A performance and energy evaluation of a dye drawn forward osmosis (FO) system for the textile industry

by
Mohammed Rahman

A thesis submitted in fulfilment of the requirements for the degree

Master of Engineering: Chemical Engineering

in the Faculty of

Engineering and Built Environment

at the

Cape Peninsula University of Technology

Supervisor: Associate Professor Marshall Sheldon
Co-supervisor: Dr Debbie De Jager

Cape Town

March 2020

DECLARATION

I, **Mohammed Rahman**, declare that the contents of this dissertation/thesis represent my unaided work and that the dissertation/thesis has not previously been submitted for academic examination towards any qualification. Furthermore, it expresses my own opinions and not necessarily those of the Cape Peninsula University of Technology.

Signed _____   **Date** _____

ABSTRACT

Continuous growth in the world population has raised significant fears with regards to the sustainability of energy and water resources. Globally, water is an indispensable resource as it is essential for the sustenance of human, animal and plant life. Water is essential for all forms of life and plays a pivotal role in economic growth. The textile industry is one of the greatest consumers of water, it is, therefore, necessary to effectively treat the large amounts of wastewater before discharge to the environment. It is estimated that annually, more than 700,000-tonnes of textile wastewater is produced by the dyeing industry. Textile wastewater is generally characterised by electrolytes, suspended solids, mineral oils and multiple textile dyes, and has therefore been classified as one of the most polluting wastewaters. These dyes are toxic and, in most cases, are not biodegradable. The presence of very small amounts (i.e. < 1 ppm) of dyes in water has aesthetic impacts and is thus undesirable. It is, therefore, necessary to treat textile wastewater before discharging.

Currently, membrane technology is widely used for wastewater treatment, as well as water purification. Forward osmosis (FO) is a promising technology for both these applications. FO is characterised by the flow of water through a semipermeable membrane from a feed solution (FS) characterised by the low solute concentration or low osmotic pressure (OP) to a draw solution (DS) characterised by the high solute concentration or high OP, due to the OP gradient across the membrane. The FO process eliminates the need for high hydraulic pressure, as required in traditional membrane technologies, and also has low fouling tendencies. Furthermore, FO has the advantage of lower energy requirements and membrane replacement costs. However, there are still many disadvantages such as reverse solute flux (RSF), membrane fouling, and concentration polarisation (CP) amongst others that still need to be addressed. Therefore, more research needs to be done in light of these limitations to better understand and mitigate these limitations to increase the effectiveness and efficiency of the FO process.

This study aimed to evaluate a dye-driven FO system for the reclamation of water from textile wastewater and synthetic brackish water (BW5) by investigating the effects of membrane orientation, system flowrate, change in DS, and membrane fouling on the FO systems performance and energy consumption. The FS used was BW5 with sodium chloride (NaCl) content of 5 g/L whereas Reactive Black 5 (i.e. a reactive dye) and Maxilon Blue GRL (i.e. a basic dye) dyes were used as a DS, respectively. The membrane utilised was a cellulose triacetate (CTA) membrane and was tested in FO mode and pressure retarded osmosis (PRO) mode whilst the system flowrate was adjusted to 400, 500 and 600 mL/min, respectively.

Experiments were performed using a bench-scale FO setup which comprised of an FO membrane cell, a double-head variable speed peristaltic pump, a digital scale, two reservoirs for the FS and DS, respectively, a digital multiparameter meter and a digital electrical multimeter to measure system energy consumption. Each experiment comprised of six steps: baseline 1 (membrane control), main experiment (dye-driven FO experiment), baseline 2 (membrane control repeat), membrane cleaning, membrane integrity (membrane damage dye identification) and membrane cleaning (preparation for next experiment). The baseline 1 and baseline 2 experiments operated for 3 h whilst each membrane cleaning procedure operated for 30 min. The main experiments operated for 5 h in the FO mode and 4 h in PRO mode whilst the membrane integrity experiments operated until a minimum of 10 mL water was recovered.

Results showed that the PRO mode achieved both higher forward flux (J_w) (i.e. 8.87, 8.71 and 9.13 L/m^2.h for flowrates of 400, 500 and 600 ml/min) and water recovery (R_e) rates compared to FO mode (i.e. 6.60, 6.88 and 7.58 L/m^2.h for flowrates of 400, 500 and 600 ml/min). The variation of flowrates had little to no influence on the J_w, J_s and Re of the system. The system consumed less energy in PRO mode (i.e. 381 kWh/m^3 average consumption for all three flowrates) than FO mode (i.e. 417 kWh/m^3 average consumption for all three flowrates). It was also observed that at a higher DS OP, the system consumed less energy. Therefore, selecting an optimum initial OP is essential for a FO process to minimise the pumping energy.

Furthermore, a change in DS from Reactive Black 5 dye to Maxilon Blue GRL dye had no significant impact on the system performance and energy consumption. In this study, no significant membrane fouling was observed, however, minute traces of fouling in the form of foreign functional groups could be observed in the attenuated total reflection Fourier transform infrared spectroscopy (ATR-FTIR) spectrums of the used membranes. Additionally, the observation of negligible changes in baseline 2 (membrane control) Re and J_w results suggested the possible occurrence of membrane fouling during the main experiment (dye-driven FO system).

Keywords: Draw solution (DS), Energy consumption, Feed solution (FS), Flowrate, Forward osmosis (FO), Membrane orientation

ACKNOWLEDGEMENTS

DEDICATION

For my mother, whose strength and resilience is an inspiration for me to follow my dreams. Thank you, mom.

TABLE OF CONTENTS

LIST OF FIGURES

LIST OF TABLES

LIST OF SYMBOLS

Nomenclature

A	Pure water permeability coefficient ($m.s^{-1}.kPa^{-1}$)
A_m	Effective membrane area (m^2)
C_i	Concentration ($g.L^{-1}$)
C_t	Reverse solute concentration ($g.L^{-1}$)
B, C and D	Viral coefficients
B_s	Salt permeability coefficient ($m.s^{-1}$)
i	Van't Hoff's solute factor (dimensionless)
J_s	Reverse solute flux ($L.m^{-2}.h^{-1}$)
J_w	Water flux ($m^3.m^{-2}.s^{-1}$)
K	Mass transfer coefficient ($m.s^{-1}$)
M	Molar concentration ($mol.L^{-1}$)
m^2	Solute molal concentration
$\dot{m}^2$	Volume molal concentration
M_w	Molecular weight ($g.mol^{-1}$)
n	Moles (mol)
R	Universal gas constant ($m^3.Pa.mol^{-1}.K^{-1}$)
T	Temperature (K)
V	Volume (m^3)

Greek Symbols

Δ	Change
$\Delta\pi$	Difference in osmotic pressures on the two sides of the membrane

LIST OF ABBREVIATIONS

BBD	Blue Basic Dye
BOD	Biological Oxygen Demand (mg/L)
BRD	Black Reactive Dye
BGW	Brackish Ground Water
BW	Brackish Water
BW5	Synthetic Brackish Water
C	Carbon
CA	Cellulose Acetate
Cl	Chloride
COD	Chemical Oxygen Demand (mg/L)
CP	Concentration Polarization
CTA	Cellulose Triacetate
DI	Deionised Water
DS	Draw Solution
ECP	External Concentration Polarisation
FO	Forward Osmosis
FS	Feed Solution
H_2O	Water
ICP	Internal Concentration Polarization
MF	Microfiltration
NaCl	Sodium Chloride
NF	Nanofiltration
OP	Osmotic Pressure (kPa)
PFD	Process Flow Diagram
PRO	Pressure Retarded Osmosis

RO	Reverse Osmosis
SRSF	Specific Reverse Solute Flux (L.m^{-2}.h^{-1})
SA	South Africa
SEC	Specific Energy Consumption
SW	Seawater
SSW	Synthetic Seawater
T&C	Textile and Clothing
TDS	Total Dissolved Solids (ppm)
TWW	Textile Wastewater
UF	Ultrafiltration
WEF	World Economic Forum

GLOSSARY

Concentration polarisation (CP)

Concentration polarisation (CP) occurs due to the manifestation of a difference in concentration at the membrane-solution interface caused by the selective transfer of species via a semi-permeable membrane (Akther *et al.*, 2015).

Desalination

Desalination (also referred to as "desalinisation" or "desalting") is the process whereby dissolved salts are removed from the water producing freshwater from seawater or brackish water (Van der Bruggen, 2003).

Draw solution

The draw solution (DS) is characterised by a high concentration and exhibits a more significant osmotic pressure (OP) than that of the saline feed solution (FS) (McCutcheon and Elimelech, 2006).

External concentration polarisation (ECP)

The external concentration polarisation (ECP) phenomena take place at the surface of the active layer of a membrane due to the occurrence of a difference in the concentration of the solution at the membrane surface compared to that of the bulk solution (Akther *et al.*, 2015).

Feed solution (FS)

The feed solution (FS) is the concentrated solution which exists on the bottom side of the permeable membrane and exhibits a lower osmotic pressure (OP) compared to that of the draw solution (DS) (McCutcheon and Elimelech, 2006).

Forward osmosis (FO)

Forward osmosis (FO) takes advantage of the naturally occurring process of osmosis, where fluid flows through a semi-permeable membrane from a lower osmotic pressure fluid to a higher osmotic pressure fluid (Al Mazrooei, 2013).

Internal concentration polarisation

Internal concentration polarisation (ICP) is the appearance of a CP layer inside the porous layer of the membrane caused by the inability of the solute to easily penetrate the dense selective segment of the diaphragm (Zhou *et al.*, 2014).

Membrane Technology

Separation process of two solutions making use of a semi-permeable membrane (Gou *et al.*, 2019).

Osmotic pressure (OP)

Osmotic pressure (OP) is the pressure that needs to be applied to a pure solvent to prevent it from passing into a given solution by osmosis. OP is often used to express the concentration of the solution (Phuntsho *et al.*, 2012)

CHAPTER 1

CHAPTER ONE: INTRODUCTION

1.1 Background

During the last few decades, a very genuine threat to the sustainable development of human society is water scarcity (Mekonnen and Hoekstra, 2016). Currently, two-thirds of the world's population resides in areas that are affected by water scarcity for at least one month a year (WWAP, 2017). According to WWAP (2017), approximately 500 million people reside in areas where water consumption exceeds the locally available renewable water resources by a factor of 2.

Most human activities using water produces wastewater. As the overall demand for water grows, the quantity and quality (i.e. total pollution load) of the wastewater produced is continuously increasing globally. Most wastewater is released directly into the environment without adequate treatment, having harmful impacts on human health, economic productivity, ambient freshwater resources quality, and ecosystems (WWAP, 2017).

Highly vulnerable areas, where non-renewable resources, such as fossil groundwater, continue to decrease, have become dependent on water supply from areas with abundant water and continually investigating affordable alternative sources of water. To support the world's growing population, a sustainable path needs to be identified for the future of water (i.e. reduced environmental impacts and promotion of reuse). Therefore, there is an increase in the demand for efficient, sustainable techniques to recover and reclaim water (Lutchmiah, 2014).

The World Economic Forum (WEF) ranked the 'Global water crisis' as one of the biggest threats to the planet over the next decade (Schwab, 2010). South Africa (SA), ranked the 30th driest country in the world, is a high water-stressed country with a harsh climate and significant rainfall variations (WRI, 2015).

The Western Cape Province, which is located in the south-western corner of SA, is categorised as a water-stressed region. Based on recent planning developments, it is anticipated that the water demand will exceed supply by 2020 in the regional water resource network. The water resources within the provinces are becoming progressively susceptible to climate variability. The recent climate change models indicate that the Western Cape will eventually become hotter and drier, resulting in reduced water availability, while experiencing more extreme rainfall events (GreenCape, 2017).

As a country with a rise in water scarcity, the economy of SA is challenging the limitations of its resource constraints. Water plays a major role in the process of electricity production and more importantly, it is also a prerequisite for the production of energy. The link between water and energy is a crucial one which has a high level of co-dependency. The entire water services organisation can be compromised as a result of a shortage of power. (Von Bormann and Gulati, 2014).

The textile and clothing industry is known to be one of the largest, as well as the oldest industries globally. This industry can be considered as one of the greatest consumers of water (Ghaly *et al.*, 2014; Han *et al.*, 2016). Forward osmosis (FO) has garnered attention as a novel technology for the recovery and reclamation of water from seawater and brackish water. FO is characterised by the osmotic transport of water through a semipermeable membrane from a feed solution (FS) characterised by the low solute concentration or low osmotic pressure (OP) to a draw solution (DS) characterised by the high solute concentration or high OP, due to the OP gradient across the membrane. Since FO does not require high pressure, it has the potential for lower energy requirements to reclaim water compared to traditional pressure-driven membrane technologies (Zhao *et al.*, 2015).

1.2 Problem Statement

FO still faces several critical challenges such as membrane fouling, reverse solute flux (J_s) and concentration polarization (CP), however, currently there is limited research available on the impact of these challenges on the performance and energy consumption of a FO system.

1.3 Research Questions

- Which operating conditions (i.e. flowrate) influence the performance and energy consumption of a dye driven FO system?
- Does change in DS influence the performance and energy requirements of a dye driven FO system?
- Does membrane orientation influence the performance and energy requirements of a dye driven FO system?

1.4 Aims and Objectives

1.4.1 Aim

The research project aimed to conduct a performance and energy evaluation of a FO system used for the production of diluted dyeing solutions using synthetic brackish water (SBW5) as the feed solution (FS). The performance was assessed using the water flux (J_w), reverse solute flux (J_s) and water recovery (R_e).

1.4.2 Objectives

The objectives of this research study were to:

- Evaluate the effect of membrane orientation on system performance and energy consumption.
- Evaluate the effect of system flowrates on system performance and energy consumption.
- Investigate the effect of membrane fouling on system performance and energy consumption.

1.5 Significance

The findings of this study will provide a better understanding of the impact of membrane orientation and system flowrate on the FO system performance and energy consumption. The findings will also provide insight into how challenges such as membrane fouling, reverse solute flux, and CP influences the dye driven FO system performance and energy consumption. The study will demonstrate whether (i) water can be reclaimed from synthetic brackish water (SBW5) using a FO system and (ii) a diluted dyeing solution can be produced that can be used in the dyeing process.

1.6 Delineation

This research project will not include:

- Determination of the type of membrane and membrane development.
- The effect of temperature on the flux.
- Modelling of water transport across the membrane.

CHAPTER 2

CHAPTER 2: LITERATURE REVIEW

2.1 Water and energy crisis in South Africa (SA)

Resources such as energy, food and water form the heart of a resilient economy. However, as a country with a rise in water scarcity, the economy of South Africa (SA) is challenging the limitations of its resource constraints. The scarcity of resources in SA means there are significant trade-offs between the food, energy and water sectors. However, water is the most significant resource constraint, since SA is a water-scarce country with a harsh climate and significant rainfall variations (Von Bormann and Gulati, 2014; WRI, 2015). At the same time, the energy sector is largely coal-fired and therefore water-intensive (Von Bormann and Gulati, 2014).

Due to the strain experienced in the energy sector, load-shedding has been a critical challenge in SA in recent years. While load-shedding persists, SA faces the even more worrying prospect of water-shedding. Similar to the energy crisis, the dreadful state of water in SA is attributed to factors such as an increase in demand, depletion and contamination of resources, as well as ineffective infrastructure. Fioramonti (2015) acknowledges that 37% of potable water is being lost through infrastructure failures (e.g. leaking pipes and dripping taps). SA is currently using 98% of its available water supply, with 40% of wastewater treatment in a critical state (Fioramonti, 2015).

2.1.1 Textile wastewater

The Textile and Clothing (TandC) industry is one of the major industries which provides employment and in turn plays a key role in the economy of many countries in the world (Keane and te Velde, 2008). According to Truett and Truett (2010), the SA TandC industry is the 6th leading employer in the manufacturing sector and the 11th largest manufactured goods exporter (Truett and Truett, 2010). Due to the production of harmful textile wastewater, the industry is considered to be one of the biggest threats to the environment. As a result of the variety of processes in the textile industry, large amounts of solid, gas and liquid wastes are produced (Ghaly et al., 2014).

The textile industry is not only responsible for the consumption of a huge amount of water but also produces contaminated textile wastewater which is highly resistant to biological treatment methods. The characteristics of the textile wastewater vary and are highly dependent on the type of chemicals being used, as well as the type of textile being manufactured. The textile wastewater is characterised by high amounts of agents which contribute negatively towards the environment and human health. The effluent consists of dissolved and suspended solids, chemicals, colour, odour, chemical oxygen demand (COD) and biological oxygen demand

(BOD) (Ghaly *et al.*, 2014). The BOD/COD ratio in the effluent is around 1:4 in most cases, signifying the existence of non-biodegradable materials (Lorimer *et al.*, 2001).

Ghaly *et al.* (2014), suggests that to produce 1 kg of textile, approximately 200 L of water is consumed. Most of the water is mainly used to apply the chemicals onto the textile and also to rinse the manufactured textiles. It is estimated that about 1000 - 3000 m^3 of wastewater is produced after the processing of approximately 12 to 20 tonnes of textiles per day. The textile wastewater effluent produced during this process is characterised by large amounts of various dyes and chemicals comprising of trace metals such as Cu, Cr, As and Zn.

These chemicals have the potential to harm both the environment and human health. The types of dyes and chemicals used are highly dependent on the type of fabric being manufactured. The three different types of dyes used to dye cellulose fibres are (Lorimer *et al.*, 2001; Ghaly *et al.*, 2014):

- ➢ Naphthol dyes: fast blue B, fast yellow GC and fast scarlet R
- ➢ Reactive dyes: cibacron F, remazol and procion MX
- ➢ Direct dyes: brown 116, congo red and direct yellow 50

The most universally used cellulose fibre dye are reactive dyes. Reactive dyes are used to dye cotton, which is also one of the most commonly used fibres. The significance of reactive dyes can be seen in the increase of its use from the year 1988 to the year 2004, where it increased from 60 000 tonnes to 178 000 tonnes (Ghaly *et al.*, 2014).

As previously mentioned, the textile industry is categorised not only by the consumption of large amounts of water but also the various types of chemicals used in the individual processes. It is, however, important to take heed of the fact that the amount of water consumed in the different processes is dependent on the type of textile industry, dyeing process and also the type of fabrics being produced. According to Ntuli *et al.* (2009), 38% of the water is consumed during the bleaching process, 8% during the printing process, 16% during the dyeing process, 14% is used for the boiler and the remaining 24% of the water is used for other purposes (Ntuli *et al.*, 2009; Ghaly *et al.*, 2014). The textile industry discharges a wide variety of pollutants during the processing of fibres, fabrics and garment production (Ghaly *et al.*, 2014).

2.2 Desalination technologies

Desalination (also referred to as "desalting") is the process whereby dissolved salts are removed from water thereby producing freshwater. The seawater desalination process divides the saline seawater into two separate streams, where one stream is characterized by a low concentration of dissolved salts and the other is characterized by concentrated brine (Van der Bruggen *et al.*, 2003). The desalination process requires a form of energy to operate and as such, it exploits various technologies for separation. There are a variety of desalination technologies such as freezing and electrodialysis, thermal distillation and membrane separation which have been industrialized over the years (Ling *et al.*, 2010).

2.2.1 Membrane technologies

Membrane technology is essentially a separation of substances whereby the membranes operate as a filter. The substances being separated can be chemical, biological or thermally modified (De Jager *et al.,* 2014; Le and Nunes, 2016). The water industry utilises membrane technologies for the desalination of brackish water and seawater as well as the treatment of wastewater. Membrane technologies have been recognised as efficient techniques to treat wastewater and produce potable water (Strathmann *et al.*, 2006). These technologies have played a pivotal role in the improvisation of the treatment of wastewater and also in the separation of micro-organisms. Due to the increase in the use of the various membrane technologies, they are well known for their purification efficiency in terms of their comprehensive preservation of particles and bacteria. According to Le and Nunes (2016), advances in membrane material is required to achieve improvements with regards to cost and affordability, energy consumption and expertise of all types of membrane technologies.

Membrane technologies display the potential to eliminate the dyestuff, allowing for reclamation of the auxiliary chemicals used for dyeing, as such, membrane technologies exhibit great potential for the treatment of textile wastewater. Examples of membrane technologies include microfiltration (MF), ultrafiltration (UF), nanofiltration (NF), reverse osmosis (RO) as well as a developing membrane technology known as forward osmosis (FO) (Strathmann *et al.*, 2006; Cath *et al.*, 2006).

2.2.1.1 Microfiltration and Ultrafiltration (MF and UF)

Microfiltration (MF) and ultrafiltration (UF) are examples of pressure-driven membrane processes. These two processes are somewhat identical with regards to their separation mechanisms and therefore the fields in which they are applied are in correspondence. The two-processes operate in crossflow as well as dead-end mode. The operating pressure and

the pore sizes of the individual process are what separates the two from one another (McGovern and Lienhard 2014).

The MF process operates at a pressure which ranges from 0.1 to 3 bars with a pore size range of 0.003 to 10 microns, compared to that of the UF process which operates at a pressure which ranges from 0.5 to 10 bars with a pore size range of 0.002 to 0.1 microns (McGovern and Lienhard 2014; De Jager *et al*, 2014).

The separation process is governed by the principle of porous filters where particles larger than the membrane pores are entirely reserved. As a result, a top layer can be observed on the surface of the membrane due to the particles being detained. This layer is responsible for holding back particles that are small and which would flow through the membrane. MF and UF are used in wastewater treatment for separation purposes. In municipal wastewater treatment, MF and UF are used for separating the sludge and water, pre-treatment that is carried out before a RO process and they are used after precipitation to remove the remaining sludge and water fractions (McGovern and Lienhard 2014). The application of MF and UF is diverse as they are also used in the treatment of industrial wastewater where they are used mostly to reprocess and re-claiming process water for several applications (Strathmann *et al.*, 2006; McGovern and Lienhard 2014).

2.2.1.2 NanoFiltration (NF)

Nanofiltration (NF) is a pressure-driven membrane bio-separation process which is mostly utilised for the reclamation of watery solutions. This technique is characterised by a crossflow operation mode with operating pressures ranging from 2 to 40 bar and a pore size range of 1 to 5 nanometres (Shon *et al.*, 2013). NF is also made use of in aqueous solutions where it plays a significant role in the separation process of the higher molecular weight components from that of the lower molecular weight components (Schader, 2006; Strathmann *et al.*, 2006). In NF, the membrane acts as a selective barrier to allow the passage of solvents while obstructing the passage of solutes (Naidu *et al.*, 2015).

2.2.1.3 Reverse Osmosis (RO)

Reverse osmosis (RO) is well known for its separation technique of the removal of undesired solutes from a solution (Motsa *et al.,* 2014). According to Peñate (2011), in RO, the dissolved solids are separated from water through the application of a pressure differential across a membrane which is permeable only to water and not to the dissolved solids. Moreover, according to Peñate (2011), the membrane, made of either cellulose acetate or polyamide, rejects most of the solids creating two streams, one of pure water, (i.e. product or permeates) and one with dissolved solids (i.e. concentrate or reject).

RO is an example of a pressure-driven membrane process (PDMP) in which hydraulic pressure is used to overcome the osmotic pressure (OP) of the feed solution (FS). As shown in Figure 2.1, hydraulic pressure (ΔP) is the driving force that allows for the transportation of water across the semi-permeable membrane, as a result, separating the solutes from the solution (Cath *et al.*, 2006; Phuntsho *et al.,* 2011). RO is characterised by operating pressures ranging from 30 to 70 bars and pore sizes of ≤0.6 nanometres (Koyuncu and Cakmakci, 2010).

2.2.1.4 Pressure Retarded Osmosis (PRO) Technology

In pressure retarded osmosis (PRO), water from a low salinity feed solution (FS) permeates through a semi-permeable membrane to a pressurised, high salinity draw solution (DS). The power required is obtained by depressurizing the permeate with a hydro turbine (Achilli *et al.*, 2009). As shown in Figure 2.1, pressure retarded osmosis (PRO) can be regarded as an in-between process between FO and RO as the hydraulic pressure is now applied in the reverse direction of the osmotic pressure (OP) gradient which is similar to that of RO. However, it is important to take heed that the net water flux flow regime remains in the direction of the concentrated DS which is similar to that of the FO process (Klaysom *et al.*, 2013). This is further supported by Klaysom *et al.* (2013), who stated that PRO is characterised by an osmotically driven membrane process as a result of the flow regime of the water which flows from a low OP FS to a high OP DS against a hydraulic pressure. PRO is a process that forms mechanical energy by converting the osmotic power within the system. The mechanical energy produced can then be converted to other forms of beneficial energy (e.g. the pressurised DS can be run through a hydro turbine to produce electricity) (Achilli *et al.*, 2009; Klaysom *et al.*, 2013).

2.2.1.5 Forward Osmosis (FO)

According to Cath *et al.* (2006) forward osmosis (FO) is the phenomena of the transportation of water through a selectively permeable membrane from an area of high-water chemical potential to an area of low water chemical potential. The process is influenced by a difference in the concentration of solutes across the membrane which stimulates the flow of water but discards most of the solute molecules or ions. The osmotic pressure (OP) is the pressure that is applied to the higher concentrated solution that would inhibit the transportation of water across the membrane (Cath *et al.*, 2006).

Cath *et al.* (2006) suggested that FO uses the OP differential across the membrane compared to that of the hydraulic pressure differential concept used in RO, as the driving force for the transportation of water across a semi-permeable membrane. The FO process is characterised by the concentration of the FS stream and the dilution of a highly concentrated DS stream

(Zhao *et al.*, 2015; Mehta *et al.*, 2014).

FO is a developing membrane technology for wastewater reclamation and seawater desalination. FO, amongst other desalination technologies, has emerged as a strong candidate to mitigate water and energy shortages as it can create clean water, and clean energy through the use of an osmotic pressure gradient across a semi-permeable membrane as the driving force for water production and power generation (Zhao *et al.*, 2015).
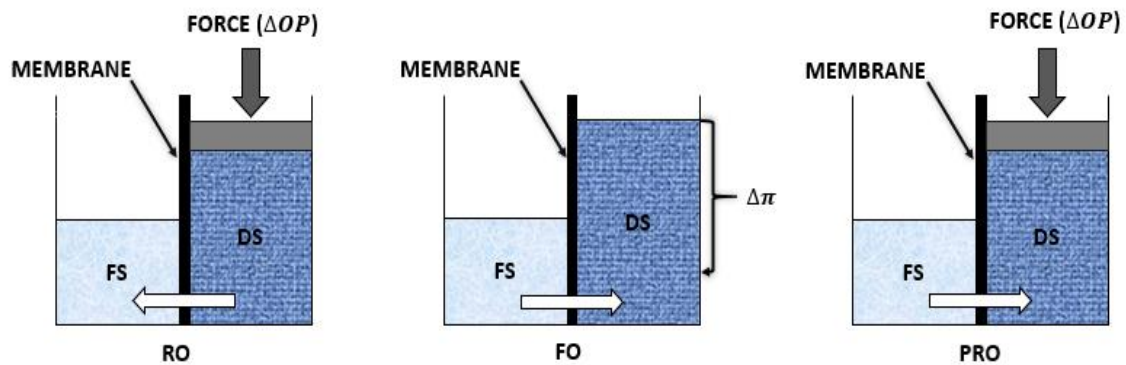
Figure 2.1: Solvent flows in RO, FO and PRO membrane technologies respectively (Adapted from Cath *et al.*, 2006)

2.2.2 Energy comparison between RO, FO and PRO

The differences between the processes of RO, FO and PRO can be seen by the water flux and energy consumption of these processes. According to Phuntsho *et al* (2012), the water flux in an osmosis process can be described by Equation 1.

$$J_w = \frac{\Delta V}{A_m.\Delta t}$$ (Equation 2.1)

Where, J_w (L.m^2.h^{-1}) is the water flux, A_m is the effective membrane area (m^2), and ΔV (m^3) is change in volume of the DS in relation to the time interval Δt (s).
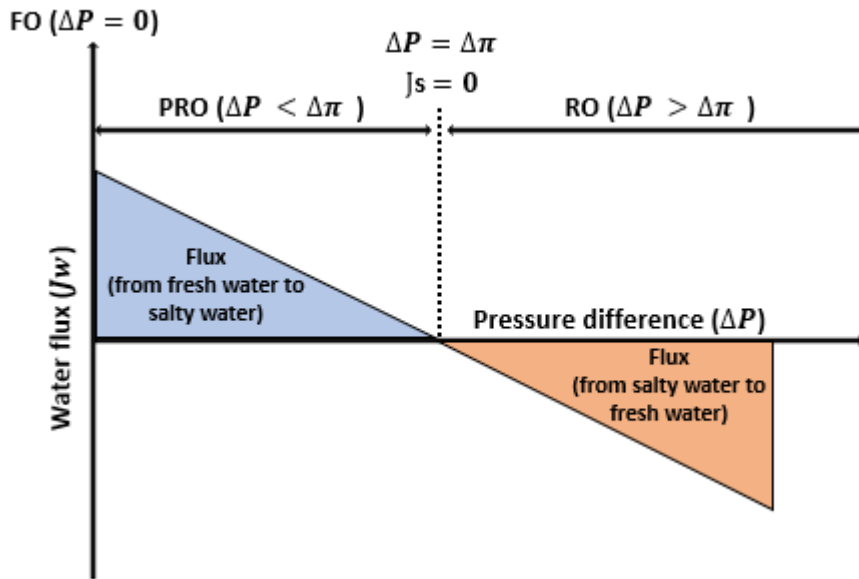
Figure 2.2: Direction of water flux with respect to forward osmosis, pressure retarded osmosis and reverse osmosis (Chou *et al.*, 2012)

Interpreting Figure 2.2, it can be seen that the process of FO does not require hydrostatic pressure differential ($\Delta P = 0$) to achieve a high-water flux (J_w) value compared to that of RO, where the hydrostatic pressure (ΔP) needs to be higher than the osmotic pressure (OP) for the process to occur. However, for PRO, hydrostatic pressure (ΔP) difference across the semi-permeable membrane is needed for the process to occur. Moreover, Figure 2.2 shows that the hydrostatic pressure in PRO has to be lower than the osmotic pressure ($\Delta P < OP$), to provide high water flux (Chou *et al.*, 2012).

Figure 2.3 illustrates the difference between the thee processes in terms of energy consumption, making it evident that the FO process indeed consumes the least amount of energy when compared to RO and PRO.

$$\Delta P = \Delta \pi$$
$$W = 0$$

FO (W = 0)

PRO ($\Delta P < \Delta \pi$)   RO ($\Delta P > \Delta \pi$)

$$\Delta P = \Delta \pi / 2$$
$$W = Wmax = \Delta \pi^2 / 4$$

Produce energy   Pressure difference (ΔP)

Power density (W)
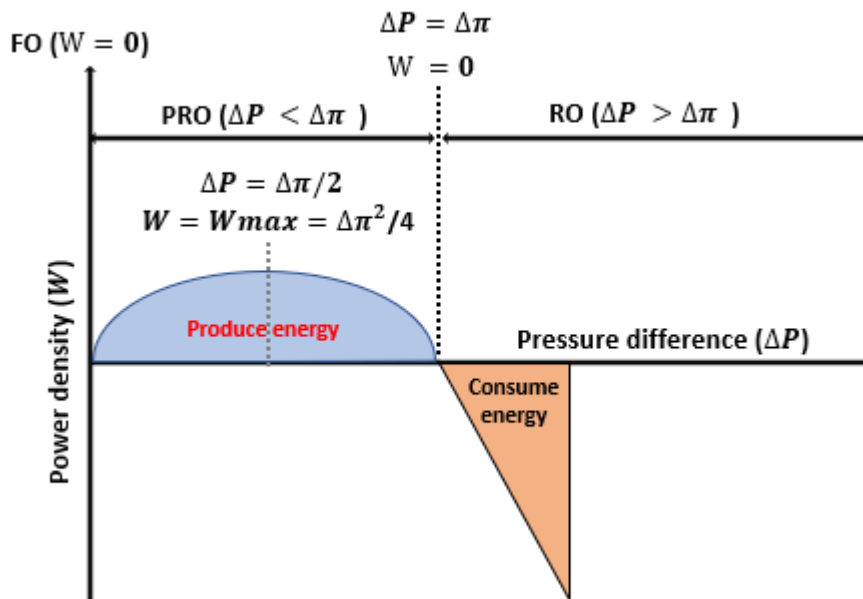
Consume energy

Figure 2.3: The energy consumption of forward osmosis, pressure retarded osmosis and reverse osmosis (Chou *et al.*, 2012)

2.2.3 Similarities and differences in RO, FO and PRO

RO, FO and PRO are membrane technologies that are characterised by common attributes. However, all three of these technologies differ in terms of the driving forces for mass transport, and water flow directions as well as solute directions. The driving force for RO is external hydraulic pressure, and it is therefore categorised as a pressure-driven membrane process. FO and PRO are different compared to that of RO because the net osmotic pressure gradient (ΔOP) across the membrane is what drives the water flux within the system (Chou *et al.*, 2012).

Observing Figure 2.2, it can be seen that in RO the water diffuses to the less saline side as a result of hydraulic pressure ($\Delta P > \Delta OP$). Furthermore, it can be seen that for FO, the pressure gradient (ΔP) is zero resulting in the water diffusing to the more saline side of the membrane. Taking into consideration PRO, the water diffuses to the more saline liquid which is under positive pressure ($\Delta OP > \Delta P$).

Due to the differences between the membrane technologies, the membrane selection criteria differ for the individual membrane processes. A comparison between RO, FO, and PRO membrane system requirements is provided in Table 2.1 (Klaysom *et al.*, 2013).

Table 2.1: Comparison between RO, FO, and PRO (Klaysom et al., 2013)

Parameter	Reverse osmosis (RO)	Forward osmosis (FO)	Pressure retarted osmosis (PRO)
Driving force	Osmotic pressure	External hydraulic pressure (P)	Osmotic pressure
Main application	➢ Water cleansing process ➢ Desalination	➢ Water cleansing process ➢ Desalination	➢ Power production
Operating conditions	Pressure: atmospheric Draw solution: Brackish water, seawater and/or synthetic draw solution like aqueous NH_3 Feed solution: Compromised water, seawater or other types of suitable feed solutions pH: 6 – 11	Pressure: 10 – 70 bar Draw solution: Brackish water and seawater pH: 6 – 7	Pressure: 10 – 15 bar Draw solution: River water, brackish water, seawater and also brine solution pH: 6 – 7
Membrane properties			
Physical morphology	➢ Thin membranes with impenetrable active layer on porous sub-layer	➢ Thick top layer and porous sub-layer ➢ Good thermal and mechanical stability	➢ Thin membranes with a thick active layer on porous sub-layer
Chemical property	➢ Highly hydrophilic ➢ High chemical stability with respect to chloride solution and synthetic draw solution	➢ High chemical stability with regards to chloride solution	➢ Highly hydrophilic
Membrane requirement	➢ High water permeability ➢ High solute preservation ➢ Stable in synthetic draw solution	➢ High water permeability ➢ High solute preservation ➢ Resilient in terms of high pressure operation	➢ High water permeability ➢ Good solute preservation to maintain the driving of the osmotic pressure ➢ Tough enough to withstand the external applied pressure
Target performance	High flux and good water recovery	High flux (at around 4 - 5 μm.s^{-1})	High power density ($>$ 5 W.m^{-2})
Challenges	➢ Internal concentration polarisation ➢ Suitable draw solution ➢ Draw solution recovery and re-concentration	➢ Energy consumption ➢ Operating cost	➢ Internal concentration polarisation ➢ Module design ➢ Membrane cleaning ➢ Feed stream pre-treatment

2.3 Forward Osmosis as a desalination technology

FO is a membrane technology which utilises the naturally occurring phenomena of osmosis, whereby the fluid flows across a semi-permeable membrane from a region of low osmotic pressure (OP) to a region of high OP fluid as illustrated in Figure 2.4b. In the FO process, a DS with a higher OP compared to that of the FS as depicted in Figure 2.4 (a) is required for the fluid to permeate across the semi-permeable membrane from the FS side to the DS side. The OP gradient between the DS and FS is known to be the driving force of the FO process (Thompson and Nicoll, 2011; Mehta *et al.*, 2014; Zhao *et al.*, 2015).
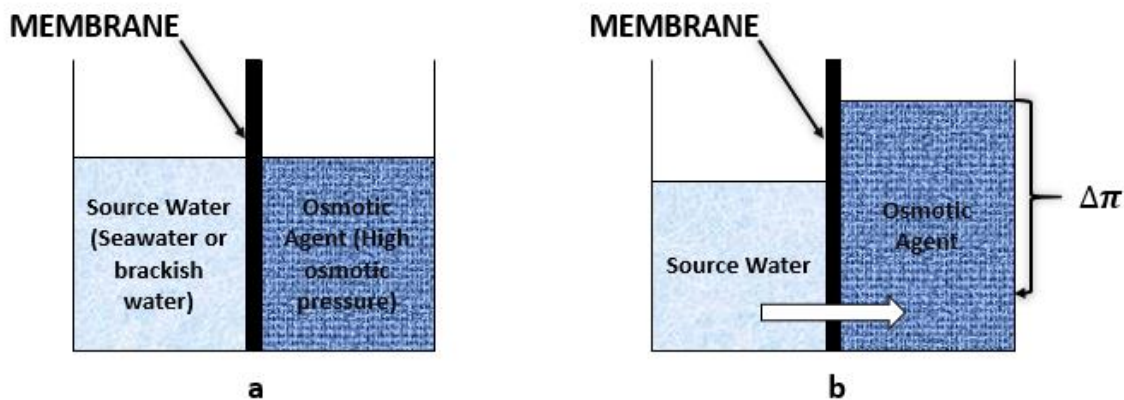
Figure 2.4: Forward osmosis process (Adapted from Thompson & Nicoll, 2011)

2.3.1 Feed Solution (FS)

According to McCutcheon and Elimelech (2006), the FS is a concentrated solution which exhibits a lower OP compared to that of the DS. A lower OP is vital for the natural OP gradient, the driving force of the FO operation. Deionised water (DI) has been used as a standard in many studies as a source of FS for comparisons (Boo *et al.*, 2013; Zhang *et al.*, 2014).

A variety of alternative FS has previously been used, which include brackish water that ranges in concentrations from 0.1 to 0.6 M of sodium chloride (NaCl) (Phunthso *et al.*, 2012). Alternative FS's also include brackish groundwater (BGW) in the range of 0.1 to 0.8 M NaCl and lastly seawater (SW) within the range of ±1 M (Gray *et al.,* 2006). The FS's mentioned are those that are most commonly used as alternative FS's (Phunthso *et al.*, 2012).

In literature, the bulk osmotic potential of the FS is predominately calculated using software made available by OLI Systems Inc. (OLI Stream Analyser 3.2) (Phuntsho *et al.,* 2011). The OLI Stream Analyser extrapolates the properties of the various solutions over a wide range of

concentrations as well as temperatures through the utilization of thermodynamic modelling which is based on published experimental data (Phuntsho *et al.,* 2011; Wilson and Stewart, 2013; Zhao *et al.,* 2016). Table 2.2 indicates various compositions for alternative FS used in previous studies.

Table 2.2: Compositions of FS used in previous studies. Osmotic potential of the FS as determined by an OLI Stream Analyser 3.2

Feed Solutions (FS)	Abbreviation	Concentration (M)	Osmotic Potential (kPa)	Reference
Deionised water	DI	0	0	(Gray *et al.,* 2006; Phuntsho *et al.,* 2012)
Brackish water	BW5	0.086	398.21	(Phuntsho *et al.,* 2012)
Seawater	SW	0.599	2837.10	(Phuntsho *et al.,* 2012)

2.3.2 Draw Solutions (DS)

The driving force of the FO process is often considered to be the concentrated DS on the permeate side of the membrane. The main criterion for the selection of a DS is that it has a higher OP compared to that of the FS (Cath *et al.,* 2006). Nicoll (2013) stated that the successful application of FO based membrane processes is highly dependent on the selection of the appropriate DS. In some processes, the DS is recovered, and its concentration is preserved by dosing. Ideally, a DS should be characterised by the following attributes (Nicoll, 2013):

- Non-toxic.
- Low cost.
- Simply recoverable or regenerated with low energy input.
- High osmotic pressure at low concentrations.
- High solubility.
- Low viscosity.
- Low reverse solute diffusion.
- Not harmfully affected by the impure ions from the FS.
- Negligible influence on internal concentration polarisation.

Ideally, all these attributes are difficult to acquire and as such in practicality a compromise solution is then adopted. The DS selection and characterisation have been the subject of many types of research with a focus on synthetic materials as well as inorganic and organic salts (Achilli *et al.*, 2010).

According to the investigations of Achilli *et al.* (2010) which was based on DS, it was found that with regards to performance $CaCl_2$, $KHCO_3$, $MgCl_2$, $MgSO_4$ and $NaHCO_3$ ranked highly. From a replenishment cost analysis point of view $KHCO_3$, $MgSO_4$, NaCl, $NaHCO_3$ and Na_2SO_4 were found to be highly ranked. Taking into consideration performance as well as replenishment cost analysis, it was found that, $KHCO_3$, $MgSO_4$ and $NaHCO_3$ ranked high with regards to both the criterions. Achilli *et al.* (2010) however suggested that the actual selection criteria are dependent on the application as well as the interaction of the DS with the different streams. The occurrence of phenomena such as reverse solute diffusion may contaminate a feed stream being concentrated using FO. The presence of scale precursors in the FS stream can also result in the contamination of the DS (Achilli *et al.*, 2010).

2.3.3 Forward osmosis membranes

FO membranes are significantly different from RO membranes in terms of the characteristics of the porous sub-layer and the compression resistance of the whole membrane. Furthermore, FO membranes are characterised by a low fouling tendency even though there are complicated mechanisms involved (Liu, 2013).

Saren *et al.* (2011) acknowledged that water flux in FO processes is limited. The limitations in water flux come as a result of a build-up of solutes in the permeable membrane support layer when the DS is against the active rejection layer of the membrane or in the case of the dilution of the DS within the support layer when the FS is against the active layer of the membrane.

Generally, for FO processes, any non-porous selectively permeable membrane can be used. The typical FO membranes are characterised by their extent of salt rejection as well as flux rate. Ideal FO membranes are characterised by their rate of salt rejection as well as flux rate. Furthermore, membranes ought to be characterised by their properties such as (Al Mazrooei, 2013):

- Low fouling propensity.
- Chlorine resistance.
- Chemical stability toward the draw solution.
- Minimum reverse osmosis.
- Tolerate mechanical stress.

Whether the individual membranes are commercially available, or custom made, all membranes are produced to maintain the above-mentioned properties. Nicoll (2013) stated that FO membranes theoretically can have similar configurations compared to that of the conventional ultra-filtration and RO membranes. FO membranes are found in a variety of configurations such as a spiral wound, flat sheet, plate and frame, tubular or hollow fibre (Cath *et al.*, 2016). Table 2.3 depicts the various FO membranes together with their specifications and attributes.

2.3.3.1 Membrane types

FO membranes are generally characterised by an asymmetric membrane which is composed of a thin selective layer together with a porous mechanical support layer. The thin-film composite (TFC) membrane is a type of FO membrane. In all types of FO membranes, the support layer functions as a boundary layer which limits the performance of the membrane. Some materials used for the construction of membranes include (Alsvik and Hagg, 2013):

- Cellulose acetate (CA)
- Polybenzimidazole (PBI)
- Polysulfone and polyethersulfone (PSF)
- Polyamide (PA)
- Poly(amide-imide) (PAI)

Each material has its individual properties which make it viable for use for the construction of membranes. Individual material properties include temperature resistance, hydrophilic nature, the extent of wetting and also the mechanical durability (Alsvik and Hagg, 2013).

2.3.4 Advantages of forward osmosis (FO)

The FO process has a variety of potential benefits as it is an osmotically driven process with a low hydraulic pressure requirement. Figure 2.5 illustrates the potential benefits of the FO process in numerous water treatment applications. FO holds the promise of achieving lower energy consumption as the system does not require an external supply of pressure for the FO process to occur. Expenditure can be lowered if the appropriate DS and its respective regeneration method can be economically and technically developed (Elimelech and Philip, 2011).
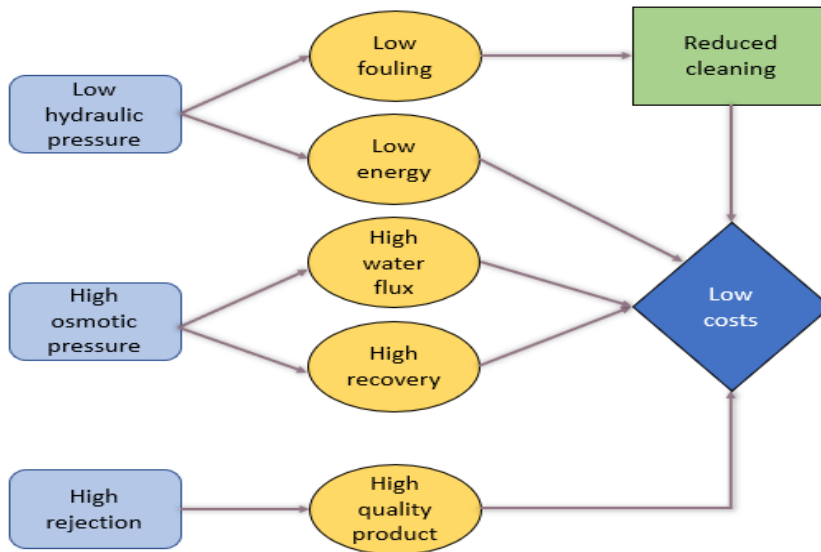
Figure 2.5: Potential benefits of forward osmosis in water treatment (Adapted from Zhao et al., 2012)

According to Achilli *et al.* (2009), studies have established that membrane fouling in FO membrane processes is reasonably low. This is supported by the absence of hydraulic pressure in FO, which depends on the osmotic gradient thus reducing the chance of fouling material to remain on the surface of the membrane, making the process more reversible (Cartinella *et al.*, 2006).

The optimisation of the hydrodynamics can further reduce the extent of fouling in the FO process (Lee *et al.*, 2010). FO is characterised by a high osmotic pressure gradient across the semi-permeable membrane as a result of which FO holds the potential to achieve high water flux and water recovery (Cartinella *et al.*, 2006). The volume of desalination brine can be reduced as a result of high-water recoveries. Desalination brine is a major environmental concern of the existing desalination plants predominantly responsible for inland desalination (McCutcheon *et al.*, 2005).

Table 2.3: Configuration of FO membranes (Cath *et al.*, 2006)

FO membrane	Disadvantages	Advantages	Application	Properties
Flat-sheet	Not suitable/ideal for applications with high volumes	Operation is simple and effective in the presence of high amounts of fouling agents in the waste streams	➢ Bio-reactors ➢ Water treatment ➢ Membrane	Area of sheets: 0.25 m^2 The thickness of membrane: 20 μm Number of sheets per module: 43 Packing density: 110 m^2/m^3 Distance between membrane sheets: 8mm
Hollow fibre	The occurrence of membrane blockages at low fouling concentrations	Suitable for applications of large volume due to its high packing density	➢ Desalination ➢ Wastewater treatment	Hollow fibre area: 0.0031 m^2 Hollow fibre diameter: 1 mm Hollow fibre wall thickness: 0.2 mm Hollow fibre length: 1 mm Packing density: $\sim$ 1600 m^2/m^3
Tubular	Water flux may be limited due to the thickness of tubes	Operation is simple while dealing with waste streams which contain large amounts of fouling agents and solutions of high viscosities	➢ Desalination industry	Tube length: 1 m Tube inner diameter: 10 mm Tube thickness: 0.4 mm Packing density: 260 m^2/m^3

2.3.5 Forward osmosis (FO) limitations

The FO membrane process is faced with many critical challenges, even though osmotically driven processes are widely suggested and investigated in an assortment of applications (Zhao *et al.*, 2012). Some of the critical challenges one is faced with when dealing with a FO process include (Al Mazrooei, 2013):

- Concentration polarization.
- Draw solution development and separation.
- Membrane development.
- Reverse solute flux.
- Fouling.

2.3.6 Membrane orientation

The efficiency of a FO membrane process depends on the selection of the ideal semi-permeable membrane for the respective application. The ideal membrane should be characterised by high water permeability and it should be thin and symmetric (McCutcheon and Elimelech 2006; Yip *et al.*, 2010). However, the use of a thin and symmetric membrane is not practical and therefore a support layer is essential to deliver mechanical strength (Yip *et al.*, 2010). The FO membrane is tested under two different orientations (FO and PRO modes). The FO membrane performances differ when the FS is positioned against the two different layers of the membrane (Gray *et al.*, 2006).

The membrane orientation is in FO mode when the FS faces the active layer of the membrane, and the permeable support layer faces the DS. In the same token, the membrane orientation is in PRO mode when the FS meets the porous support layer, and the DS meets the active layer of the membrane. The membrane orientation of the FO process plays a significant impact on the extent of internal concentration polarisation (ICP), the presence of which causes a decline in the water flux (Gray *et al.*, 2006; McCutcheon and Elimelech 2006).

Figure 2.6 demonstrates the flux direction of the permeating fluid in the respective FO and PRO modes. Also, in Figure 2.6, the orientation type of the asymmetric membrane is indicated where in FO mode the FS faces the active layer of the membrane compared to that of the PRO mode where the DS meets the active layer of the membrane (Achilli *et al.*, 2009).
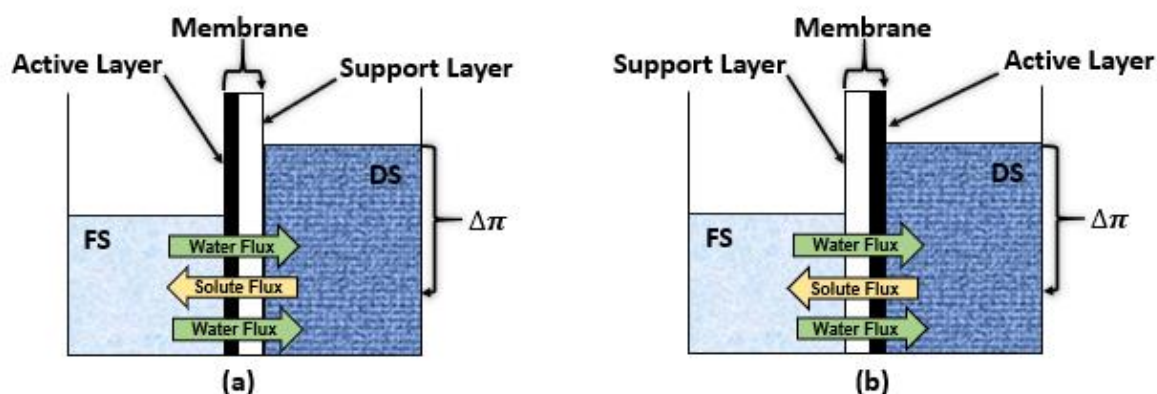
Figure 2.6: Depiction of the solvent flow regime in the FO and PRO mode. The membrane orientation in each system is indicated by the thick black line which represents the active layer of the membrane. (a) FS faces the active layer (FO mode) and (b) DS faces the active layer (PRO mode) (Adapted from Achilli *et al.*, 2009)

2.3.7 Concentration polarization in osmotic processes

Concentration polarization (CP) is a phenomenon that occurs in most membrane separation processes irrespective of whether it is an osmotically driven or a pressure-driven process. The development of CP is caused by the occurrence of a concentration difference at the interface of the membrane-solution which occurs due to the flow of species across a semi-permeable membrane (Darwish *et al.*, 2016). In osmotically driven membrane processes like PRO and FO, CP occurs due to the development of a concentration gradient between the DS and the FS across an asymmetric FO membrane. The occurrence of CP in FO processes can be categorised as internal concentration polarisation (ICP) and external concentration polarisation (ECP). ICP occurs at the membrane support layer compared to that of the ECP which occurs at the surface of the membrane active layer (Akther *et al.*, 2015).

In FO, the water flux, as well as the recovery process, is controlled by the effective transmembrane osmotic pressure (ETOP) (Akther *et al.*, 2015). According to literature (Darwish *et al.*, 2016), the effect of ETOP is greatly reduced with the occurrence of CP on both sides of the FO membrane. This phenomenon is one of the major contributing factors towards the decline in both water flux and the recovery process across the semi-permeable membranes (Sagiv *et al.*, 2014).

2.3.7.1 External concentration polarisation (ECP)

The phenomena of ECP is common to both FO and RO processes. ECP takes place at the membranes active layer surface and is caused by the development of a concentration gradient of the solution at the surface of the membrane compared to that of the bulk solution (Akther *et al.*, 2015). The role of ECP is of great significance as it plays a pivotal role in reducing the osmotic gradient and as a result inhibiting the flux of water across the membrane. The degree of ECP however, is significantly smaller compared to that of ICP in the FO process. According to literature (Jung *et al.*, 2011) by regulating the water flux together with raising the turbulence and shear rate of flow across the membrane, the influence of ECP on the permeate flux can be alleviated. The influence of ECP is negligible in accordance with low levels of permeate water flux. In essence, the selection of DS is of great importance as the level of ECP is dependent on the type of DS in question (Chanukya *et al.*, 2013).

Concentrative external concentration polarization (CECP) is the phenomena where the solute accumulates above the membrane active layer as a result of the permeation of water across the membrane, which then causes an increase in the feed concentration and a reduction in the ΔOP (Suh and Lee, 2013).

In the same token, the phenomena of the dilution of the DS against the porous layer as a result of the permeation of water across the membrane is referred to as dilutive external concentration polarization (DECP). By increasing the fluid flow and turbulence, a reduction in both ECPs may be observed. Figure 2.7 shows the effect of both DECP and CECP (Al Mazrooei, 2013)
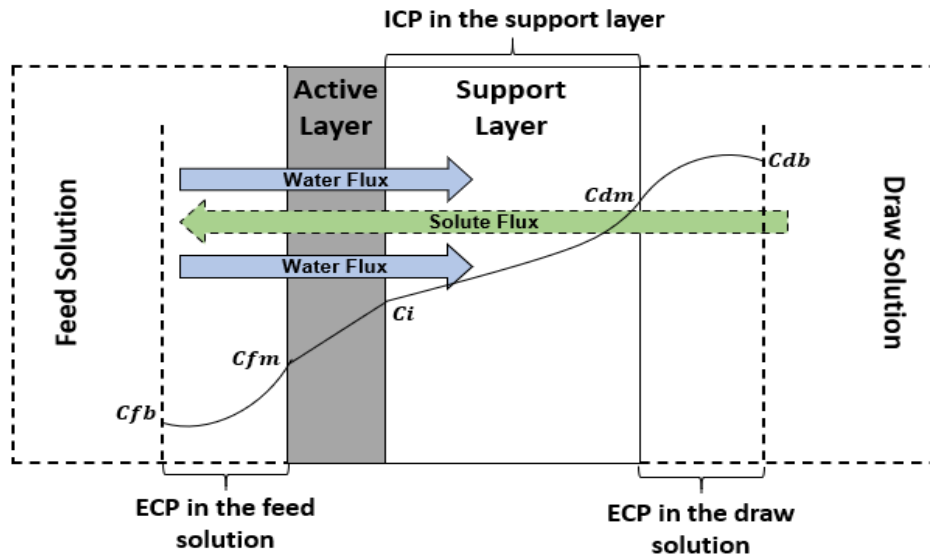
Figure 2.7: CECP and DECP (Adapted from Suh and Lee, 2013)

Only CECP can occur in pressure-driven processes compared to that of osmotically driven processes where both CECP and DECP can occur in accordance with the individual membrane orientation (Akther *et al.*, 2015). According to the results obtained by Sagiv *et al.* (2014) through the combination of hydrodynamics and mass transfer equations, it was proposed that the counter-current flow regime in FO improves the water flux and also reduces the cross-flow of solutes.

2.3.7.2 Internal concentration polarization (ICP)

It is apparent from the literature that the reduction in water flux is mainly due to the occurrence of ICP. ICP is essentially the development of a CP layer inside the support layer of the membrane which occurs as a result of the incapability of the solute to pierce the dense selective layer of the membrane with ease (Zhou *et al.*, 2014). Although FO has lower fouling tendencies compared to that of other membrane processes, FO faces major disadvantages in terms of maintaining a high level of transmembrane flux which has inhibited the commercialisation of FO technology. The development of phase inverted asymmetric membranes which are characterised by an active layer which is fabricated at the top of a permeable support layer such as polysulfone (PS) and polyethersulfone (PES) has transformed the membrane separation sector. It is, however, important to consider that according to initial studies, ICP is said to reduce the water flux by over 80% (Sagiv *et al.*, 2014).

There exist two types of ICP, namely, concentrative ICP (CICP) and dilutive ICP (DICP). The development of the individual ICP depends on the orientation of the asymmetric membranes. The CICP occurs when the saline FS is characterised by low water flux (Wei *et al.*, 2011). CICP can be observed while operating in PRO mode where the feed is against the permeable

support layer of the membrane. In PRO mode, the penetration of the solute across the active layer causes the solution to concentrate which results in the formation of an immobile region within the permeable support layer where the flow solute rises mainly because of hindered diffusion; thereby causing a reduction in the effective osmotic driving force (Tow and McGovern, 2015).

DICP can be observed when the DS is diluted due to the permeation of water within the membrane support layer. As a result of the dilution of the DS, the OP reduces thereby causing a decline in the water flux. DICP plays a pivotal role in limiting the progress of FO membranes as the membrane has to be characterised by low ICP levels as well as being impermeable to salt leakage (Al Mazrooei, 2013).

Figure 2.8 shows the effect of both DICP and CICP. The water concentration and salt solution profiles are depicted by the dotted and solid lines respectively. In Figure 2.8 (a) the FS is against the active layer (FO mode) in comparison to Figure 2.8 (b) where the FS is against the support layer (PRO mode). C_5 and C_1 represent the bulk concentrations of the FS and DS of the respective feed and draw sides. C_4 and C_2 represent the concentrations of the FS and DS at the boundary layer of the respective feed and draw sides. C'_3 and C_3 represent the concentrations of the FS and DS at the support and active layer intersection when the salt solution and water were used as a source of feed. The lines of the boundary near the active layer and the support layer are represented by the vertical dotted lines (Akther *et al.*, 2015).
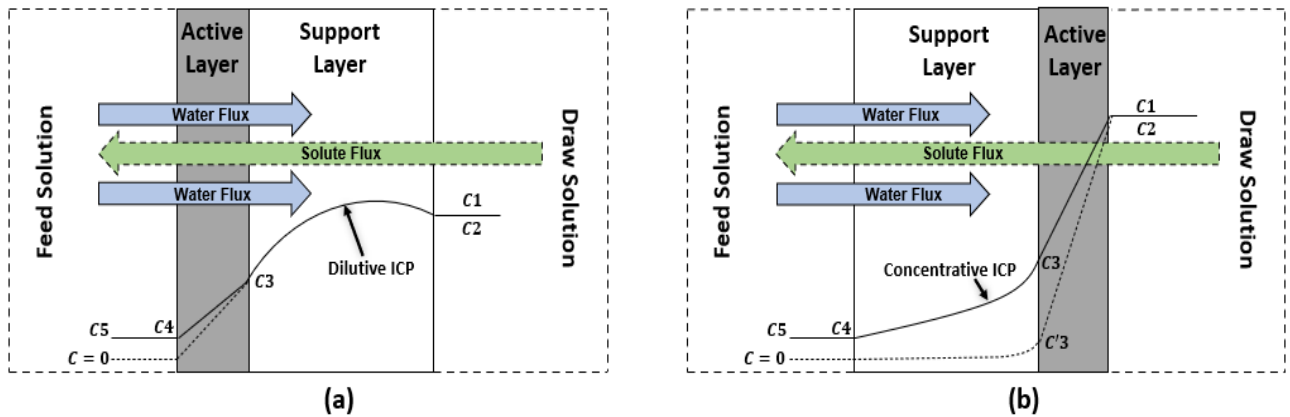
Figure 2.8: (a) represents a system in FO mode and hence describes DICP. Whereas, (b) represents a system in PRO mode hence describes CICP (Adapted from Akther et al., 2015)

Although there are a variety of FO membranes found in various configurations, each configuration has its advantages and disadvantages. The FO membranes are different from that of the conventional membranes in that the FO membranes are characterised by four flow connections (feed-in, concentrated feed-out, draw in and dilute draw out) (Nicoll, 2013).

2.3.8 Factors affecting the performance of FO and the implications thereof

The driving force in the FO process is the OP gradient and as such no hydraulic pressure is required; thereby the energy requirement of the system is reduced in turn lowering the susceptibility to membrane fouling compared to that of the traditional pressure-driven membrane processes such as RO. Additionally, in FO no chemicals are needed for the removal of fouling because the fouling is removed by physical cleaning, hence lowering costs. Due to the physical cleaning, FO exhibits higher water recovery and higher removal of an extensive range of ion contaminants is also achievable (Achilli *et al.*, 2009; Zhang *et al.*, 2010). There are numerous challenges faced by FO which limits its application in large scale processes, this is despite the fact that the FO process possesses many favourable characteristics (Martinetti *et al.*, 2009).

2.3.8.1 Influence of membrane properties on the FO performance

For the FO process, any selectively permeable membrane material can be used. However, the efficiency of the FO process is hindered greatly by the properties of the membrane (Cath *et al.*, 2006; Lay *et al.*, 2012). According to Phuntsho *et al.* (2013), the modification of the structural properties of the membrane support layer can considerably improve the extent of water flux. The use of high performing membranes will have a significant impact on the capital as well as the operational costs of the desalination plant (Phuntsho *et al.*, 2013).

2.3.8.2 Influence of draw solution (DS) properties on the FO performance

Phuntsho *et al.* (2013), suggested that the type of DS has a bigger impact on the FO process compared to that of the OP of the DS. Although an adequate OP of the DS is desirable for the FO process, the impact of the OP of the DS is less significant at higher OPs. The selection of an optimum initial OP is crucial to reduce the required pumping energy for the FO process because pumping energy is affected by the fluid density and the viscosity of the DS (Phuntsho *et al.*, 2013).

2.3.8.3 Influence of feed solution (FS) properties on the FO performance

The concentration of the total dissolved solids (TDS) in the FS, can influence the extent of the OP gradient or the driving force in the FO process (McCutcheon *et al.*, 2006). Based on the observations of Phuntsho *et al.* (2013), the concentration of the TDS in the FS can hinder the performance of the FO process to a certain extent. However, the impact of the concentration of TDS in the FS is somewhat negligible for FS TDS concentration which is greater than 20,000 mg/L signifying the promising potential of the use of FO with feed water characterised by high TDS concentrations (Phuntsho *et al.*, 2013).

Studies undertaken by Phuntsho *et al.* (2013), proposed that water flux reduces at higher feed TDS. It was also observed that the reverse solute flux (J_s) and specific reverse solute flux (SRSF) reduces as at higher feed TDS. The studies conducted by Phuntsho *et al.* (2013) are of great significance as it can assist in the reduction of the loss of draw solutes and replenishment costs when making use of high TDS feed like seawater.

2.3.8.4 Influence of reverse solute flux on FO process

It is highly imperative that we consider the extent of the draw solute's reverse flux as it might negatively hinder the FO process (Hancock and Cath, 2009). Lee *et al.* (2010) and Lay *et al.* (2010) demonstrated that the extent of the draw solute's reverse flux can increase membrane fouling by amplifying the effect of the cake enhanced osmotic pressure (CEOP). Hancock and Cath (2009), suggested that FO membrane selection is impacted by the specific reverse solute flux (SRSF) or the ratio of the reverse flux of the draw solute to the forward flux of water. A higher ratio results in a lower FO efficiency and thus reduces membrane selectivity (Hancock and Cath, 2009). Besides salt rejection and permeate flux, SRSF is considered to be the third evaluation parameter for FO performance. Reverse solute diffusion is one of the major limiting factors which is governed by factors like membrane design (Tang and Ng, 2008), membrane orientation (Zhao *et al.*, 2012) as well as the concentration and nature of the DS and FS (DS and FS temperature) (Wong *et al.*, 2012).

Akther *et al.* (2015) suggested that one of the major challenges in FO is reverse solute diffusion and as such, it should be taken into consideration for evaluation. The extent of reverse solute diffusion should be reduced in the course of the future development of draw solutes and FO membranes. Tables 2.4, 2.5 and 2.6 gives a general overview of reported fluxes and testing conditions in accordance with membrane orientation. The reported fluxes are tabulated to demonstrate the dependence of FO performance on draw agents and their applied operating conditions.

Table 2.4: Reported water fluxes and testing conditions in FO mode

Mode	Draw Solution (DS)	Feed solution (FS)	Operating conditions	J_w (L/m².h)	References
FO	1M Sodium Chloride	Deionized water	➢ Standard Protocol: TFC membrane ➢ Cross flowrate: 0.25 m/s ➢ Draw solution: 1 M NaCl ➢ Temperature: 20 ℃	50	(Cath *et al.*, 2013)
FO	1M Hydroacid complex {Na₄[Co (C₆H₄O₇)₂] 2H₂O (Na–Co–CA)}	2000 ppm heavy metal solution	➢ Cross flowrate: 0.2 L/min ➢ Draw solution concentration: 1 M ➢ Feed: 2000 ppm heavy metal solution ➢ Temperature: 23 – 60 ℃	11-16	(Cui *et al.*, 2014)
FO	Polyelectrolytes (polyacrylic acid sodium salts-PAA-NA)	Deionized water	➢ Cross flowrate: 6.4 cm/s ➢ PAA-NA molecular weight: 1800 Dalton ➢ Draw solution concentration: 0.08 mol/L (70 atm) ➢ Osmotic pressure difference: 20 atm ➢ Temperature: 25 ± 0.5 ℃	7	(Ge *et al.*, 2012)
FO	Trimethylamine–carbon dioxide	Deionized water	➢ Cross flow: 17.1 cm/s ➢ Draw solution concentration: 1 M TMA–CO₂ ➢ Draw osmotic pressure: 48.8 atm ➢ Temperature: 25 ± 0.5 ℃	14.5	(Boo *et al.*, 2015)
FO	Electro-responsive polymer hydrogels	2000 ppm NaCl	➢ Cross flowrate: 22.22 cm/s ➢ Draw hydrogel: 0.6 g ➢ Applied voltage: 6–9 V ➢ Feed: Deionized water	1.7	(Zhang *et al.*, 2014)
FO	Polyelectrolytes (polyacrylamide)	Dyeing wastewater (0.05 g/L dye)	➢ Cross flowrate: 10 cm/s ➢ Draw agent: 20–40 g/L ➢ Draw osmotic pressure: 366–824 mOsm/kg H₂O ➢ Temperature: 35 ± 0.5 ➢ pH: 6.37	3-5	(Zhao *et al.*, 2015)

Table 2.5: Reported water fluxes and testing conditions in PRO mode

Mode	Draw solution (DS)	Feed solution (FS)	Operating conditions	Jw (L/m².h)	References
PRO	Sodium Chloride	Deionized water	➢ Standard Protocol: TFC membrane ➢ Cross flowrate: 0.25 m/s ➢ Draw solution concentration: 1 M NaCl ➢ Temperature: 20 ℃	30	(Cath *et al.*, 2013)
PRO	Ammonium bicarbonate	Deionized water	➢ Cross flowrate: 30 cm/s ➢ Osmotic pressure difference: 236.2 atm ➢ Temperature: 50 ℃	30	(McCutcheon *et al.*, 2006)
PRO	Magnetic nanoparticles (polyacrylic acid)	Deionized water	➢ Cross flowrate: 6.4 cm/s ➢ Draw solution concentration: 0.15 mol/L ➢ Temperature: 22 ± 0.5 ℃	7.7-10	(Ling *et al.*, 2010)
PRO	Polymer hydrogels-poly (sodium acrylate)	2000 ppm NaCl	➢ Draw agent amount: 1 g ➢ Hydrogel density: 1 g/cm³ ➢ Draw agent size: 100 to 200 lm	1.06-0.49	(Li *et al.*, 2013)
PRO	Hydrophillic nanoparticles	Deionized water	➢ Cross flowrate: 6.4 cm/s ➢ Draw solution concentration: 0.08 mol/L (70 atm) ➢ Temperature: 22 ± 0.5 ℃	18	(Ling and Chung, 2011)
PRO	Polyelectrolytes (polyacrylic acid sodium salts-PAA-NA)	Deionized water	➢ Cross flowrate: 6.4 cm/s ➢ PAA-NA molecular weight: 1800 Dalton ➢ Draw solution concentration: 0.08 mol/L (70 atm) Osmotic pressure difference: 20 atm ➢ Temperature: 25 ± 0.5 ℃	12	(Ge *et al.*, 2012)
PRO	Polymer hydrogels	2000 ppm NaCl	N/A	0.24	(Cai *et al.*, 2013)
PRO	Trimethylamine–carbon dioxide	Deionized water	➢ Cross flow: 17.1 cm/s ➢ Draw solution concentration: 1 M TMA–CO₂ ➢ Draw osmotic pressure: 48.8 atm ➢ Temperature: 25 ± 0.5 ℃	33.4	(Boo *et al.*, 2015)
PRO	Polyelectrolytes (polyacrylamide)	Dyeing wastewater (0.05 g/L dye)	➢ Cross flowrate: 10 cm/s; ➢ Draw agent: 20 - 40 g/L ➢ Draw osmotic pressure: 366–824 mOsm/kg H₂O ➢ Temperature: 35 ± 0.5 ➢ pH: 6.37	5-8	(Zhao *et al.*, 2015)

Table 2.6: Water flux (J_w) and reverse solute flux (J_s) based on membrane orientation

Draw solution: NaCl (M)	FO mode		PRO mode		Operating conditions	References
	J_w (L/m².h)	J_s(g/m².h)	J_w (L/m².h)	J_s(g/m².h)		
0.25	1.34	0.32	2.11	0.46	**Draw solution**:0.25–2.0 M NaCl at the lumen side **Feed**: DI water at the lumen shell side **Membrane**: hollow fibre **Temperature**: 25 ℃	(Su *et al.*, 2013)
0.50	2.9	0.56	4.41	0.86		
1.00	4.15	0.85	7.08	1.38		
1.50	7.48	1.29	9.92	1.98		
2.00	8.43	1.44	12.65	2.43		

2.3.8.5 Influence of fouling on FO performance

Fouling is the deposition of retained matter (i.e. particles, colloids, macromolecules, salts, etc.) which occurs on the surface of the membrane or within the pores. Fouling can be categorised into four groups; organic fouling, colloidal fouling, inorganic fouling (i.e. scaling) and biofouling (Amy, 2008). The interface between the foulants and membrane surface causes a reduction in the membrane water flux which can either be temporary or permanent. Furthermore, the foulants can also be responsible for the chemical degradation of the membrane material (Rana and Matsuura, 2010).

Fouling is considered to be a problem that occurs in most liquid membrane methods and therefore it impacts the operation with respect to the economics. Therefore, most research is focused on reducing the extent of fouling in pressure-driven membrane processes. The problem can be resolved by regulating the operating conditions, cleaning or by modifying the membrane. Membrane fouling properties can also be mitigated by employing strategies such as surface modification and material selectivity (Alsvik and Hägg, 2013).

Figure 2.9 illustrates fouling in osmotically driven membrane processes in accordance with the respective membrane orientation (Alsvik and Hägg, 2013). The deposition of foulants occurs on different membrane surfaces, depending on the orientation of the membrane. In the FO mode, the foulant deposition occurs on the relatively smooth active layer compared to that of the PRO mode where the foulant deposition takes place on the rough support layer side or in some cases inside the support layer (Seidel and Elimelech, 2002).
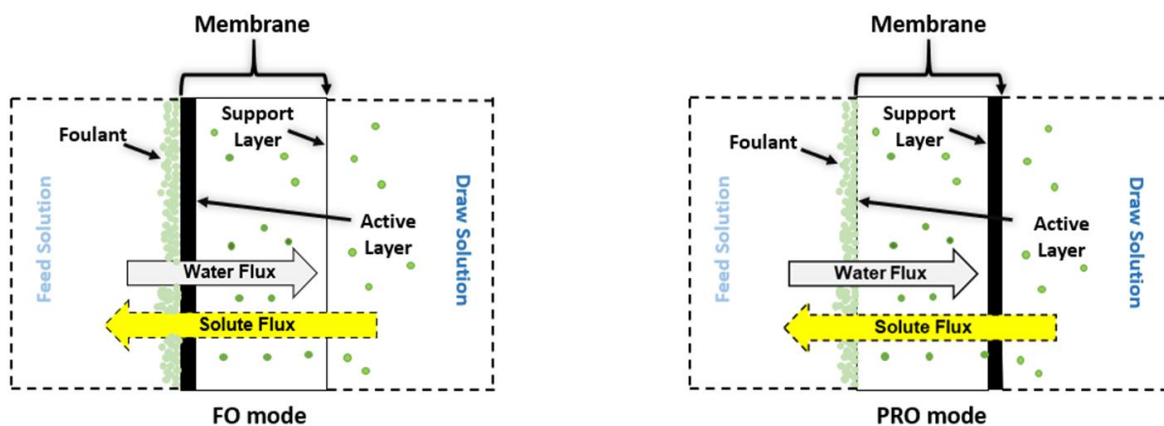
Figure 2.9: Illustration of the fouling mechanisms in osmotically driven membrane processes (Adapted from Seidel & Elimelech, 2002)

2.4 Applications of FO

Recent interest in the use of FO can be attributed to two major advantages over current membrane technologies: 1.) FO utilises lower energy than current membrane technologies because of the nature of the driving force used (i.e. osmotic as opposed to the hydraulic); 2.) FO membranes have lower fouling propensity than current membrane technologies because the flow channels in FO modules are not pressurised (Mi and Elimelech, 2008; Tang *et al*., 2010; Lee *et al*., 2010), resulting in FO to be considered for further commercial and large-scale utilisation, thus explaining the sudden interest and rapid development by researchers globally (Hsiang, 2011).

FO has been studied in a variety of applications such as wastewater treatment, seawater/brackish water desalination, food processing as well as power generation. All the applications can be categorised under three general areas: life science, water, and energy as illustrated in Figure 2.10. The illustrations portray all types of applications with a focus on current applications (Zhao *et al*., 2012). Furthermore, Table 2.7 summarises the benefits and challenges for some applications of FO.
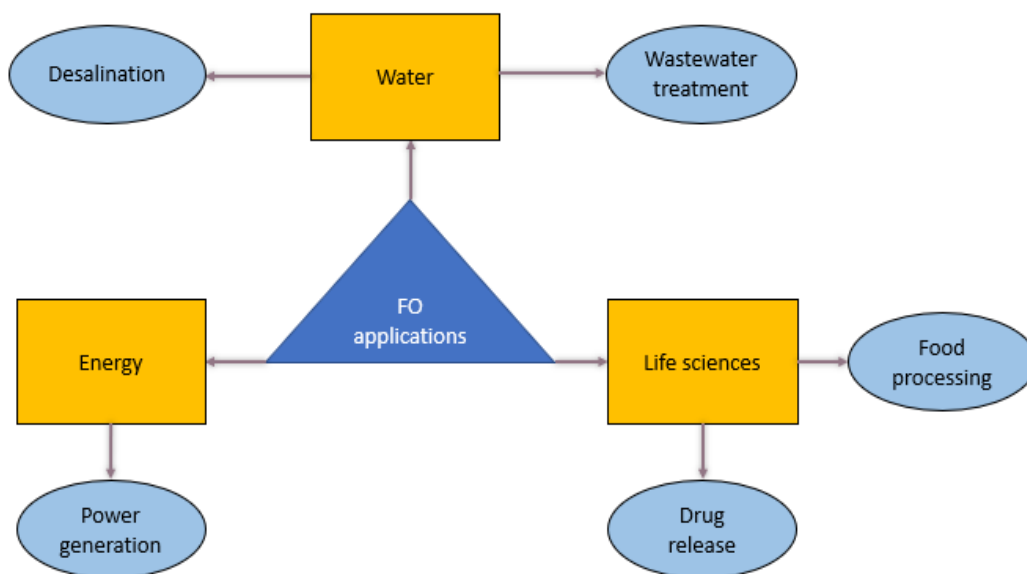
Figure 2.10: Applications of FO in the fields of water, energy and life science (Adapted from Zhao *et al*., 2012)

Table 2.7: Benefits and challenges of different applications of FO (Chaoui *et al.*, 2019)

Applications of FO	Benefits	Challenges
Desalination	Low energy consumption for the transport of water across the semi-permeable membrane	Ineffective membranes; lack of cost-effective draw solutes
Direct fertigation	Fertilisers are natural draw solutes; a diluted DS is useful for irrigation	Limited application sites
Osmotic power generation	Seawater is a natural draw solute	Pre-treatments of seawater and river water; fouling due to the high pressure in the seawater compartment
Osmotic membrane bioreactor	Low fouling and low energy consumption	Need to find low cost and easy recyclable draw solutes

2.5 Energy consumption in FO systems

FO is globally recognised as an energy-efficient process and or an energy-efficient pre-treatment procedure for a consequent desalination process such as RO (Zou *et al.*, 2016). The consumption of energy in the FO process occurs as a result of functions such as pre-treatment of the FS and DS, reconcentration of the DS, fouling control, FS post-treatment as well as the recirculation pump(s). The process of physical backwashing can be employed to accomplish approximately 90% recovery in terms of performance from fouling with low energy input. Studies conducted by Zou *et al.* (2016) found that 71% to 98% of the total energy that is quantified as the specific energy consumption (SEC - kWh per m^3 reclaimed water) is a prerequisite for the reconcentration process of the solute. A study conducted on a hybrid FO-RO system projected a SEC of 25 kWh.m^{-3}, 76% (19 kWh.m^{-3}) of which had been consumed by the solute reconcentration process (i.e. RO) (Shaffer *et al.*, 2015; Zou *et al.*, 2016).

McGinnis and Elimelech, (2007) suggested that desalination processes use between 1.6 to 3.02 kWh.m^{-3} of electrical power. According to studies done by Cath *et al*, (2005), the elimination of the energy-intensive RO process was made possible through the use of a $NH_3 - CO_2$ DS which was thermally reconcentrated through the use of waste heat. As a result of this technique, the SEC for the entire system (0.84 kWh.m^{-3}) was significantly reduced of which 71% (0.60 kWh.m^{-3}) was consumed by the reconcentration process and 29% (0.24 kWh.m^{-3}) was used by the recirculation pumps. Many studies (McGinnis and Elimelech, 2007; Zou *et al.*, 2016) thereafter used a benchmark value of 0.25 kWh.m^{-3} when adhering to energy-related issues in FO systems with the exclusion of solute reconcentration. Moreover, it was found that the recirculation energy accounted for approximately 25% to 30% of the total SEC demand for systems that are dependent on reconcentration. The SEC percentage is of significance; however, it is appropriate as most bench-scale FO systems are operated using flowrates which range between 400 mL.min^{-1} to 1000 mL.min^{-1} (1.0-cm pipe). It is quite apparent that the recirculation costs will essentially be one of the decisive factors in terms of FO competitiveness as FO systems are tested in greater scales (Cath *et al.*, 2005; McGinnis and Elimelech, 2007; Zou *et al.*, 2016). Table 2.8 tabulates the energy consumption of a variety of FO processes found in the literature.

Table 2.8: Energy consumption of FO processes

SEC (kWh.m^{-3})	Feed solution (FS)	Draw solution (DS)	Operating conditions	Reference
0.09 ± 0.02	Deionised water (DI)	Fertiliser DS	DS concentration:25% Operation H: 72h Temperature: ~ 20 ℃ Draw recirculation flowrate: 25mL.m^{-1}(2.1cm.s^{-1})	(Xiang *et al.*, 2017)
0.37 ± 0.08	Deionised water (DI)	Fertiliser DS	DS concentration:50% Operating h: 72h Temperature: ~ 20 ℃ Draw recirculation flowrate: 50mL.m^{-1}(4.2cm.s^{-1})	(Xiang *et al.*, 2017)
1.30 ± 0.28	Deionised water (DI)	Fertiliser DS	DS concentration:100% Operating h: 72h Temperature: ~ 20 ℃ Draw recirculation flowrate: 100mL.m^{-1}(8.5cm.s^{-1})	(Xiang *et al.*, 2017)
3.58	NaCl	aqueous NaCl	Feed TDS: 35000 ppm System recovery: 50% Osmotic pressure difference: 19.4 bar Feed temperature: 25 ℃	(McGovern and Lienhard, 2014)
1.6	Synthetic wastewater	Brine	Feed recovery: 50% Temperature: 20 ℃ High-pressure pump efficiency: 80% Inlet feed pressure: 4 bar	(Kim *et al.*, 2015)

2.5.1 Recirculation pumps: The neglected aspect

The recirculation pumps are a vital part of FO systems as they are responsible for the transfer of solutions to the membrane and deliver hydraulic shear forces to reduce the ECP as well as fouling. Despite the significance of the recirculation pumps, very few studies account for the energy consumption of the recirculation pumps (Zou *et al.*, 2016). After conducting numerous experiments, Zou and He (2016) reported that with a flowrate of 10 mL.min^{-1} (0.5 cm tubing), a FO system can reclaim 155 mL of water within 24 h rendering an SEC of approximately 0.02 kWh.m^{-3} to 0.01 kWh.m^{-3}. According to Zou and He (2016), the estimated SEC of 11.93 kWh.m^{-3} to 3.08 kWh.m^{-3} for a flowrate of 250 mL min^{-1} was greater. Furthermore, Zou and He (2016), also stated that during the proceedings of their experiments, the development of mass transfer was limited by higher flowrates (water recovery of 182 at 250 mL.min^{-1}) as a result of the negligible ECP at relatively low water fluxes. For experimental purposes, Zou and He (2016) estimated that a minimum SEC of 1.86 ± 0.47 kWh.m^{-3} and 11.93 ± 3.08 kWh.m^{-3} would be mandatory for their FO system with accordance to velocities of 8.50 cm.s^{-1} and 21.25 cm.s^{-1} which are typical values reported in the FO studies.

2.6 Osmotic Pressure (OP)

The OP is described as the pressure that is applied by the movement of water across a semi-permeable membrane which is separating two solutions with different solute concentrations. In essence, it can be defined as the pressure difference required to stop the flow of solvent across the semi-permeable membrane. The OP of a solution is proportional to the molar concentration of the solute particles present in the solution (Kutchai, 2003).

2.6.1 Methods to determine OP

2.6.1.1 Van't Hoffs equation

Phuntsho *et al.* (2012), states that the Van't Hoff's equation (i.e. Equation 2.2) is the most common osmotic pressure theory which applies to ideal diluted mixtures that consist of ions which behave drastically from one another:

$$\pi = i \left(\frac{n}{v} \right) RT = iC_iRT \qquad \text{(Equation 2.2)}$$

Where R is the universal gas constant (R = 8.314 $m^3.Pa.mol^{-1}.K^{-1}$), T is the absolute temperature (K), C_i refers to the molarity of a solution of a non-dissociating solute (C_i = $mol.L^{-1}$) and i is the Van't Hoff's index which accounts for solute dissociation (Wilson and Stewart 2013).

2.6.1.2 Viral equation

Phuntsho *et al.* (2011) acknowledged that the electrostatic interactions between the ions increases and becomes a non-ideal solution as a result of higher ionic concentrations. This phenomenon causes a reduction in the activity coefficient of each ion and also the OP of the solution.

Therefore, the OP for common solutions can be specified with regards to the concentration dependence osmotic equation referred to as the Viral equation (i.e. Equation 2.3):

$$\frac{\pi}{c} = RT \left[\frac{1}{M_w} + B\ (C_i) + C(C_i)^2 + D(D_i)^3 + \dots N(N_i)^n \right] \qquad \text{(Equation 2.3)}$$

Where C_i represents concentration ($g.L^{-1}$) and B, C, D, are the osmotic viral coefficients.

2.6.1.3 Osmometer

An osmometer is an instrument used to measure osmolality in $osmoles.kg^{-1}$ of water in correspondence to the method of freezing point depression. The osmometer use is limited to solutions characterised by infinite dilutions and therefore are not suited for use at high concentrations (Phuntsho *et al.*, 2011).

The freezing point osmometer (Osmomat 3000) is responsible for the calculation of the overall osmolality of aqueous solutions. Osmometers require minute sample volumes, therefore, it can be utilised for extreme measuring tasks. The speediness of the osmometer permits serial measurements within a short period of time (Gonotech, 2014).

The determination of the total osmolality of aqueous solutions is accomplished via the comparative measurements of the freezing points of pure water and that of the solutions. The freezing point of water is 0 °C compared to that of a solution with a saline concentration of 1 Osmol/kg which is characterised by a freezing point of -1.858 °C (Gonotec, 2014). Figure 2.11 provides a graphical description of how the Osmomat 3000 measures the OP of solutions.

Ice Crystal   Lower Probe   Needle Injection   Crystallization
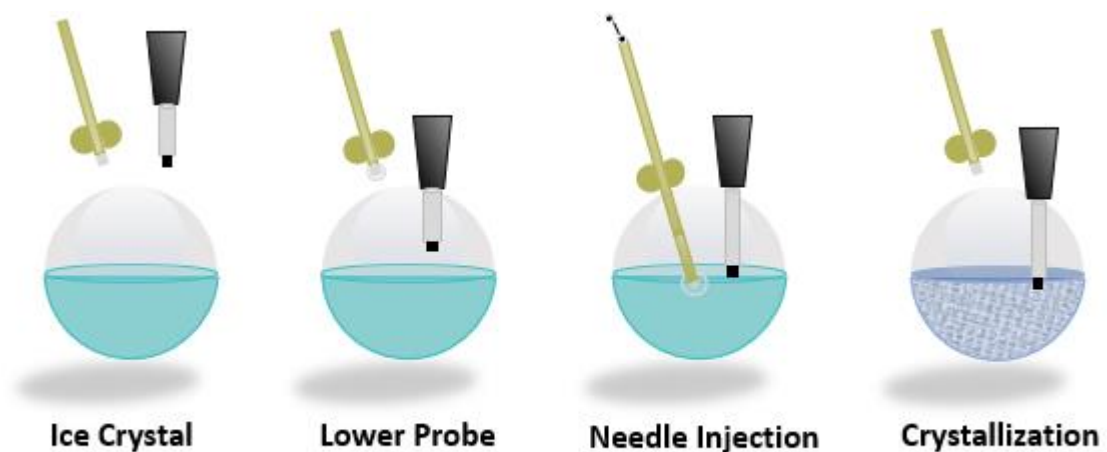
Figure 2.11: Step-by-step illustration of the mechanism behind the measurement of OP using the Osmomat 3000 (Adapted from Gonotech, 2014)

CHAPTER 3

CHAPTER 3: MATERIALS AND METHODS

3.1 Introduction

This chapter describes in detail the operating conditions and procedures of experiments conducted as well as the analytical methods used for the data produced from the experiments. In addition, this chapter further elaborates on the bench-scale FO system used to conduct the experiments.

3.2 Bench-scale FO system

3.2.1 FO setup

The bench-scale FO system used for this study shown in Figure 3.1 and 3.2 consisted of:

- Double-head variable speed peristaltic pump (Watson-Marlow, 323E/D, Dune Engineering, South Africa),
- FO membrane cell (Sterlitech Co., CF042D, USA),
- Membrane (Flat-sheet CTA, Fluid Technology Solutions Inc., USA),
- Digital electrical multimeter (ToptronicTBM250 series, Yebo Electronics, SA),
- Tubings (Masterflex Tygon E-Food (B-44-4X)),
- Digital multipurpose meter (Lovibond SensoDirect 150, Selectech (Pty) Ltd, SA),
- Electronic weighing scale (Labex WA606, Weighing Instrument Services (Pty) Ltd, SA) and
- 2 L beaker × 2 (store FS and DS).

Figure 3.1 represents a schematic diagram of the bench-scale FO system and Figure 3.2 presents a picture of the bench-scale FO system.
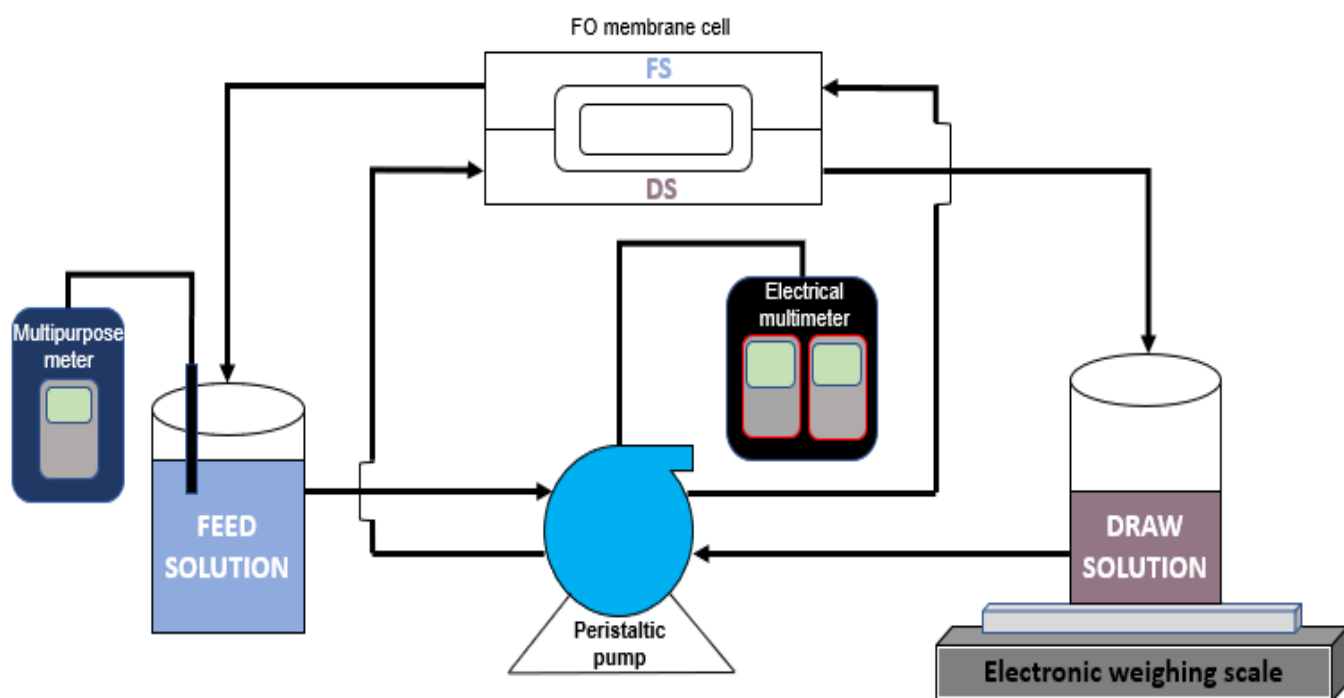
Figure 3.1: Process flow diagram of the laboratory bench-scale FO system
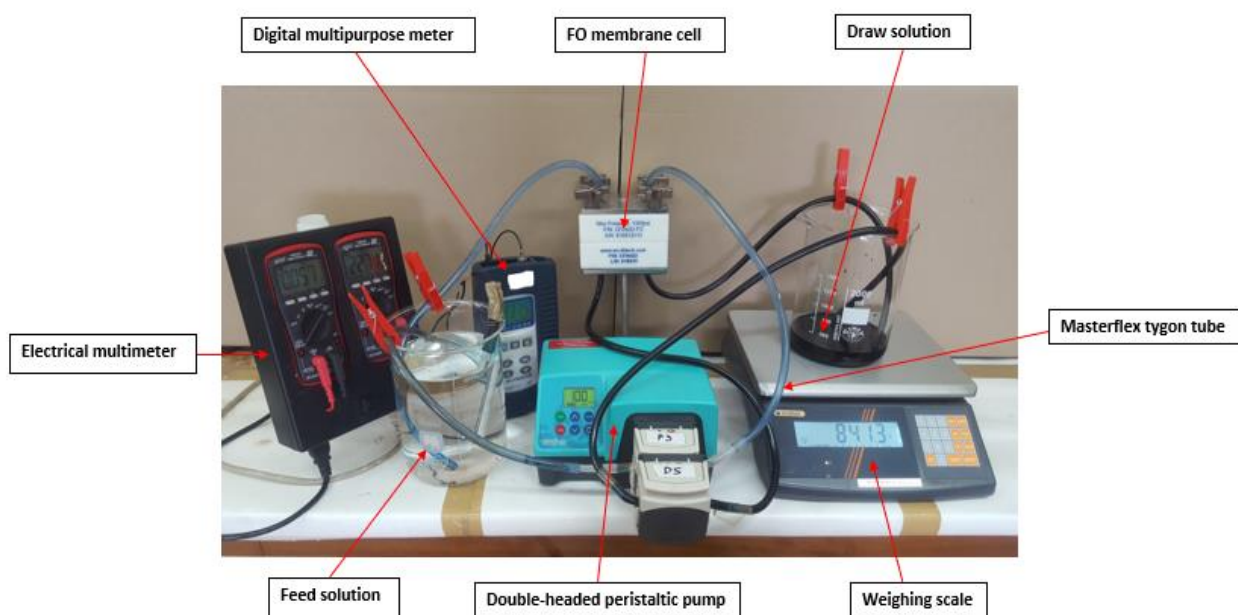
Figure 3.2: Picture of the laboratory bench-scale FO system taken by Mohammed Rahman in lab 4.4 at Cape Peninsula University of Technology, Cape Town, SA

The FO system (Sterilitech, USA) was operated in batch mode with the FS and DS in a counter-current flow regime. The FO operation in the counter-current mode is preferred since it provides an improvement in water flux and significantly lowers the extent of reverse solute flux relative to FO operation in the co-current mode (Sagiv *et al.*, 2014).

The FO membrane cell had outer dimensions of 0.13 x 0.10 x 0.08 m, a flow channel of 0.09 x 0.05 x 0.002 m and a total membrane area of 0.0042 m^2. The membrane cell was placed horizontally such that the FS was flowing into the top channel and the DS into the bottom channel of the membrane cell. This orientation was favoured mainly to allow the water flux to flow with gravity.

The FO set-up was a tubed model that was constructed using Masterflex Tygon tubing of 0.7 mm diameter and 0.2 mm wall thickness. The only energy required for this process was the energy for operating the double-head variable speed peristaltic pump (approximately 0.2 bar). The double-head variable speed peristaltic pump was used to transport the FS and DS in the FO system, with equal flowrates and pressures on both sides of the membrane, i.e. no hydraulic pressure gradient.

A digital custom-built multimeter was used to measure the extent of energy consumption for the duration of the experiments. The digital custom-built multimeter comprised of two identical multimeters. The one multimeter was set to alternating current (AC) mode and the other in AC voltage mode to account for the current drawn and the voltage supplied by the double-head variable speed peristaltic pump for the duration of the experiments.

Before commencing with the experimental studies, a flow curve between the pump revolutions per minute (RPM) and system flowrate was required to be established as the pump speed could only be regulated in RPM. The crossflow velocity across the system was determined by dividing the attained flowrates with the tube cross-sectional area of 0.00105 m^2. Table 3.1 tabulates the relationship between the pump RPM, flowrate and crossflow velocity.

Table 3.1: Relationship between pump RPM, flowrate and crossflow velocity

RPM	Flowrate (ml/min)	Crossflow velocity (cm/s)
50	200	3.2
100	400	6.3
125	500	7.8
150	600	9.5

The FS and DS were stored in sperate 2 L beakers for all experiments and maintained at ambient temperature ($\pm$ 25℃). A digital multipurpose meter was used to measure the physicochemical parameters such as pH, electrical conductivity (EC) and temperature of the FS and DS, respectively. The electronic weighing scale was used to measure the varying mass of the DS over time.

3.2.2 CTA membrane

The flat-sheet CTA membrane (Fluid Technology Solutions, USA) used for this study is one of the most commonly used commercially available FO membrane (Sunohara and Masuda, 2011). This FO membrane has a polyester mesh embedded between the cellulose material for mechanical support, as opposed to a thick support layer typically found in RO membranes. With a thickness of about 50 μm, it was purported to reduce the effect of internal concentration polarization owing to the thick porous support layer of the membrane (McCutcheon *et al.,* 2005). The membrane was selected mainly due to its availability and utilisation as reported by previous studies (Lambrechts, 2018; Augustine, 2017). Refer to Appendix C for details regarding the membrane preparation for each experiment.
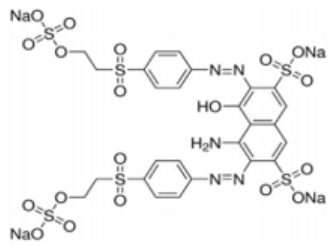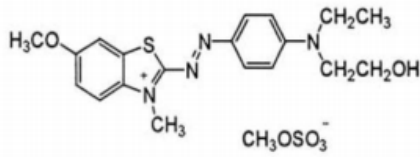
3.2.3 Feed solution (FS)

The FS utilised for baseline 1 and baseline 2 experiments was deionised (DI) water. The FS for the main experiment was a synthetic brackish water (SBW5) solution containing a salt content of 5000 mg/L (5 g/L) NaCl. SBW5 was selected due to its salinity and concentration that mimics the properties of brackish water which is available in the Western Cape (Refer to Appendix A).

3.2.4 Draw solution (DS): Dyeing solution

The DS used for the main experiment was a dyeing solution consisting of a mixture of dye and NaCl in a mass ratio of 1:10, respectively for Reactive Black 5 and Maxilon Blue GRL dye (refer to Appendix A) (Jingxi, 2017). From previous studies conducted by Sheldon *et al.* (2018), the Reactive Black 5 and Maxilon Blue GRL dye solutions at a concentration 0.02 mol/L generated a higher OP compared to other dyes and were therefore selected to be used as DS in this study. Table 3.2 illustrates the specifications of the dyes used in this study.

Table 3.2: Specifications of the dyes used

Dye	Mw (g/mol)	Chemical Formula	Chemical structure	Reference
Reactive Black 5	991	$C_{26}H_{21}N_5Na_4O_{19}S_6$		Han *et al.*, (2016)
Maxilon Blue GRL	482	$C_{20}H_{22}N_4O_6S_2$		Aljeboree *et al.*, (2014)

3.3 Experimental process

An entire experiment consisted of six phases. Each experiment was duplicated to attain results that are reliable and accurate: Each experiment was completed in approximately 2 days as shown in Table 3.3 illustrating the operating time of each phase of the experiment, respectively.

Table 3.3: Operating time for each of the experiments

Phase	Operating time
Phase 1: Control experiment 1 (Baseline 1) – (FS: DI; DS: Reactive Black 5 and Maxilon Blue GRL)	3 h
Phase 2: Main experiment (FS: SBW5 and DS: Reactive Black 5)	FO: 5 h (400 ml/min, 500 ml/min and 600 ml/min); PRO: 4 h (400 ml/min, 500 ml/min and 600 ml/min)
Phase 2: Main experiment (FS: SBW5 and DS: Maxilon Blue GRL)	FO: 143 h (400 ml/min); 147 h (500 ml/min); 171 h (600 ml/min)
Phase 3: Control Experiment 2 (Baseline 2) – (FS: DI; DS: Reactive Black 5 and Maxilon Blue GRL)	3 h
Phase 4: Membrane cleaning	1 h
Phase 5: Membrane integrity test	40 min
Phase 6: Membrane autopsy	12 h

3.3.1 Phase one: Control experiment 1 (Baseline 1)

Control experiments 1 and 2 were conducted before and after the Main experiment, respectively to be used as a basis of comparison to determine the extent of fouling and its impact on the energy consumption and system performance. The parameters such as pH, EC, temperature, OP, and DS weight were periodically recorded for the duration of the experiment. Parameters such as the water flux (J_w), reverse solute flux (J_s), recovery rate (R_e), as well as the specific energy consumption (SEC), was calculated as an indication of system performance.

The experiment was conducted in a counter-current flow regime with respect to the FS and DS flow in both membrane orientations. The membrane orientation was in FO mode when the

FS faces the active layer of the membrane, and the permeable support layer faces the DS. Furthermore, the membrane orientation is in PRO mode when the FS faces the porous support layer, and the DS meets the active layer of the membrane.

Experiments using Reactive Black 5 dye were performed in both FO and PRO modes, while experiments for Maxilon Blue GRL dye were operated in FO mode only as it was assumed that the change in orientation would have very little to no impact on the system performance and energy consumption of the FO system in question. Table 3.4 tabulates the operating conditions utilised for the Control experiment 1.

Table 3.4: Operating conditions for Control experiment 1

Mode	FS	DS	Operating conditions
FO and PRO	DI	Reactive black 5	➢ System flowrate: 200 ml/min (50 rpm) ➢ DS concentration: 1 M NaCl ➢ Volume: 2 L (FS); 0.2 L (DS) ➢ Duration: 3 h ➢ Flow regime: Counter current ➢ Temperature: Room temperature ($\pm\,25\,°C$)
FO	DI	Maxilon Blue GRL	➢ System flowrate: 200 ml/min (50 rpm) ➢ DS concentration: 1 M NaCl ➢ Volume: 2 L (FS); 0.2 L (DS) ➢ Duration: 3 h ➢ Flow regime: Counter current ➢ Temperature: Room temperature ($\pm\,25\,°C$)

3.3.2 Phase two: Main experiment

The Main experiment was conducted after the completion of the Control experiment. The main experiment was crucial in indicating the energy consumption and system performance in producing a diluted dyeing solution suitable for direct use with respect to the specifications stipulated in dyeing recipes obtained from textile industries. Parameters such as the J_w, J_s, R_e as well as the SEC of the system were calculated as an indication of system performance.

The experiment was conducted in a counter-current flow regime with respect to the FS and DS flow in both the membrane orientations (FO and PRO mode). Table 3.5 tabulates the operating conditions utilised for the Main experiment. The duration of the main experiment, as

well as the time required in reaching the respective target concentration, varied when using Maxilon Blue GRL as DS.

The target concentration of experiments using the basic dye (Maxilon Blue GRL) solution as DS was 0.004 M corresponding to an OP of 8853 kPa. The target concentration using the reactive (Reactive Black 5) dye solution as DS was 0.002 M corresponding to an OP of 8580 kPa. Table 3.5 presents the operating conditions utilised for the conduction of the Main experiment.

Table 3.5: Operating conditions for the main experiment

Mode	FS	DS	Operating conditions
FO and PRO	SBW5	Reactive Black 5	➢ System flowrate: 400 ml/min (100 rpm); 500 ml/min (125 rpm); 600 ml/min (150 rpm) ➢ Draw solution initial concentration: 0.02 M ➢ Feed solution initial concentration: 5 g/L ➢ Volume: 2 L (FS); 0.2 L (DS) ➢ Duration: 5 h (FO) and 4 h (PRO) ➢ Flow regime: Counter current ➢ Temperature: Room temperature ($\pm$ 25 ℃)
FO	SBW5	Maxilon Blue GRL	➢ System flowrate: 400 ml/min (100 rpm); 500 ml/min (1250 rpm); 600 ml/min (1500 rpm) ➢ Draw solution initial concentration: 0.02 M ➢ Feed solution initial concentration: 5 g/L ➢ Volume: 2 L (FS); 0.2 L (DS) ➢ Duration: 143 h (400 ml/min); 147 h (500 ml/min); 171 h (600 ml/min) ➢ Flow regime: Counter current ➢ Temperature: Room temperature ($\pm$ 25 ℃)

3.3.3 Phase three: Control experiment 2 (Baseline 2)

Control experiment 2 which proceeded after the Main experiment, was conducted to determine the extent of fouling and its impact on energy consumption and system performance. Parameters such as the J_w, J_s, R_e as well as the SEC of the system was determined for the duration of the experiment.

The experiment was conducted in a counter-current flow regime with respect to the FS and DS flow and for each membrane orientation. Table 3.6 tabulates the operating conditions utilised for the Control experiment 2.

Table 3.6: Operating conditions for control experiment 2

Mode	FS	DS	Operating conditions
FO and PRO	DI	Reactive black 5	➤ Cross flowrate: 200 ml/min (50 rpm) ➤ Draw solution concentration: 1M NaCl ➤ Volume: 2 L (FS); 0.5 L (DS) ➤ Duration: 3 h ➤ Flow regime: Counter current ➤ Temperature: Room temperature ($\pm$ 25℃)
FO	DI	Maxilon Blue GRL	➤ Cross flowrate: 200 ml/min (50 rpm) ➤ Draw solution concentration: 1M NaCl ➤ Volume: 2 L (FS); 0.5 L (DS) ➤ Duration: 3 h ➤ Flow regime: Counter current ➤ Temperature: Room temperature ($\pm$ 25℃)

3.3.4 Phase four: Membrane cleaning

The Membrane cleaning experiment was conducted to obtain an indication of the energy consumption of the cleaning process, prepare the membrane for the integrity of the membrane for reuse and to ensure that a clean membrane was used for the duplicate experiment.

The membrane was soaked in a 200 mL solution (10% wt. citric acid) for 40 min. After soaking the membrane for 40 min, the membrane was then placed in the membrane cell and rinsed for an additional 30 min as indicated in Table 3.7 which tabulates the operating conditions utilised for the membrane rinsing process with DI water. The current and voltage readings were recorded at 10 min intervals to consider the extent of the energy consumption of the system for the duration of the 30 min.

Table 3.7: Operating conditions for the rinsing process

Mode	FS	DS	Operating conditions
FO and PRO	DI	DI	➢ Flowrate: 600 ml/min (150 rpm) ➢ Volume: 2 L (FS); 0.5 L (DS) ➢ Duration: 30 min ➢ Temperature: Room temperature ($\pm25℃$)

3.3.5 Phase five: Membrane integrity

The membrane integrity experiment was conducted to obtain an indication of the extent of the damage on the membrane after the completion of an entire set of experiments. This phase was performed in FO mode. The FS comprised of a methyl violet dye ($C_{25}H_{30}ClN_3$) content of 1.5 mL. The methyl violet dye was used for the identification of damage on the surface of the membrane. The DS for this experiment was 2 M NaCl. The experiment was conducted until a minimum of 10 ml (approximately 10 g in weight) was gained by the DS. Refer to Appendix B for more details on the preparation of the FS and DS for the membrane integrity test.

After approximately 40 min, the membrane was removed from the FO membrane cell for inspection. An indication of membrane damage was a hint of purple colour stain on the surface of the membrane as opposed to an undamaged membrane that had no indication of any form of stain on the surface of the membrane. If the damage was observed, the membrane was discarded, and not used for the duplicate experiment.

The power consumption of the system was monitored by recording the voltage and current of the system at 10 min intervals. The weight was also monitored manually at 10 min intervals by recording the varying DS mass values reflected on the electronic weighing scale. Table 3.8 tabulates the operating conditions utilised for the Membrane integrity experiment.

Table 3.8: Operating conditions utilised for the conduction of the membrane integrity experiment

Mode	FS	DS	Operating conditions
FO and PRO	DI	DI	➢ Flowrate: 200 ml/min (50 rpm) ➢ Volume: 0.5 L (FS); 0.5 L (DS) ➢ Duration: 40 min ➢ Temperature: Room temperature ($\pm$ 25℃)

3.3.6 Phase six: Membrane autopsy

After all, experiments were conducted, the CTA FO membranes were preserved in DI water and stored in a sealed container in preparation to study the morphology of the membranes using the attenuated total reflection Fourier transform infrared spectroscopy (ATR-FTIR) technique. The ATR-FTIR study was conducted using the horizontal ATR (HATR) instrument (FT-IR, Nicolet 6700, Thermo Electron CO., USA). The ATR-FTIR spectra for each membrane sample were collected from wavenumbers between 650 and 4500 cm^{-1} at a resolution of 8 cm^{-1}. The resolution was at 8 wavenumbers (cm^{-1}) and a total of 64 scans was collected per sample. The major functional groups on the membrane surfaces after use were identified.

3.4 Measurements and analytical methods

3.4.1 Osmotic pressure (OP)

The OP of the FS and DS was determined by utilising a cryoscopic osmometer (OSMOMAT 3000, Gonotec, Germany). An osmometer is an instrument used to measure osmolality in osmoles.kg^{-1} of water in correspondence to the method of freezing point depression (refer to Chapter 2, section 2.6 for more details). The OP obtained from the osmometer was recorded in osmoles.kg^{-1} which was then converted to kPa using Equation 3.1. The relationship between concentration and pressure is as follows (Burton, 2008) (See Appendix E for sample calculations).

$$1\frac{mOsmol}{kg}\ water =\ 19.32\ mmHg; 1\ mmHg = 0.13\ kPa \qquad \text{(Equation 3.1)}$$

3.4.2 Determination of water flux (J_w)

Water flux (Jw) was obtained by taking into consideration the weight change of the DS as a function of time. Water flux was calculated using Equation 3.2 (Han *et al.,* 2016):

$$J_w = \frac{\Delta V}{A_m.\Delta t} \qquad \text{(Equation 3.2)}$$

Where A_m (m^2) is the effective membrane area, ΔV (m^3) is the volume change in the DS in time interval Δt (s) (Han *et al.,* 2016).

3.4.3 Determination of reverse solute flux (J_s)

Reverse solute flux (Js) was determined by using Equation 3.3 (Han *et al.,* 2016):

$$J_S = \frac{\Delta(C_t V_t)}{A_m . \Delta t}$$

(Equation 3.3)

Where, C_t is the reverse solute concentration and V_t is the feed volume which is measured at the end of the FO bench-scale analyses (Han *et al.,* 2016).

To determine the C_t, a standard curve of conductivity vs concentration was used. A standard curve is a general method for determining the concentration of a substance in an unknown sample by comparing the unknown to a set of standard samples of known concentration. Figures 3.3 and 3.4 are the standard curves generated for Reactive Black 5 and Maxilon Blue GRL, respectively.
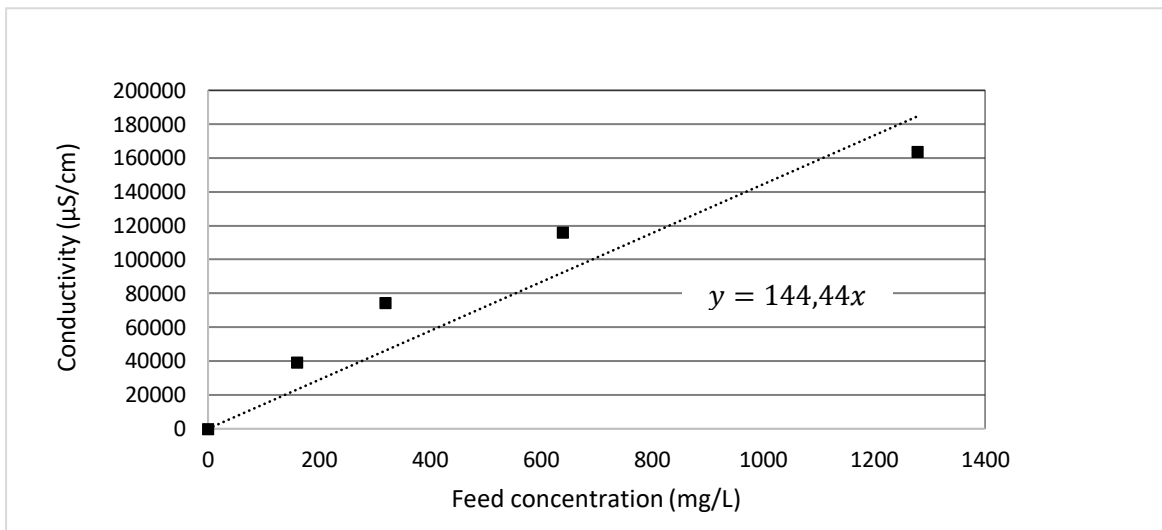
Figure 3.3: Standard curve of Reactive Black 5 dye
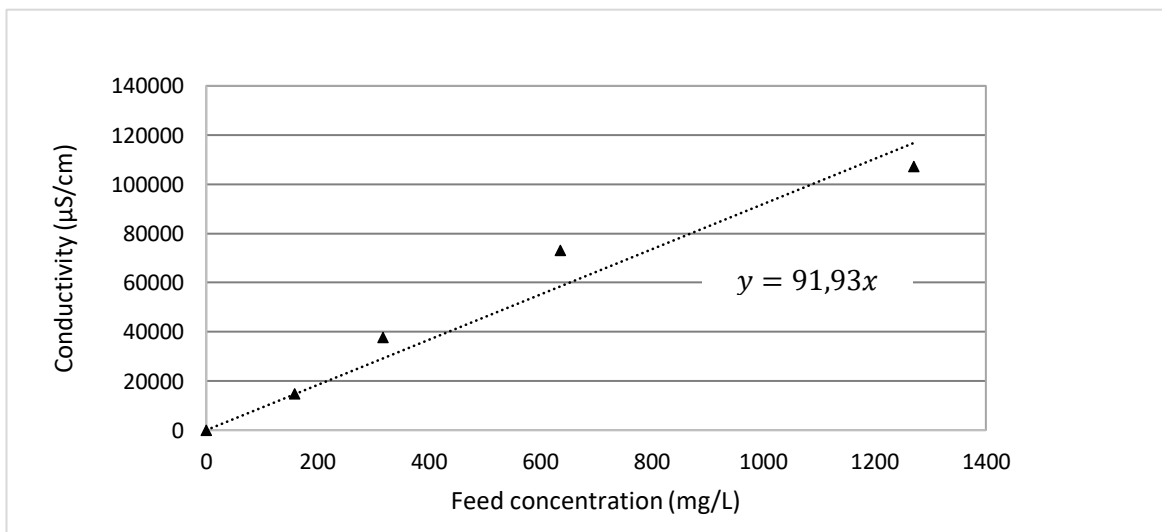
Figure 3.4: Standard curve of Maxilon Blue GRL dye

3.4.4 Determination of water recovery

The feed water recovery (R_e) was calculated using Equation 3.4 (Han *et al.*, 2016):

$$R_e = \frac{\Delta V}{V_{f,i}} \times 100 \qquad \text{(Equation 3.4)}$$

Where initial volume of the feed solution (FS) in litres is represented by V_{fi} and ΔV is change in volume of the FS (L) (Han *et al.*, 2016).

3.4.5 Determination of the specific energy consumption (SEC)

The SEC was determined by making use of the data gathered from the digital multimeter (TBM250 series). The data which entails values in terms of amperes and voltage was then used to calculate the energy in terms of kW/h after which the SEC was then determined for the respective experiments.

The specific energy consumption (SEC in kWh.m^{-3}) for unit recovered water was determined using Equation 3.5 and 3.6 (Xiang *et al.,* 2017):

$$SEC = \frac{P_{pump}}{Water\ flux\ volumetrcic\ flowrate} \qquad \text{(Equation 3.5)}$$

$$Water\ flux\ volumetric\ flow\ rate = \frac{Vf_{DS} - Vi_{DS}}{\rho_{water} \times time\ interval} \qquad \text{(Equation 3.6)}$$

Where, P_{pump} is the consumed power of the recirculation pump in kW and water flux volumetric flowrate in m^3.h^{-1}, respectively. The Vf_{DS} and Vi_{DS} is the final and initial volume of DS recovered per time interval in L.

<u>NB:</u> It was considered that the solution crossing the membrane from the FS to the DS mimics the properties of water, therefore it was assumed that the ρ_{water} was 1000 g/L

3.4.6 Sampling methods

For the conductivity and pH measurements, the conductivity and pH probes of the digital multipurpose meter (Lovibond SensoDirect 150) were directly immersed into the FS and DS to obtain the respective conductivity and pH measurements.

3.4.7 Microscopic observations

The CTA FO membranes were preserved (in DI water) in a sealed container in preparation to study the morphology of the membranes using the attenuated total reflection Fourier transform infrared spectroscopy (ATR-FTIR) technique. An ATR accessory operates by measuring the changes that occur in an internally reflected (IR) beam when the beam comes into contact with a sample. An IR beam is directed onto an optically dense crystal with a high refractive index at a certain angle. This internal reflectance creates an evanescent wave that extends beyond the surface of the crystal into the sample held in contact with the crystal (PerkinElmer precisely, 2005).

In regions of the IR spectrum where the sample absorbs energy, the evanescent wave will be attenuated. The attenuated beam returns to the crystal, then exits the opposite end of the crystal and is directed to the detector in the IR spectrometer. The detector records the attenuated IR beam as an interferogram signal, which can then be used to generate an IR spectrum. Figure 3.5 provides a visual depiction of the beam paths during the ATR-FTIR analysis (PerkinElmer precisely, 2005).
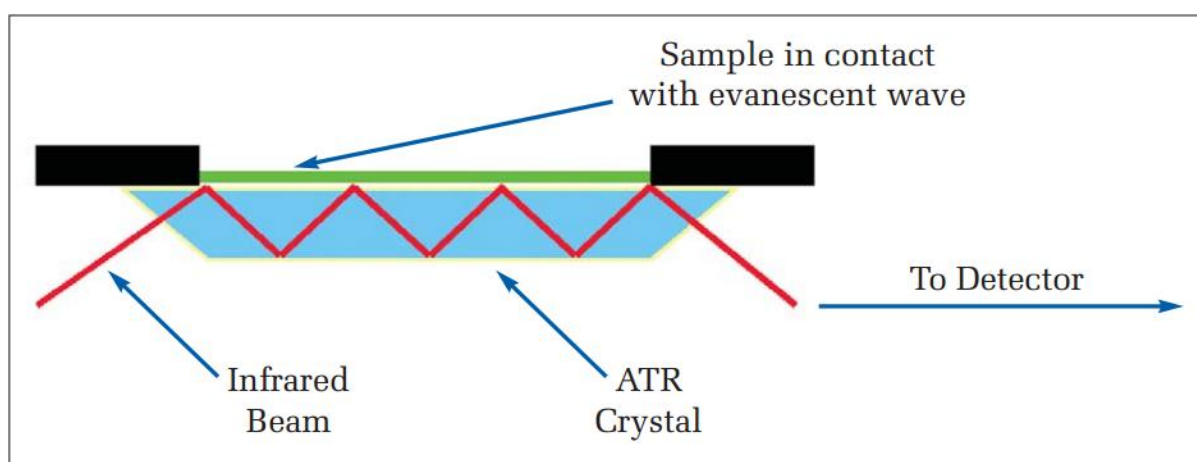
Figure 3.5: Beam paths of ATR-FTIR

CHAPTER 4

CHAPTER 4: RESULTS AND DISCUSSION OF THE EFFECT OF MEMBRANE ORIENTATION

4.1 Introduction

This chapter provides the results of the performance and energy evaluation of baseline 1, main experiment and baseline 2 as described in Chapter 3. The system performance was evaluated in terms of J_w, J_s, R_e and SEC.

4.2 Dye solution: Reactive Black 5

4.2.1 Effect of membrane orientation (FO and PRO mode) on system performance and energy consumption: Baseline 1

The study was conducted as a basis of comparison to determine the extent of fouling on the cellulose triacetate (CTA) membrane used and its impact on system performance and the energy consumption of the dye driven FO system. For this part of the study, deionised water (DI) was used as the FS and Reactive Black 5 dye was used as the DS. Refer to Chapter 3 section 3.2 for details of the operating conditions. To evaluate the effect of membrane orientation on the system performance, experiments were run in both FO and PRO modes.

4.2.1.1 Water Flux (J_w)

Table 4.1 tabulates the initial and final ΔOP and J_w in FO and PRO mode. It can be seen that the initial ΔOP in FO and PRO modes have a difference of 485 kPa, due to fresh FS and DS being prepared per experiment. It was therefore not possible to obtain identical initial ΔOP values. The final ΔOP in FO mode was 1946 kPa higher compared to that of PRO mode. Comparing the initial and final J_w in FO and PRO mode, it can be seen that a higher J_w was achieved in PRO mode compared to that of the FO mode.

Table 4. 1: The initial and final ΔOP and J_w in FO and PRO mode

Mode	Initial ΔOP (kPa)	Final ΔOP (kPa)	Initial J_w (L/m².h)	Final J_w (L/m².h)
FO	16827	11292	9.7	7.16
PRO	16342	9346	11.7	9.1

Figure 4.1 illustrates the J_w and J_s obtained during a 3 h operation for three Baseline 1 experiments (i.e. Test 1, Test 2 and Test 3) using CTA membranes while operating in FO and PRO mode at a flowrate of 200 ml/min, respectively. It can be observed that the J_w in PRO mode was higher than the FO mode. The average J_w in PRO and FO mode were 8.78 and 6.79 L/m^2.h, respectively. Furthermore, Figure 4.1 demonstrates that both J_w and J_s decreases over time in both PRO and FO mode.

The difference in J_w in the FO mode and PRO mode can be attributed to the difference in the membrane resistance depending on the orientation of the support layer. In the FO mode, the porous support layer of the membrane faces the DS, while the active layer faces the FS. The J_w from the feed side dilutes the DS at the membrane's surface and within the membrane's porous support layer, reducing the ΔOP at the membrane's surface and lowering the J_w. Since the osmotic pressure of the DS at the membrane boundary layer is crucial to the FO process, dilutive ICP severely affects J_w in the FO process (Zhao *et al.*, 2015). It has been demonstrated that the membrane orientation in FO poses critical impacts on internal concentration polarization (ICP), which dominates the J_w decline (McCutcheon and Elimelech, 2006).

When the process is operated in PRO mode, the CP phenomenon reverses. Since in PRO mode, the membrane active layer faces the DS. The phenomenon is dilutive ECP, which can be mitigated by the crossflow shear provided on the membrane surface. Although concentrative ICP occurs on the feed side of the membrane, its effect is less severe than the dilutive ICP (McCutcheon and Elimelech, 2006).

Regardless of the operating conditions, higher J_w have previously been achieved in PRO mode than in FO mode as demonstrated by Suh and Lee (2013) and Zhao *et al.* (2015), respectively. With a DS of 1M NaCl and a FS of DI water, Suh and Lee (2013) reported a J_w of 4.15 and 7.08 L/m^2.h in FO and PRO modes, respectively. Furthermore, the same phenomenon was reported by Zhao *et al.* (2015), where a J_w of 3 to 5 and 5 to 8 L/m^2.h in FO and PRO mode, respectively, was achieved using a DS of dyeing wastewater (0.05 g/L dye) and a FS of polyelectrolytes (polyacrylamide)

Figure 4.1: Baseline 1 J_w and J_s as a function of time in both FO and PRO mode at 200 ml/min in a) Test 1 b) Test 2 and c) Test 3

4.2.1.2 Reverse solute flux (J_s)

Reducing reverse solute flux (J_s) is one of the main challenges in FO systems (She *et al.*, 2012). The solutes passing through the membrane from the draw side to the feed side effectively reduces the osmotic driving force and thus dictates the need to supplement the DS, all of which adversely impact the FO performance. Moreover, the J_s can contribute to fouling on the membrane through cake-enhanced OP (Boo *et al.*, 2012; She *et al.*, 2012).

Table 4.2 tabulates the initial and final J_s in FO and PRO mode. It can be seen that there is no significant difference in PRO mode compared to that of FO mode. The J_s achieved in both FO and PRO mode ranged between 0.03 and 0.04 g/m^2.h which is much less than the J_s achieved by Augustine (2017) and Jingxi (2017).

Table 4.2: The initial and final J_s in FO and PRO mode

Mode	Initial J_s (g/m^2.h)	Final J_s (g/m^2.h)
FO	0.03	0.02
PRO	0.04	0.02

From Figure 4.1 and Table 4.2, it can be seen that the average J_s in PRO mode and FO mode was 0.04 and 0.02 g/m^2.h, respectively. A slightly higher J_s was achieved in the PRO mode initially compared to that of FO mode. Higher J_s has previously been obtained in PRO mode by Suh and Lee (2013), who reported a J_s of 0.85 and 1.38 g/m^2.h in FO and PRO mode, respectively. The achievement of higher J_s in PRO mode can be attributed to the presence of a higher draw solute concentration at the membrane active layer compared to that of FO mode. The selection of membrane orientation in FO applications is mainly determined by the water flux performance. However, the J_s should be considered in the selection of membrane orientation because it may jeopardize the FO performance (Hancock and Cath, 2009; Yen *et al.*, 2010).

4.2.1.3 Water recovery (R_e)

Figure 4.2 illustrates the volume of water recovered and expressed as percentage recovery (R_e) over a 3 h period in both FO and PRO modes. Figure 4.2 demonstrates that the recovery in both FO and PRO mode decreased with respect to time. The R_e in PRO mode decreased by 46% compared to the 20% decrease in FO mode over the same period of time.

a)

b)

c)

Figure 4.2: Baseline 1 water recovery (R_e) with respect to water recovered as a function of time in both FO and PRO mode of operation at 200 ml/min in a) Test 1 b) Test 2 and c) Test 3

However, higher recovery was achieved in PRO mode compared to that of FO mode over the same period. The low percentage of water recoveries achieved for both FO and PRO modes compared to literature (references) can be attributed to the duration of the experiments (i.e. 3 h for this study).

4.2.1.4 Energy consumption (SEC)

Figure 4.3 demonstrates the SEC with respect to time in FO and PRO modes. It can be seen that the system consumed less energy in the PRO mode compared to that of FO mode over the same period. The SEC obtained for Test 3 was different from that of Test 1 and Test 2, which can be attributed to the change in the tubing of the system resulting in a change in the energy consumption of the system. The average SEC in FO and PRO modes was 252.52 and 212.96 kW.h/m^3, respectively. The energy consumption in both FO and PRO modes of the operation increased with respect to time. However, the percentage of SEC increase in FO and PRO modes was 22% and 20%, respectively, over the same period.
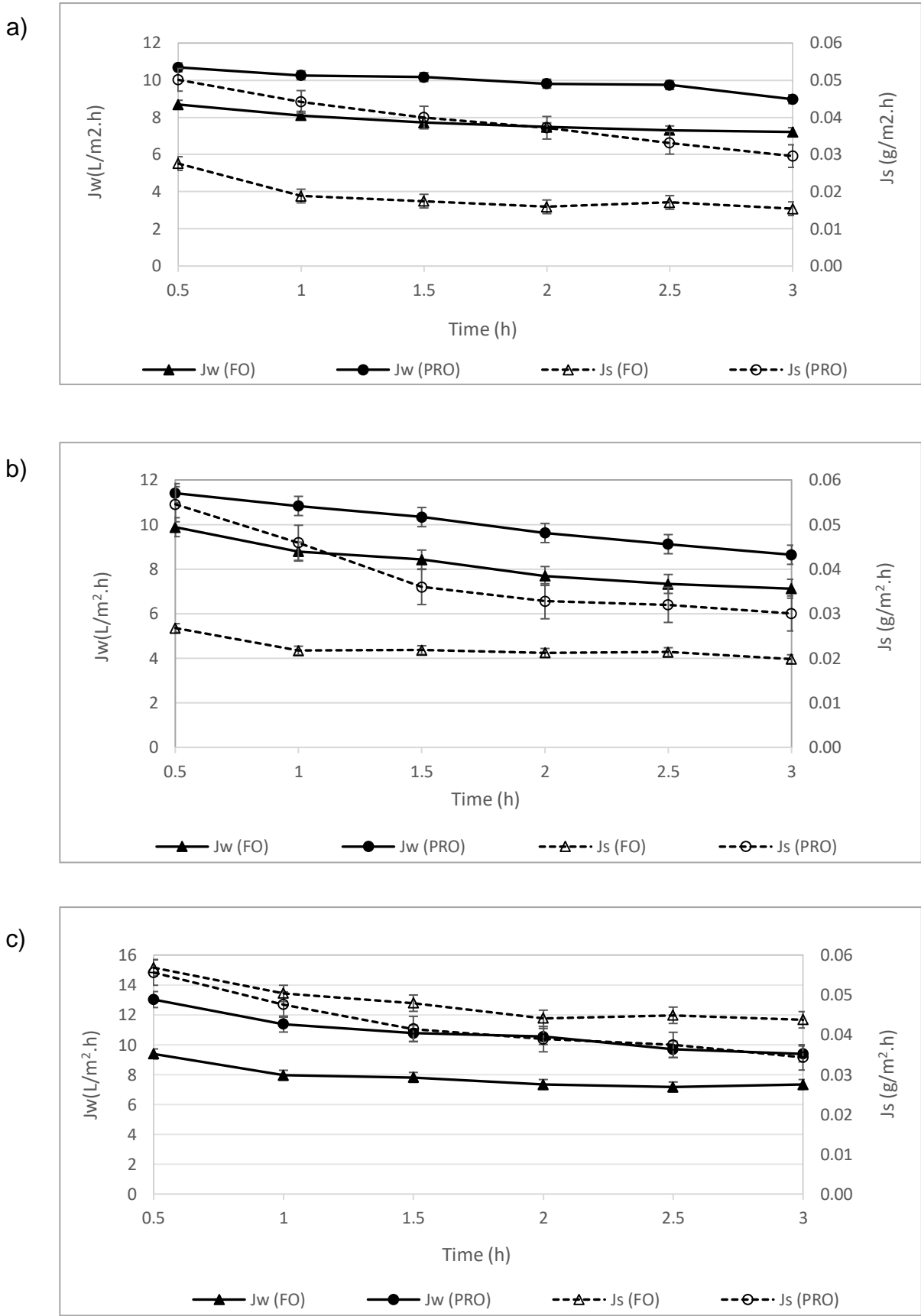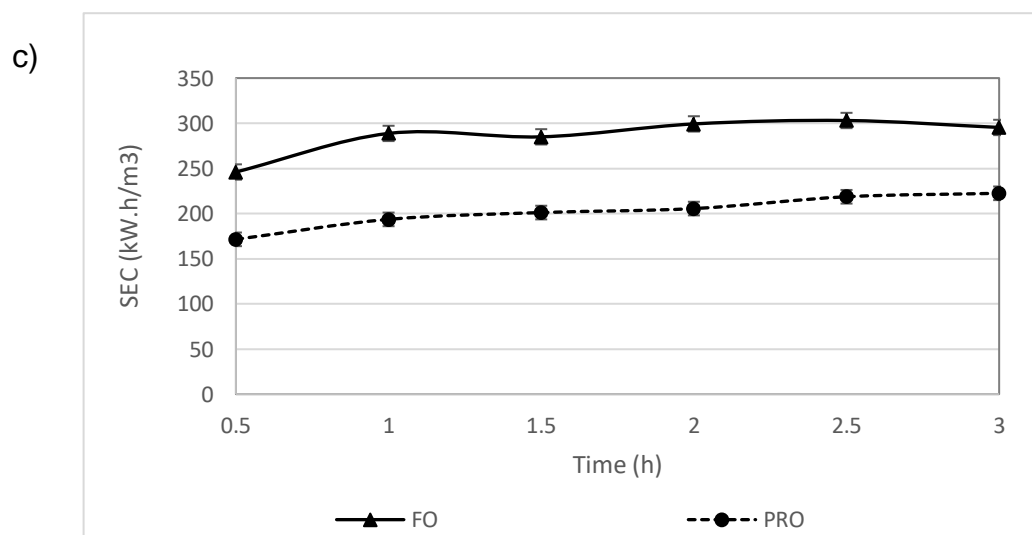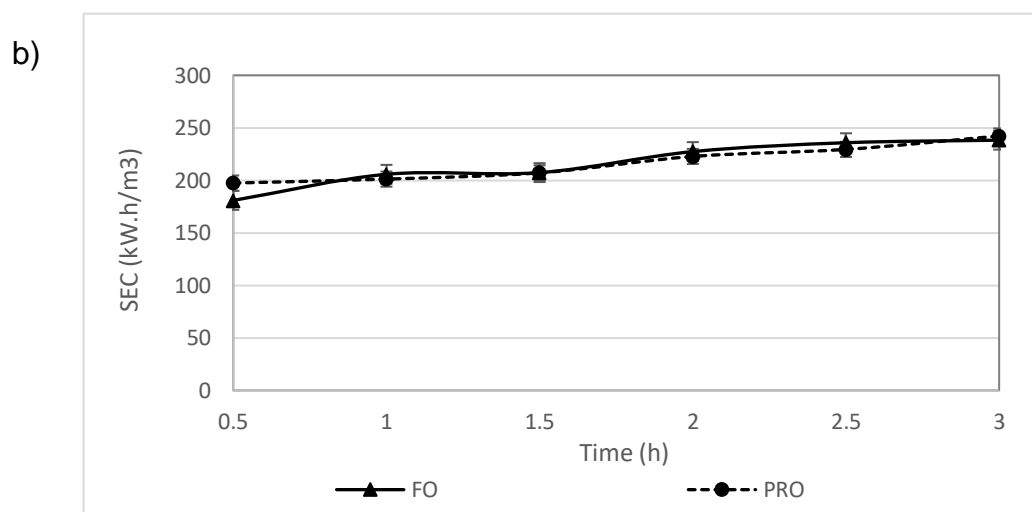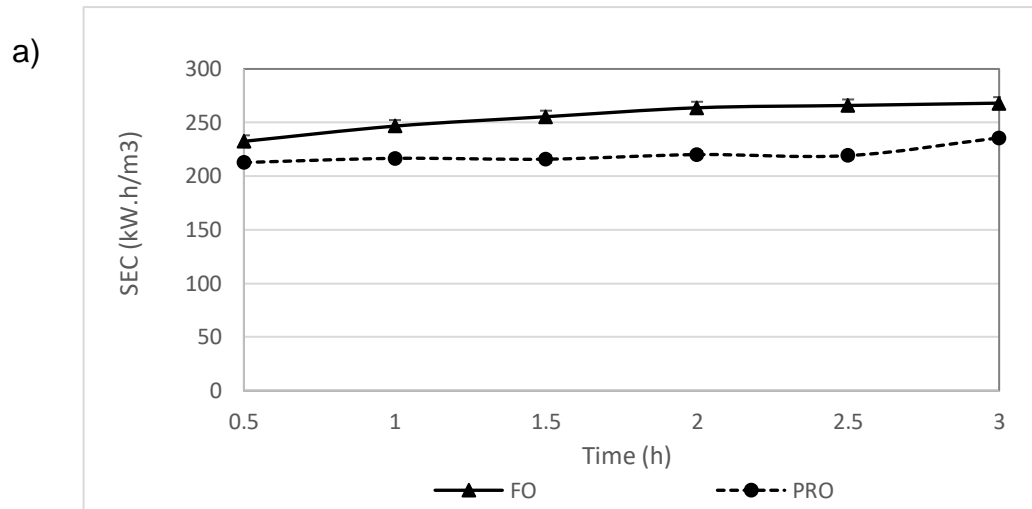
Figure 4.3: Baseline 1 SEC as a function of time in both FO and PRO mode at 200 ml/min in a) Test 1 b) Test 2 and c) Test 3

4.2.2 Effect of membrane orientation (FO and PRO mode) on system performance and energy consumption: Main experiment using Reactive Black 5

The Main experiment was crucial in indicating the performance and energy consumption of a dye driven FO system at different flowrates.

4.2.2.1 Water flux (J_w)

Figure 4.4 illustrates the J_w and FS electrical conductivity (EC) obtained during a 5 h operation in FO mode and 4 h operation in PRO mode for flowrates of 400, 500 and 600 ml/min, respectively. Experiments were run to achieve the target diluted concentration of the dye solution and as such, it was found that in FO mode, the target concentration was achieved after 4 h in comparison to the 5 h in PRO mode. Figure 4.4 (a), (b) and (c) illustrates the EC increase in FO mode from an initial EC of 9.38 mS/cm to a final EC of 10.15, 10.09 and 9.90 mS/cm for flowrates of 400, 500 and 600 mL/min, respectively. Furthermore, Figure 4.4 (a), (b) and (c) demonstrates a decrease in the J_w over time in the FO mode from an initial J_w of 7.25, 8.30 and 9.11 L/m^2.h to a final J_w of 6.05, 6.17 and 6.61 L/m^2.h for flowrates of 400, 500 and 600 mL/min, respectively.

Additionally, Figure 4.4 (a), (b) and (c) illustrates the EC increase in PRO mode from an initial EC of 9.08 mS/cm to a final FS EC of 9.77, 9.68 and 9.74 mS/cm for flowrates of 400, 500 and 600 mL/min, respectively. Figure 4.4 (a), (b) and (c) also demonstrates the J_w decrease over time in the PRO mode from an initial J_w of 10.01, 10.56 and 11.55 L/m^2.h to a final J_w of 7.99, 6.95 and 7.55 L/m^2.h for flowrates of 400, 500 and 600 mL/min, respectively.

Observations from Figure 4.4 (a), (b) and (c) indicate that the final EC's in FO and PRO mode were close, which suggests that membrane orientation had little to no impact on the reverse solute flux. Figure 4.4 (a), (b) and (c) shows that the EC on the feed side increases with a decrease in the J_w in both FO and PRO mode. However, when observing the J_w in Figure 4.4 (a), (b) and (c) in FO and PRO mode, it can be seen that greater flux was achieved in PRO mode compared to that of FO mode.
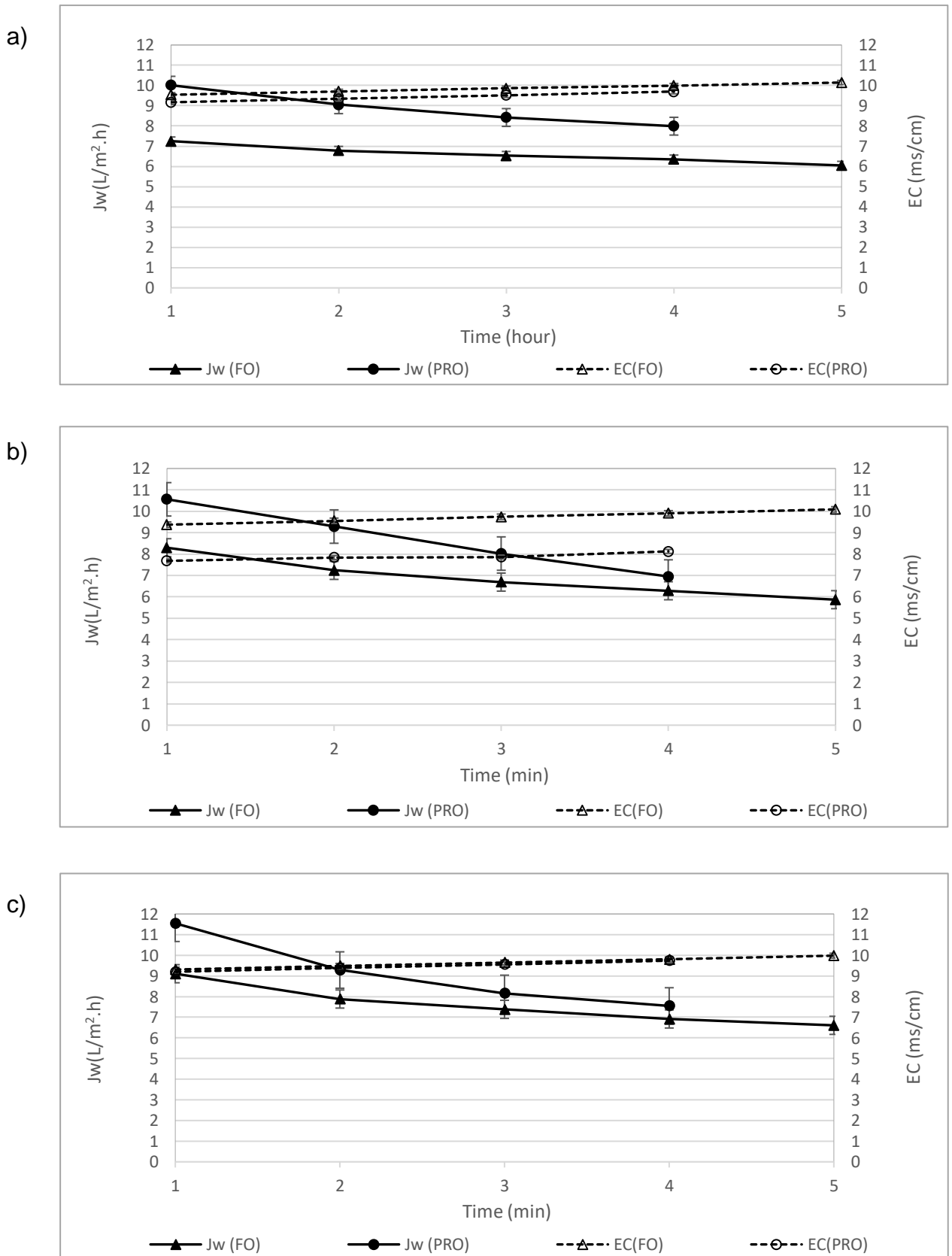
Figure 4.4:Main experiment J_w and EC as a function of time in both FO and PRO mode at a flowrate of a) 400 b) 500 and. c) 600 ml/min

4.2.2.2 Water recovery (R_e)

Water recovery is cumulative (i.e. total water recovered increases over time) but recovery per unit time decreases due to a reduction in flux which results from a decrease in the ΔOP as the target concentration is approached. Figure 4.5 demonstrates a comparison between percentage recovery (R_e) and water recovered (L) with respect to time in FO and PRO mode. The feed recovery rate decreased with respect to time in both FO and PRO mode. In this experiment an average R_e of 7.4% and 7.5%, respectively, for the FO and PRO modes was achieved. These R_e values are higher than the R_e values obtained for Baseline 1 since these experiments ran over a longer period of time (i.e. 5 h for FO mode and 4 h for PRO mode) than the Baseline 1 experiment (i.e.3 h).

A colour Hazen analysis (refer to Appendix D for the procedure) was done on the DS at the beginning and end of the study to assess the extent of DS dilution due to water flux and reverse solute flux. It was found that in the FO mode on average the DS colour concentration decreased from 1048 mg/L Pt to 1033 mg/L Pt. For the PRO mode on average, the colour concentration of the DS decreased from 1041 mg/L Pt to 1026 mg/L Pt. The greater decrease of the colour concentration in the DS observed in PRO mode can be linked to the higher fluxes achieved in the PRO mode.

Comparing R_e in FO and PRO modes, it can be seen that the R_e was greater in the PRO mode. Although the duration of the experiment in PRO mode was shorter compared to that of FO mode, a higher colour concentration decrease was achieved in PRO mode due to the achievement of higher J_w over a shorter time period (i.e. 4 h opposed to 5 h in FO mode). Due to the achievement of higher J_w and colour concentration decrease in PRO mode with respect to time, there is a possibility of achieving higher R_e in PRO mode.
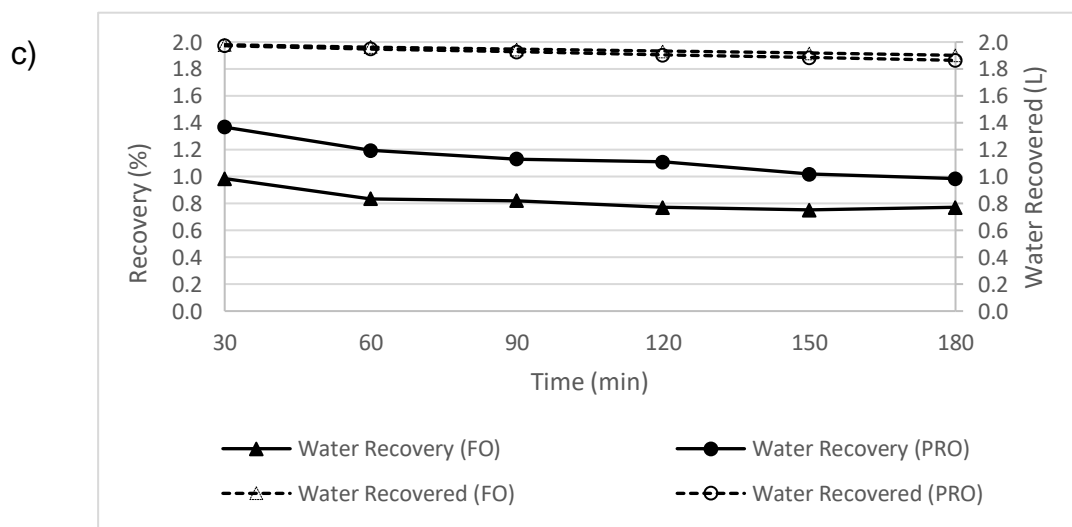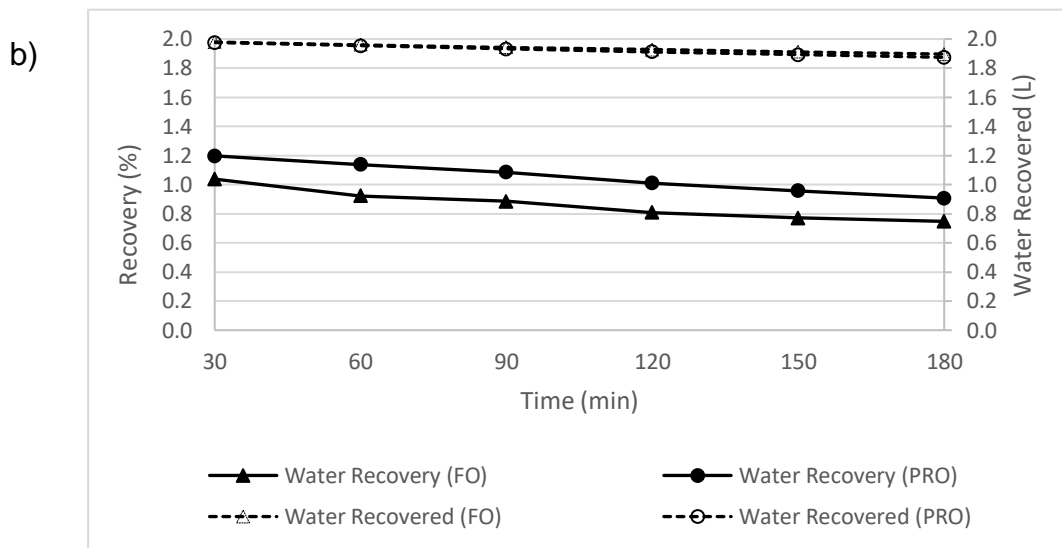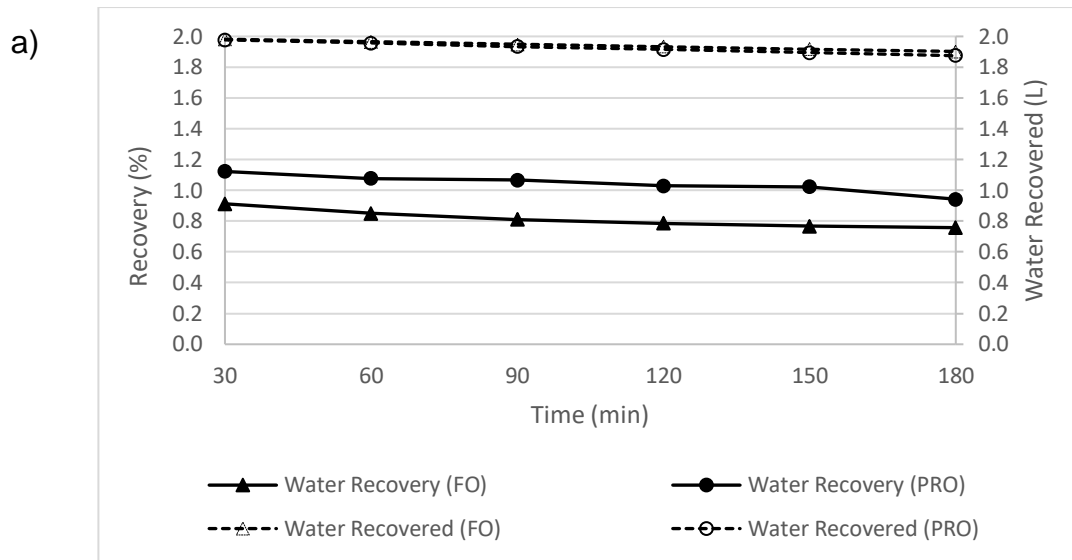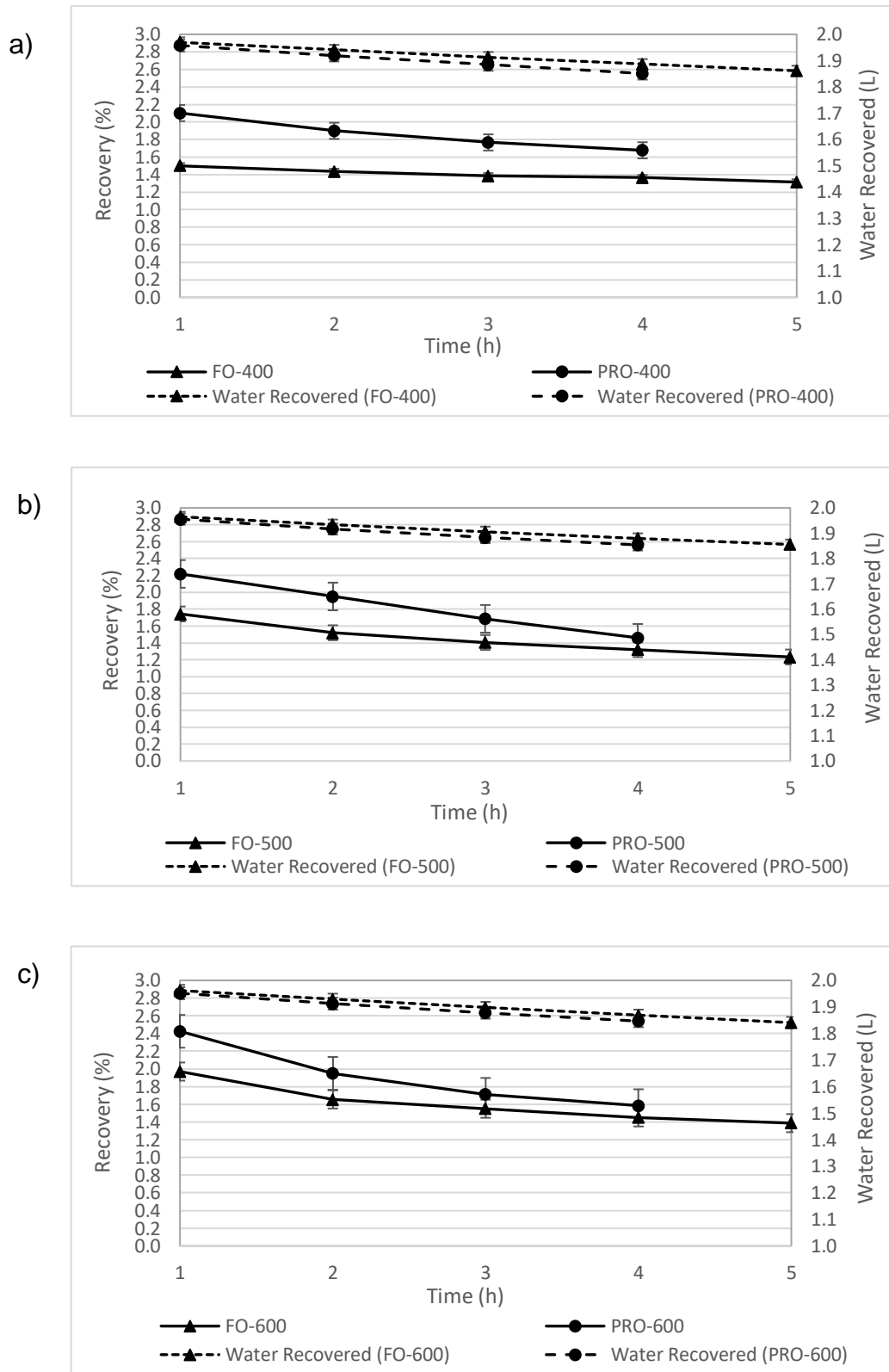
Figure 4.5: Water recovery (R_e) with respect to water recovered as a function of time in both FO and PRO mode of operation in accordance with the respective flowrate of a) 400 b) 500 and c) 600 ml/min

4.2.2.3 Energy consumption (SEC)

FO has been widely referred to as an "energy-efficient" process or an energy-efficient pre-treatment process for a subsequent desalination process (i.e. RO or distillation). However, energy consumption data has rarely been reported in the literature (Shaffer *et al.*, 2015). It should be noted that in this study energy consumption was represented by the energy demand of the recirculation pump, and the energy required for membrane cleaning was not included.

Permeate flux is driven by the ΔOP between the feed and draw solutions. Hydraulic pressure is not required in the FO system other than for recirculation of the FS and DS (Shaffer *et al.*, 2015). Limited research has been published concerning the effect of membrane orientation on the SEC of recirculation pumps in FO systems.

Figure 4.6 illustrates SEC with respect to time in FO and PRO modes. Less energy was consumed in PRO mode compared to that of FO mode with respect to time. The average SEC in PRO and FO mode was 380.6 and 417.3 kW.h/m^3, respectively. Although the duration of study in PRO mode was shorter than that of FO mode (i.e. 4 h as opposed to 5 h in FO mode), SEC in the PRO mode was lower compared to that of FO mode over the same time period (i.e. comparison over the 4 h period of study).

The average initial SEC in FO mode is 365.9 kW.h/m^3 compared to the average initial SEC of 317.2 kW.h/m^3 in PRO mode. The same observation can be made for the average final SEC, where the average final SEC of FO and PRO mode was 462.3 and 442.8 kW.h/m^3, respectively. This further illustrates the fact that the energy consumption in PRO mode was much less than that of FO mode with respect to time.
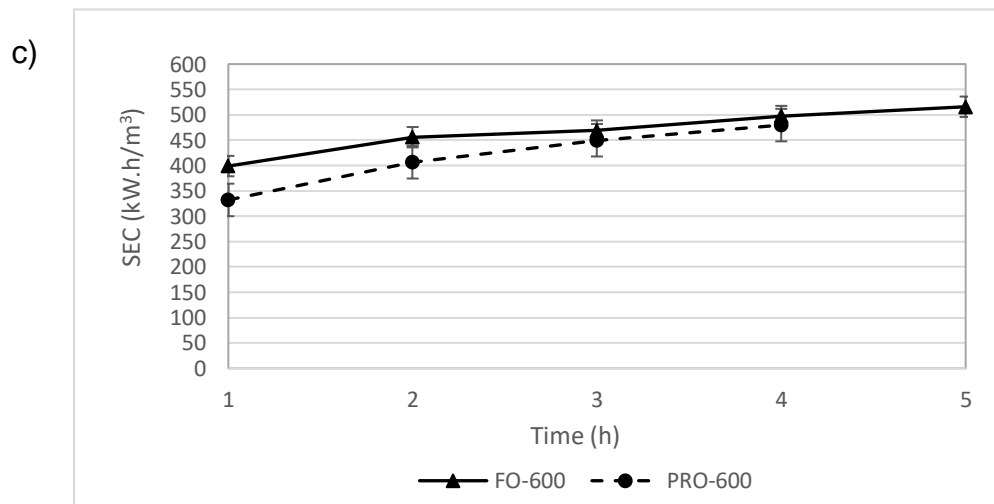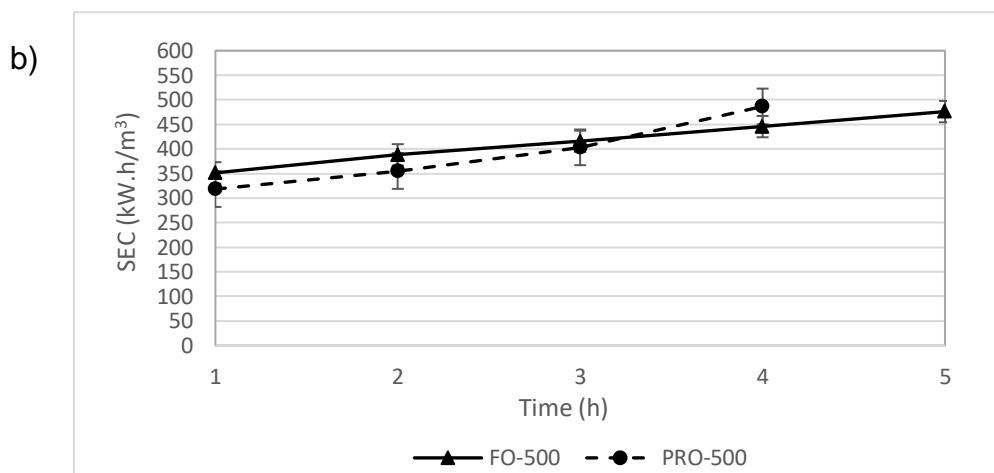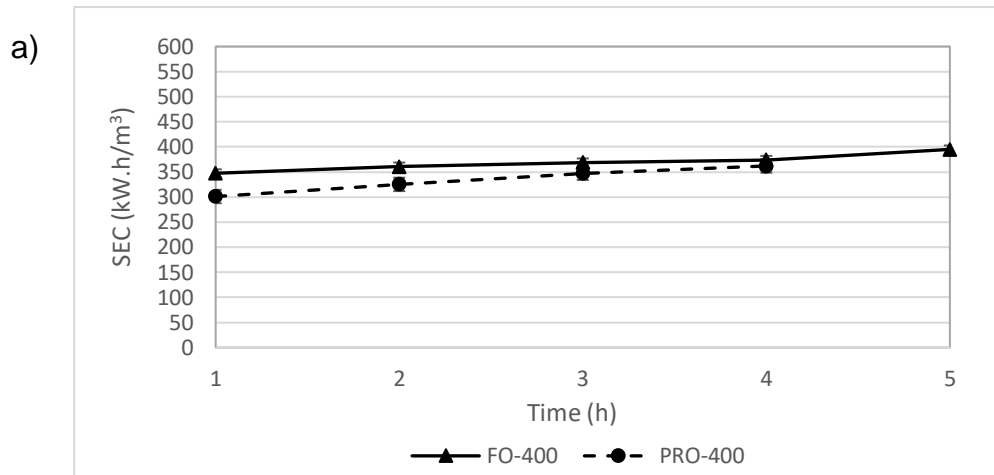
Figure 4.6: Main Experiment SEC as a function of time in both FO and PRO mode at flowrates of a) 400 b) 500 and c) 600 ml/min

A trend can be observed by the increase in SEC with respect to time where the SEC increase in PRO mode is larger with respect to time compared to that of FO mode (i.e. 14% increase in PRO mode compared to that of the 10% increase in FO mode from 1-2 h of study). The percentage increase of SEC in PRO and FO mode over the 4 h period of study is 40% and 20%, respectively. Taking into consideration the percentage increase of SEC in PRO and FO modes, it can be concluded that although less energy was consumed in PRO mode in this experiment, more energy would be consumed in the PRO mode with an increase in the duration of the experimental time.

4.2.3 Effect of membrane orientation (FO and PRO modes) on system performance and energy consumption: Baseline 2

This phase was conducted to be used as a basis of comparison with Baseline 1 to determine the extent of fouling and its impact on the system performance and energy consumption of a dye driven FO system in FO and PRO modes.

4.2.3.1 Water Flux (J_w)

Figure 4.7 compares the J_w and J_s of Baseline 1 and Baseline 2 as a function of time in FO and PRO modes. From Figure 4.7 (b) (Baseline 2), It can be observed that the water flux (J_w) in PRO mode is higher than in FO mode. In this phase, the average J_w in PRO mode and FO mode was 9.73 and 7.63 L/m^2.h, respectively. In the PRO mode, the draw solute concentration at the membrane surface is higher than it is in FO mode of operation, which generates a higher driving force and consequently higher water flux (Lay *et al.*, 2012). Higher water flux has previously been reported for PRO mode than in FO mode (Jung *et al.*, 2011; Lay *et al.*, 2012).

Table 4.3 illustrates the average J_w achieved in baseline 1 (B1) and baseline 2 (B2) experiments in FO and PRO mode, respectively. Higher J_w was achieved in PRO mode for both B1 and B2 experiments. Furthermore, observing the trends illustrated in Figure 4.7, it was found that the J_w decreased over time in both FO and PRO mode for B1 and B2 experiments.

Table 4.3: Average J_w achieved in Baseline 1 and 2 experiments in FO and PRO mode

Experiment	Mode	Average J_w (L/m^2.h)
Baseline 1	FO	6.79
	PRO	8.78
Baseline 2	FO	7.63
	PRO	9.73

Comparing J_w for B1 and B2 shows that there was no fouling on the membrane as similar J_w was achieved for B2 experiments in FO and PRO mode, respectively.

Figure 4.7: Comparison of the J_w and J_s of Baseline 1 (B1) and Baseline 2 (B2) experiments as a function of time in both a) FO and b) PRO mode of operation in accordance with the respective flowrates of i) Test 1 ii) Test 2 and iii) Test 3

4.2.3.2 Reverse solute flux (J_s)

Figure 4.7 demonstrates the comparison of J_s between baseline 1 (B1) and baseline 2 (B2) experiments in FO and PRO modes at a flowrate of 200 ml/min, respectively. Interpreting Figure 4.7 (b) (i), (ii) and (iii) it can be seen that the average J_s in PRO mode and FO mode are 0.02 and 0.04 g/m^2.h, respectively. The J_s in FO mode is higher than that of PRO mode.

Table 4.4 illustrates the average J_s achieved in B1 and B2 experiments in FO and PRO mode, respectively. The same J_s was achieved for FO and PRO modes in both B1 and B2 experiments indicating the absence of fouling. Furthermore, observing the trends illustrated in Figure 4.7, it was found that the J_s decreased over time in both FO and PRO mode for B1 and B2 experiments.

Table 4.4: Average J_s achieved in Baseline 1 and 2 experiments in FO and PRO mode

Experiment	Mode	Average J_s (g/m^2.h)
Baseline 1	FO	0.04
	PRO	0.02
Baseline 2	FO	0.04
	PRO	0.02

Table 4.4 indicated that membrane orientation had no impact on J_s However, the J_s should be considered in the selection of membrane orientation because it may jeopardise the FO performance (Hancock and Cath, 2009; Yen *et al.*, 2010).

4.2.3.3 Water recovery (R_e)

This study attempts to relate recovery to system performance to elaborate on the significance of recovery with respect to system performance. Figure 4.8 illustrates the percentage of R_e in relation to the water recovered for baseline 1 (B1) and baseline 2 (B2) experiments as a function of time in FO and PRO modes.

Evaluating Figure 4.8 (b) (i), (ii) and (iii) it can be observed that the R_e in both FO and PRO modes decreased with respect to time. The percentage recovery in PRO mode decreased by 32% compared to the 28% decrease in FO mode over the same period. However, the rate of recovery in PRO mode was higher than that of FO mode over the same period. Comparing Figure 4.8 (a) and (b), it can be seen that higher R_e was achieved in PRO mode for B1 and B2 experiments. Furthermore, the rate of R_e decreased over time in FO and PRO modes for both B1 and B2 experiments.
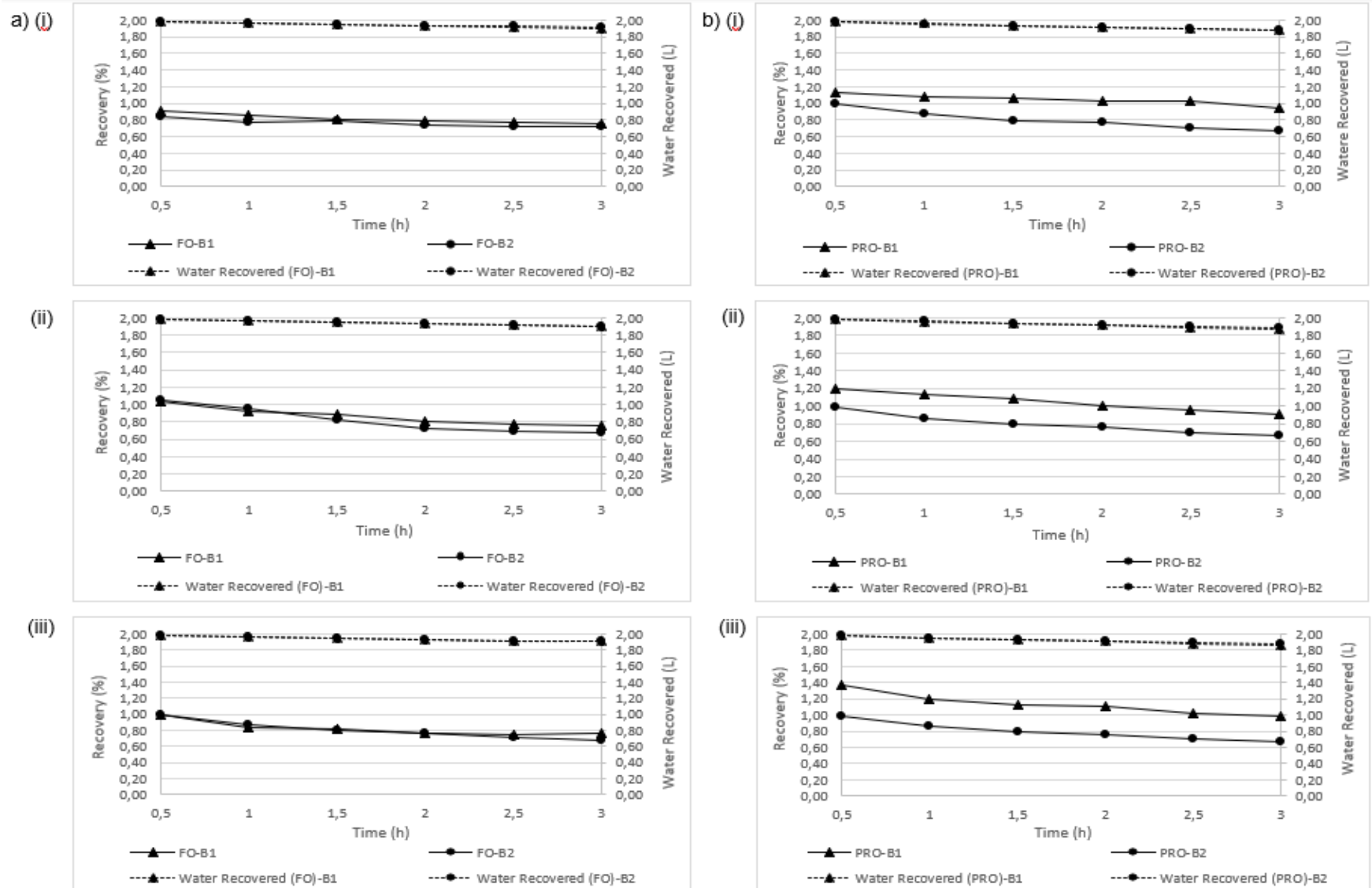
Figure 4.8: Comparison of R_e with respect to water recovered of the Baseline 1 (B1) and Baseline 2 (B2) experiments as a function of time in both a) FO and b) PRO modes in accordance with the respective flowrate of 200 ml/min in i) Test 1 ii) Test 2 and iii) Test 3

4.2.3.4 Energy consumption (SEC)

Figure 4.9 demonstrates the *SEC* with respect to time in FO and PRO modes for B1 and B2 experiments, respectively. Figure 4.9 (a), (b) and (c) compare the results of SEC between B1 and B2 experiments. From Figure 4.9, it can be seen that less energy was consumed in the PRO modes compared to FO mode over the same period. The average SEC in FO and PRO mode was 256.11 and 226.70 kW.h/m^3, respectively. The energy consumption in both FO and PRO modes of operation increased with respect to time. The percentage increase of SEC in FO and PRO modes was 31% and 13% over the same period, respectively.

Table 4.5 illustrates the average SEC achieved in B1 and B2 experiments in FO and PRO modes, respectively. Results tabulated in Table 4.5, indicates that higher SEC was achieved in FO mode for B1 and B2 experiments. Furthermore, the SEC decreased over time in FO and PRO mode for both B1 and B2 experiments. Comparing the average SEC in Table 4.5, it can be concluded that there was very little to no fouling in the FO system as the SEC obtained in FO and PRO modes, respectively, for both B1 and B2 experiments were similar.

Table 4.5: Average SEC achieved in Baseline 1 and 2 experiments in FO and PRO mode

Experiment	Mode	Average SEC (kW.h/m^3)
Baseline 1	FO	252.52
	PRO	226.70
Baseline 2	FO	256.11
	PRO	212.96

Observing the trend of the percentage increase in SEC in FO and PRO modes for B1 and B2 experiments, it was found that over time, SEC in PRO mode would surpass that of the SEC in FO mode.
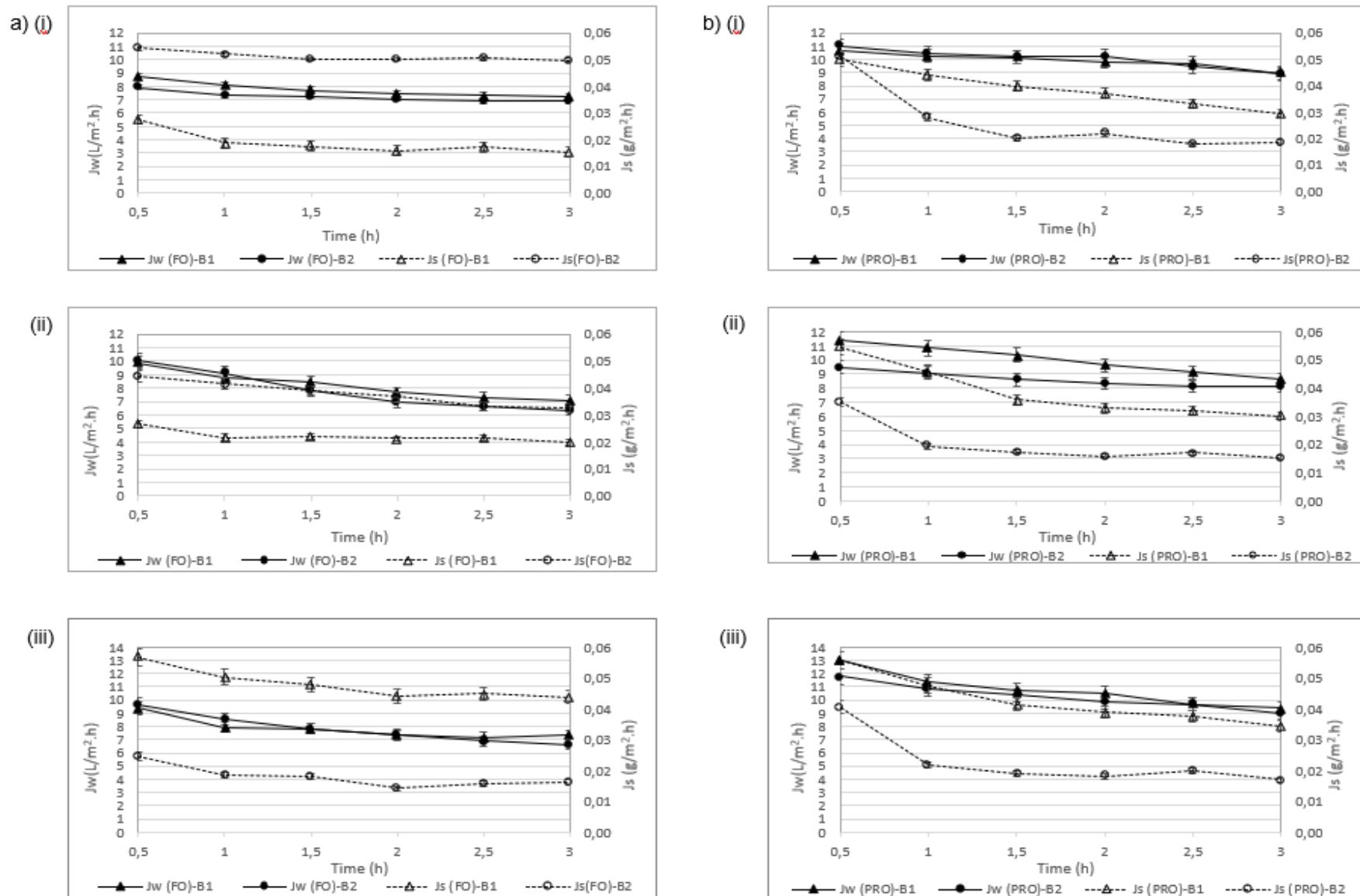
a)

b)

c)
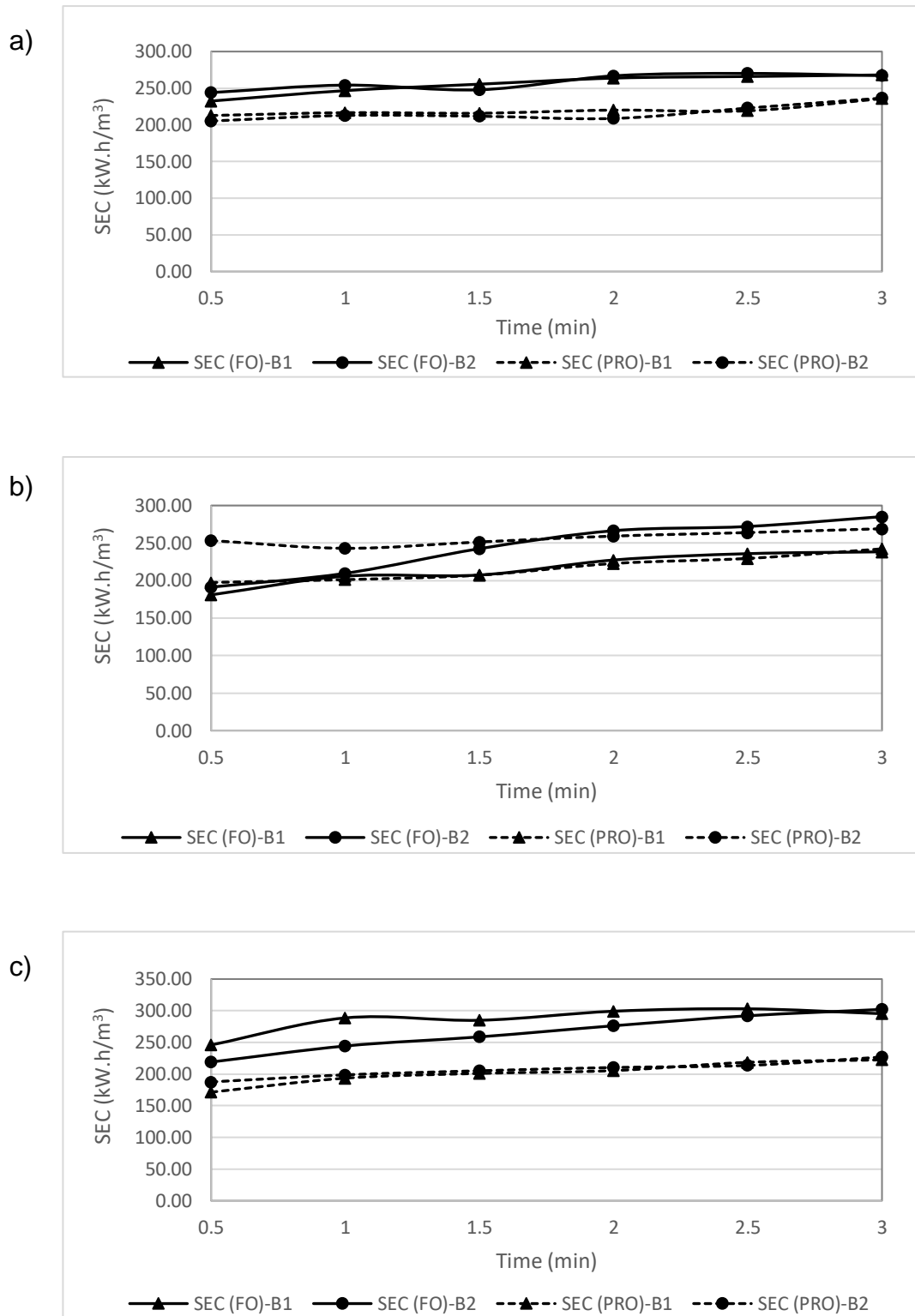
Figure 4.9: Comparison of the SEC of the Baseline 1 (B1) and Baseline 2 (B2) experiments as a function of time in both FO and PRO modes in accordance with the respective flowrate of 200 ml/min in a) Test 1 b) Test 2 and c) Test 3

4.3 Dye solution: Maxilon Blue GRL

Maxilon Blue GRL was used as a DS for a basis of comparison with the Reactive Black 5 to investigate the impact of change in DS on the performance and energy of the FO system. The system performance was evaluated in terms of Jw, Js, R_e and SEC. Due to the duration of the Main Experiments ($\pm$ 140 h), while using Maxilon Blue GRL as the DS, a decision was made to conduct experiments only in FO mode for comparison purposes.

4.3.1 System performance and energy consumption: Baseline 1

For this study, DI was used as the FS and Maxilon Blue GRL dye was used as the DS. Refer to Chapter 3 (section 3.2) for details of the operating conditions of this study.

4.3.1.1 Water Flux (J_w)

Table 4.6 tabulates the initial and final ΔOP and J_w in FO mode for Baseline 1 experiments with DS of Maxilon Blue GRL and Reactive Black 5, respectively. It can be seen that the initial and final ΔOP while using Reactive Black 5 as DS in FO mode was 8998.5 and 10780 kPa greater compared to that of Maxilon Blue GRL. Comparing the initial and final J_w it can be seen that lower J_w was achieved while using Maxilon Blue GRL as DS in FO mode.

Table 4.6: The initial and final ΔOP and J_w in FO mode

DS	Initial ΔOP (kPa)	Final ΔOP (kPa)	Initial J_w (L/m².h)	Final J_w (L/m².h)
Reactive Black 5	16827	11292	9.7	7.16
Maxilon Blue GRL	7828.5	512	6.31	4.70

Figure 4.10 illustrates the J_w and J_s obtained for the duration of a 3 h operation Baseline 1 experiment using Maxilon Blue GRL and Reactive Black 5 as the DS whilst operating in FO mode at a flowrate of 200 ml/min. In comparing the J_w, it can be observed that higher fluxes were achieved in experiments where Reactive Black 5 was used as the DS. From Figure 4.10 (a), (b) and (c), it can be observed that the average (i.e. test 1, 2 and 3) initial and final J_w for experiments using Reactive Black 5 as the DS were 9.32 and 7.22 L/m².h in comparison to the 6.31 and 4.70 L/m².h achieved while using Maxilon Blue GRL as the DS.

Figure 4.10: Water flux (J_w) and J_s as a function of time using Maxilon Blue GRL (BBD) and Reactive Black 5 (BRD) as DS in FO mode at 200 ml/min in a) Test 1 b) Test 2 and c) Test 3

4.3.1.2 Reverse solute flux (J_s)

Table 4.7 summarises the initial and final J_s in FO mode for Baseline 1 experiments with DS of Maxilon Blue GRL and Reactive Black 5, respectively. It can be seen from Table 4.7 that the initial and final J_s achieved while using Maxilon Blue GRL and Reactive Black 5 as DS in FO mode was similar in comparison.

Table 4.7: The initial and final J_s in FO mode using Maxilon Blue GRL and Reactive Black 5 as DS

DS	Initial J_s (g/m².h)	Final J_s (g/m².h)
Reactive Black 5	0.04	0.03
Maxilon Blue GRL	0.05	0.03

Figure 4.10 illustrates the J_w and J_s obtained for the duration of the 3 h operation for Baseline 1 experiments using Maxilon Blue GRL and Reactive Black 5 as DS whilst operating in FO mode at a flowrate of 200 ml/min. While comparing the J_s achieved using Maxilon Blue GRL and Reactive Black 5 as DS, it was observed that similar J_s was achieved in both sets of experiments. From Figure 4.10 (a), (b) and (c), it can be observed that the average initial and final J_s for experiments using Reactive Black 5 as the DS are 0.04 and 0.03 g/m².h in comparison to 0.05 and 0.03 g/m².h achieved while using Maxilon Blue GRL as the DS.

4.3.1.3 Water recovery (R_e)

Figure 4.11 illustrates the R_e and water recovered (L) for the duration of the 3 h operation for Baseline 1 experiments using Maxilon Blue GRL and Reactive Black 5 as DS whilst operating in FO mode at a flowrate of 200 ml/min. Evaluating Figure 4.11 (a), (b) and (c), it was observed that the rate of recovery decreased with respect to time. From Figure 4.11 (a), (b) and (c), it can be observed that the average initial and final R_e for experiments using Reactive Black 5 as the DS are higher compared to when using Maxilon Blue GRL as the DS. Furthermore, R_e is directly related to J_w and as such, it was expected that higher R_e is obtained while using Reactive Black 5 as the DS due to the higher J_w achieved.

Figure 4.11: Water recovery (R_e) with respect to water recovered (L) as a function of time using Maxilon Blue GRL (BBD) and Reactive Black 5 (BRD) as DS in FO mode at 200 ml/min in a) Test 1 b) Test 2 and c) Test 3

4.3.1.4 Energy consumption (SEC)

Figure 4.12 illustrates the SEC for the duration of a 3 h operation for Baseline 1 experiments using Maxilon Blue GRL and Reactive Black 5 as DS whilst operating in FO mode at a flowrate of 200 ml/min. From Figure 4.12 (a), (b) and (c), it can be observed that the average initial and final SEC for experiments using Reactive Black 5 as the DS were 219.80 and 267.24 kW.h/m^3 in comparison to the 369.19 and 433.77 kW.h/m^3 achieved while using Maxilon Blue GRL as the DS. It can be seen that the system consumes less energy while using Reactive Black 5 as the DS in comparison to Maxilon Blue GRL. Furthermore, it can be observed in Figure 12 (a), (b) and (c) that the energy consumption increased with respect to time.

Figure 4.12: Energy consumption (SEC) as a function of time using Maxilon Blue GRL (BBD) and Reactive Black 5 (BRD) as DS in FO mode at 200 ml/min in a) Test 1 b) Test 2 and c) Test 3

4.3.2 System performance and energy consumption: Main experiment using Maxilon Blue GRL

In this section, a comparison will be made in terms of system performance (J_w and Re) and energy consumption in relation to the use of Maxilon Blue GRL and Reactive Black 5 as DS in the Main experiment.

4.3.2.1 Water flux (J_w)

Figure 4.13 illustrates the water flux (J_w) and feed solution electrical conductivity (FS EC) obtained using Maxilon Blue GRL and Reactive Black 5 as DS in FO mode for flowrates of 400, 500 and 600 ml/min, respectively. It can be observed from Figure 4.13 that the duration of experiments using Reactive Black 5 as DS was approximately 5 h for the respective flowrates of 400, 500 and 600 ml/min. However, the duration of experiments using Maxilon Blue GRL as DS was approximately 143, 147 and 171 h for the respective flowrates to reach the target concentration. The difference in the duration of experiments is attributed to the difference in molecular weight of the DS as well as the ΔOP across the FO system.

Figure 4.13 (a), (b) and (c) illustrates the FS EC increase using Maxilon Blue GRL as DS from an initial EC of 9.14 mS/cm to a final FS EC of 13.23, 21.40 and 23.70 mS/cm for flowrates of 400, 500 and 600 mL/min, respectively. Figure 4.13 (a), (b) and (c) further illustrates that J_w decreased using Maxilon Blue GRL as DS from an initial J_w of 5.33, 5.35 and 5.43 L/m^2.h to a final J_w of 0.64, 0.12 and 0.10 L/m^2.h for flowrates of 400, 500 and 600 mL/min, respectively.

Additionally, Figure 4.13 (a), (b) and (c) illustrates the FS EC increase using Reactive Black 5 as DS from an initial EC of 9.38 mS/cm to a final FS EC of 10.15, 10.09 and 9.90 mS/cm for flowrates of 400, 500 and 600 mL/min, respectively. Furthermore, Figure 4.13 (a), (b) and (c) also illustrates that J_w decreased using Reactive Black 5 as DS from an initial J_w of 7.25, 8.30 and 9.11 L/m^2.h to a final J_w of 6.05, 6.17 and 6.61 L/m^2.h for flowrates of 400, 500 and 600 mL/min, respectively.

Observations from Figure 4.13 (a), (b) and (c) indicate identical trends for FS EC's in relation to the use of two different DS. Greater FS EC's were achieved using Maxilon Blue GRL as DS as a result of the increased duration of experiments relative to the respective flowrates. When comparing the J_w with FS EC's in Figure 4.13 (a), (b) and (c), it can be seen that the FS EC's increase with a decrease in the J_w. However, greater J_w was achieved using Reactive Black 5 dye as a DS when compared to Maxilon Blue GRL dye as a DS, due to the higher ΔOP (i.e. 16827 kPa) achieved across the FO system resulting from the higher molecular weight (i.e. 991 g/mol (Reactive Black 5) compared to 482 g/mol (Maxilon Blue GRL dye), respectively).
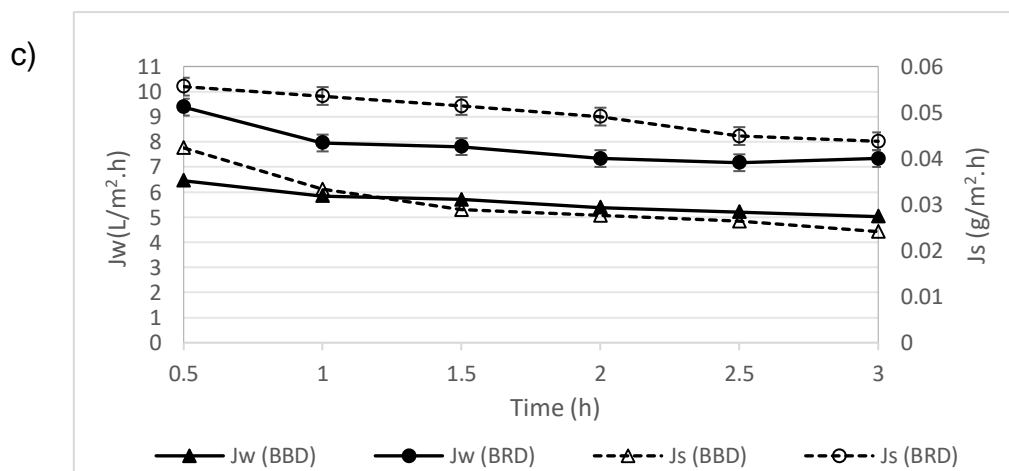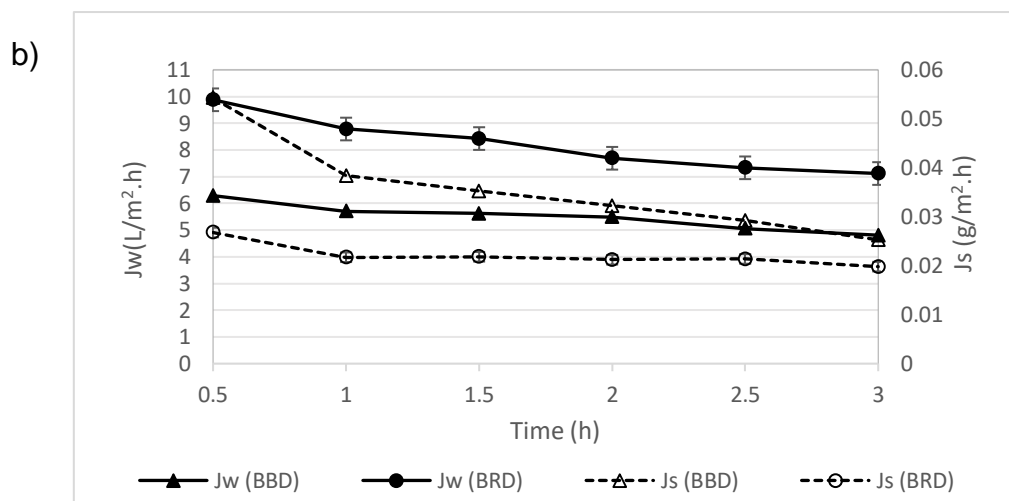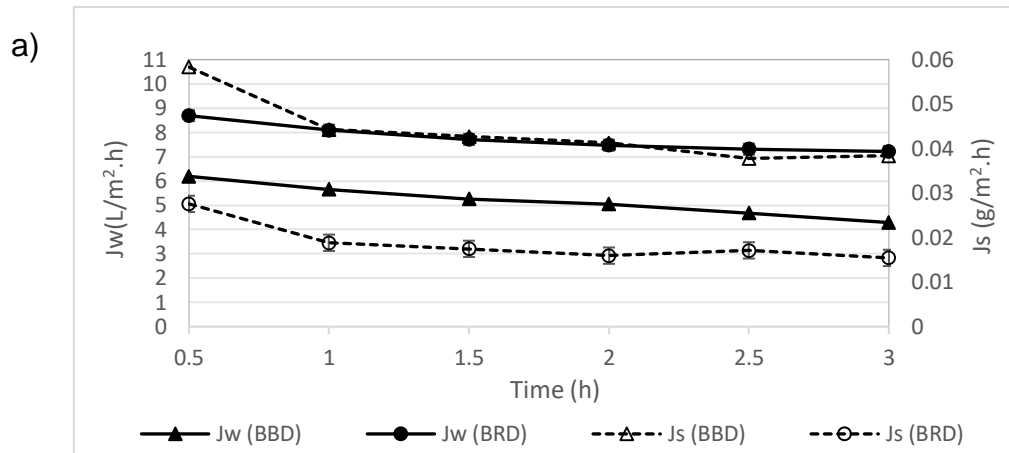
Figure 4.13: Water flux (J_w) and EC as a function of time using Maxilon Blue GRL (BBD) and Reactive Black 5 (BRD) as DS in FO mode at a) 400 b) 500 and c) 600 ml/min

4.3.2.2 Water recovery (R_e)

Figure 4.14 (a), (b) and (c) illustrates the R_e obtained using Maxilon Blue GRL and Reactive Black 5 as DS whilst operating in FO mode at flowrates of 400, 500 and 600 ml/min, respectively. It can be seen that whilst using Reactive Black 5 as DS, it took approximately 5 h to reach the target concentration in comparison to the 143, 147 and 171 h while using Maxilon Blue GRL as DS with respect to the flowrates of 400, 500 and 600 ml/min. According to Figure 4.14, a higher recovery rate was achieved whilst using Reactive Black 5 as the DS. In Figure 4.14 (a), (b) and (c), it can be observed that the average initial and final R_e using Reactive Black 5 as DS was higher in comparison to the use of Maxilon Blue GRL as the DS for the same period (i.e. 5 h).
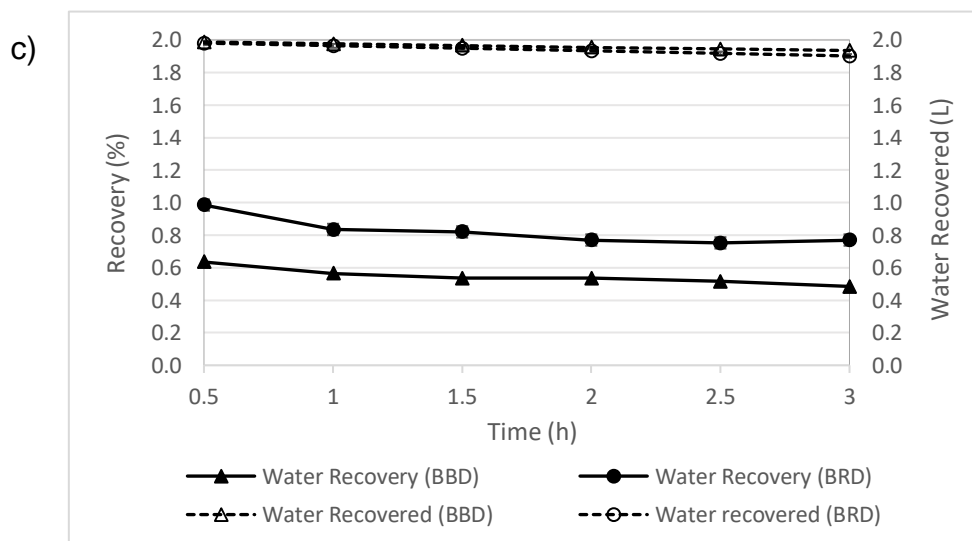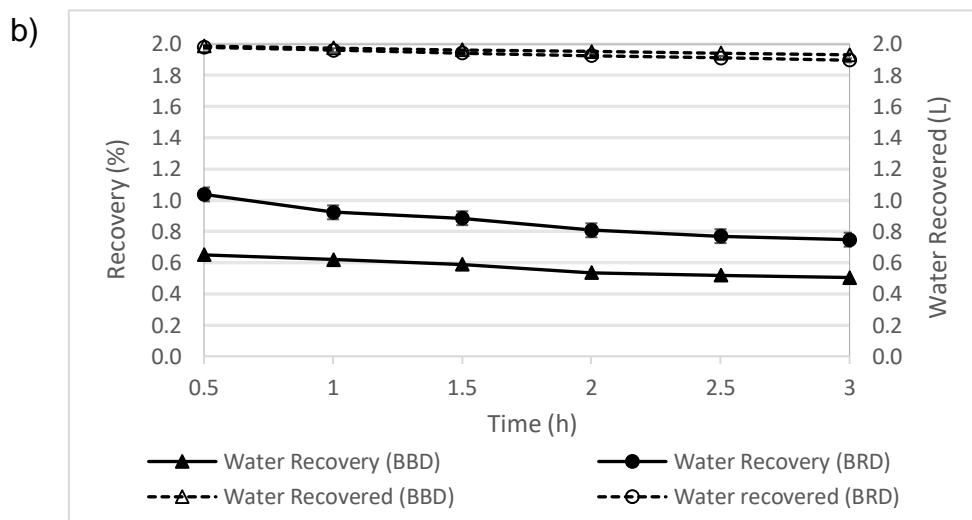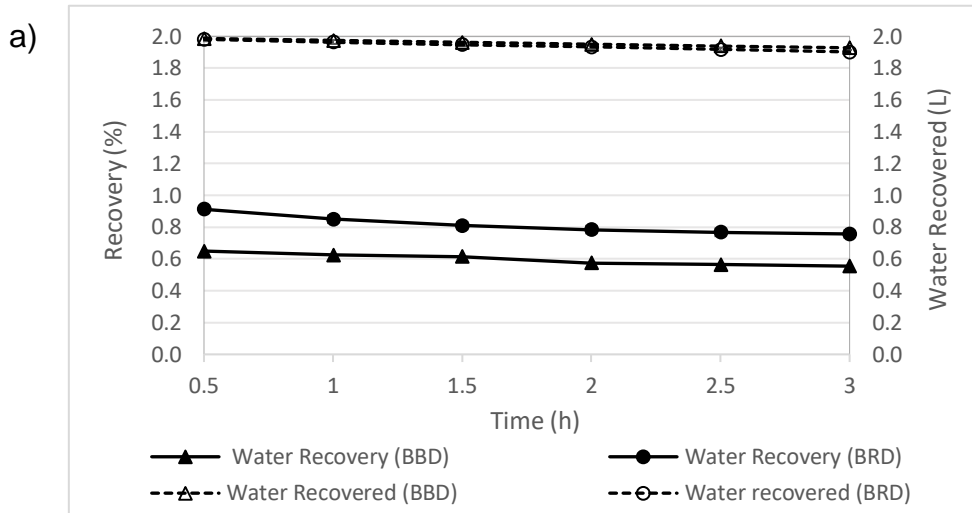
Figure 4.14: Water recovery (R_e) and water recovered as a function of time using Maxilon Blue GRL (BBD) and Reactive Black 5 (BRD) as DS in FO mode at a) 400 b) 500 and c) 600 ml/min

4.3.2.3 Energy consumption (SEC)

Figure 4.15 (a), (b) and (c) illustrate the SEC obtained using Maxilon Blue GRL and Reactive Black 5 as DS whilst operating in FO mode at flowrates of 400, 500 and 600 ml/min, respectively. It can be seen that whilst using Reactive Black 5 as DS, it took approximately 5 h to reach the target concentration in comparison to the 143, 147 and 171 h while using Maxilon Blue GRL as DS with respect to the flowrates of 400, 500 and 600 ml/min. According to Figure 4.15 (a), (b) and (c), less energy was consumed using Reactive Black 5 as the DS. In Figure 4.15 (a), (b) and (c), it can be observed that the average initial and final SEC using Reactive Black 5 as DS were 365.88 and 462.23 kW.h/m^3 in comparison to the 650.77 and 946.89 kW.h/m^3 achieved while using Maxilon Blue GRL as the DS for the same period (i.e. 5 h).
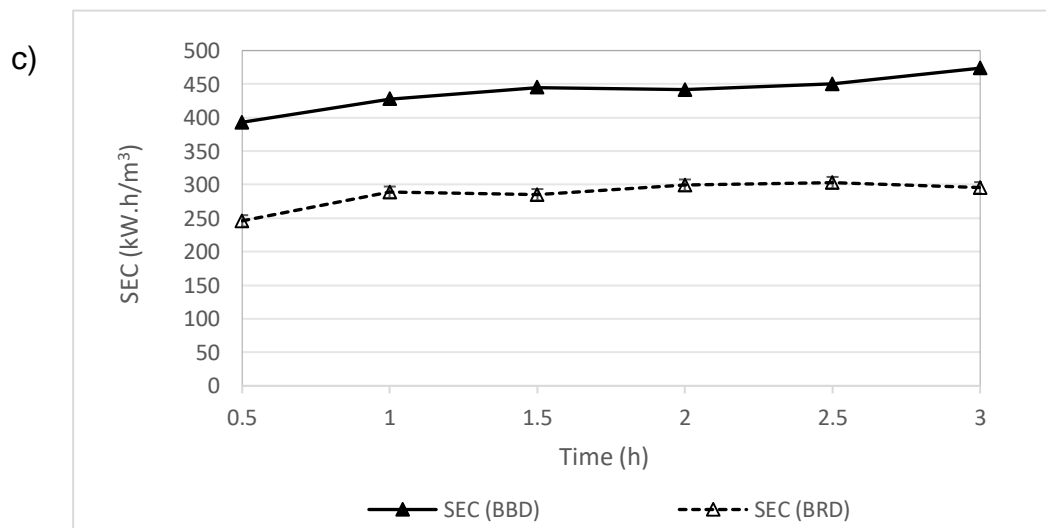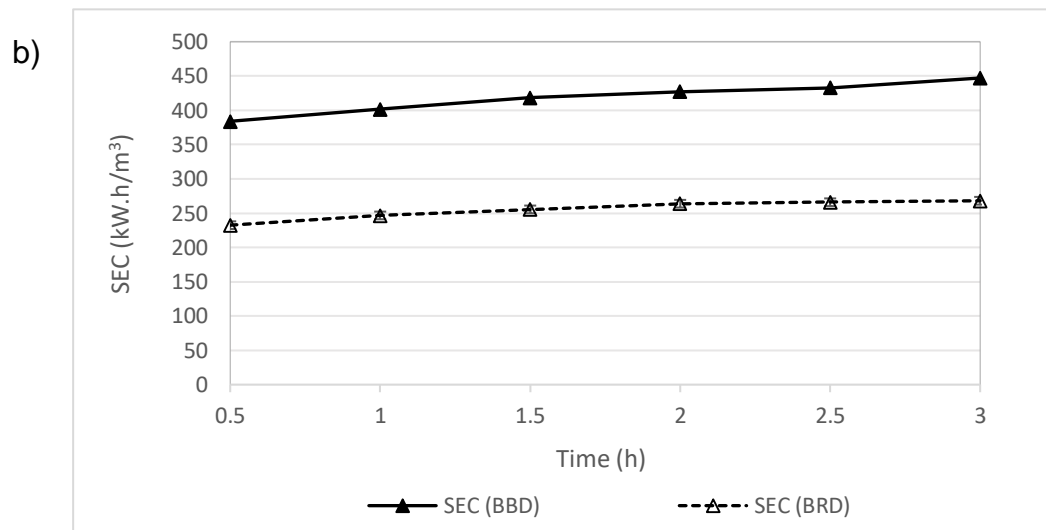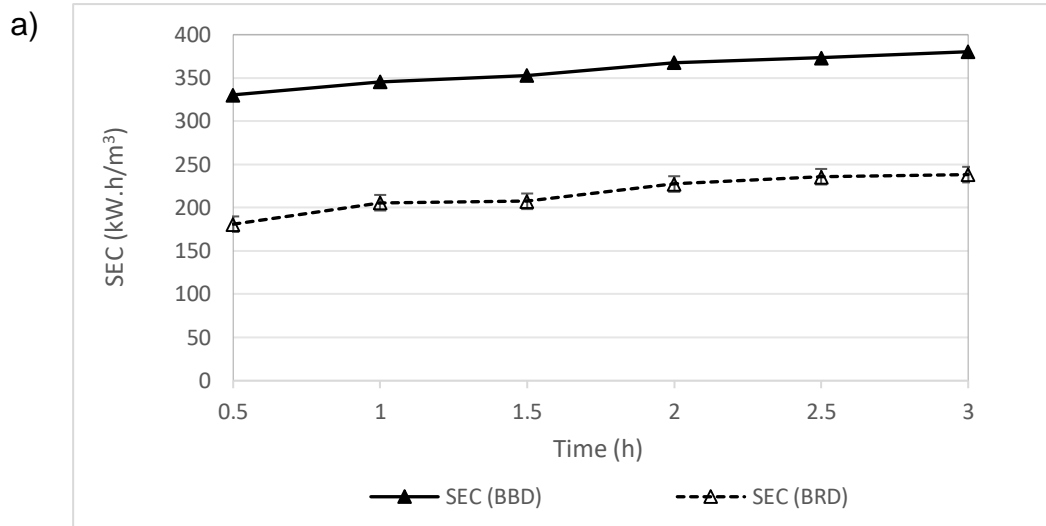
Figure 4.15: Energy consumption (SEC) as a function of time using Maxilon Blue GRL (BBD) and Reactive Black 5 (BRD) as DS in FO mode at a) 400 b) 500 and c) 600 ml/min

4.3.3 System performance and energy consumption: Baseline 2

This study was used as a basis of comparison with Baseline 1 to determine the extent of fouling and its impact on the energy consumption of the FO system. To evaluate the effect of membrane orientation on system performance, experiments were run in FO mode.

4.3.3.1 Water Flux (J_w)

Figure 4.16 illustrates the J_w and J_s obtained for the duration of a 3 h operation for Baseline 2 experiments using Maxilon Blue GRL and Reactive Black 5 as DS whilst operating in FO mode at a flowrate of 200 ml/min. It can be observed that greater J_w was achieved whilst using Reactive Black 5 as the DS in comparison to Maxilon Blue GRL. From Figure 4.16 (a), (b) and (c), it was observed that the average initial and final J_w for experiments using Reactive Black 5 as the DS were 9.21 and 6.61 L/m^2.h compared to the 5.66 and 4.20 L/m^2.h achieved while using Maxilon Blue GRL as the DS.
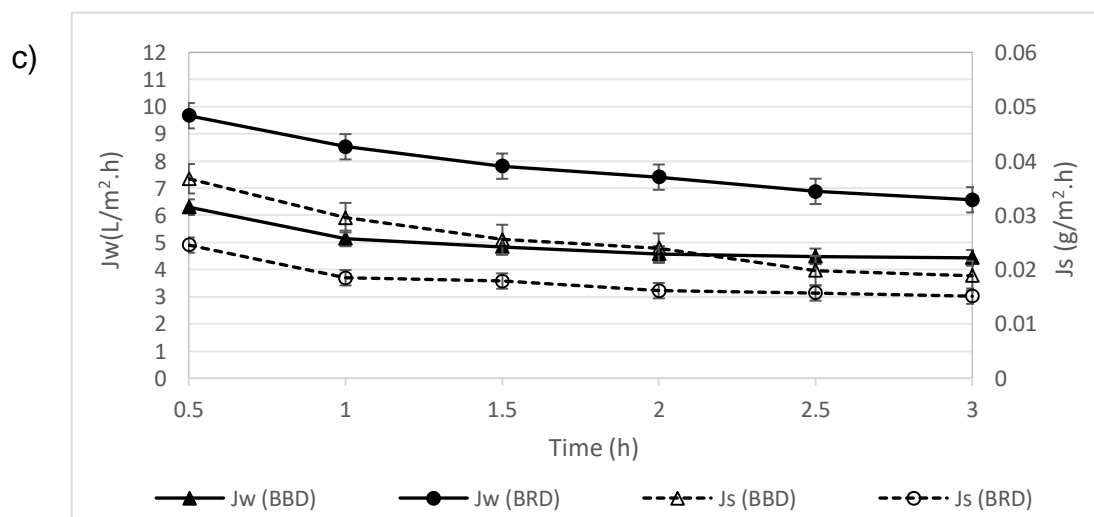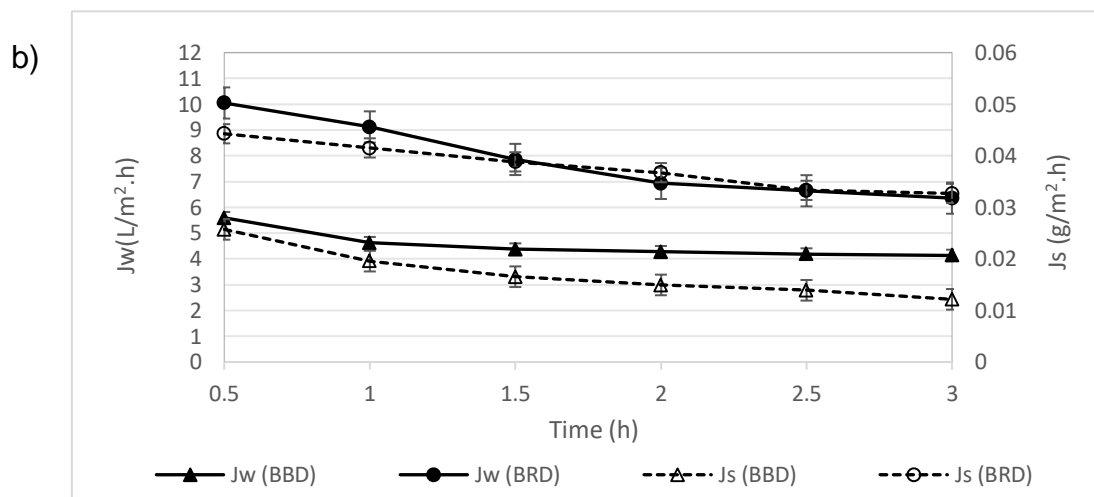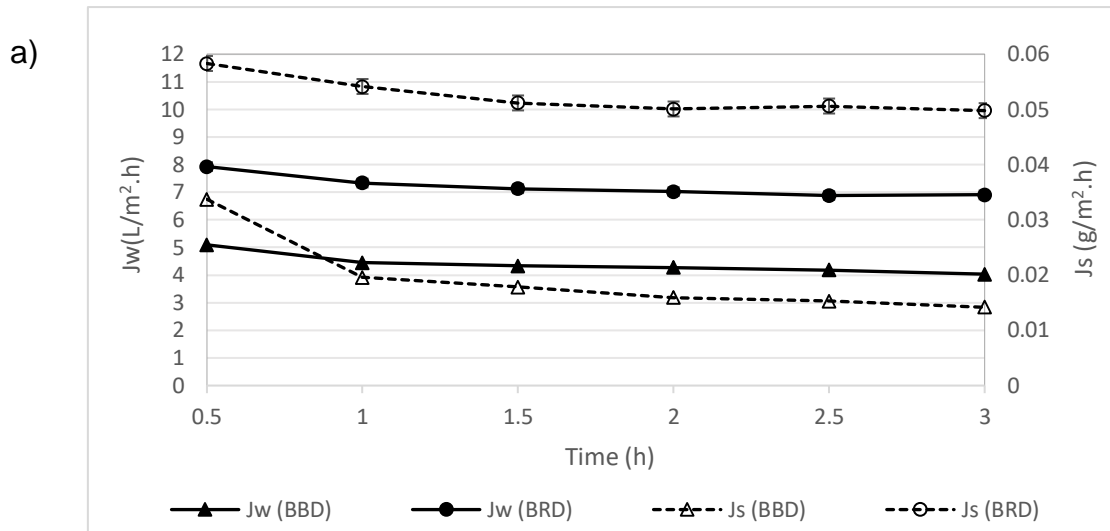
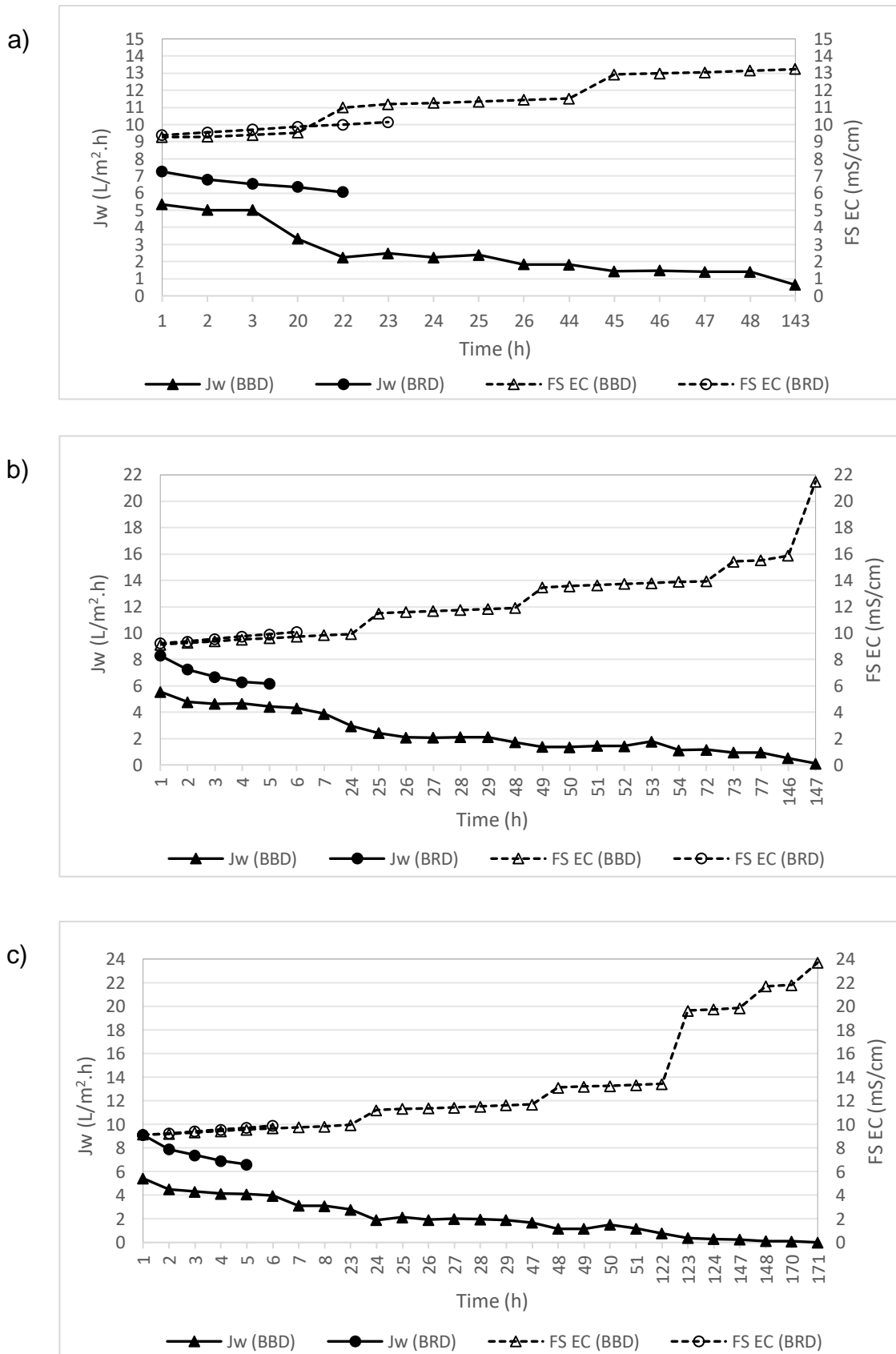Figure 4.16: Water flux (J_w) and J_s as a function of time using Maxilon Blue GRL (BBD) and Reactive Black 5 (BRD) as DS in FO mode at 200 ml/min in a) Test 1 b) Test 2 and c) Test 3

4.3.3.2 Reverse solute flux (J_s)

Table 4.8 tabulates the initial and final J_s in FO mode for Baseline 2 experiments with a DS of Maxilon Blue GRL and Reactive Black 5, respectively. It can be seen from Table 4.8 that the initial and final J_s achieved using Maxilon Blue GRL and Reactive Black 5 as DS in FO mode was similar in comparison. The J_s achieved is minute in this study which borders the idea of negligibility.

Table 4.8: The initial and final J_s in FO mode using Maxilon Blue GRL and Reactive Black 5 as DS

DS	Initial J_s (g/m^2.h)	Final J_s (g/m^2.h)
Reactive Black 5	0.04	0.03
Maxilon Blue GRL	0.05	0.03

Figure 4.16 illustrates the J_w and J_s obtained for the duration of a 3 h operation for Baseline 1 experiments using Maxilon Blue GRL and Reactive Black 5 as DS whilst operating in FO mode at a flowrate of 200 ml/min. While comparing the J_s achieved using Maxilon Blue GRL and Reactive Black 5 as DS, it can be observed that similar J_s were achieved in both sets of experiments. From Figure 4.16 (a), (b) and (c), it can be observed that the average initial and final J_s for the experiments using Reactive Black 5 as the DS were 0.04 and 0.03 g/m^2.h in comparison to the 0.05 and 0.03 g/m^2.h achieved while using Maxilon Blue GRL (BBD) as the DS.

4.3.3.3 Water recovery (R_e)

Figure 4.17 illustrates the R_e and water recovered (L) for the duration of a 3 h operation for Baseline 2 experiments using Maxilon Blue GRL and Reactive Black 5 as DS whilst operating in FO mode at a flowrate of 200 ml/min. Evaluating Figure 4.17 (a), (b) and (c), it can be observed that the rate of recovery decreased with respect to time. The average initial and final R_e for experiments using Reactive Black 5 as the DS were higher in comparison to the R_e achieved while using Maxilon Blue GRL as the DS. The low percentages achieved can be attributed to the duration of the experiments. Furthermore, water recovery is directly related to water flux and as such, it was expected that higher water recovery be obtained when using Reactive Black 5 as the DS as higher J_w was achieved when using Reactive Black 5.
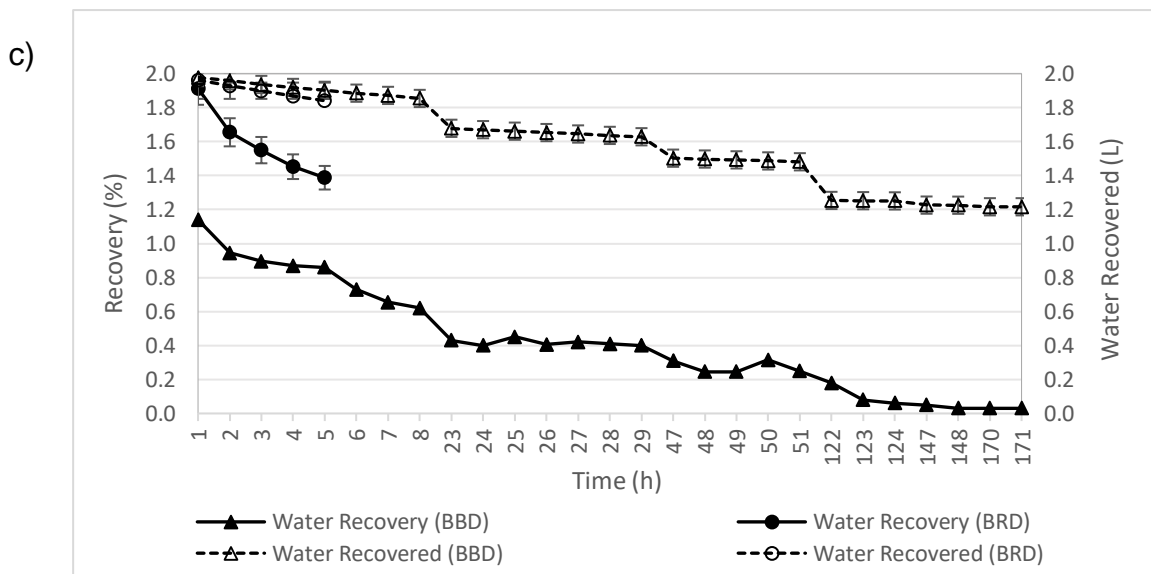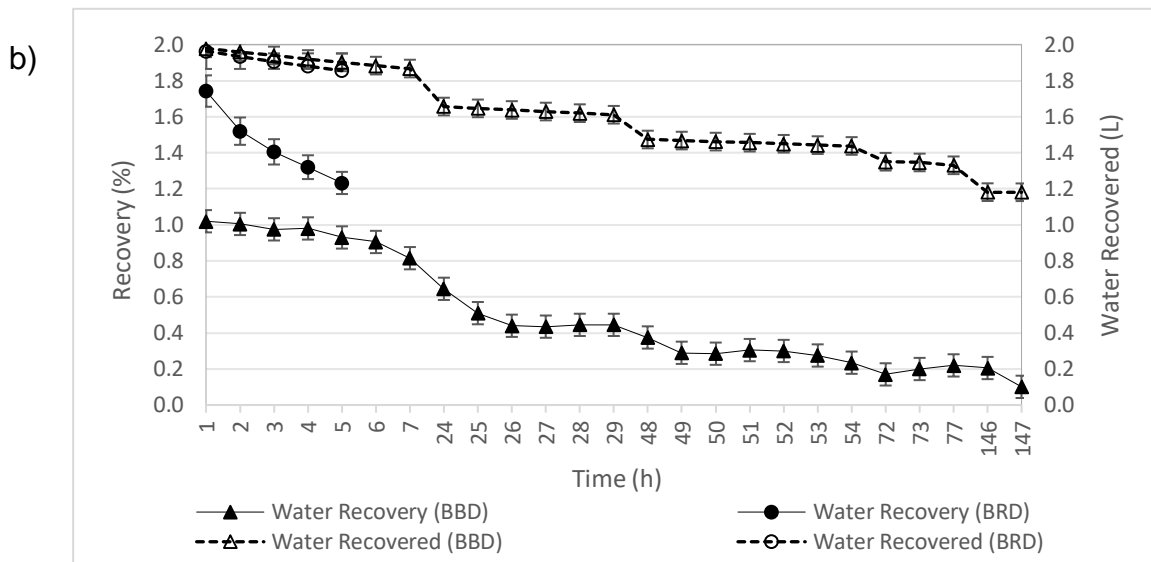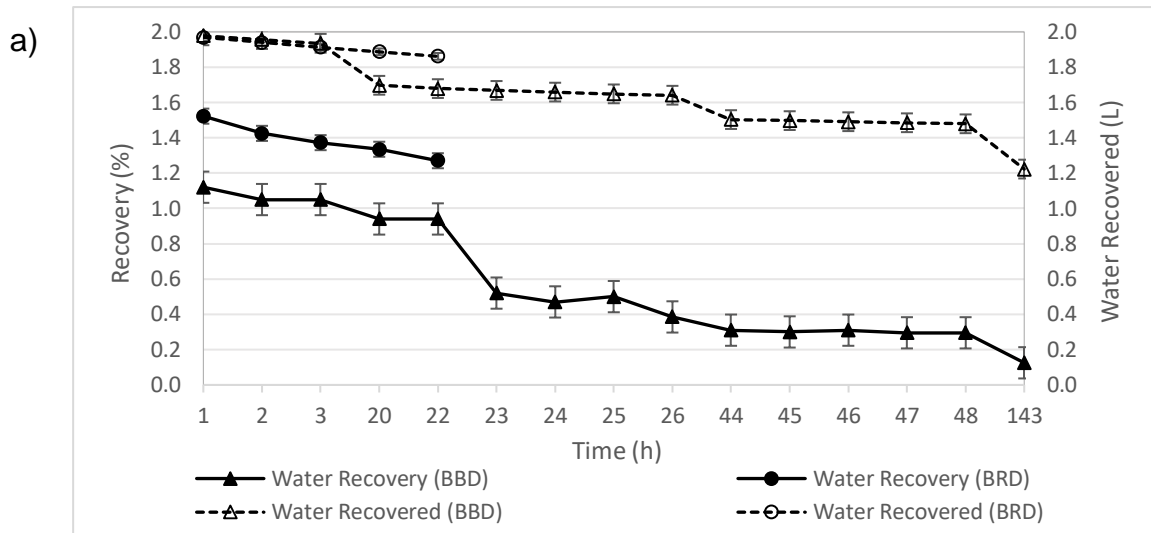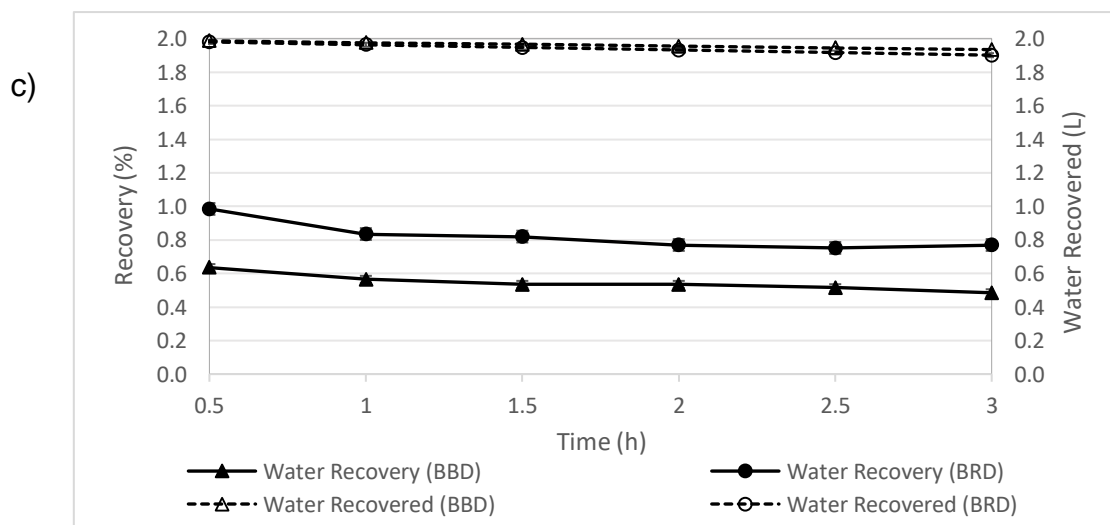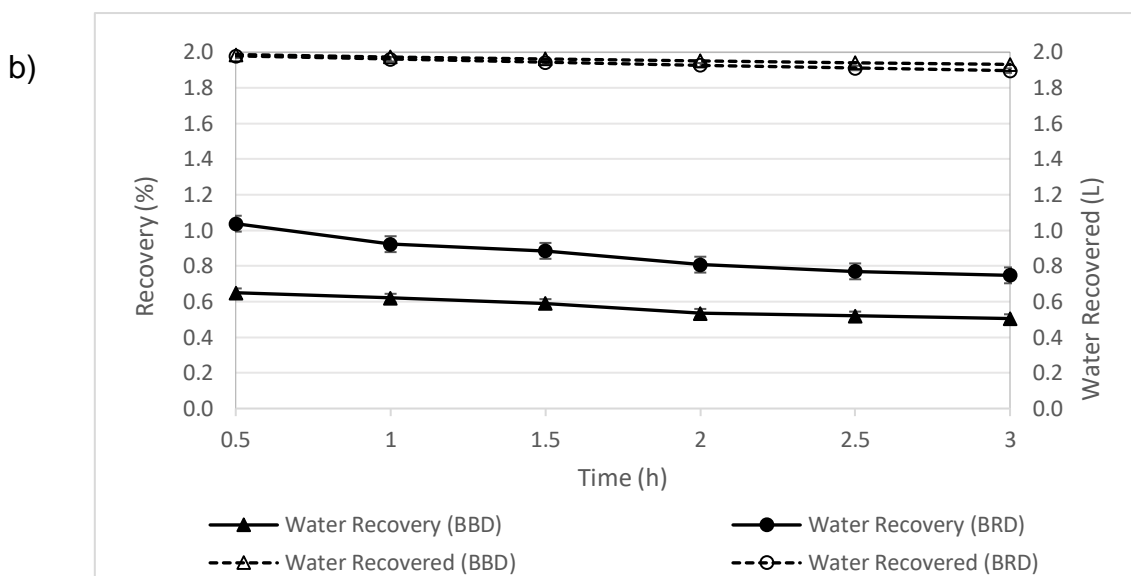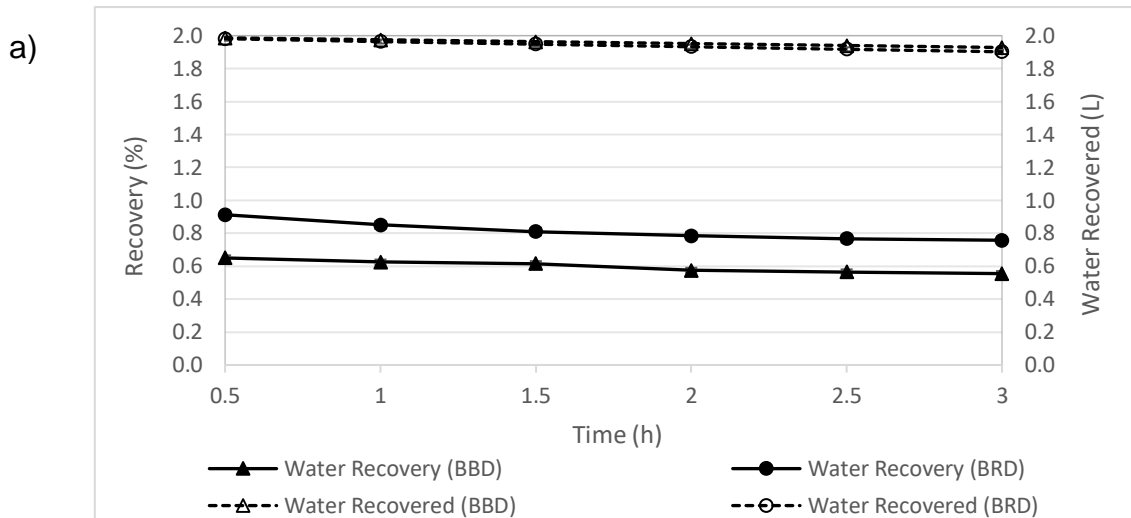
Figure 4.17: Water recovery (R_e) with respect to water recovered (L) as a function of time using Maxilon Blue GRL (BBD) and Reactive Black 5 (BRD) as DS in FO mode at 200 ml/min in a) Test 1 b) Test 2 and c) Test 3

4.3.3.4 Energy consumption (SEC)

Figure 4.18 illustrates the SEC for the duration of a 3 h operation for Baseline 2 experiments using Maxilon Blue GRL and Reactive Black 5 as DS whilst operating in FO mode at a flowrate of 200 ml/min. From Figure 4.18 (a), (b) and (c), it can be observed that the average initial and final SEC for experiments using Maxilon Blue GRL as DS were 1116.30 and 1411.50 kW.h/m^3 in comparison to the 218.09 and 284.84 kW.h/m^3 achieved when using Reactive Black 5 as the DS. It can be seen that the system consumes less energy while using Reactive Black 5 as the DS in comparison to Maxilon Blue GRL. Furthermore, it was observed in Figure 4.18 (a), (b) and (c) that the energy consumption increased with respect to the increase in time and flowrate. The use of Maxilon Blue GRL as DS resulted in an increase in energy consumption mainly due to the increase in the duration of the experiments.
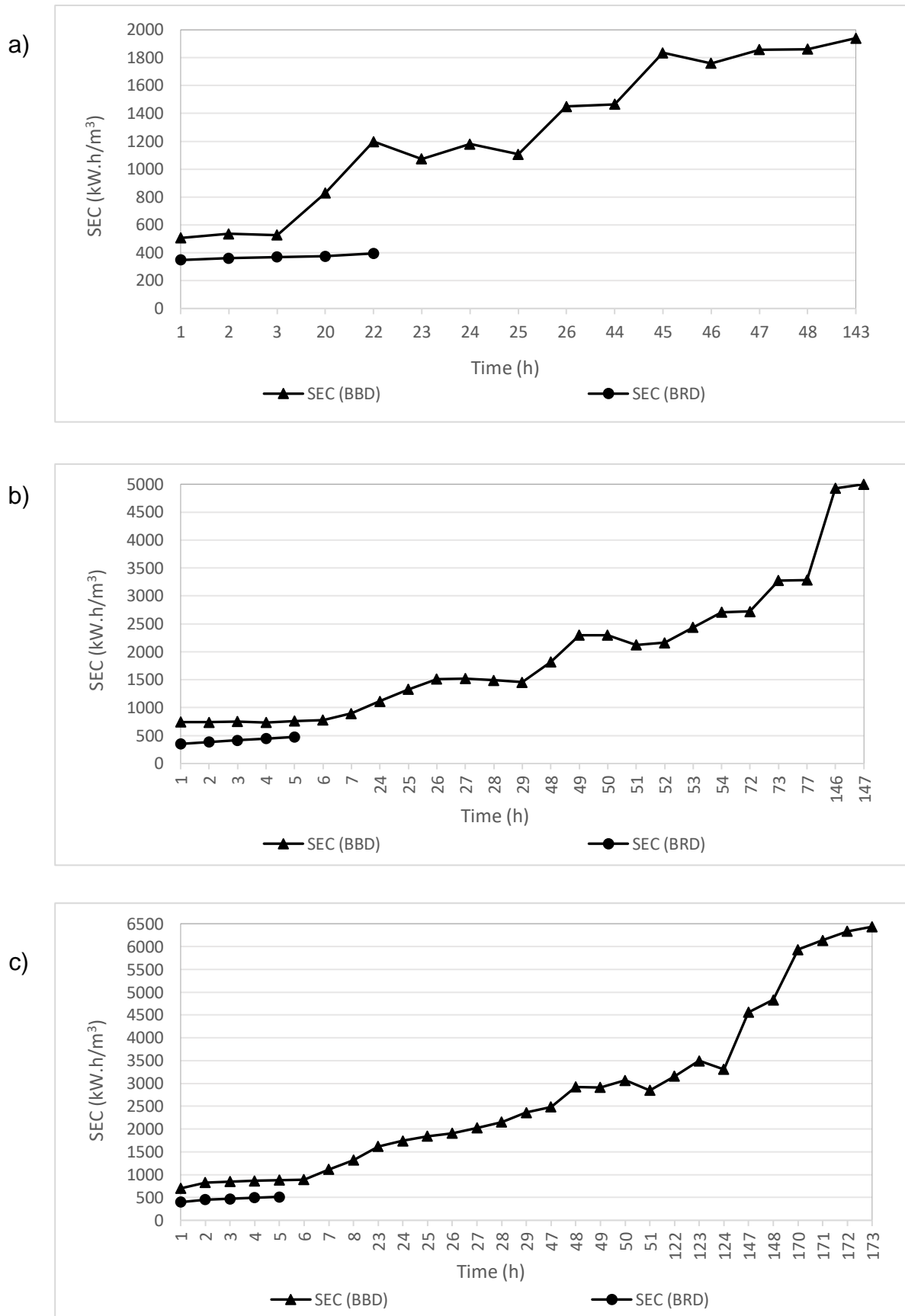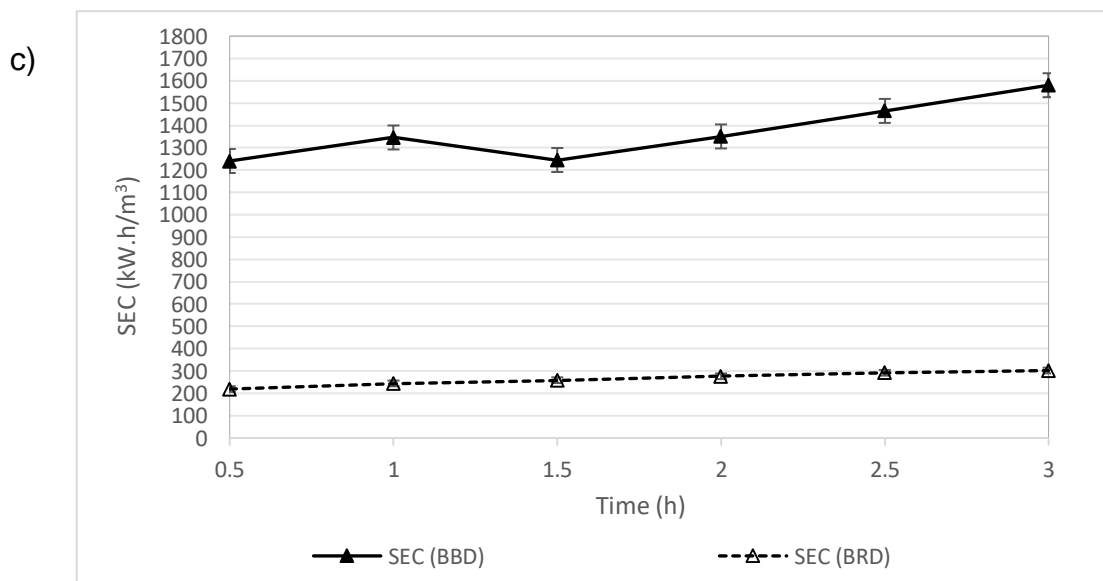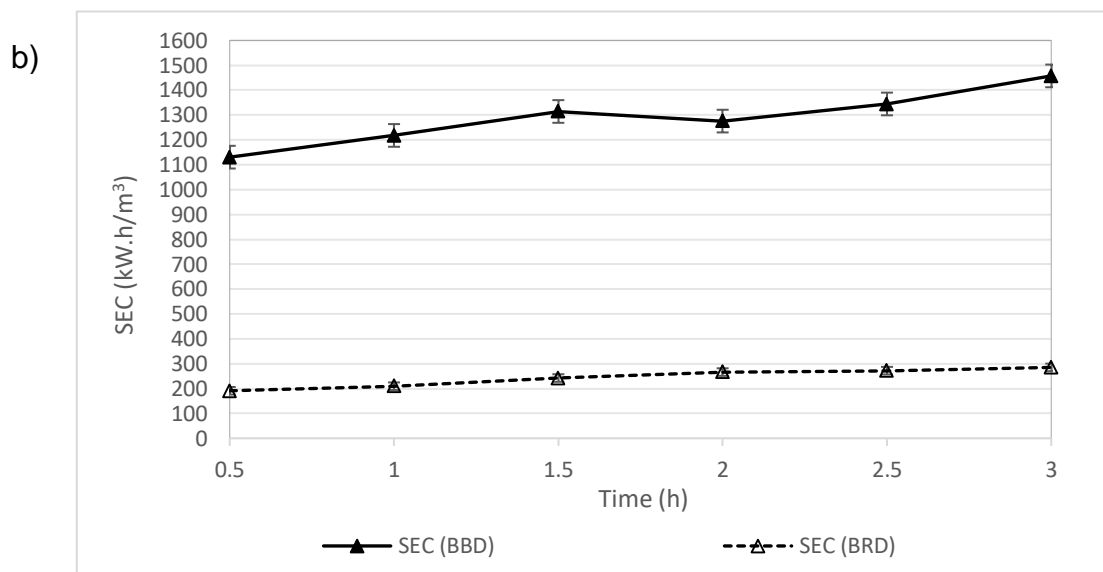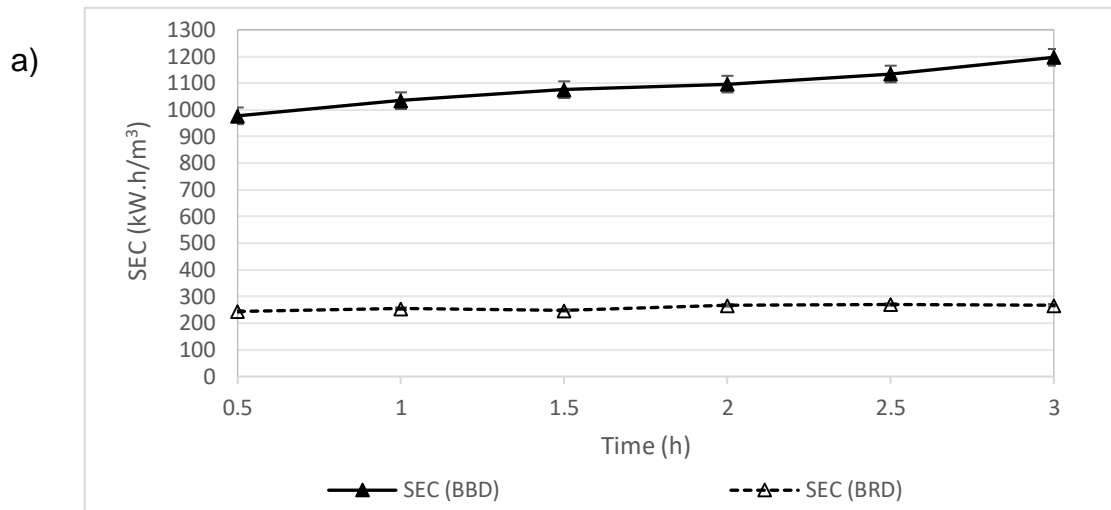
Figure 4.18: Energy consumption (SEC) as a function of time using Maxilon Blue GRL (BBD) and Reactive Black 5 (BRD) as DS in FO mode at 200 ml/min in a) Test 1 b) Test 2 and c) Test 3

4.4 Summary

Membrane integrity (refer to section 3.3.5 in Chapter 3) was investigated after the completion of an entire set of experiments to obtain an indication of the extent of damage on the membrane surface. No significant damage was observed on the membrane surface for any of the membrane integrity experiments as no visible methyl violet dye adhered to the membrane surface, therefore no results were available to report and discuss.

A change in membrane orientation had no significant impact on system performance and energy consumption. However, change in membrane orientation provided insight with regards to the magnitude of the energy consumption of the FO system while operating with Reactive Black 5 and Maxilon Blue GRL dye, respectively. Additionally, the observation of negligible changes in baseline 2 (membrane control) R_e and J_w results suggested the possible occurrence of membrane fouling during the main experiment (dye-driven FO system).

CHAPTER 5

CHAPTER 5: EFFECT OF FLOWRATES ON THE SYSTEM PERFORMANCE AND ENERGY CONSUMPTION OF A DYE DRIVEN FO SYSTEM

5.1 Introduction

This chapter provides the results of the impact of flowrates (i.e. feed and draw solution flowrates) on the performance and energy evaluation of Baseline 1, the Main and Baseline 2 experiments as described in Chapter 3. The system performance was evaluated in terms of J_w; J_s; and Re. The energy was evaluated in terms of SEC.

5.2 Dye solution: Reactive Black 5

5.2.1 Effect of flowrates on system performance and energy consumption: Baseline 1

This part of the study was conducted to be used as a basis of comparison to determine the impact on the energy consumption and system performance of the dye driven FO system. For the purposes of this part of the study, deionised water (DI) was used as the FS and Reactive Black 5 dye was used as the DS. Refer to Chapter 3 (section 3.2) for details of the operating conditions for this study.

5.2.1.1 Water flux (J_w)

Figure 5.1 illustrates the J_w obtained for the duration of a 3 h operation for Baseline 1 experiments whilst operating in a) FO and b) PRO modes at a flowrate of 200 ml/min. From Figure 5.1 (a), the average initial J_w was 9.70 L/m^2.h after which it steadily declined due to osmotic dilution to result in an average final J_w of 7.16 L/m^2.h. In Figure 5.1 (b), an average initial J_w of 11.71 L/m^2.h was obtained after which it can be seen that the J_w steadily declined to a final average J_w of 9.10 L/m^2.h.

The difference in water fluxes in the FO mode and PRO mode can be attributed to the difference in the membrane structural resistance depending on which sides of the solutions the support layer of the membrane is oriented. In the FO mode, the DS faces the porous support layer of the membrane, while the feed faces the active layer. The incoming water flux from the feed side dilutes the DS at the membrane's surface and within the membrane's porous support layer, reducing the net OP at the membrane's surface and lowering the Jw.

Since the OP of the DS at the membrane boundary layer is crucial to the FO process, dilutive ICP severely affects water flux in the FO process. It has been demonstrated that the

membrane orientation in FO poses critical impacts on internal concentration polarization (ICP), which dominates the water flux decline (McCutcheon and Elimelech, 2006).

a)

b)

Figure 5.1: Water fluxes (J_w) obtained for the duration of a 3 h operation for Baseline 1 experiments whilst operating in a) FO and b) PRO modes at a flowrate of 200 ml/min, respectively.

When the process is operated in PRO mode, the CP phenomenon reverses. Since the DS in PRO mode faces the membrane active layer, the phenomenon is dilutive ECP, which can be mitigated by the crossflow shear provided on the membrane surface. Although concentrative ICP occurs on the feed side of the membrane, its effect is less severe than dilutive ICP, and this is the reason why J_w in PRO mode is higher than in FO mode. Even though PRO mode results in higher J_w in the laboratory scale studies under controlled conditions, in a practical

situation, PRO mode is not suitable for desalination because the membrane is prone to severe membrane fouling as the porous support layer is directly exposed to the feed water containing scaling and fouling species (Tang *et al.*, 2010; Zou *et al.*, 2011; Zhao *et al.*, 2012).

5.2.1.2 Reverse solute flux (J_s)

From Figure 5.2 (a), the average initial J_s was 0.03 g/m^2.h (with an exception to test 3, which can be attributed to change in the tubing of the system due to deterioration) after which it steadily declined to an average final J_s of 0.02 g/m^2.h. In Figure 5.2 (b), an average initial J_s of 0.04 g/m^2.h was obtained after which it can be seen that the J_s decreased to a final average J_s of 0.02 g/m^2.h.

It can be observed that the J_s obtained in FO mode was less than that obtained in PRO mode. This observation agrees with other reports in the literature (Phuntsho *et al.*, 2013). This anticipated higher solute concentration at the membrane active layer in the PRO mode compared to the FO mode results in an increase in the osmotic driving force within the system which in turn results in a greater J_w and also increases the J_s .
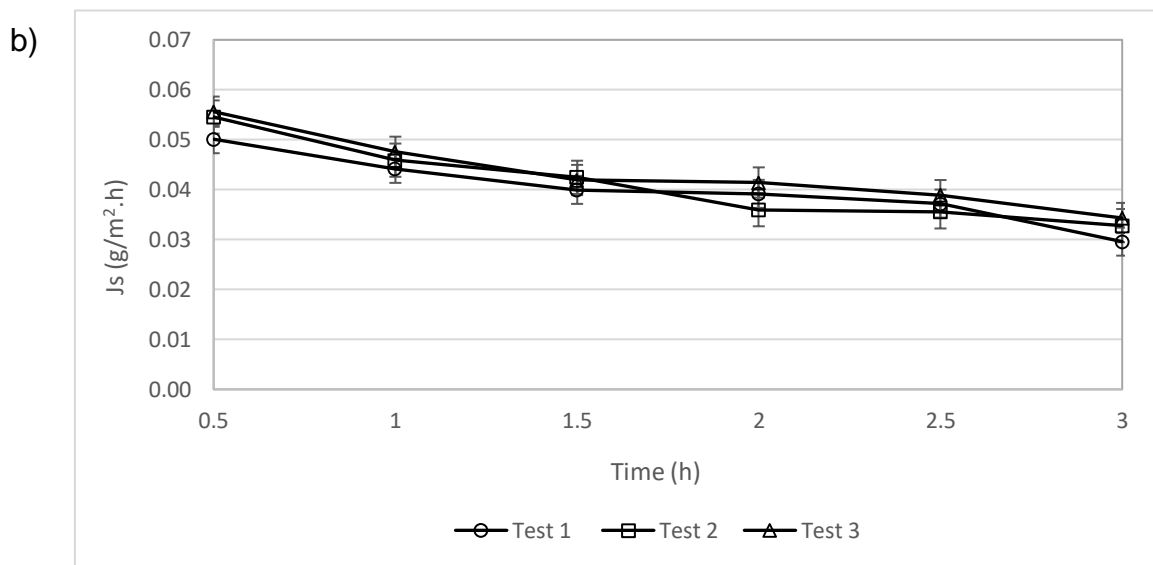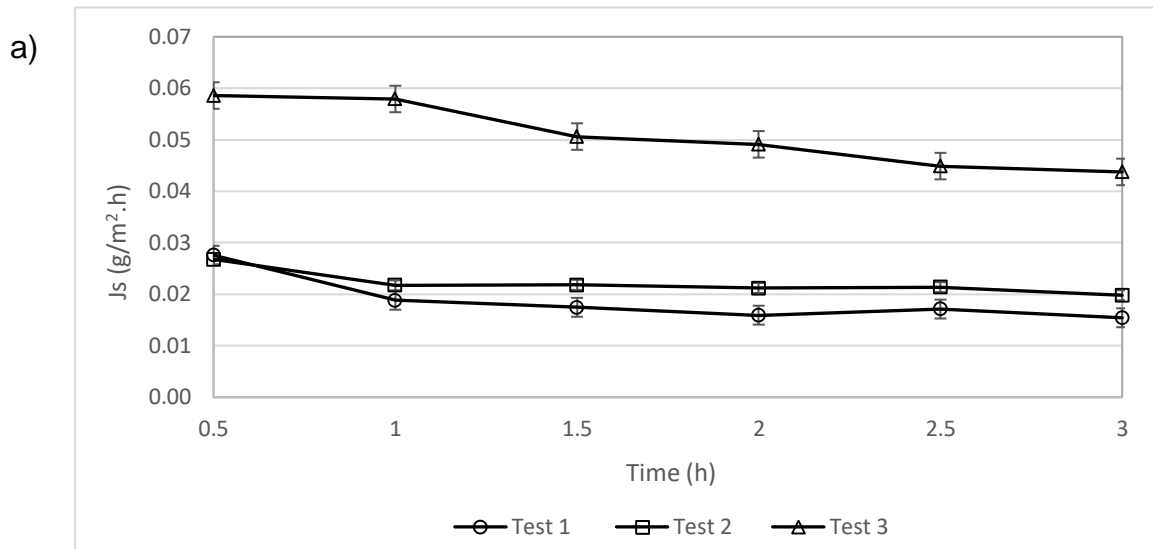
Figure 5.2: Reverse solute flux (J_s) obtained for the duration of a 3 h operation for Baseline 1 experiments whilst operating in a) FO and b) PRO modes at a a flowrate of 200 ml/min, respectively.

5.2.1.3 Water recovery (R_e)

Water recovery is directly related to water flux and as such, it can be observed from Figure 5.3 (a), a lower percentage of water was recovered in FO mode compared to that of the PRO mode in Figure 5.3 (b). The low percentages achieved can be attributed to the duration of the experiments. The experiments lasted for 3 h in comparison to experiments in literature which are run for 24 h for example. This phenomenon was assumed to be owing to the presence of CP as mentioned in Section 4.
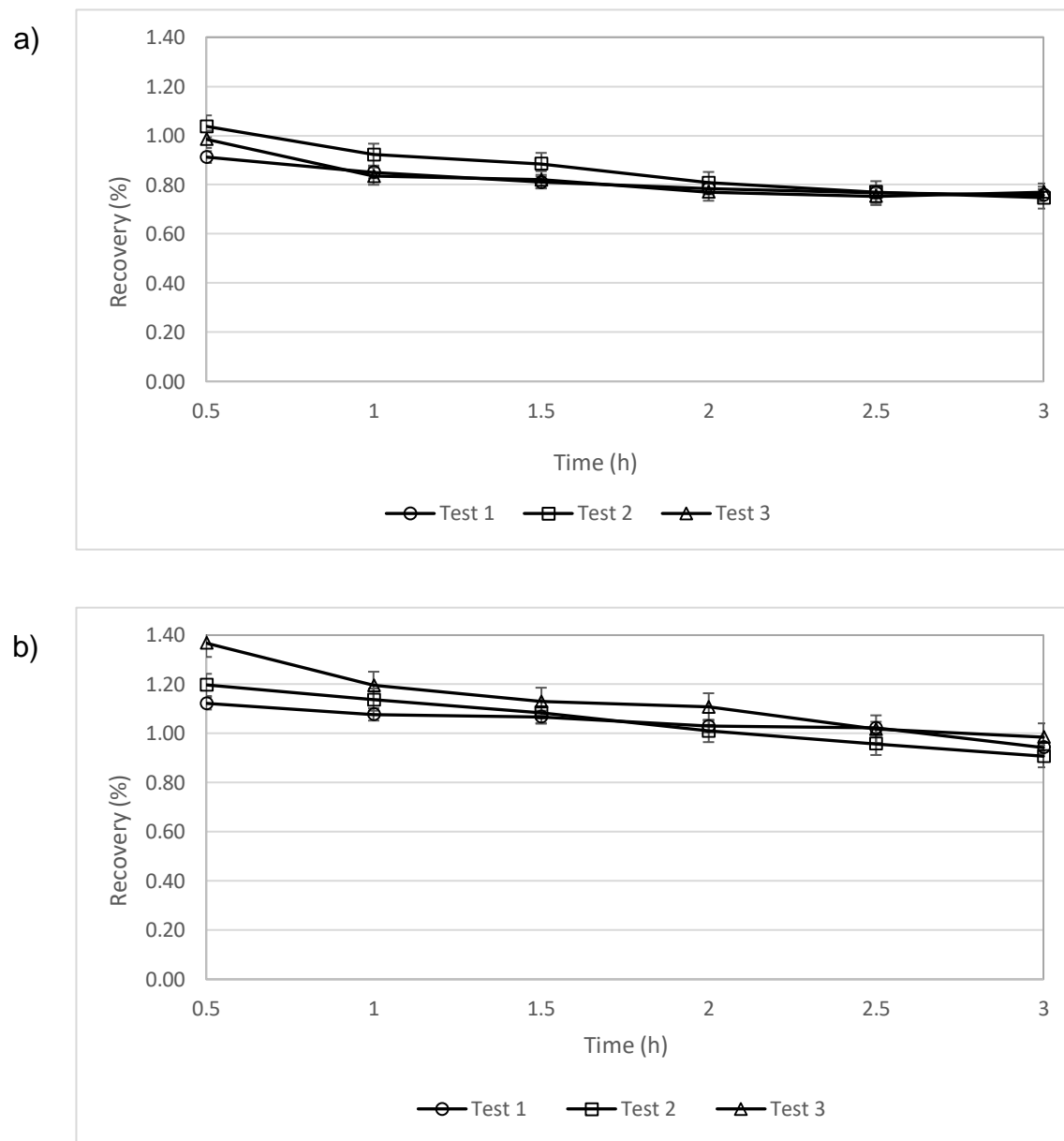
Figure 5.3: Percentage recovery (R_e) obtained for the duration of a 3 h operation for Baseline 1 experiments whilst operating in a) FO and b) PRO modes at a flowrate of 200 ml/min.

5.2.1.4 Energy consumption (SEC)

From Figure 5.4 (a), the average initial SEC was 219.80 kW.h/m^3 after which it steadily increased to an average final SEC of 267.24 kW.h/m^3. In Figure 5.4 (b), an average initial SEC of 193.89 kW.h/m^3 was obtained after which it steadily increased to a final average SEC of 233.49 kW.h/m^3. It can be observed that the SEC obtained in FO mode was much higher than that of the SEC obtained in PRO mode. The higher SEC obtained in FO mode can be attributed to the longer duration of experiments in FO mode in comparison to PRO mode, i.e. higher pump energy was required to operate for a more extended period. It was expected that the SEC increase would be directly proportional to the rise in flowrate as the pump would require more power to pump faster at a higher flowrate. According to studies conducted by Lambrechts (2018), higher SEC was obtained with higher flowrates.

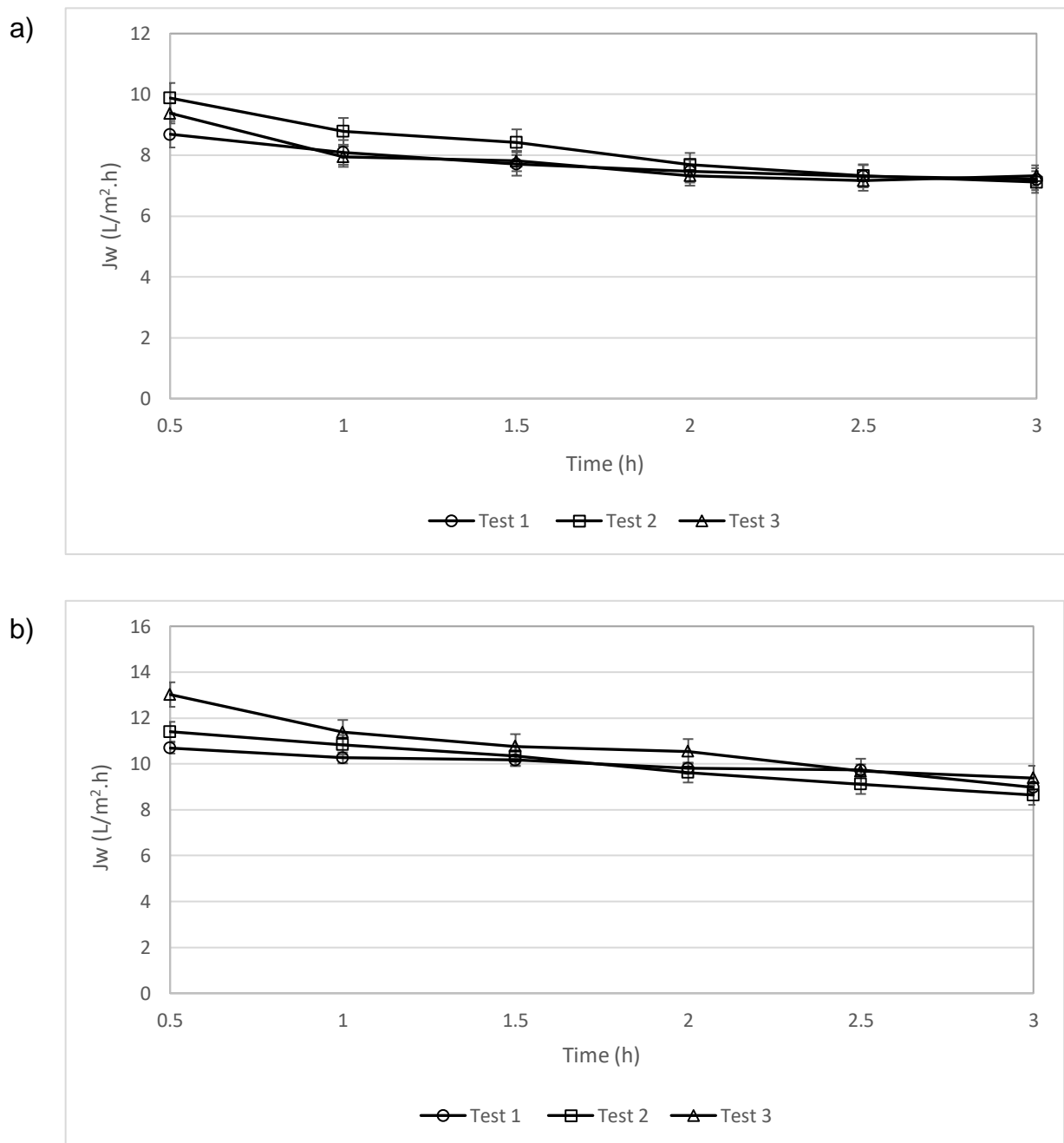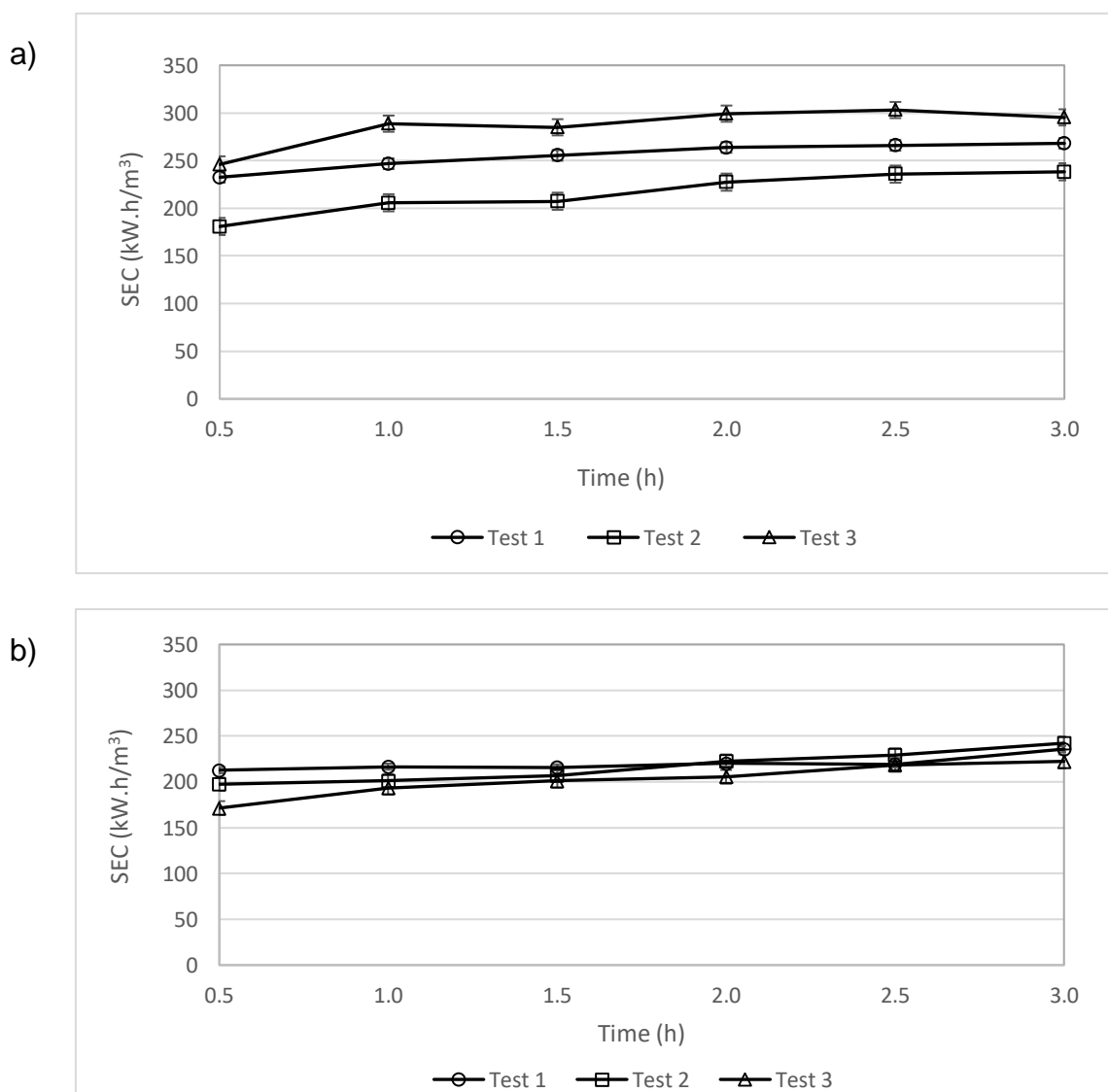Figure 5.4: Energy consumption (SEC) obtained for the duration of a 3 h operation for Baseline 1 experiments whilst operating in a) FO and b) PRO modes at a flowrate of 200 ml/min.

5.2.2 Effect of flowrates on system performance and energy consumption: Main experiment using Reactive Black 5

For the purposes of this part of the study, SBW5 was used as the FS and Reactive Black 5 dye was used as the DS. Refer to Chapter 3 (section 3.3) for details of the operating conditions. To evaluate the effect of flowrates on the system performance which relates to the water flux (J_w), reverse solute flux (J_s) and water recovery (Re), experiments were run at 400, 500 and 600 ml/min, respectively.

5.2.2.1 Water Flux (J_w)

Figure 5.5 illustrates the J_w obtained whilst operating in a) FO and b) PRO modes with SBW5 as the FS and Reactive Black 5 dye as DS (for flowrates of 400, 500 and 600 ml/min), respectively. Operating at the lowest flowrate of 400 ml/min, it can be seen in Figure 5.5 (a) that an initial J_w of 7.25 L/m^2.h was attained which decreased linearly to a final flux of 6.05 L/m^2.h. Furthermore, at a flowrate of 500 ml/min an initial J_w of 8.30 L/m^2.h was achieved which once again decreased linearly for the 5 h duration to a final J_w of 5.87 L/m^2.h. Finally, at the highest flowrate of 600 ml/min, an initial J_w of 9.11 L/m^2.h was achieved which decreased to a final flowrate of 6.61 L/m^2.h.

Taking into consideration Figure 5.5 (b), it can be seen that at the lowest flowrate of 400 ml/min, an initial J_w of 10.01 L/m^2.h was achieved which decreased to a final flux of 7.99 L/m^2.h at the end of the 4 h duration. At a flowrate of 500 ml/min, it was found that an initial J_w of 10.56 L/m^2.h was achieved which decreased to a final J_w of 6.95 L/m^2.h at the end of the 4 h duration. Lastly, it can be seen that at the highest flowrate of 600 ml/min, an initial J_w of 11.55 L/m^2.h was attained which again decreased to a final J_w of 7.55 L/m^2.h at the end of the 4 h duration.

Interpreting the trend in Figure 5.5 (a) and (b), it can be seen that the J_w achieved for flowrates of 400, 500 and 600 ml/min, followed the same phenomena of achieving a higher initial J_w which decreases to a final J_w nearing the completion of the individual experiments. It can also be observed that at 400 ml/min, the lowest J_w is achieved whilst, the highest J_w was achieved at the highest flowrate of 600 ml/min. However, when comparing Figure 5.5 (a) to Figure 5.5 (b), it can be seen that higher J_w is achieved in PRO mode compared to that of FO mode.

In literature, it was observed that there is a significant improvement in the system performance of a FO operation in conjunction with an increase in the system flowrate. In accordance with the film theory which states that an increase in the flowrate of the system will result in the varying of the flow regime of the system, in response to which the formation of the ECP would be reduced (Wang *et al.*, 2016; Phuntsho *et al.*, 2013).

The similarity of the J_w trends observed in accordance with the varying flowrates of 400, 500 and 600 ml/min, can be attributed to the low ECP formation. It can be observed that higher J_w was achieved at higher flowrates which is indicative of the fact that at higher flowrates, the effect of ECP is mitigated more efficiently. The decrease in J_w with respect to time can be attributed to the reduction of the osmotic driving force within the system which in turn contributed to a reduction in the water flow across the system. The results in Figure 5.5 indicated that the J_w increased when the FO system was operated at higher flowrates which corroborates well with previous studies (Lee *et al.*, 2010; Lambrechts, 2018).

Figure 5.5: Water flux (J_w) obtained operating in a) FO (5 h) and b) PRO (4 h) modes for flowrates of 400, 500 and 600 ml/min, respectively.

5.2.2.2 Water recovery (R_e)

Figure 5.6 (a) and (b) illustrates the R_e obtained for flowrates of 400, 500 and 600 ml/min, whilst operating in a) FO and b) PRO modes with SBW5 as the FS and Reactive Black 5 dye as DS, respectively.

Interpreting the trend observed in Figure 5.6 (a) and (b), it was observed that the R_e achieved for flowrates of 400, 500 and 600 ml/min, followed the same phenomena of achieving a higher initial R_e which proceeded to a lower final R_e nearing the completion of the individual experiments. It was also observed that at the lowest flowrate of 400 ml/min, the lowest R_e was achieved whilst the highest R_e was achieved at the highest flowrate of 600 ml/min. However, when comparing Figure 5.6 (a) to Figure 5.6 (b), it can be seen that higher R_e was achieved in Figure 5.6 (b) compared to that of Figure 5.6 (a).

As mentioned in the previous text, an increase in the flowrate contributes to an improvement of the system performance as a result of which the layers of ECP are reduced. The reduction of ECP contributes to the production of a greater effective osmotic driving force within the system and in turn, greater R_e is achieved. The varying flowrates could have played a role in the mitigation of ECP which resulted in greater R_e.
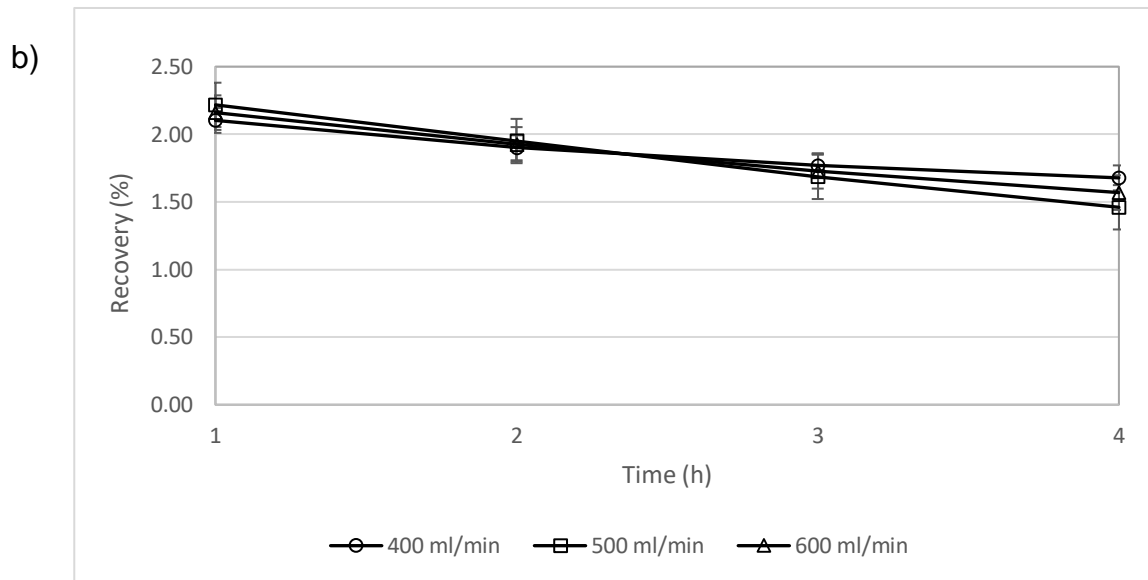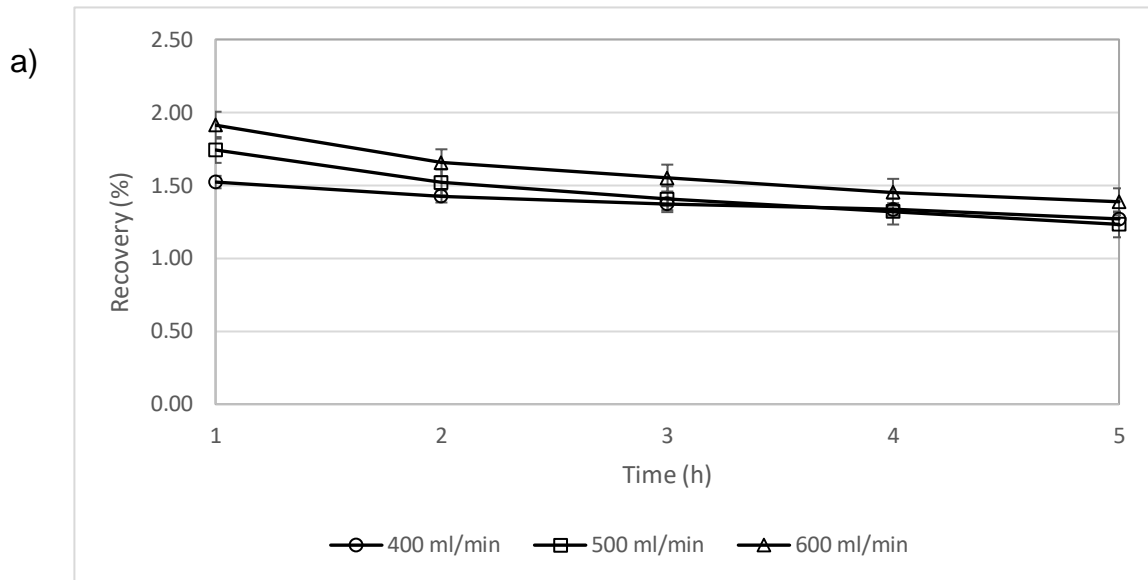
Figure 5. 6: Water recovery (R_e) obtained operating in a) FO (5 h) and b) PRO (4 h) modes with SBW5 as the FS and Reactive Black 5 dye as the DS for flowrates of 400, 500 and 600 ml/min, respectively.

5.2.2.3 Energy consumption (SEC)

Figure 5.7 (a) and (b) illustrate the SEC obtained whilst operating in a) FO and b) PRO modes with SBW5 as the FS and Reactive Black 5 dye as DS for flowrates of 400, 500 and 600 ml/min, respectively. Operating at the lowest flowrate of 400 ml/min, it can be seen in Figure 5.7 (a) that an initial SEC of 347.41 kW.h/m^3 was attained which increased to a final SEC of 394.99 kW.h/m^3 at the end of the 5 h duration. Furthermore, at a flowrate of 500 ml/min, an initial SEC of 351.35 kW.h/m^3 was achieved which once again increased to a final SEC of 476.02 kW.h/m^3. Finally, at the highest flowrate of 600 ml/min, an initial SEC of 398.87 kW.h/m^3 was achieved which increased to a final SEC of 515.88 kW.h/m^3.

Taking into consideration Figure 5.7 (b), it can be seen that at the lowest flowrate of 400 ml/min, an initial SEC of 301.05 kW.h/m^3 was achieved which increased to a final SEC of 362.02 kW.h/m^3. At a flowrate of 500 ml/min, it was found that an initial SEC of 344.27 kW.h/m^3 was achieved which increased to a final SEC of 471.94 kW.h/m^3. Lastly, it can be seen that at the highest flowrate of 600 ml/min, an initial SEC of 332.08 kW.h/m^3 was attained which increased to a final SEC of 479.75 kW.h/m^3 at the end of the 4 h duration.

Observations from Figure 5.7 (a) and (b) indicated that higher SEC was achieved at higher flowrates. The phenomena observed with respect to the SEC achieved in accordance with the respective flowrates is valid as it is expected that the SEC would increase with an increase in the flowrates as the pump would naturally require more power to pump faster at a higher flowrate. However, the fluctuation in the SEC trend can be attributed to the replacement of tubing within the pump head. Due to the use of a peristaltic pump, the tubing within the pump head was highly prone to damage as a result of which tubing within the head was replaced. An increase in the power consumption of the system was observed with the introduction of new tubing. It is proposed that the lack of flexibility of the new tubing instigated a resistance in relation to the rotation of the pump head. Due to the presence of the resistance, an increase in pump power consumption was expected as the pump would require more power to overcome the excess resistance. Over time, with the degradation of the tubing, a reduction in the pump power consumption was observed as a result of the increase in flexibility of the tubing contributing to a decrease in the resistance in the rotation of the pump head. The phenomena are further validated by the findings of Lambrechts (2018).
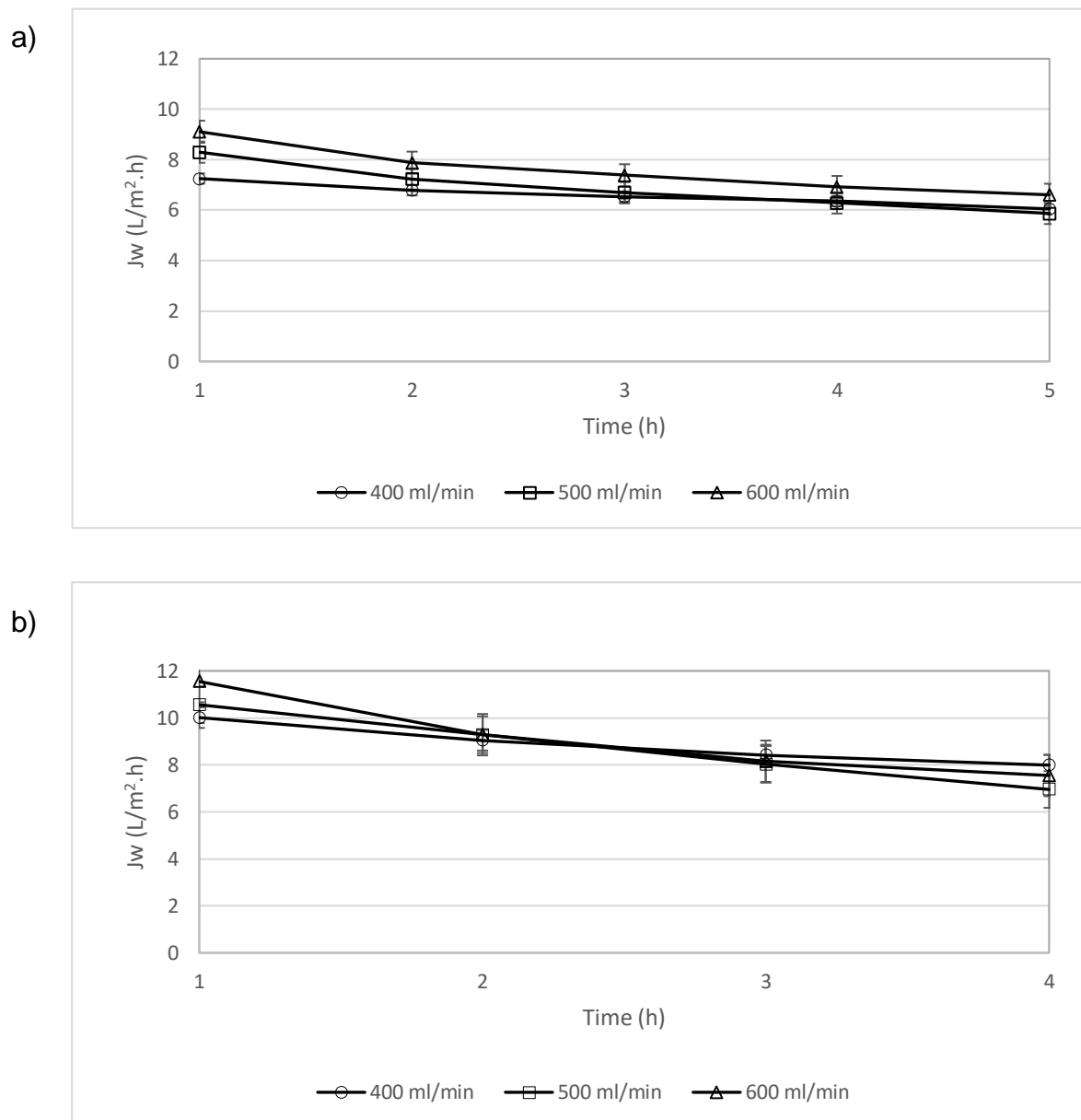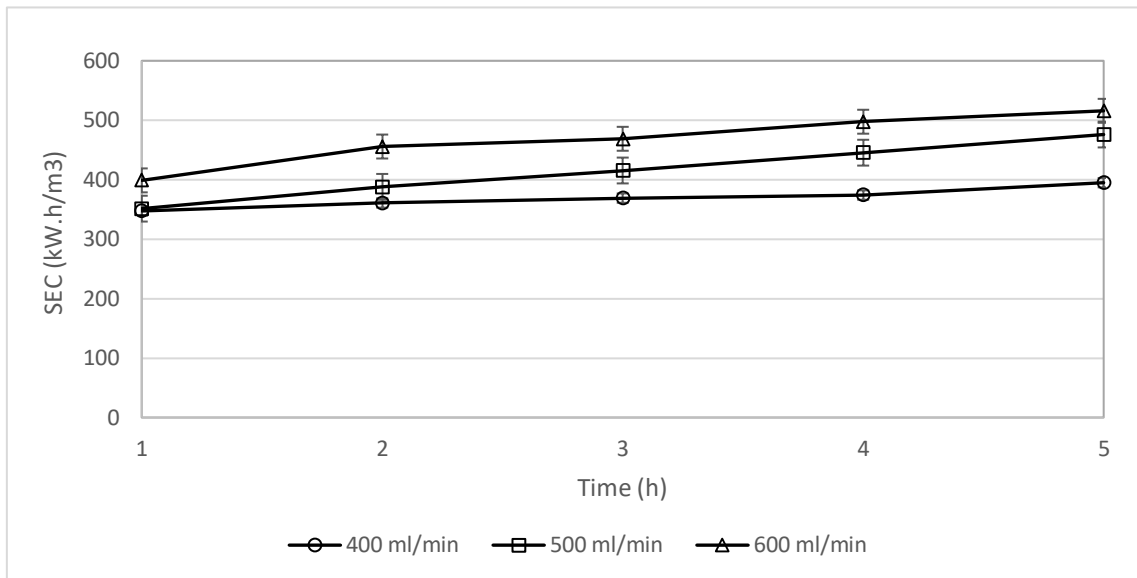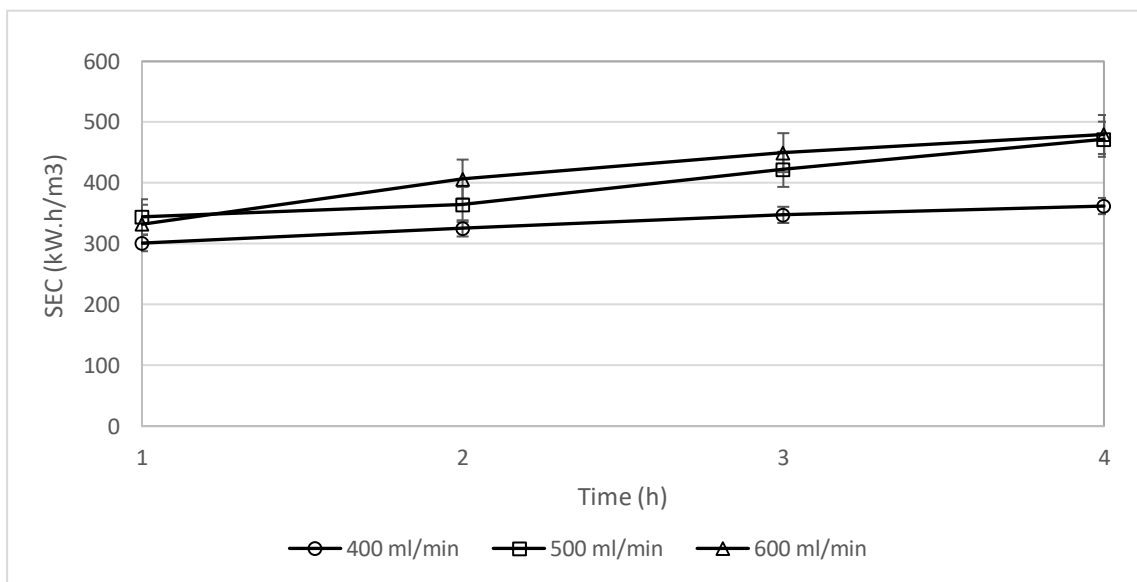
Figure 5.7: Energy consumption (SEC) obtained operating in a) FO (5 h) and b) PRO (4 h) modes for flowrates of 400, 500 and 600 ml/min, respectively.

5.2.3 Effect of flowrates on system performance and energy consumption: Baseline 2

This part of the study was conducted as a basis of comparison with Baseline 1 experiments to determine the extent of fouling and its impact on the system performance and energy consumption of a dye driven FO system. Deionised (DI) water was used as the FS and Reactive Black 5 dye was used as the DS. Refer to Chapter 3 (section 3.4) for details of the operating conditions for this part of the study. The system performance was related to the water flux (J_w), reverse solute flux (J_s), water recovery (R_e) and SEC.

5.2.3.1 Water flux (J_w)

From Figure 5.8 (a), the average initial J_w was 9.21 L/m^2.h after which it steadily decreased due to osmotic dilution to result in an average final J_w of 6.61 L/m^2.h. In Figure 5.8 (b), an average initial J_w of 10.76 L/m^2.h was obtained after which it can be seen that the J_w steadily decreased to a final average J_w of 8.68 L/m^2.h. The higher flux achieved in Figure 5.8 (b) was attributed to the presence of ICP as mentioned in the previous text.

Table 5.1 tabulates the initial and final J_w of baseline 1 and baseline 2 experiments. When comparing the J_w it could be seen that lower J_w was achieved in baseline 2 experiments compared to that of baseline 1. The decrease in J_w from baseline 1 to baseline 2, imply that fouling might have occurred during the experiments. However, no discernable trend can be observed between baseline 1 and 2 experiments indicating different degrees of fouling within the respective experiments. Furthermore, the extent of fouling could also not be established due to a lack of correlation between the experiments indicating inconsistent system performances.

Table 5.1: Comparison of the initial and final J_w of baseline 1 and baseline 2 experiments at a flowrate of 200 ml/min

Experiment	J_w (L/m^2.h)		
	Initial	Final	Average
Baseline 1	10.51	8.11	9.31
Baseline 2	9.99	7.65	8.82

a)

b)
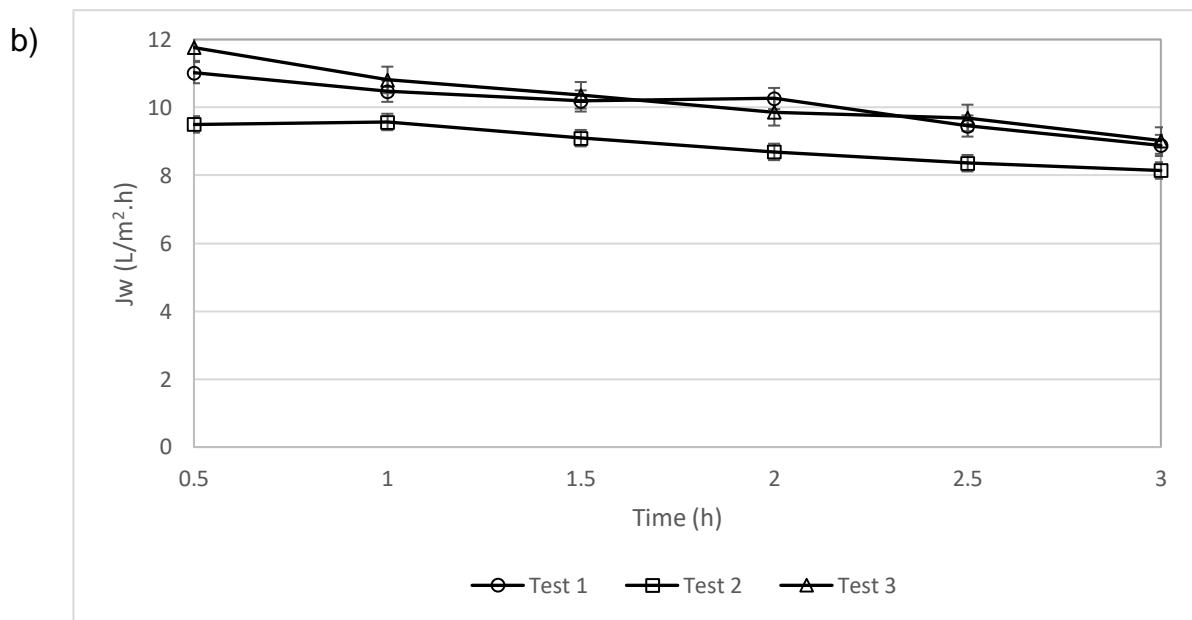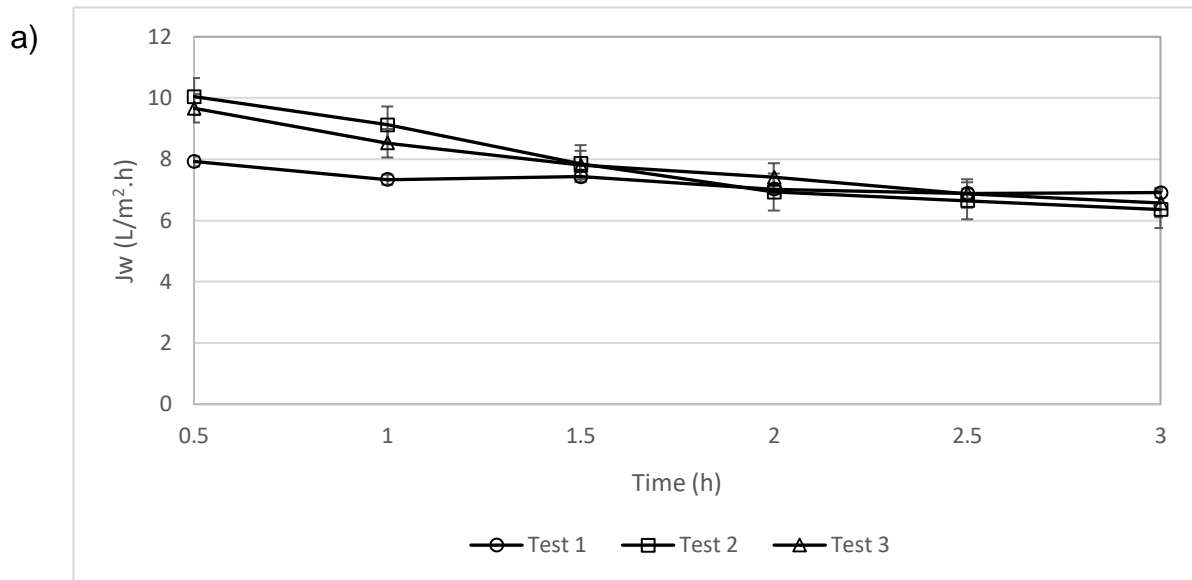
Figure 5.8: Water flux (J_w) obtained for the duration of a 3 h operation for Baseline 2 experiments whilst operating in a) FO and b) PRO modes at a flowrate of 200 ml/min, respectively.

5.2.3.2 Reverse solute flux (J_s)

Interpreting Figure 5.9 (a), the average initial J_s was 0.037 g/m^2.h after which it steadily declined to an average final J_s of 0.036 g/m^2.h. In Figure 5.9 (b), an average initial J_s of 0.042 g/m^2.h was obtained after which the J_s decreased to a final average J_s of 0.017 g/m^2.h. It can be observed that the J_s obtained in Figure 5.9 (a) was more than that of the J_s obtained in Figure 5.9 (b). Low J_s was expected due to the high solute rejection properties of CTA membranes (Chen *et al.*, 2017). Furthermore, the lower J_s achieved can also be attributed to the duration of experiments.

Table 5.2 tabulates the initial and final J_s of baseline 1 and baseline 2 experiments. When comparing the J_s , it could be seen that similar J_s was achieved in baseline 1 and 2 experiments. However, the average J_s achieved in baseline 2 was lower than that of the average J_s achieved in baseline 1 experiments. However, no distinct trend can be observed between baseline 1 and baseline 2 experiments indicating different degrees of fouling within the respective experiments. Furthermore, the extent of fouling could also not be established due to a lack of correlation between the experiments indicating inconsistent system performances.

Table 5.2: Comparison of the initial and final J_s of baseline 1 and baseline 2 experiments at a flowrate of 200 ml/min

Experiment	J_s (g/m^2.h)		
	Initial	Final	Average
Baseline 1	0.04	0.03	0.04
Baseline 2	0.04	0.03	0.03
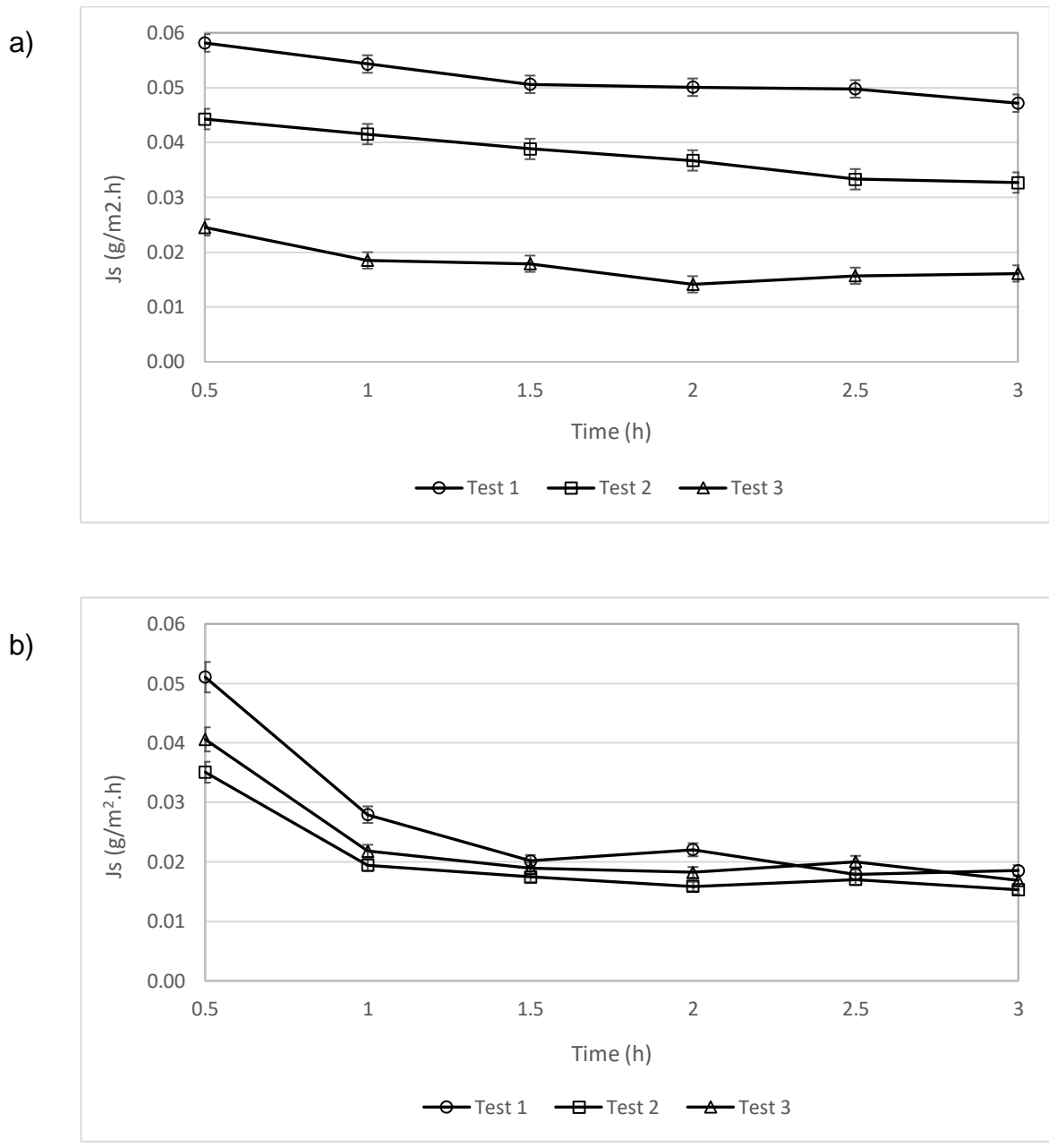
Figure 5.9: Reverse solute flux (J_s) obtained for the duration of a 3 h operation for Baseline 2 experiments whilst operating in a) FO and b) PRO modes at a flowrate of 200 ml/min, respectively.

5.2.3.3 Water recovery (Re)

Figure 5.10 (a) and (b) illustrates the R_e obtained whilst operating in a) FO and b) PRO modes using deionised (DI) water as the FS and Reactive Black 5 dye as DS, respectively. The low percentages achieved can be attributed to the duration of the experiments. The experiments lasted for 3 h in comparison to experiments in literature which are run for 24 h for example. As previously mentioned, there is a direct correlation between water flux and water recovery. Thus, it can be seen that on average, a higher water recovery was achieved in PRO mode in comparison to FO mode.
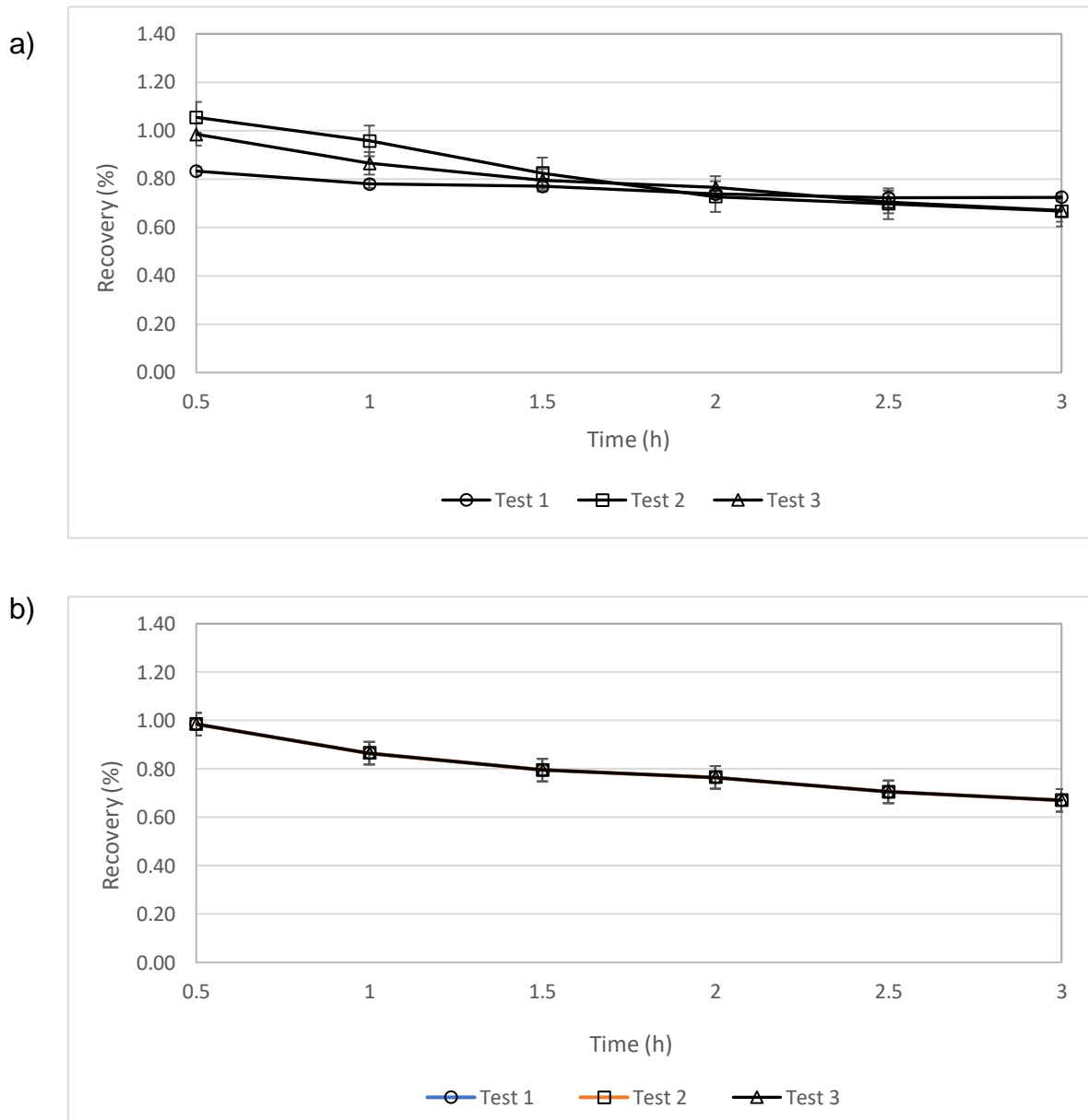
Figure 5.10: Water recovery (R_e) obtained for the duration of a 3 h operation for baseline 2 experiments whilst operating in a) FO and b) PRO modes at a flowrate of 200 ml/min, respectively.

5.2.4.4 Energy consumption (SEC)

From Figure 5.11 (a), the average initial SEC was 218.09 kW.h/m^3 after which it steadily increased to an average final SEC of 284.84 kW.h/m^3. In Figure 5.11 (b), an average initial SEC of 215.38 kW.h/m^3 was obtained after which it steadily increased to a final average SEC of 244.16 kW.h/m^3. It can be observed that the SEC obtained in Figure 5.11 (a) was much greater than that of the SEC obtained in Figure 5.11 (b).

Table 5.3 tabulates the initial and final SEC of baseline 1 and baseline 2 experiments. When comparing the SEC it could be seen that a higher SEC was achieved in baseline 2 experiments compared to that of baseline 1 experiments.

Table 5.3: Comparison of the initial and final SEC of baseline 1 and baseline 2 experiments

Experiment	SEC (kW.h/m^3)		
	Initial	Final	Average
Baseline 1	206.84	250.37	228.61
Baseline 2	216.74	264.50	240.62

a)

b)
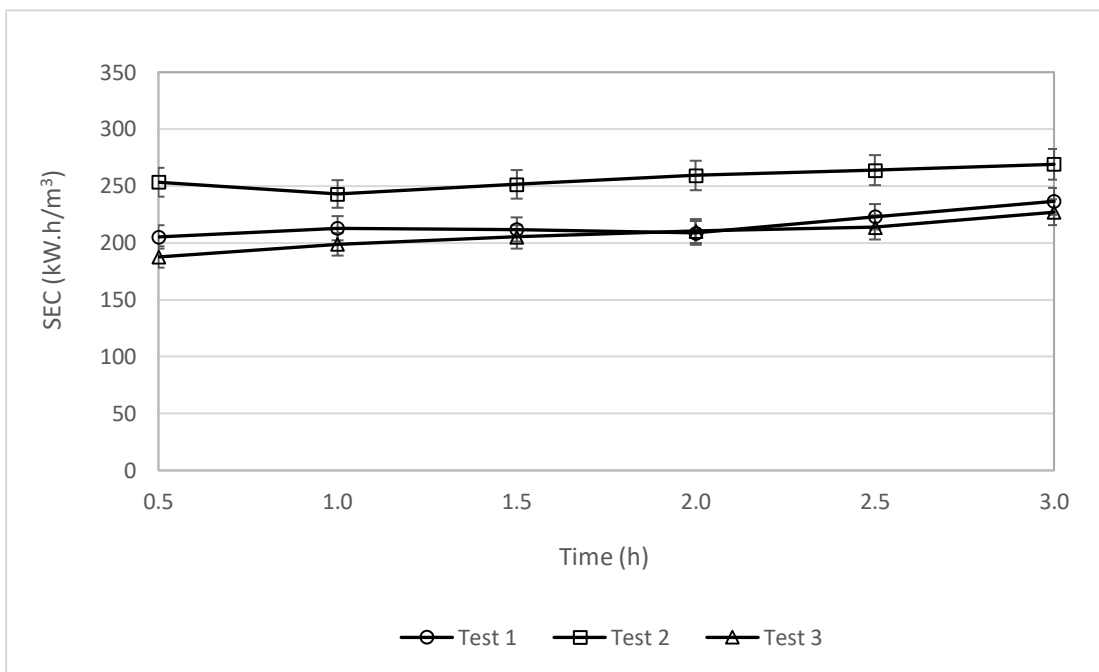
Figure 5.11: Energy consumption (SEC) obtained for baseline 2 experiments whilst operating in a) FO and b) PRO modes at a flowrate of 200 ml/min, respectively.

5.3 Dye solution: Maxilon Blue GRL

Maxilon Blue GRL was used as a DS as a basis of comparison with the Reactive Black 5 to investigate the impact of the change in DS on the performance and energy of the FO system. Due to the duration of the Main Experiments ($\pm$ 140 h to reach target concentration), while using the Maxilon Blue GRL as DS, a decision was made to conduct experiments only in the FO mode for purposes of comparison.

5.3.1 Effect of flowrates on system performance and energy consumption: Baseline 1

For this part of the study, deionised water (DI) was used as the FS and Maxilon Blue GRL was used as the DS. Refer to Chapter 3 section 3.2 for details of the operating conditions for this study. To evaluate the effect of flowrates on the system performance and energy consumption, the water flux (J_w), reverse solute flux (J_s), water recovery (R_e) and SEC was determined.

5.3.1.1 Water flux (J_w)

Figure 5.12 illustrates the J_w obtained Baseline 1 experiments using (a) Maxilon Blue GRL and (b) Reactive Black 5 dye as DS, whilst operating in the FO mode at a flowrate of 200 ml/min. From Figure 5.12 (a), the average initial J_w was 6.31 L/m^2.h after which it steadily declined due to osmotic dilution to result in an average final J_w of 4.70 L/m^2.h. In Figure 5.12 (b), an average initial J_w of 9.32 L/m^2.h was obtained after which the J_w steadily declined to a final average J_w of 7.22 L/m^2.h.

Observing Figure 5.12 (a) and (b), it can be seen that greater J_w was achieved whilst using Reactive Black 5 dye as DS in comparison to Maxilon Blue GRL dye. At a dye concentration of 0.02 mol/l, a ΔOP of $\pm$ 16000 kPa was achieved using Reactive Black 5 dye as DS in comparison to the ΔOP of $\pm$ 8000 kPa achieved using Maxilon Blue GRL dye as DS at a dye concentration of 0.02 mol/l. Furthermore, the molecular weight of Reactive Black 5 dye was 991 g/mol in comparison to the 482 g/mol of Maxilon Blue GRL dye. The phenomena observed with regards to J_w was expected as Reactive Black 5 dye has a greater molecular weight and also the ΔOP across the FO system is much greater as a result of which higher solute flow across the membrane cell is made possible due to which greater fluxes were achieved.

Figure 5.12: Water flux (J_w) obtained for baseline 1 experiments using a) Maxilon Blue GRL and b) Reactive Black 5 as DS whilst operating FO mode at a flowrate of 200 ml/min

5.3.1.2 Reverse solute flux (J_s)

Figure 5.13 (a) and (b) illustrates the reverse solute flux (J_s) obtained for baseline 1 experiments using a) Maxilon Blue GRL dye and b) Reactive Black 5 dye as DS whilst operating in FO mode at a flowrate of 200 ml/min. From Figure 5.13 (a), the average initial J_s was 0.052 g/m^2.h after which it steadily declined to an average final J_s of 0.029 g/m^2.h. In Figure 5.13 (b), an average initial J_s of 0.037 g/m^2.h was obtained after which it can be seen that the J_s declined to a final average J_s of 0.026 g/m^2.h. It can be observed that the J_s obtained in Figure 5.13 (a) and (b) were quite similar (with an exception to test 3, which can be attributed to change of tubing due to deterioration) insinuating the fact that the change in DS had little to no impact on J_s.
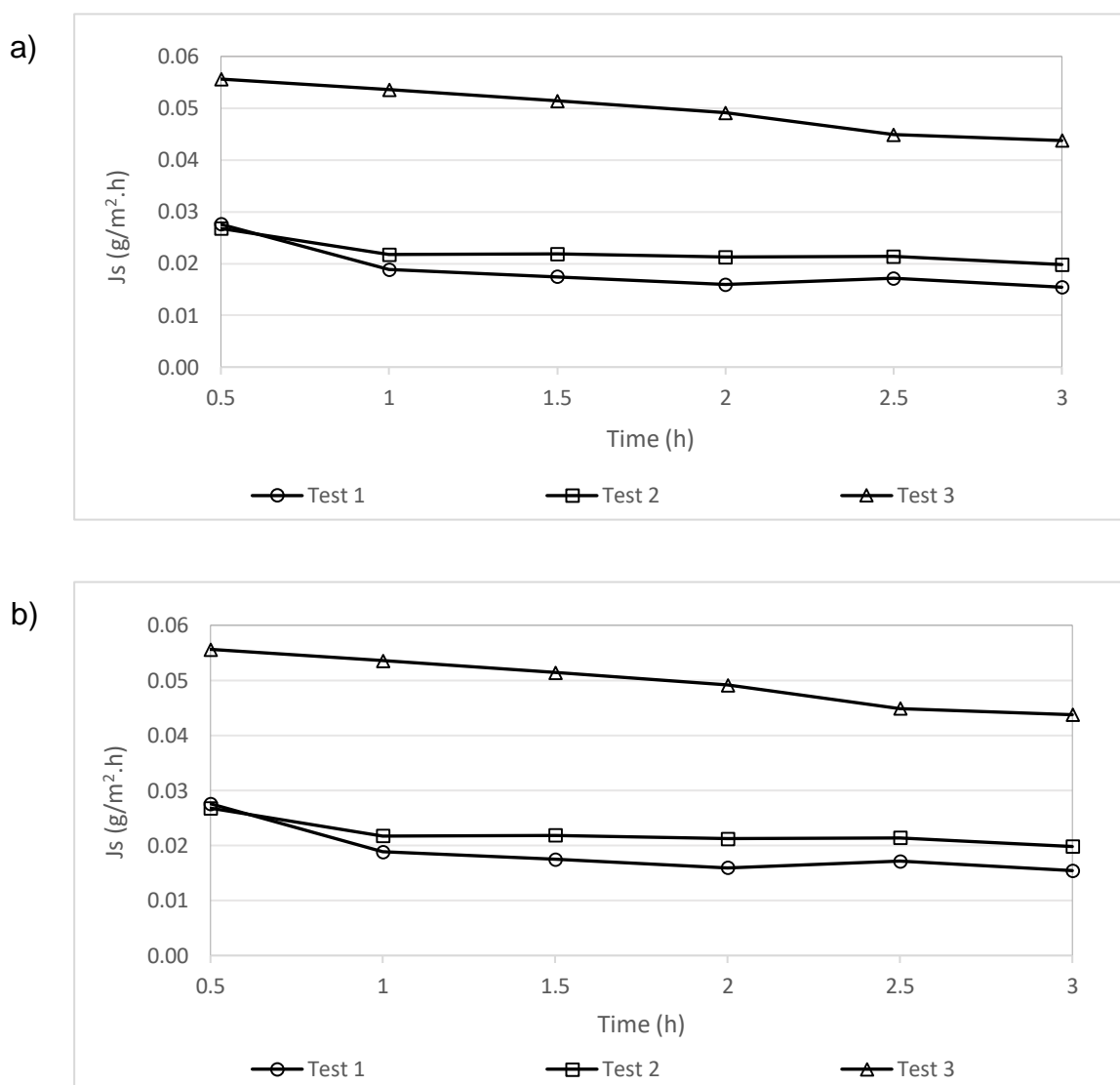
Figure 5.13: Reverse solute flux (J_s) obtained for baseline 1 experiments using a) Maxilon Blue GRL and b) Reactive Black 5 as DS whilst operating FO mode at a flowrate of 200 ml/min

5.3.1.3 Water recovery (R_e)

Figure 5.14 (a) and (b) illustrates the R_e obtained for baseline 1 experiments using a) Maxilon Blue GRL dye and b) Reactive Black 5 dye as DS whilst operating in FO mode at a flowrate of 200 ml/min. The low percentages achieved can be attributed to the duration of the experiments. The experiments lasted for 3 h in comparison to experiments in literature which are run for 24 h for example. Observing Figure 5.14 (a) and (b), it can be concluded that the change in DS had no impact on the water recovery as similar recoveries were achieved in both Figure 5.14 (a) and (b).

a)

b)
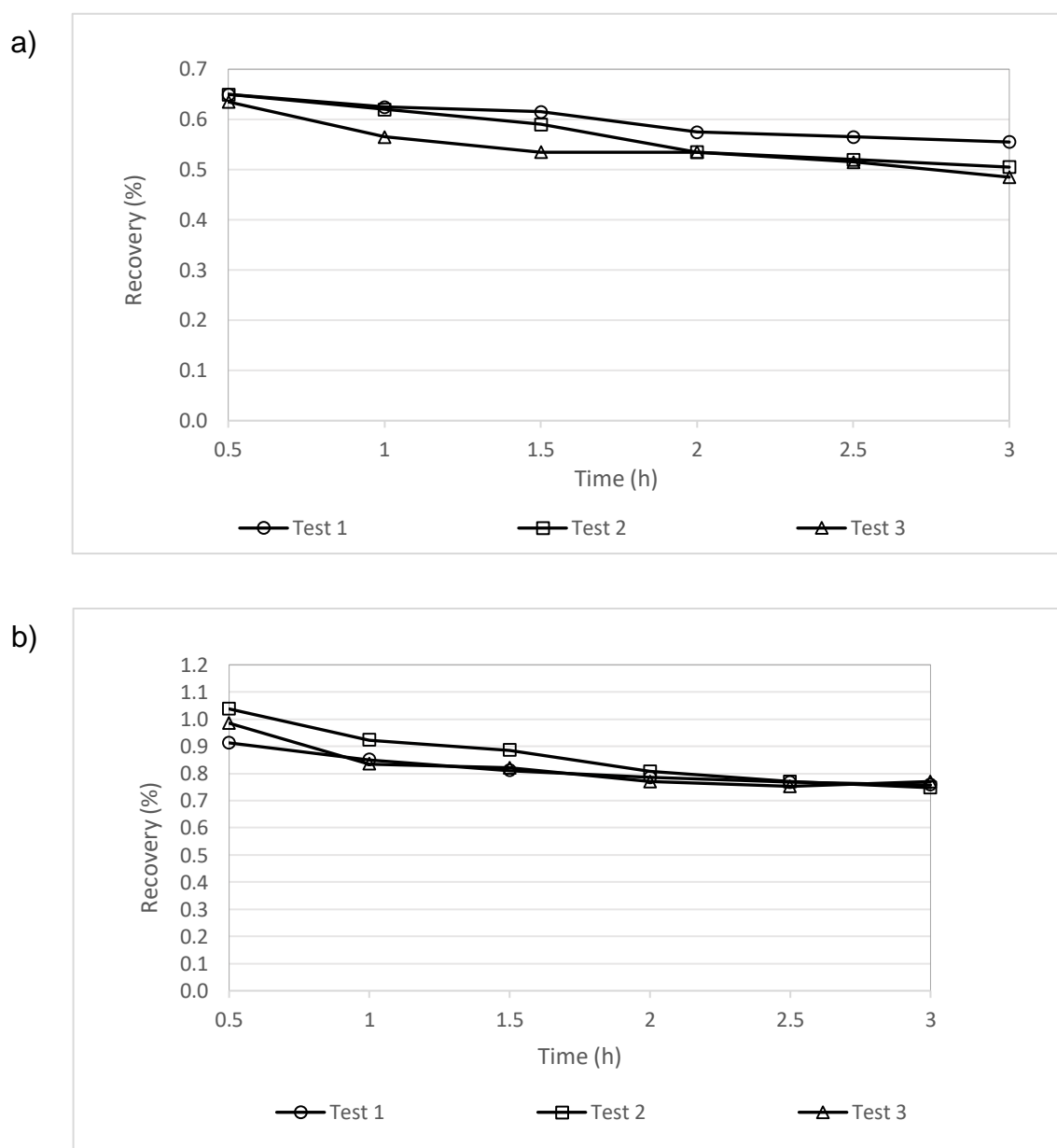
Figure 5.14: Water recovery (R_e) obtained for the duration of a 3 h operation for Baseline 1 experiments using a) Maxilon Blue GRL and b) Reactive Black 5 as DS whilst operating in FO mode at a flowrate of 200 ml/min.
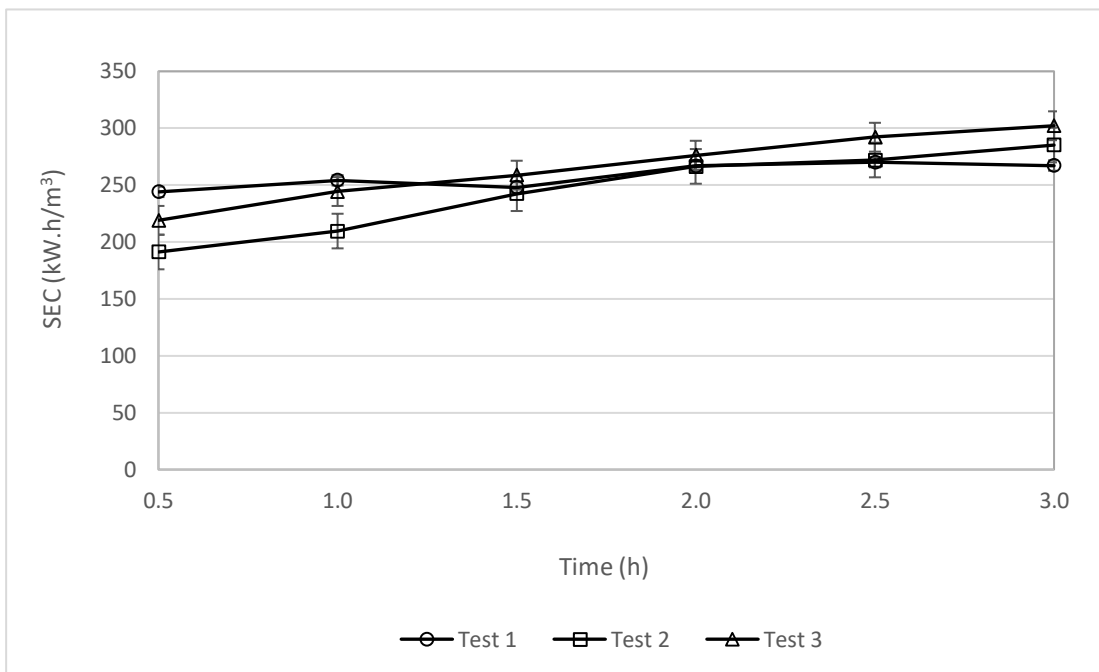
5.3.1.4 Energy consumption (SEC)

From Figure 5.15 (a), the average initial SEC was 369.19 kW.h/m³ after which it steadily increased to an average final SEC of 433.77 kW.h/m³. In Figure 5.15 (b), an average initial SEC of 219.80 kW.h/m³ was obtained after which it steadily increased to a final average SEC of 267.24 kW.h/m³. It can be observed that the SEC obtained in Figure 5.15 (a) was greater than that of the SEC obtained in Figure 5.15 (b). A ΔOP of $\pm$ 16000 kPa was achieved using Reactive Black 5 dye as DS in comparison to the ΔOP of $\pm$ 8000 kPa achieved using Maxilon Blue GRL dye as DS. Due to the lower ΔOP across the FO system, when using Maxilon Blue GRL dye as DS, more pump energy was required to overcome the resistance of flow across the FO system, resulting in greater energy consumption.

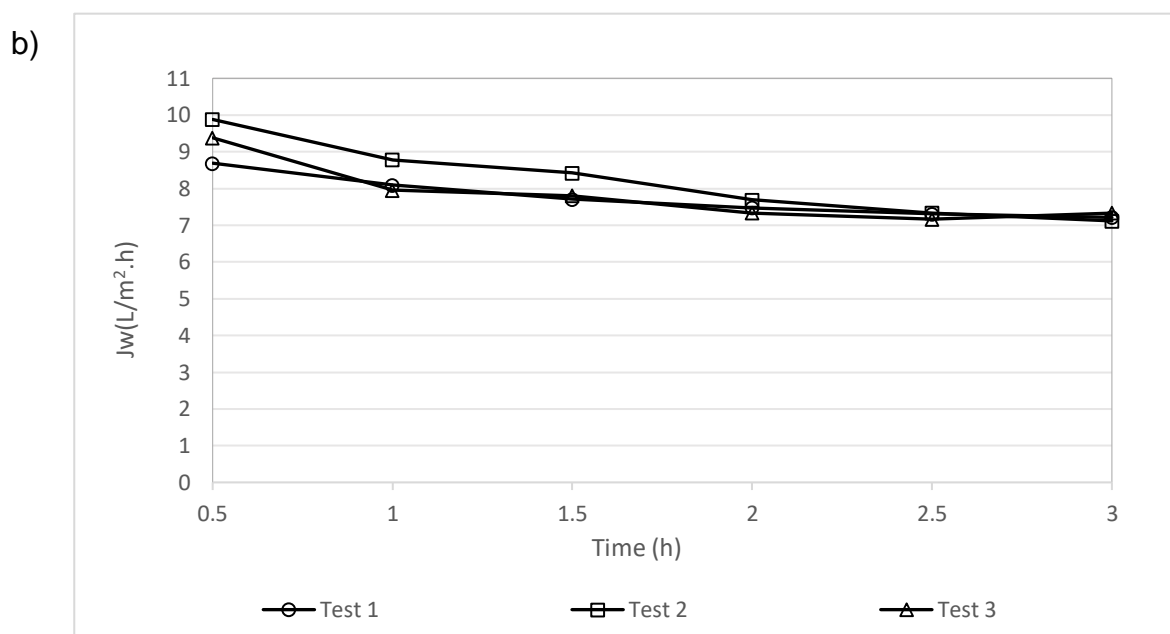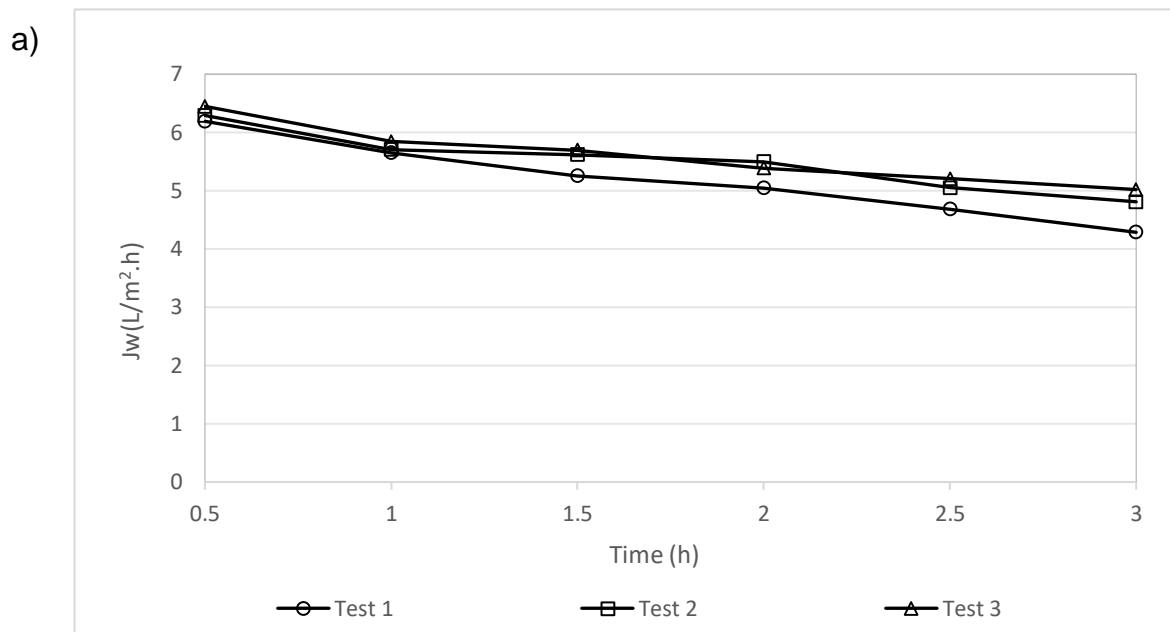Figure 5.15: Energy consumption (SEC) obtained for baseline 1 experiments using a) Maxilon Blue GRL and b) Reactive Black 5 as DS whilst operating in FO mode at a flowrate of 200 ml/min.

5.3.2 Effect of flowrates on system performance and energy consumption: Main experiment using Maxilon Blue GRL and Reactive Black 5

For this part of the study, SBW5 was used as the FS and Maxilon Blue GRL dye was used as the DS. Refer to Chapter 3 (section 3.3) for details of the operating conditions for this study. To evaluate the effect of flowrates on the system performance which relates to the water flux (J_w), reverse solute flux (J_s), water recovery (R_e) and SEC. Experiments were run in FO mode at flowrates of 400, 500 and 600 ml/min, respectively.

5.3.2.1 Water Flux (J_w)

Figure 5.16 (a) illustrates the J_w obtained using Maxilon Blue GRL as DS whilst operating in FO mode at flowrates of 400, 500 and 600 ml/min, respectively. Operating at the lowest flowrate of 400 ml/min, it can be seen in Figure 5.16 (a) that an initial J_w of 5.33 L/m^2.h was attained which decreased to a final J_w of 0.64 L/m^2.h at the end of the 143 h. Furthermore, at a flowrate of 500 ml/min an initial J_w of 5.56 L/m^2.h was achieved which once again decreased for the 147 h to a final J_w of 0.12 L/m^2.h. Finally, at the highest flowrate of 600 ml/min, an initial J_w of 5.83 L/m^2.h was achieved which decreased to a final flowrate of 0.12 L/m^2.h at the end of the 171 h.

Figure 5.16 (b) illustrates the J_w obtained using Reactive black 5 as DS whilst operating in FO mode at flowrates of 400, 500 and 600 ml/min, respectively. Taking into consideration Figure 5.16 (b), operating at the lowest flowrate of 400 ml/min, it can be seen that an initial J_w of 7.25 L/m^2.h was attained which decreased to a final J_w of 6.05 L/m^2.h at the end of the 5 h. Furthermore, at a flowrate of 500 ml/min an initial J_w of 8.30 L/m^2.h was achieved which once again decreased for the 5 h to a final J_w of 5.87 L/m^2.h. Finally, at the highest flowrate of 600 ml/min, an initial J_w of 9.11 L/m^2.h was achieved which decreased to a final J_w of 6.61 L/m^2.h at the end of the 5 h.

Interpreting the trend in Figure 5.16 (a) and (b), it can be seen that the J_w achieved for flowrates of 400, 500 and 600 ml/min, followed the same phenomena of achieving a higher initial J_w which gradually decreased to a lower final J_w nearing the completion of the individual experiments. It can also be observed that at the lowest flowrate of 400 ml/min, the lowest J_w is achieved whilst the highest J_w is achieved at the highest flowrate of 600 ml/min. However, when comparing Figure 5.16 (a) to (b), it can be seen that greater J_w was achieved while using Reactive Black 5 as the DS in comparison to Maxilon Blue GRL. Lower J_w was expected to be achieved whilst using Maxilon Blue GRL as DS due to the low ΔOP across the FO system. A ΔOP of $\pm$ 16000 kPa was achieved using Reactive Black 5 dye as DS in comparison to the ΔOP of $\pm$ 8000 kPa achieved using Maxilon Blue GRL dye as DS. Whilst using Maxilon Blue

GRL as DS, the duration of experiments increased with respect to an increase in flowrate, however, no significant increase in J_w could be observed in relation to the increase in flowrates. Considering the observations in relation to the change in DS, it can be concluded that there was little to no impact of the change in DS on the J_w with respect to the varied flowrates.

Figure 5.16: Forward flux (J_w) obtained using a) Maxilon Blue GRL and b) Reactive Black 5 as DS whilst operating in FO mode at flowrates of 400, 500 and 600 ml/min,

5.3.2.2 Water recovery (R_e)

Figure 5.17 (a) and (b) illustrates the R_e obtained using Maxilon Blue GRL and Reactive Black 5 as DS whilst operating in FO mode at flowrates of 400, 500 and 600 ml/min, respectively. Interpreting the trend observed in Figure 5.17 (a) and (b), it can be seen that the R_e achieved for flowrates of 400, 500 and 600 ml/min, followed the same phenomena of achieving a higher initial R_e which proceeds to a lower final R_e nearing the completion of the individual experiments. It can also be observed from Figure 5.17 (a) and (b) that there is no significant increase in R_e in relation to an increase in flowrate. Furthermore, the change in DS once again had no impact on R_e as similar recoveries were achieved in Figure 5.17 (a) and (b) in relation to the varied flowrates.

Figure 5.17: Water recovery (R_e) obtained using a) Maxilon Blue GRL and b) Reactive Black 5 as DS whilst operating in FO mode at flowrates of 400, 500 and 600 ml/min, respectively.

5.3.2.3 Energy consumption (SEC)

Figure 5.18 (a) and (b) illustrates the SEC obtained using Maxilon Blue GRL and Reactive Black 5 as DS whilst operating in FO mode at flowrates of 400, 500 and 600 ml/min, respectively. Operating at the lowest flowrate of 400 ml/min, an initial SEC of 505.80 kW.h/m^3 was achieved which increased to a final SEC of 1940.33 kW.h/m^3 at the end of the 143 h. At a flowrate of 500 ml/min, it was found that an initial SEC of 746.20 kW.h/m^3 was achieved which increased to a final SEC of 5000 kW.h/m^3 at the end of the 147 h. Lastly, it can be seen that at the highest flowrate of 600 ml/min, an initial SEC of 700.31 kW.h/m^3 was attained which increased to a final SEC of 6434.30 kW.h/m^3 at the end of the 171 h.

Taking into consideration Figure 5.18 (b), it can be seen that at the lowest flowrate of 400 ml/min, an initial SEC of 347.41 kW.h/m^3 was attained which increased to a final SEC of 394.99 kW.h/m^3 at the end of the 5 h. Furthermore, at a flowrate of 500 ml/min an initial SEC of 351.35 kW.h/m^3 was achieved which once again increased for the 5 h to a final SEC of 476.02 kW.h/m^3. Finally, at the highest flowrate of 600 ml/min, an initial SEC of 398.87 kW.h/m^3 was achieved which increased to a final SEC of 515.88 kW.h/m^3 at the end of the 5 h.

Interpreting the trend observed in Figure 5.18 (a) and (b), it can be seen that the SEC achieved for flowrates of 400, 500 and 600 ml/min, followed the same phenomena of achieving a lower initial SEC which proceeds to a higher final SEC nearing the completion of the individual experiments. It can also be observed that at the lowest flowrate of 400 ml/min, the lowest SEC is achieved whilst the highest SEC is achieved at the highest flowrate of 600 ml/min. However, when comparing Figure 5.18 (a) to (b), it can be observed that the average initial and final SEC using Reactive Black 5 as DS were 365.88 and 462.23 kW.h/m^3 in comparison to the 650.77 and 946.89 kW.h/m^3 achieved while using Maxilon Blue GRL as the DS for the same time period (i.e. 5 h). Higher SEC was expected to be achieved whilst using Maxilon Blue GRL as DS due to the lower ΔOP across the FO system as previously mentioned. Whilst operating with Maxilon Blue GRL as DS, the duration of experiments increased with respect to an increase in flowrate, as a result of which a significant increase in SEC could be observed in relation to the increase in flowrates.

The phenomena observed with respect to the high SEC achieved when using Maxilon Blue GRL as DS in accordance to the respective flowrates is valid because the pump is being used for a longer period of time and also with an increase in the flowrates, the pump would naturally require more power to pump faster. Taking into consideration the change in DS, it can be concluded that more energy was consumed whilst operating with Maxilon Blue GRL as DS. The identical trends observed while using Maxilon Blue GRL and Reactive Black 5 as DS in

relation to the increase in SEC with respect to the varied flowrates, further validates the phenomena of the greater energy consumption with an increase in flowrate.

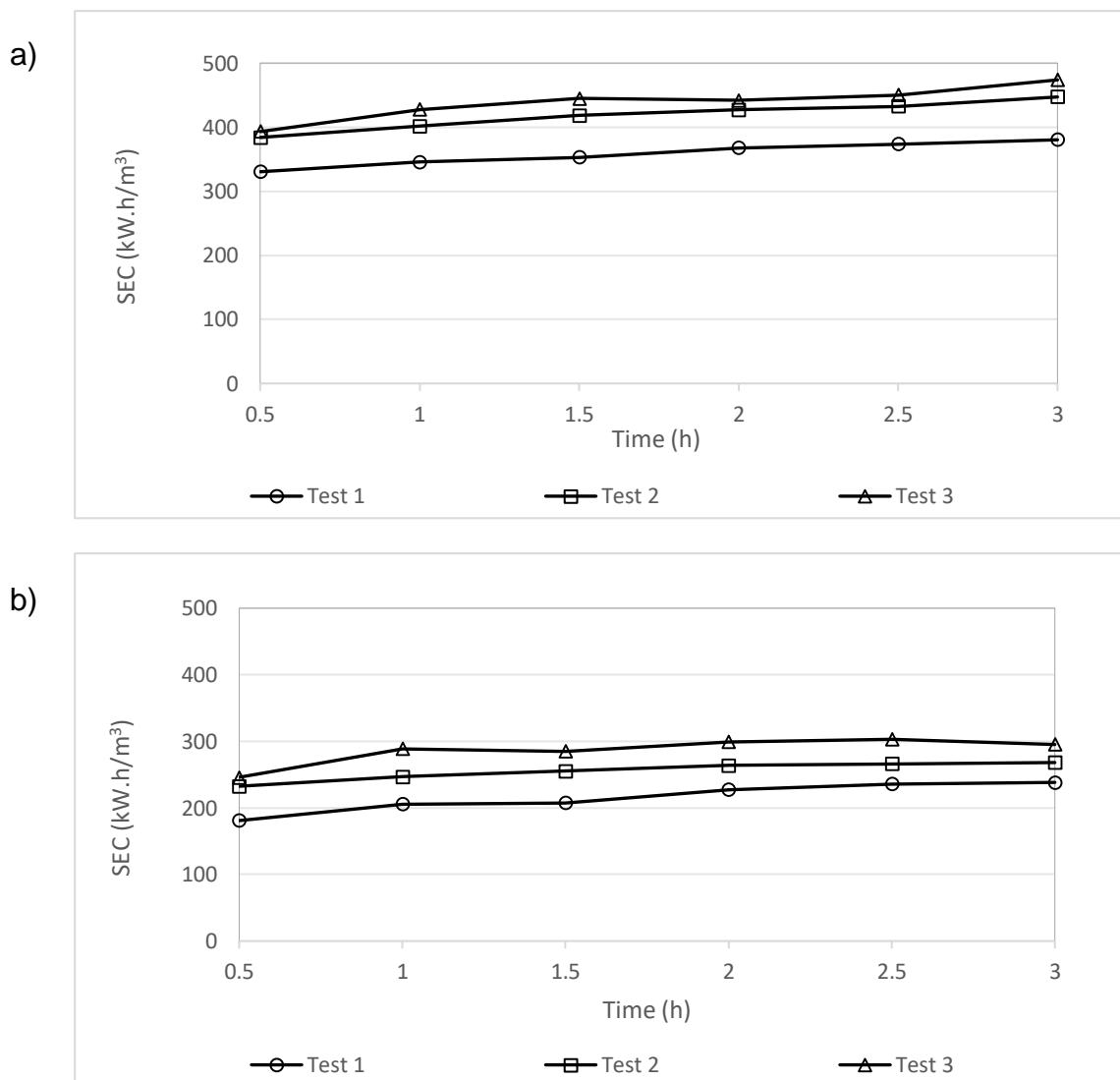

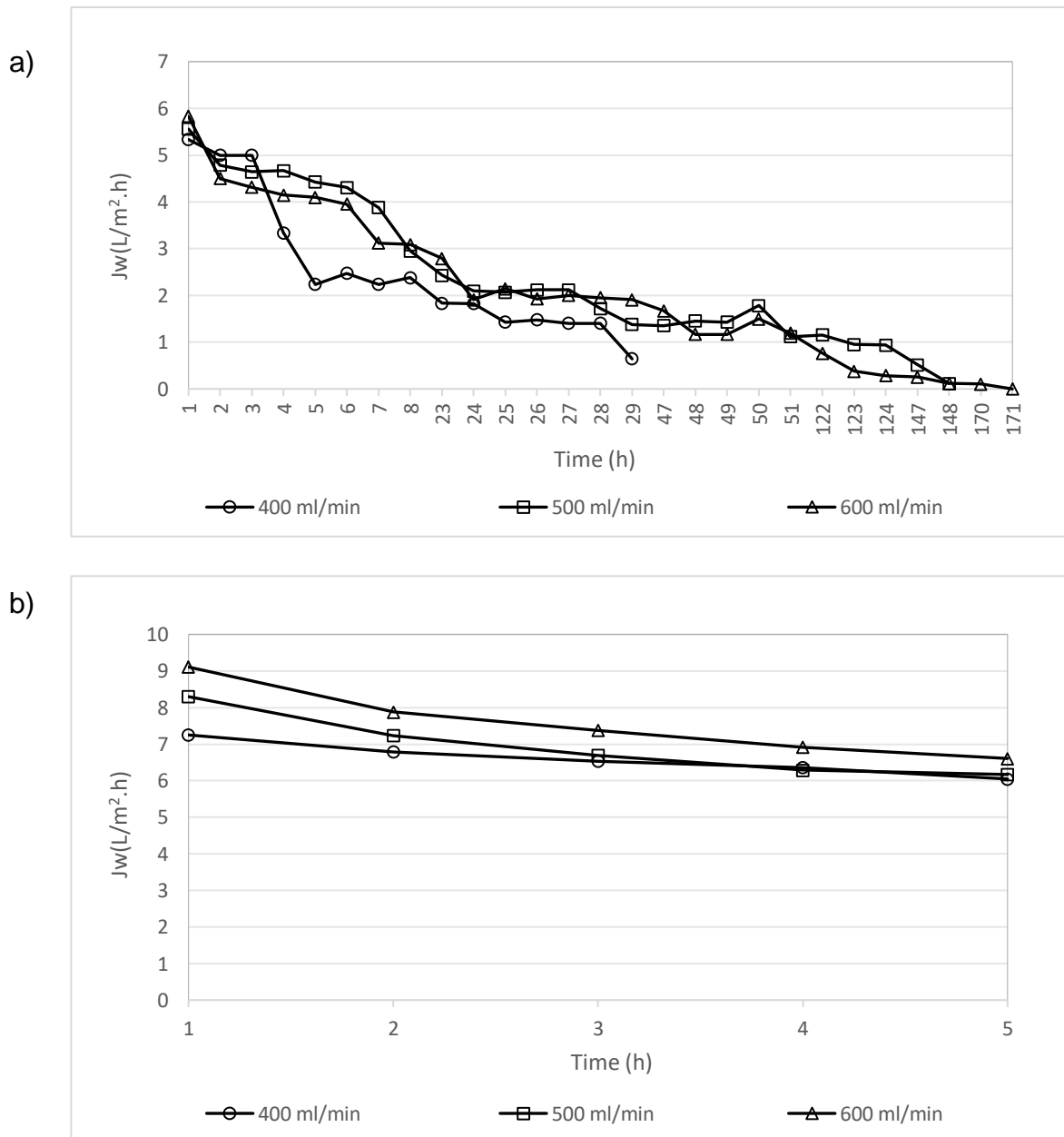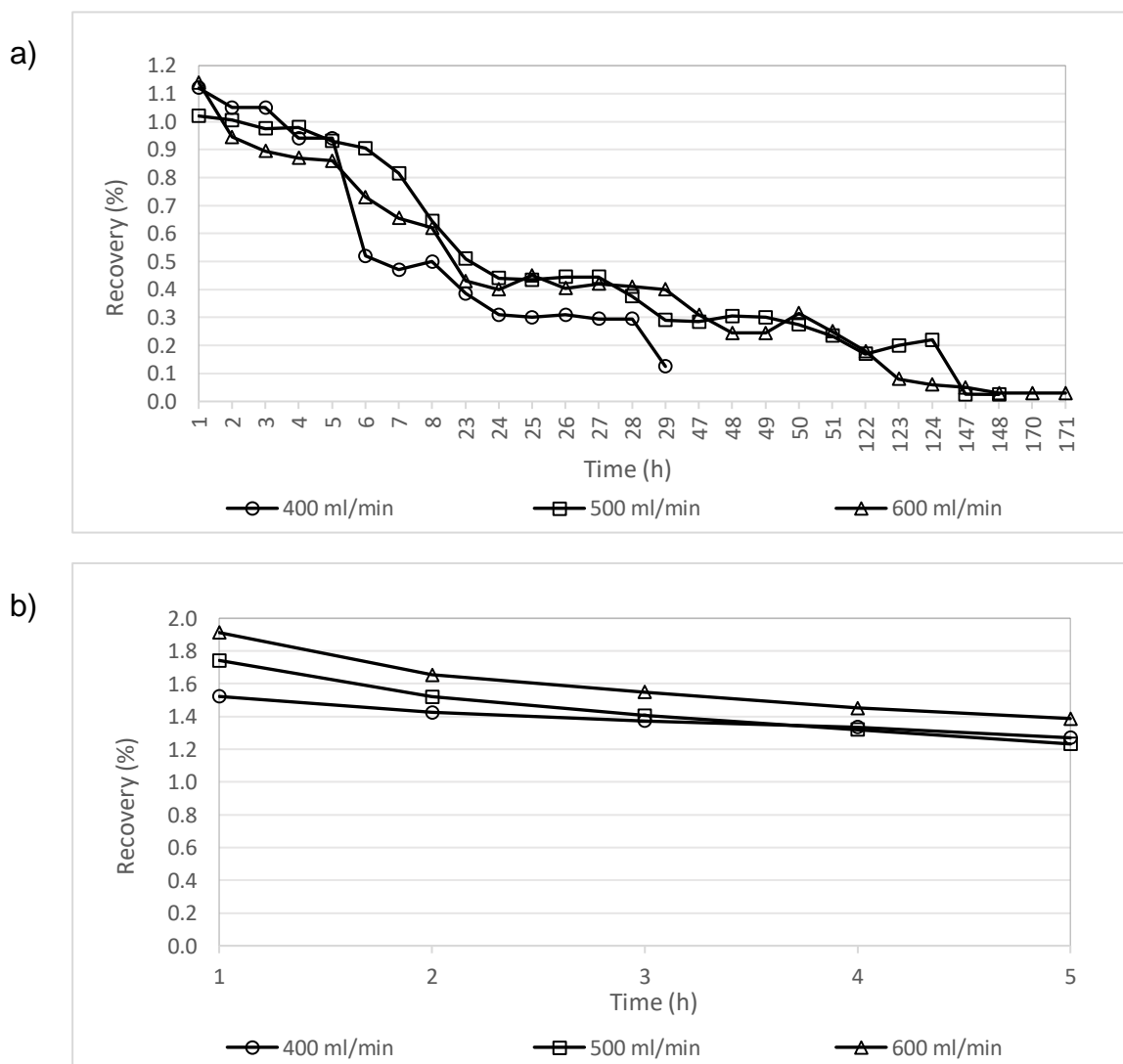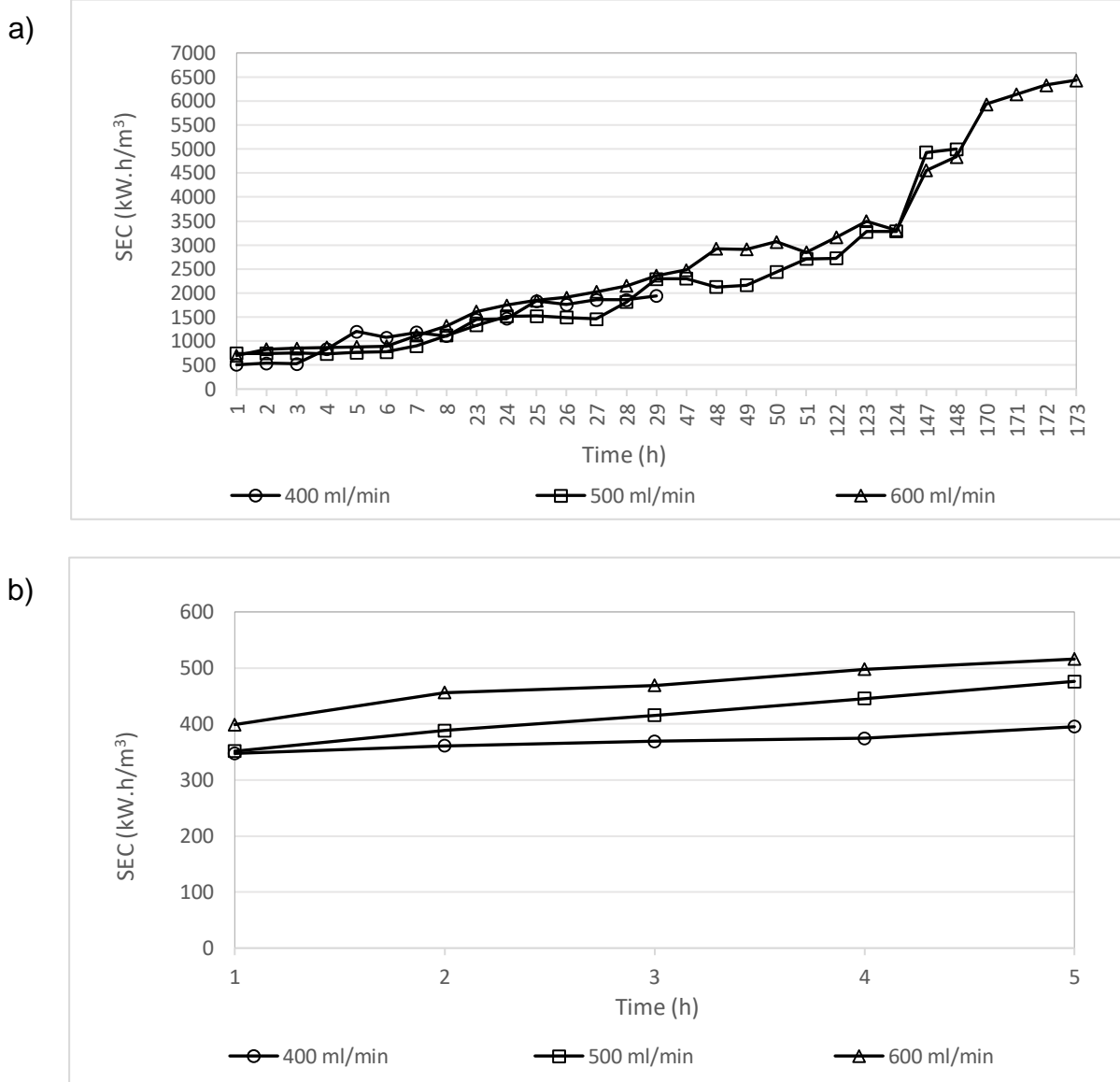Figure 5.18: Energy consumption (SEC) obtained using a) Maxilon Blue GRL and b) Reactive Black 5 as DS whilst operating in FO mode at flowrates of 400, 500 and 600 ml/min, respectively.

5.3.3 Effect of flowrates on system performance and energy consumption: Baseline 2

This part of the study was conducted to be used as a basis of comparison with Baseline 1 experiments to determine the extent of fouling and its impact on the energy consumption and system performance of a dye driven FO system. For this study, deionised water (DI) was used as the FS and Maxilon Blue GRL dye was used as the DS. Refer to Chapter 3 (section 3.4) for details of the operating conditions for this study. To evaluate the effect of flowrates on the system performance which relates to the water flux (J_w), reverse solute flux (J_s), water recovery (R_e) and SEC, experiments were run in FO mode at a flowrates of 200 ml/min.

5.3.3.1 Water flux (J_w)

Table 5.4 tabulates the average initial and final J_w obtained for the duration of a 3 h operation for Baseline 1 and 2 experiments using Maxilon Blue GRL and Reactive Black 5 as DS whilst operating in FO mode at a flowrate of 200 ml/min. When comparing the J_w, it could be seen that lower J_w was achieved in Baseline 2 experiments compared to that of Baseline 1. The decrease in J_w from Baseline 1 to Baseline 2, was indicative of the efficiency of the cleaning procedure. Furthermore, the decrease was also an indication that there was little no fouling in the system.

Table 5.4: Comparison of the initial and final J_w of Baseline 1 and Baseline 2 experiments

Experiment	DS	Average initial J_w (L/m^2.h)	Average final J_w (L/m^2.h)
Baseline 1	Maxilon Blue GRL	6.31	4.70
	Reactive Black 5	9.32	7.22
Baseline 2	Maxilon Blue GRL	5.66	4.20
	Reactive Black 5	9.21	6.61

From Figure 5.19 (a), an average initial J_w of 5.66 L/m^2.h was obtained after which it can be seen that the J_w steadily decreased to a final average J_w of 4.20 L/m^2.h. In Figure 5.19 (b), the average initial J_w was 9.21 L/m2.h after which it steadily declined due to osmotic dilution to result in an average final J_w of 6.61 L/m^2.h. Higher J_w was achieved whilst operating with Reactive Black 5 as DS in comparison to Maxilon Blue GRL.

a)

b)

Figure 5.19: Forward flux (J_w) obtained for Baseline 2 experiments using a) Maxilon Blue GRL and b) Reactive Black 5 as DS whilst operating in FO mode at a flowrate of 200 ml/min

5.3.3.2 Reverse solute flux (J_s)

Table 5.5 tabulates the average initial and final J_s obtained for the duration of a 3 h operation for Baseline 1 and 2 experiments using Maxilon Blue GRL and Reactive Black 5 as DS whilst operating in FO mode at a flowrate of 200 ml/min. When comparing the J_s , it could be seen that the J_s achieved in Baseline 2 experiments was similar to that of the J_s achieved in Baseline 1. However, the average J_s achieved in Baseline 2 was lower than that of the average J_s achieved in Baseline 1 experiments.

Table 5.5: Comparison of the initial and final J_s of Baseline 1 and Baseline 2 experiments

Experiment	DS	Average initial J_s (g/m².h)	Average final J_s (g/m².h)
Baseline 1	Maxilon Blue GRL	0.05	0.03
	Reactive Black 5	0.04	0.03
Baseline 2	Maxilon Blue GRL	0.03	0.02
	Reactive Black 5	0.04	0.03

Interpreting Figure 5.20 (a), the average initial J_s was 0.03 g/m².h after which it steadily declined to an average final J_s of 0.02 g/m².h. In Figure 5.20 (b), an average initial J_s of 0.04 g/m².h was obtained after which it can be seen that the J_s decreased to a final average J_s of 0.03 g/m².h. It can be observed that the J_s obtained in Figure 5.20 (a) and (b) were similar in comparison.
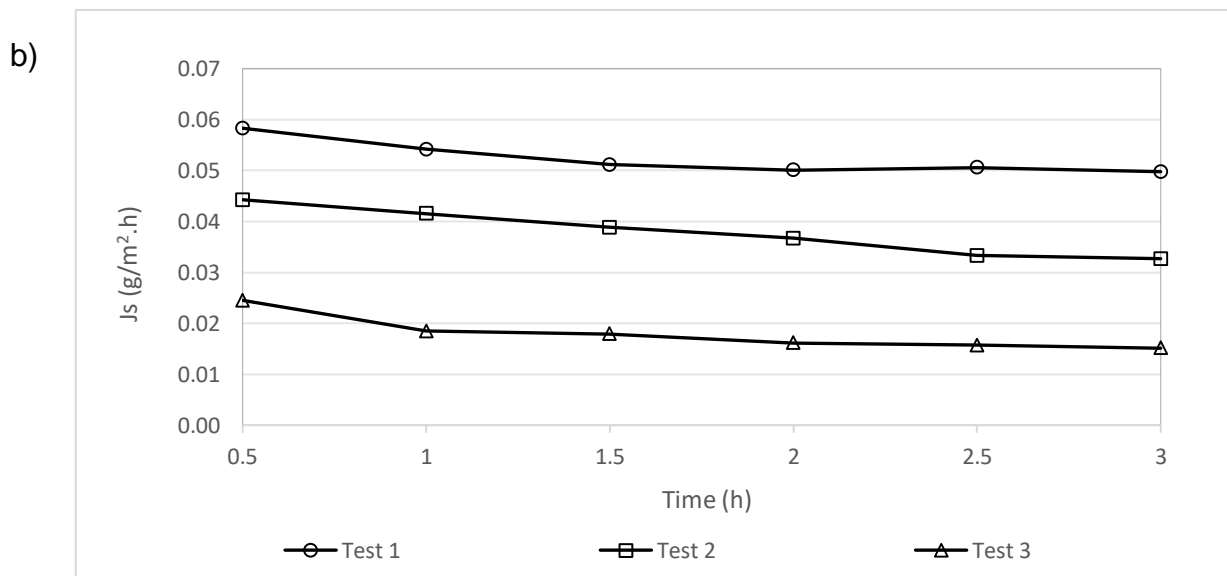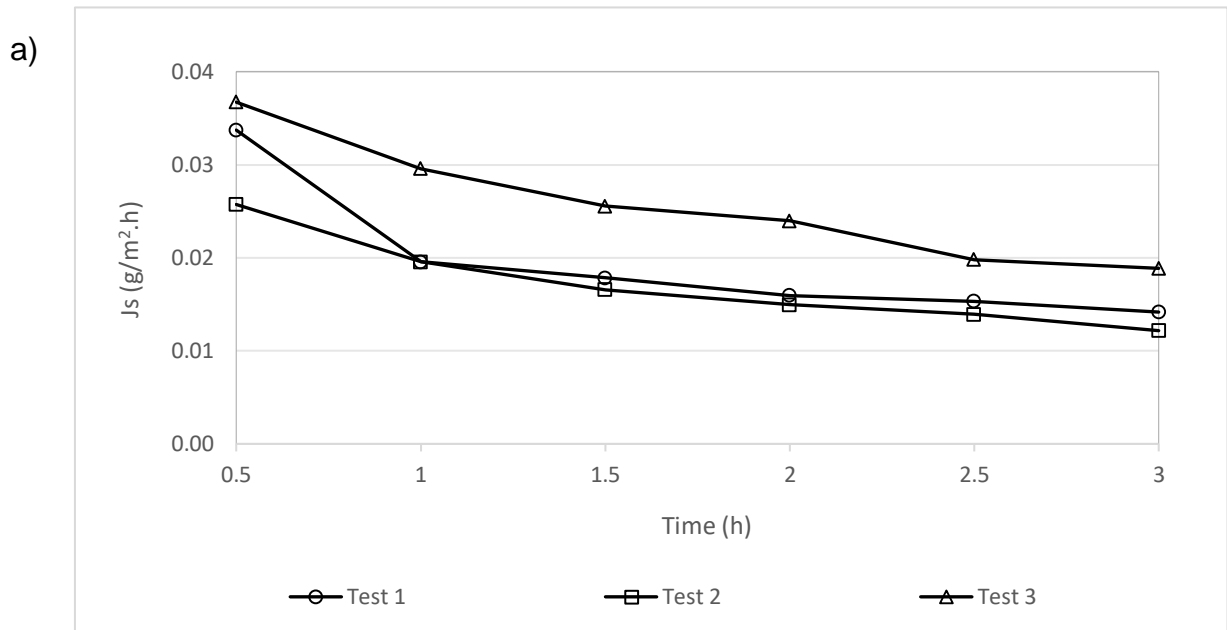
Figure 5.20: Figure 5.20: Reverse solute flux (J_s) obtained for Baseline 2 experiments using a) Maxilon Blue GRL and b) Reactive Black 5 as DS whilst operating in FO mode at a flowrate of 200 ml/min

5.3.3.3 Water recovery (R_e)

Figure 5.21 (a) and (b) illustrates the R_e obtained whilst operating in FO mode using a) Maxilon Blue GRL and b) Reactive Black 5 as DS whilst operating in FO mode at a flowrate of 200 ml/min. Table 5.6 tabulates the average initial and final R_e obtained for the duration of a 3 h operation for Baseline 1 and 2 experiments using Maxilon Blue GRL and Reactive Black 5 as DS whilst operating in FO mode at a flowrate of 200 ml/min. When comparing the R_e it can be seen that similar R_e was achieved in Baseline 1 experiments compared to that of Baseline 2 experiments.

Table 5.6: Comparison of the initial and final R_e of Baseline 1 and Baseline 2 experiments

Experiment	DS	Average initial Re (%)	Average final Re (%)
Baseline 1	Maxilon Blue GRL	0.98	0.76
	Reactive Black 5	0.65	0.52
Baseline 2	Maxilon Blue GRL	0.54	0.39
	Reactive Black 5	0.96	0.69

a)

b)
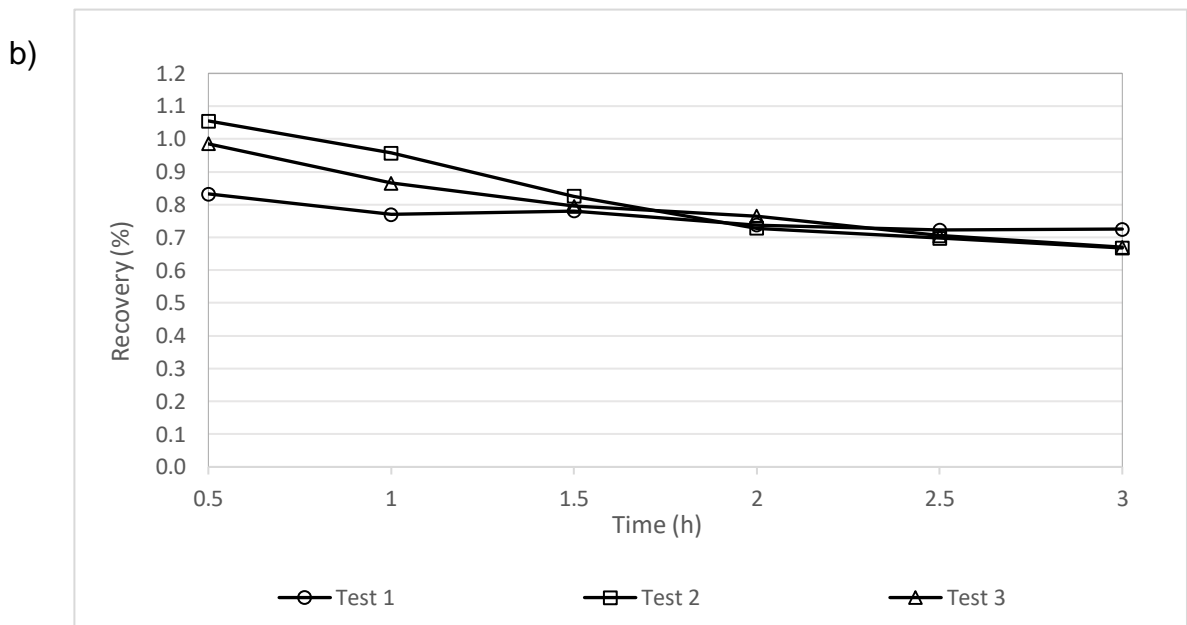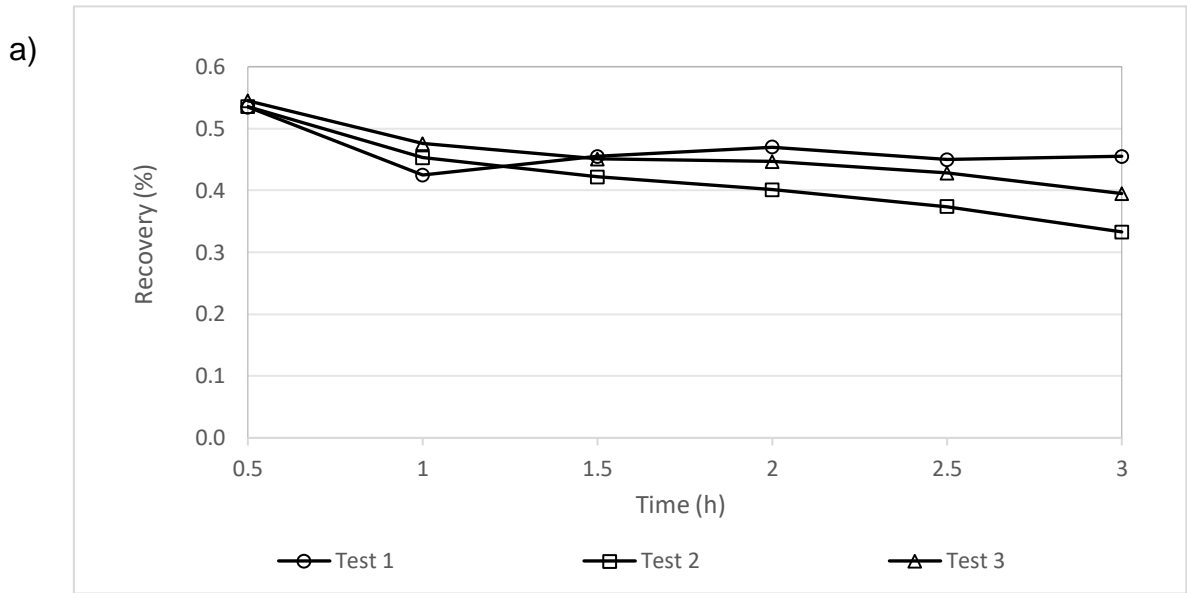
Figure 5.21: Water recovery (R_e) obtained for Baseline 2 experiments using a) Maxilon Blue GRL and b) Reactive Black 5 as DS whilst operating in FO mode at a flowrate of 200 ml/min

5.3.3.4 Energy consumption (SEC)

Figure 5.22 (a) and (b) illustrate Baseline 2 experiments using a) Maxilon Blue GRL and b) Reactive Black 5 as DS whilst operating in FO mode at a flowrate of 200 ml/min. From Figure 5.22 (a), the average initial SEC was 1116.30 kW.h/m^3 after which it increased to an average final SEC of 1411.50 kW.h/m^3. In Figure 5.22 (b), an average initial SEC of 218.09 kW.h/m^3 was obtained after which it increased to a final average SEC of 284.84 kW.h/m^3. It can be observed that the SEC obtained in Figure 5.22 (a) was much greater than that of the SEC obtained in Figure 5.22 (b). As mentioned previously, the higher SEC achieved using Maxilon Blue GRL as DS can be attributed to the lower ΔOP across the FO system.

Table 5.7 tabulates the average initial and final SEC obtained for the duration of a 3 h operation for Baseline 1 and 2 experiments using Maxilon Blue GRL and Reactive Black 5 as DS whilst operating in FO mode at a flowrate of 200 ml/min. When comparing the SEC it could be seen that a higher SEC was achieved in Baseline 2 experiments compared to that of Baseline 1 experiments. The higher SEC obtained in Baseline 2 experiments was due to the wear and tear of the tubing which contributed to an increase in resistance to flow resulting in higher pump energy consumption.

Table 5.7: Comparison of the initial and final SEC of Baseline 1 and Baseline 2 experiments

Experiment	DS	Average initial SEC (kW.h/m^3)	Average final SEC (kW.h/m^3)
Baseline 1	Maxilon Blue GRL	369.19	433.77
	Reactive Black 5	219.80	267.24
Baseline 2	Maxilon Blue GRL	1116.30	1411.50
	Reactive Black 5	218.09	284.84

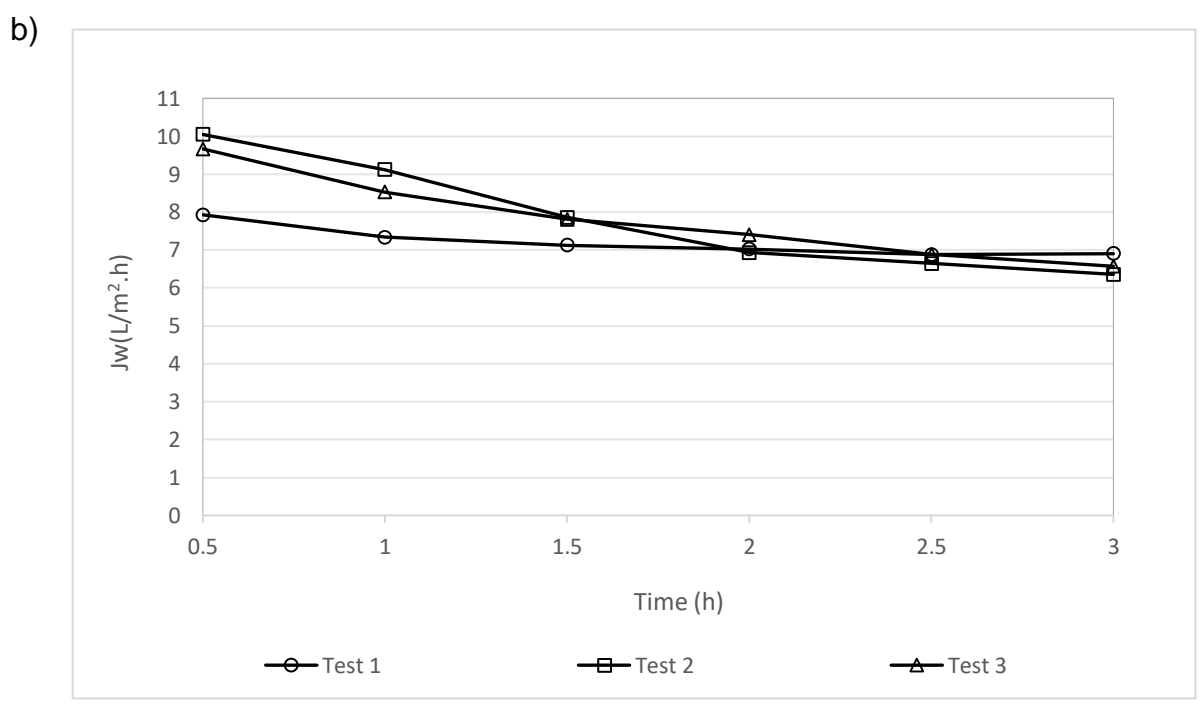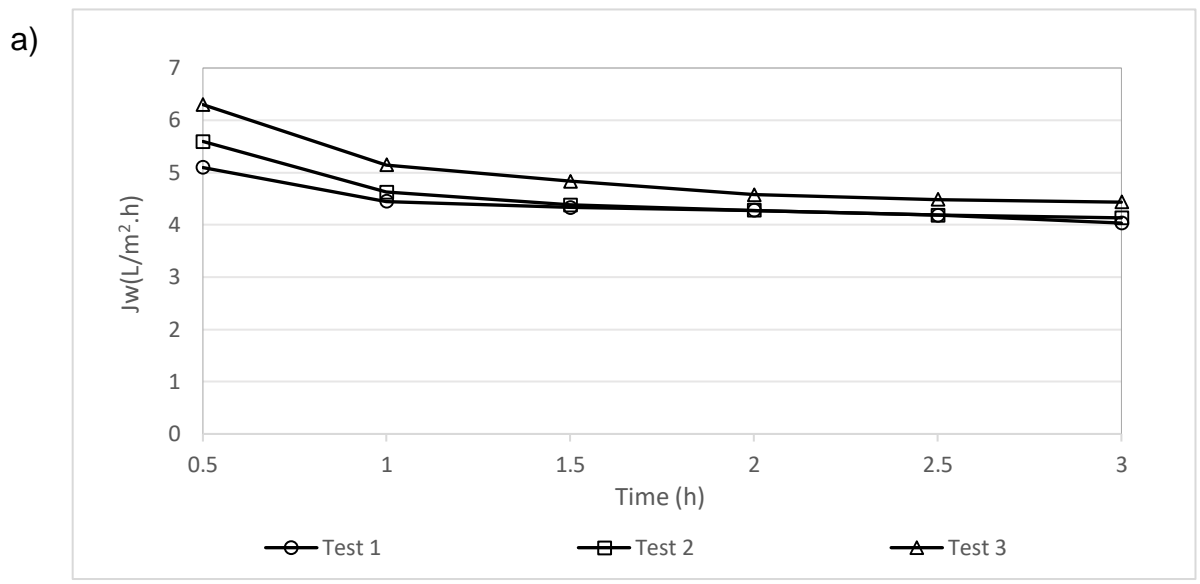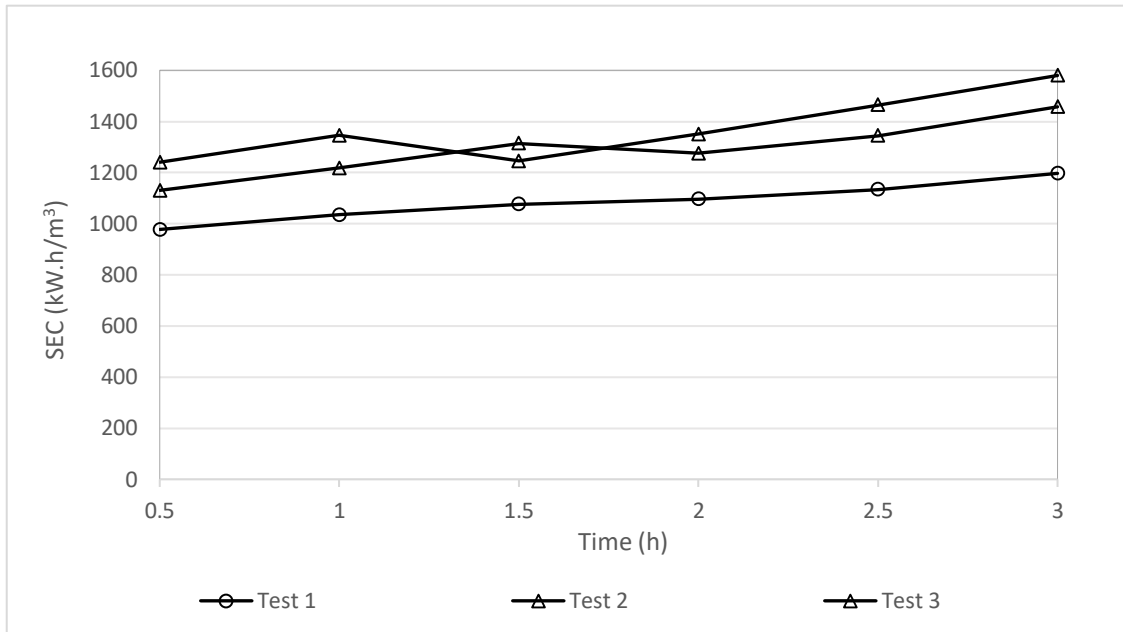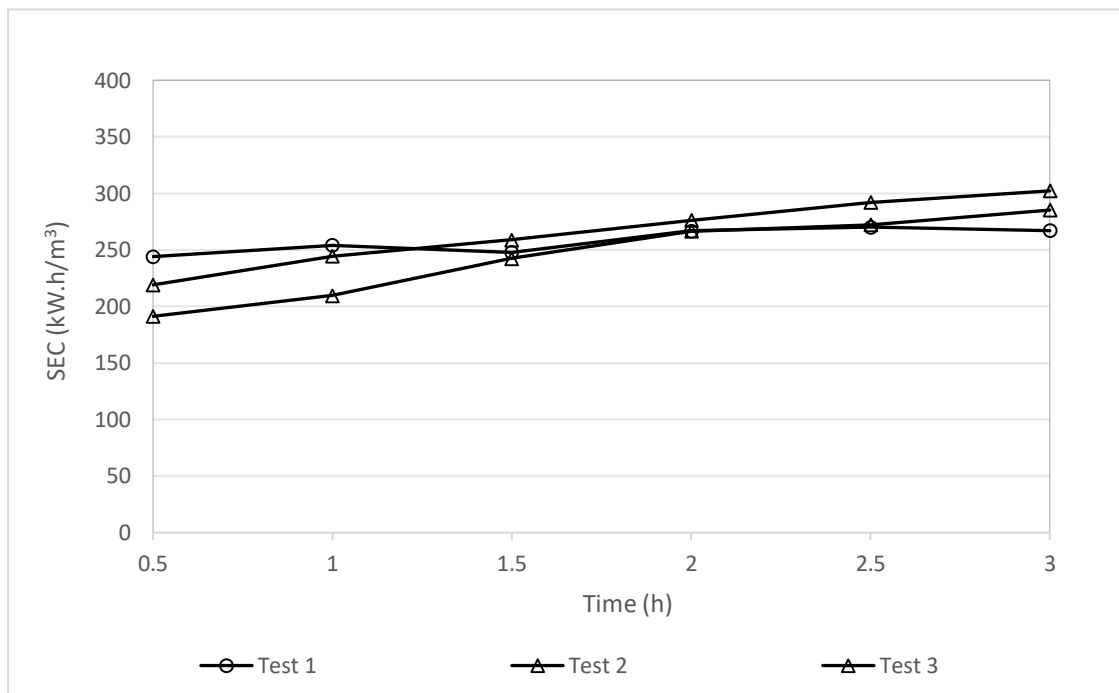Figure 5.22: Energy consumption (SEC) obtained for Baseline 2 experiments using a) Maxilon Blue GRL and b) Reactive Black 5 as DS whilst operating in FO mode at a flowrate of 200 ml/min

5.4 Summary

A change in DS from Reactive Black 5 dye to Maxilon Blue GRL dye had no significant impact on the system performance and energy consumption. Variations in flowrate provided insight with regards to the magnitude of the energy consumption of the FO system while operating with Reactive Black 5 and Maxilon Blue GRL dye, respectively. Furthermore, a change in orientation did not contribute to any noteworthy impacts on system performance and energy consumption. Additionally, the observation of negligible changes in baseline 2 (membrane control) R_e and J_w results suggested the possible occurrence of membrane fouling during the main experiment (dye-driven FO system). Therefore, minute traces of fouling in the form of foreign functional groups may be observed in the attenuated total reflection Fourier transform infrared spectroscopy (ATR-FTIR) spectrums of the used membranes (refer to Chapter 6).

CHAPTER 6

CHAPTER 6: INVESTIGATION OF MEMBRANE MATERIAL BY ATTENUATED TOTAL REFLECTION-FOURIER TRANSFORM INFRARED (ATR-FTIR) SPECTROSCOPY

6.1 Introduction

Based on the comparison of the results obtained for baseline 1 and 2 experiments it was concluded that the physical cleaning procedure (refer to Table 3.7, section 3.3.4 in Chapter 3), which consumed ± 0.045 kWh electrical power per procedure, was effective. However, a further investigation that allowed surface characterization was very important to investigate the molecular structure and organisation of membranes. Attenuated total reflection-Fourier transform infrared (ATR-FTIR) spectroscopy was therefore used to investigate the extent of fouling by screening the clean and fouled CTA membranes, by investigating/identifying the presence (i.e. absorbance) of different functional groups in the wavenumber range of 4000 - 600 cm^{-1}. The ATR-FTIR spectra for each membrane sample were recorded within the range of 4000 - 600 cm^{-1} at a resolution of 8 wavenumbers (cm^{-1}) and a total of 64 scans were collected per sample.

6.2 Membrane Analysis: Virgin membrane

Figure 6.1 illustrates the spectra of ATR-FTIR spectroscopy of the active and support layers of a virgin CTA membrane. The ATR-FTIR spectra in Figure 6.1 indicated that the distinct and sharp absorption bands of the virgin CTA membrane were overwhelmed by rather broad absorption peaks between the region of 600 - 1800 cm^{-1}. The wide absorption bands observed in the region 3480–3000 cm^{-1} can be as a result of the presence of alcohols and phenols ($O - H$ stretching modes), while the less intense absorption bands at 2957 – 2853 cm^{-1} are attributed to Alkanes ($C - H$ stretching modes). The distinct absorption band located around 1730 cm^{-1} can be attributed to stretching vibrations of the carbonyl group.

In the wavenumber range from 1300 cm^{-1} to 1500 cm^{-1}, a peak at 1367 cm^{-1} corresponding to valence vibration of sulfoxides ($S = O$ stretching modes) can be observed. The absorption bands centered around 1220 – 1030 cm^{-1}, corresponding to stretching modes of $C - O$ single bonds. The absorption bands centered around 900 – 600 cm^{-1} observed closer to the end of the spectrum correspond to stretching vibrations of groups of aromatics.
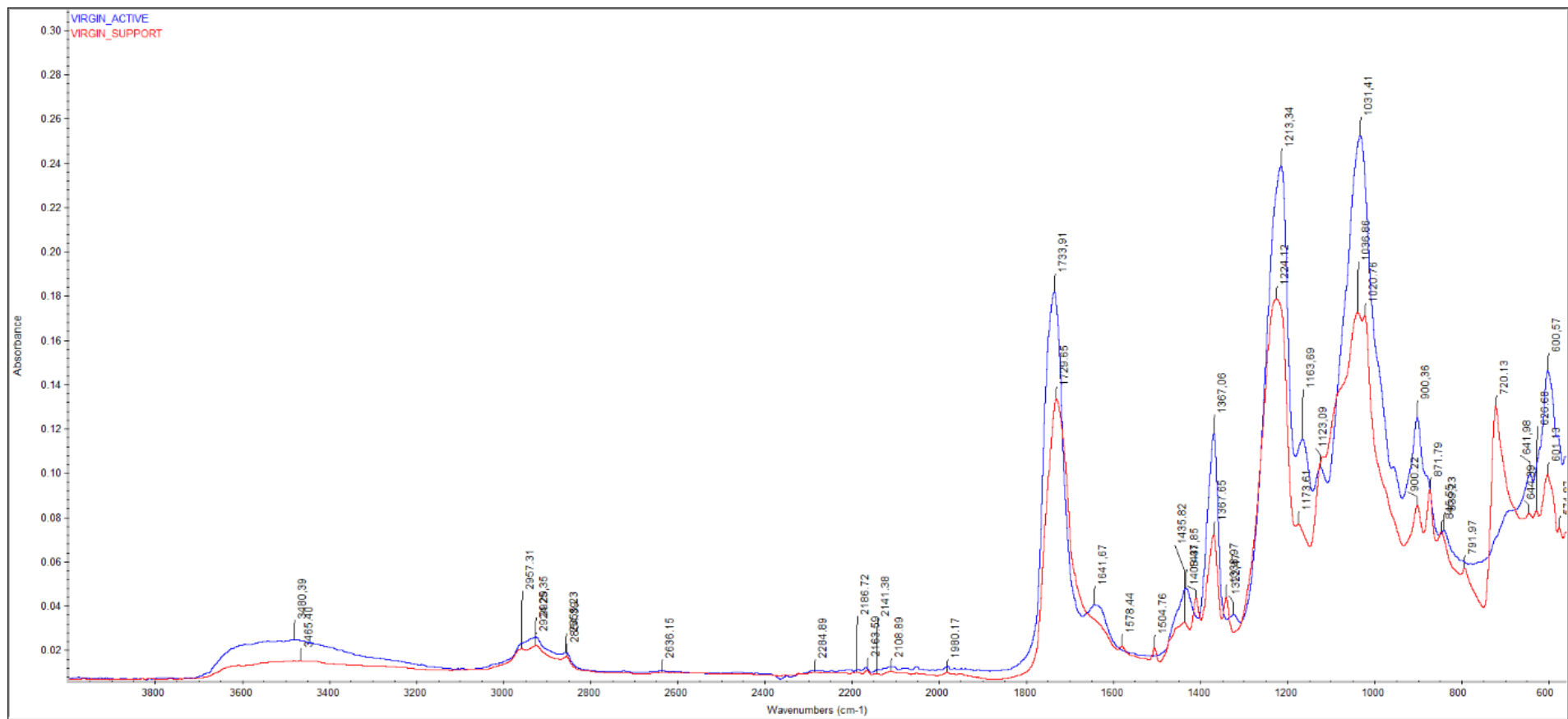
Figure 6.1: ATR-FTIR spectra of the active (blue) and support (red) layer of the virgin CTA membrane (graph markers not included as such view in colour)

In the wavenumber range from 1300 cm^{-1} to 1500 cm^{-1}, a peak at 1367 cm^{-1} corresponding to valence vibration of sulfoxides ($S = O$ stretching modes) can be observed. The absorption bands centered around 1220 – 1030 cm^{-1}, correspond to stretching modes of $C - O$ single bonds. The absorption bands centered around 900 – 600 cm^{-1} observed closer to the end of the spectrum correspond to stretching vibrations of groups of aromatics.

6.3 Membrane Analysis: Used membrane

6.3.1 Membrane Analysis: Reactive Black 5 dye as DS (FO mode)

Figure 6.2 illustrates the ATR-FTIR spectra of the membrane exposed to Reactive Black 5 dye in FO mode in accordance with the respective flowrates of i) 400 ii) 500 and iii) 600 ml/min. Observing the ATR-FTIR spectra with respect to flowrates of i) 400 ii) 500 and iii) 600 ml/min, sharp absorbance peaks appeared at 870 cm^{-1}, 720 cm^{-1} and 600 cm^{-1} for all flowrates investigated, in addition to the prominent peaks observed in the virgin CTA membrane in Figure 6.1. Taking into consideration the observations made of the ATR-FTIR spectra in accordance with the respective flowrates, the variations of flowrates had similar impacts on the molecular structure of the membrane.

Considering the chemical structure of Reactive Black 5 dye (refer to Table 3.2, section 3.2.4 in Chapter 3), it was expected that functional groups such as amines, aromatics, and sulfoxides relating to wavenumbers of 1000- 1350 cm^{-1}, 3050-3150 cm$^{-1,}$ and 1050 cm^{-1}, respectively, would be present on the surface of the membrane. When comparing the ATR-FTIR spectra of the membrane exposed to Reactive Black 5 dye to the virgin membrane, very little deviations in relation to absorbance peaks were observed. Furthermore, the used ATR-FTIR spectra exhibited minute traces of the expected functional groups on the surface of the membranes. Based on the observations made from the ATR-FTIR spectra of the membranes exposed to Reactive Black 5 dye, it can be concluded that the molecular structure of the membrane was not compromised as a result of exposure to the dye in question.
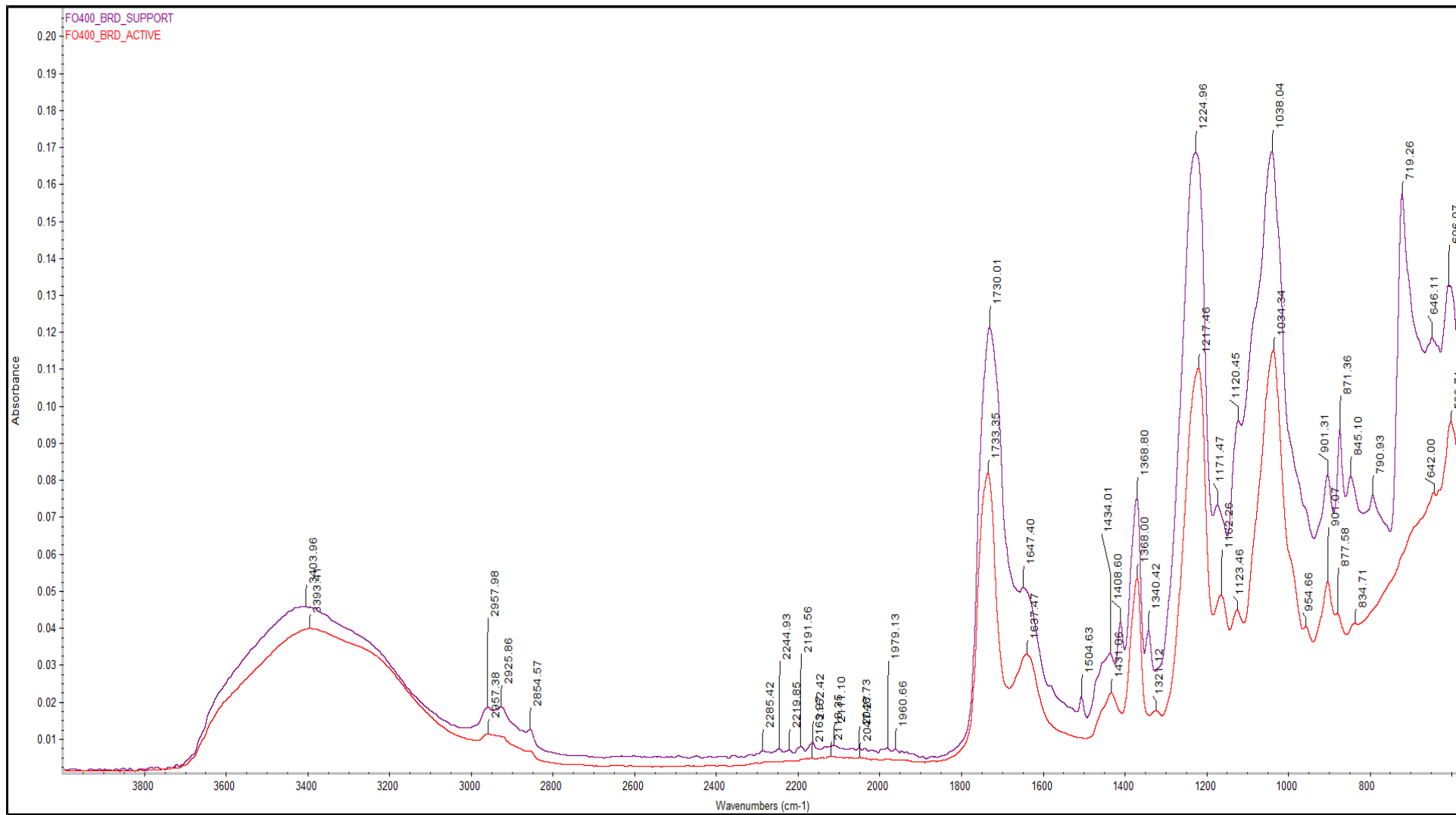
a) (i)
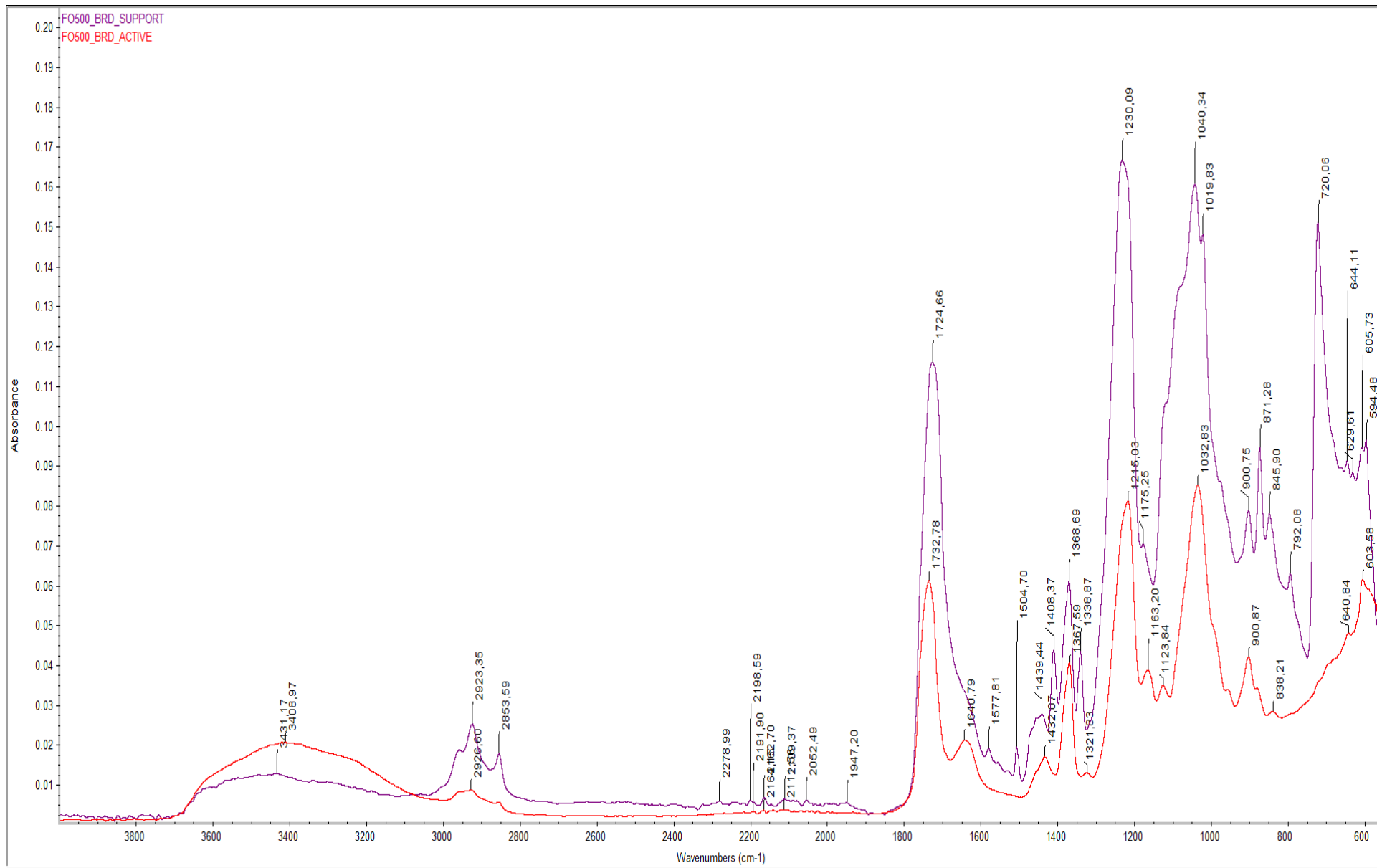
(ii)

Figure 6.2: ATR-FTIR spectrum of the active (blue) and support (red) layer of the CTA membrane exposed to Reactive black 5 dye in FO mode in accordance to the respective flowrate of i) 400 ii) 500 and iii) 600 ml/min (graph markers not included as such view in colour)

6.3.2 Membrane Analysis: Reactive Black 5 dye as DS (PRO mode)

Figure 6.3 illustrates the ATR-FTIR spectra of the membrane exposed to Reactive Black 5 dye in PRO mode in accordance with the respective flowrates of i) 400 ii) 500 and iii) 600 ml/min. Observing the ATR-FTIR spectra in accordance to the respective flowrates of i) 400 ii) 500 and iii) 600 ml/min, sharp absorbance peaks once again appeared at 870 cm^{-1}, 720 cm^{-1} and 600 cm^{-1} for all flowrates investigated, in addition to the prominent peaks observed in the virgin CTA membrane in Figure 6.1. Considering the chemical structure of Reactive Black 5 dye (refer to Table 3.2, section 3.2.4 in Chapter 3), it was expected that functional groups such as amines, aromatics, and sulfoxides relating to wavenumbers of 1000- 1350 cm^{-1}, 3050-3150 cm$^{-1,}$ and 1050 cm^{-1}, respectively, would be present on the surface of the membrane. Taking into consideration the observations made of the ATR-FTIR spectra in accordance with the respective flowrates, the variations of flowrates had similar impacts on the molecular structure of the membrane.

When comparing the ATR-FTIR spectra of the membrane exposed to Reactive Black 5 dye to the virgin membrane, very little deviations in relation to absorbance peaks were observed. Furthermore, the used ATR-FTIR spectra exhibited minute traces of the expected functional groups on the surface of the membranes. Based on the observations made on the ATR-FTIR spectra of the membranes exposed to Reactive Black 5 dye, it can be concluded that the molecular structure of the membrane was not compromised as a result of the exposure to the dye in question.

(i)

(ii)

Figure 6.3: ATR-FTIR spectrum of the active (blue) and support (red) layer of the CTA membrane exposed to Reactive black 5 dye in PRO mode in accordance to the respective flowrates of i) 400 ii) 500 and iii) 600 ml/min (graph markers not included as such view in colour)

### 6.3.3 Membrane Analysis: Maxilon Blue GRL dye as DS (FO mode)

Figure 6.4 illustrates the ATR-FTIR spectra of the membranes exposed to Maxilon Blue GRL dye in FO mode only in accordance with the respective flowrates of i) 400 ii) 500 and iii) 600 ml/min. Observing the ATR-FTIR spectra in accordance to the respective flowrates of i) 400 ii) 500 and iii) 600 ml/min, sharp absorbance peaks once again appeared at 870 cm^{-1}, 720 cm^{-1} and 600 cm^{-1} for all flowrates investigated, in addition to the prominent peaks observed in the virgin CTA membrane in Figure 6.1. Considering the chemical structure of Maxilon Blue GRL dye (refer to Table 3.2, section 3.2.4 in Chapter 3), it was expected that functional groups such as amines, amides, alcohols, aromatics, and ethers relating to wavenumbers of 1000- 1350 cm^{-1}, 3100-3500 cm^{-1}, 3200- 3400 cm^{-1}, 3050-3150 cm$^{-1,}$ and 1000-1300 cm^{-1}, respectively, would be present on the surface of the membranes. Taking into consideration the observations made of the ATR-FTIR spectra in accordance with the respective flowrates, the variations of flowrates had similar impacts on the molecular structure of the membranes.

When comparing the ATR-FTIR spectra of the membranes exposed to Maxilon Blue GRL dye to the virgin membrane, very little deviations in relation to absorbance peaks were observed. Furthermore, the used ATR-FTIR spectra exhibited minute traces of the expected functional groups on the surface of the membranes. Based on the observations made on the ATR-FTIR spectra of the membrane exposed to the Maxilon Blue GRL dye, it can be concluded that the molecular structure of the membrane was not compromised as a result of the exposure to the dye in question.
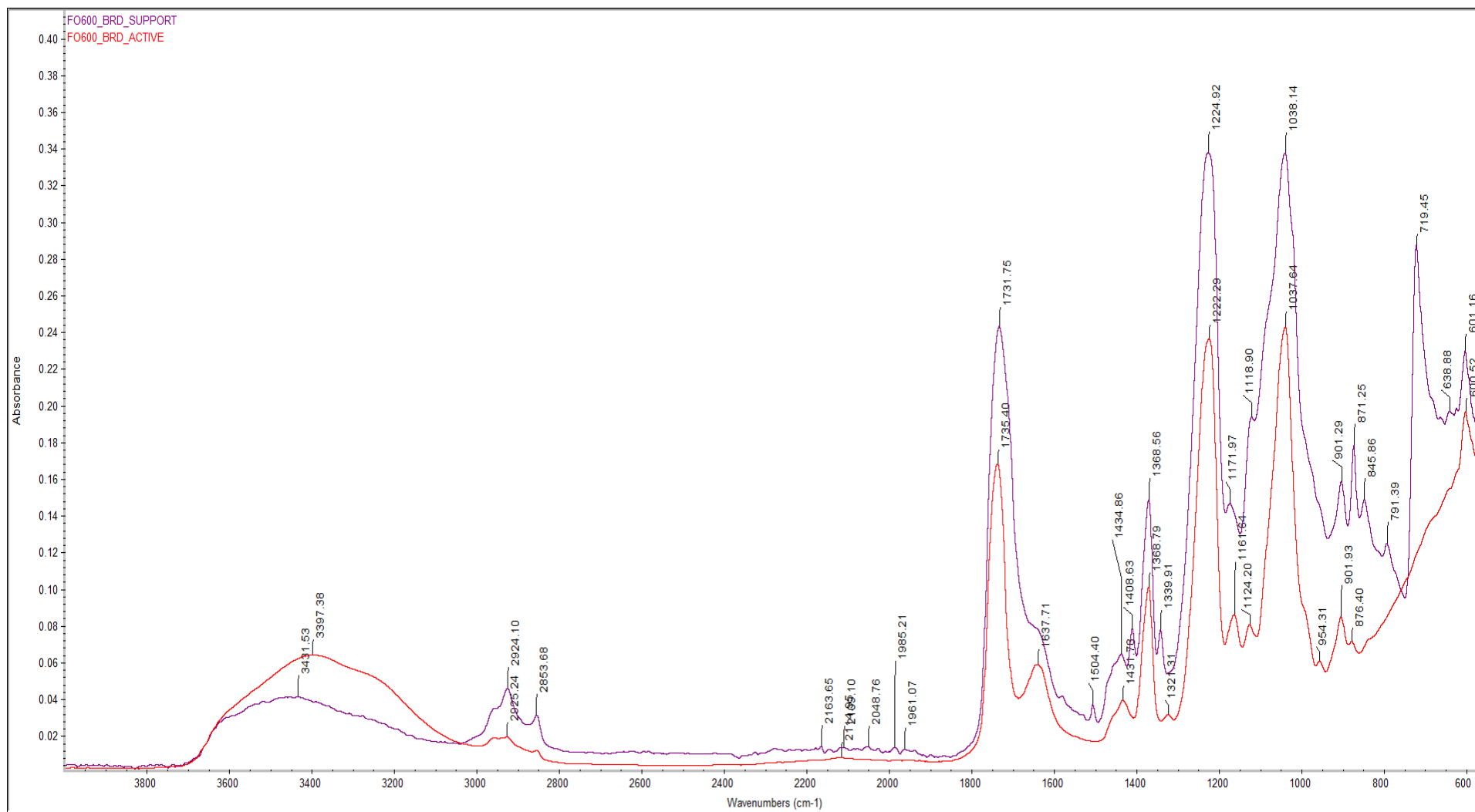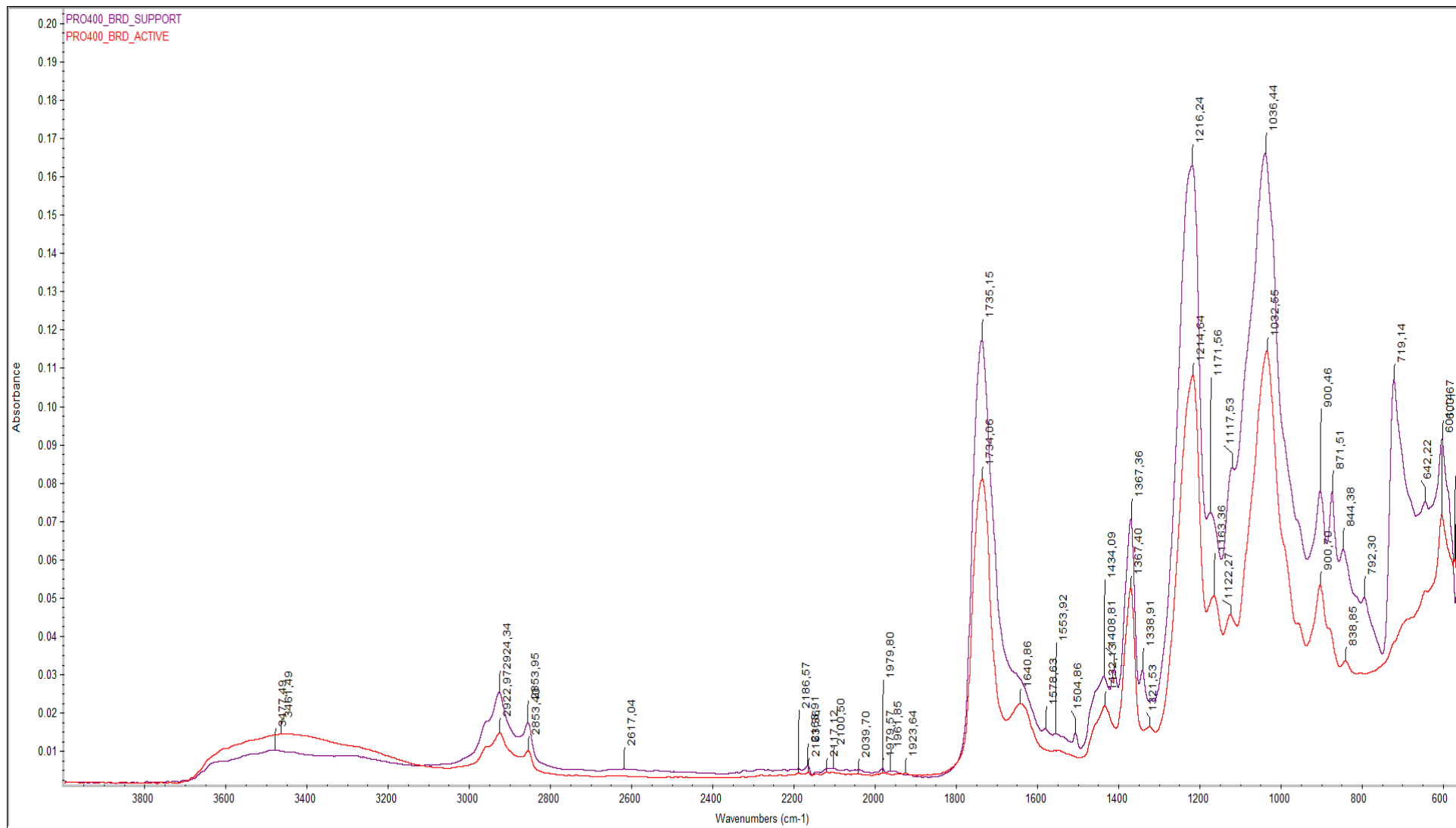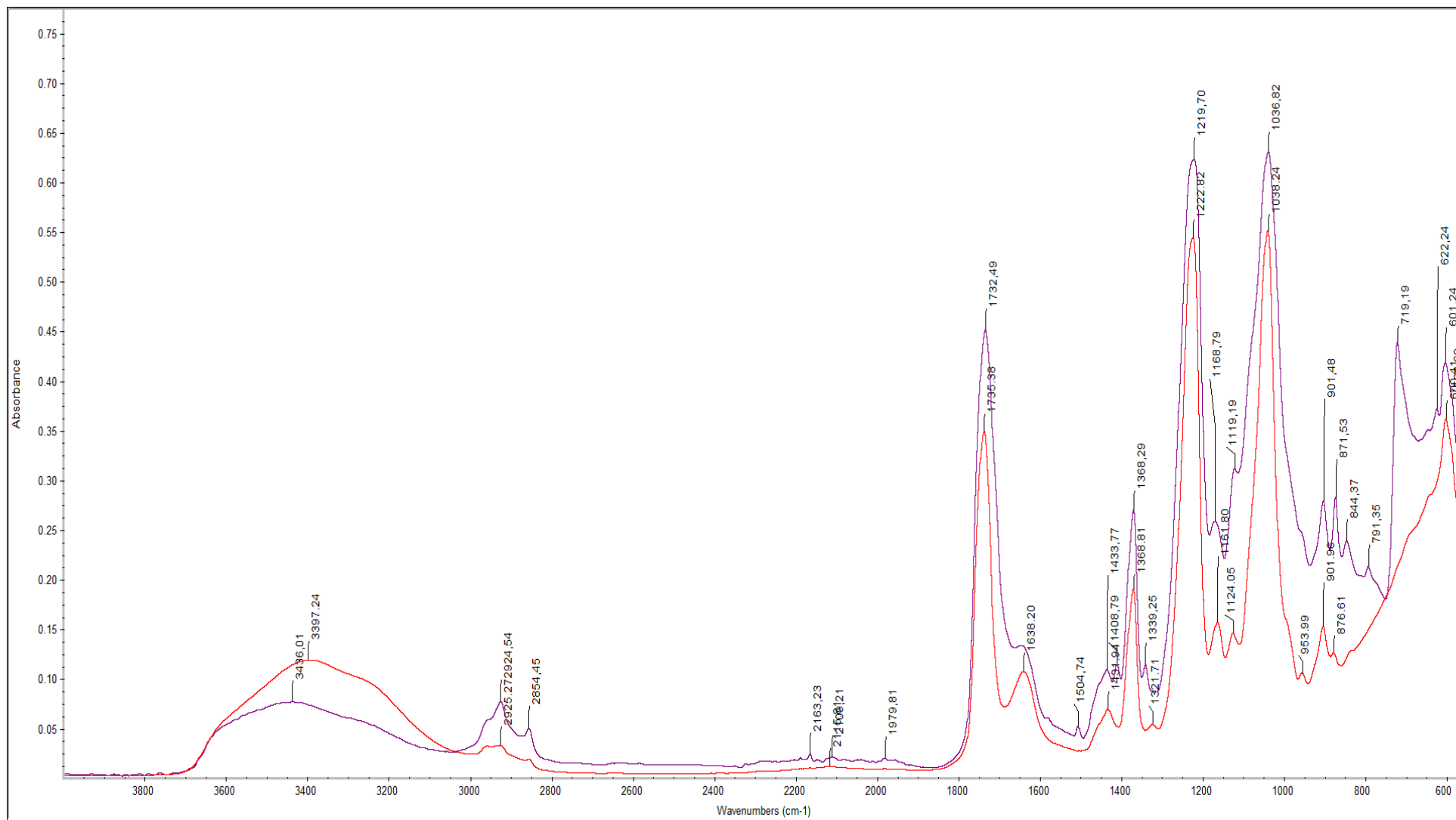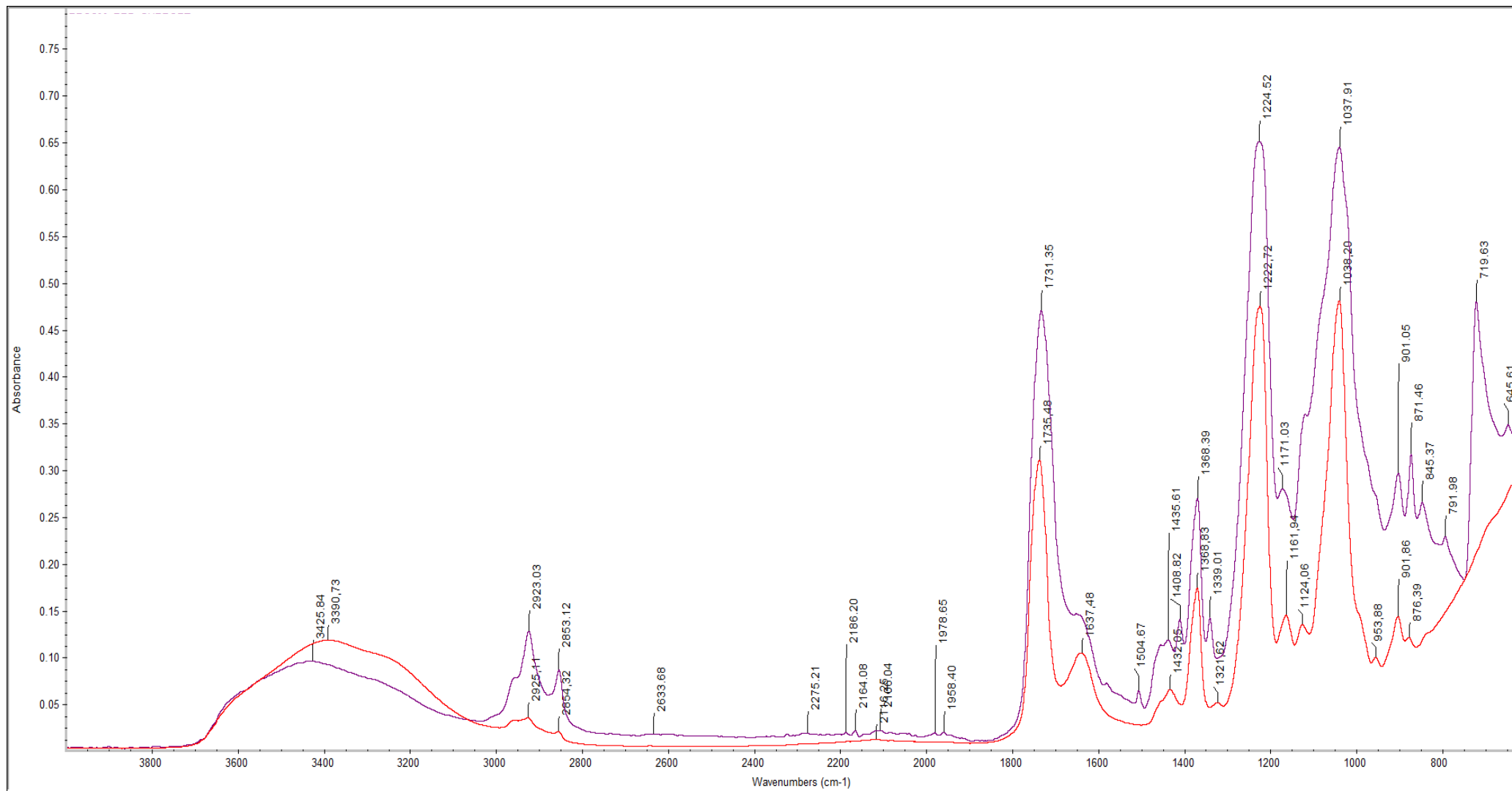
(i)

(ii)
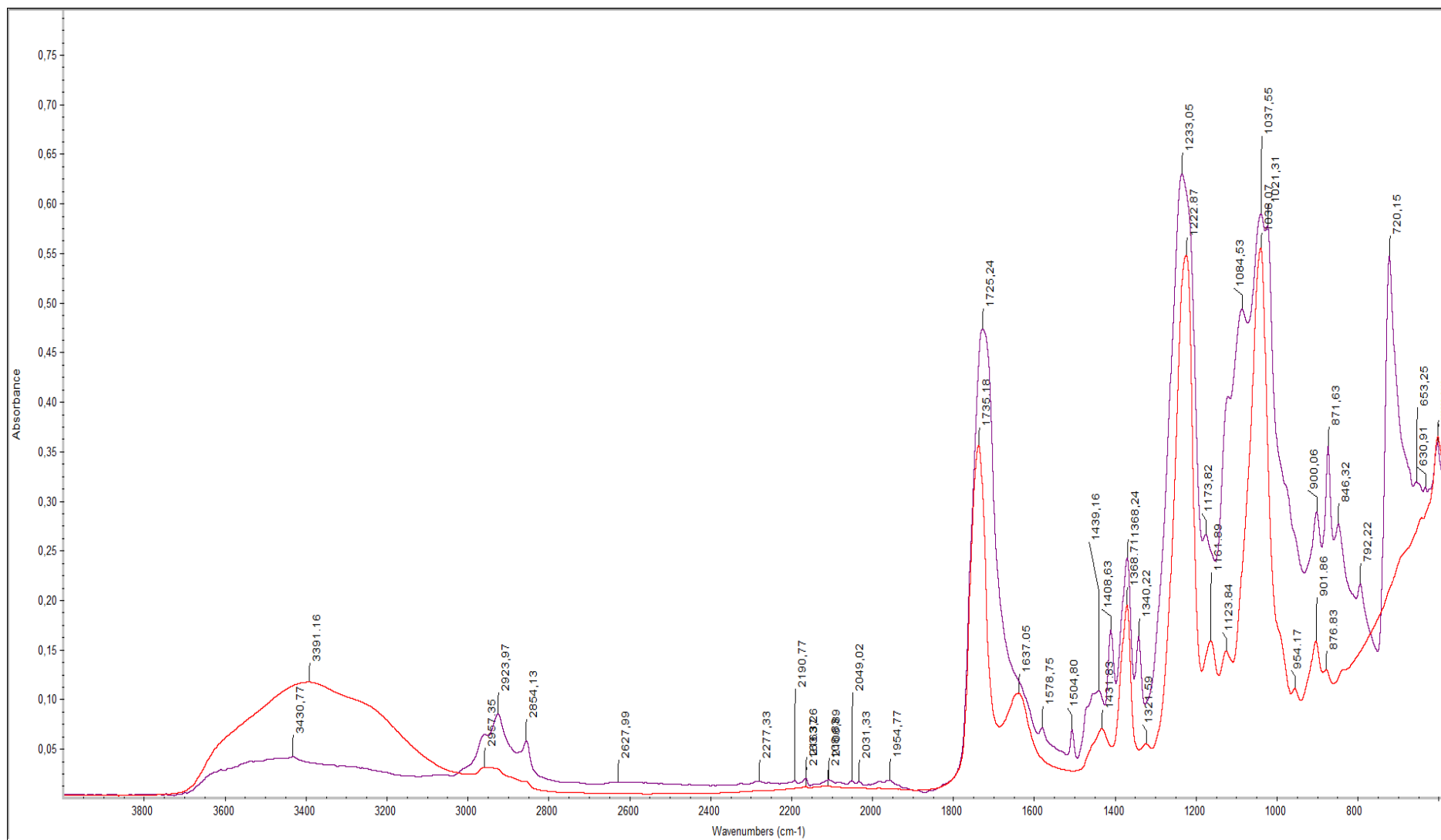
Figure 6.4: ATR-FTIR spectrum of the active (blue) and support (red) layer of the CTA membrane exposed to Maxilon blue GRL dye in FO mode in accordance to the respective flowrates of i) 400 ii) 500 and iii) 600 ml/min (graph markers not included as such view in colour)

6.4 Summary

In the ATR-FTIR spectrum of the virgin CTA membrane in Figure 6.1, four specific peaks were observed at locations 1734 cm^{-1}, 1367 cm^{-1}, 1213 $cm^{-1,}$ and 1031 cm^{-1}, respectively. However, after long-term operation with the respective dye (i.e. Reactive Black 5 and Maxilon Blue GRL), the specific peaks of the virgin CTA membrane maintained their prominence, demonstrating that the membrane surface was not altered by any membrane foulants of significance. Taking into consideration the ATR-FTIR spectra of the membranes exposed to Reactive Black 5 and Maxilon Blue GRL dye, no significant impact in terms of membrane molecular structure was observed. Furthermore, the deviations in flowrate had little to no impact on the membrane molecular structure.

CHAPTER 7

CHAPTER 7: CONCLUSIONS AND RECOMMENDATIONS

7.1 Introduction

Chapter 7 draws conclusions on the study evaluating a dye-driven forward osmosis (FO) system for the reclamation of synthetic brackish water (BW5) by investigating the effects of membrane orientation, system flowrate, membrane fouling and change in dye DS on the systems performance and energy consumption. The system performance was evaluated in terms of the water flux (J_w), reverse solute flux (J_s) and water recovery (Re) whilst the system energy consumption was evaluated in terms of the specific energy consumption (SEC). The effects and extent of membrane fouling on the FO system were evaluated by comparing the results of baseline 1 and baseline 2 experiments.

7.1.1 Membrane orientation

Varying the membrane orientation from FO to PRO mode contributed to a change in the system performance and energy consumption. Results showed that the PRO mode achieved both higher water flux (J_w) (i.e. 8.87, 8.71 and 8.90 L/m^2.h for flowrates of 400, 500 and 600 ml/min) and water recovery (Re) rates compared to FO mode. The difference between PRO and FO mode was further validated by the t-test which indicated a p-value below 0.05, suggesting a significant difference between the two modes. The system consumed less energy in PRO mode (i.e. 381 kWh/m^3 average consumption with respect to all three flowrates) than FO mode (i.e. 417 kWh/m^3 average consumption with respect to all three flowrates). Furthermore, it was observed that at a higher DS osmotic pressure (OP), the system consumed less energy. Therefore, selecting an optimum initial OP is essential for an FO process to minimise the pumping energy. It was concluded that the extent of the impact of varying the membrane orientation on system performance and energy consumption would be more conclusive with a longer duration of the respective experiments.

7.1.2 Flowrate

The increase in flowrate did not make a significant impact on the system performance as the J_w, J_s and R_e achieved were fairly similar in relation to the variated flowrates. However, it was observed that slightly higher J_w was achieved with an increase in flowrate from 400, 500 and 600 ml/min, respectively. Furthermore, higher SEC was achieved with an increase in flowrates from 400, 500 and 600 ml/min, respectively. The increase in SEC did not make a significant impact on the system power consumption. It was suggested that the low increase in the pump power consumption was a result of the short duration of experiments. Slight deviations in the

SEC increase with respect to flowrate increase were attributed to the replacement of tubing due to wear between experiments.

7.1.3 Membrane fouling

In this study, no significant membrane fouling was observed, however, minute traces of fouling in the form of foreign functional groups could be observed in the attenuated total reflection Fourier transform infrared spectroscopy (ATR-FTIR) spectrums of the used membranes. Additionally, the observation of negligible changes in baseline 2 (membrane control) J_w, J_s and R_e results suggested the possible occurrence of membrane fouling during the main experiment. However, the extent of the impact of membrane fouling on the system performance and energy consumption of the dye-driven FO system was not fully established due to a lack of correlation between baseline 1 and baseline 2 experimental results.

7.2 Conclusions

In conclusion, alteration in the membrane orientation contributed to an improvement in the system performance and energy consumption of a dye-driven FO system. It was found that the system performance and energy consumption in the PRO mode were more favorable and ideal in comparison to the FO mode of operation. Furthermore, it is advised that the PRO mode should be considered to be the more viable orientation for experiments with lower duration.

An increase in flowrate did not contribute to a beneficial impact on the system performance, however, a change in the energy consumption of the dye-driven FO system was observed at a higher flowrate. In light of this, to optimise operational costs, it is advised that lower flowrates be favoured as equivalent system performances can be achieved with lower flowrates in comparison to higher flowrates. No significant membrane fouling was observed throughout the study. Taking into consideration the ATR-FTIR spectrums of the used membranes and the experimental results of baseline 1 and baseline 2 experiments, it was concluded that membrane fouling might have occurred. However, the extent of membrane fouling could not be quantified due to a lack of correlation between baseline 1 and baseline 2 experiments.

Experiments were run until the target concentration (i.e. 0.002 M and 0.004 M for Reactive Black 5 and Maxilon Blue GRL dyes, respectively) of the resulting dye solution was achieved and as such dictated the duration of experiments within the study. However, the system performance parameters (i.e. J_w, J_s, R_e and SEC) were compared over the same period to draw reliable conclusions. Taking the J_w, J_s, R_e and SEC results into consideration, for the same period, it can be concluded that the FO system performed better whilst operating with

Reactive Black 5 dye as a DS in comparison to Maxilon Blue GRL dye. From the results obtained, it was observed that the ΔOP, as well as the target concentration of the experiments, impacted the system performance. It is therefore recommended that a study incorporating the use of a FS and DS yielding higher ΔOP and water flux be undertaken at a dye concentration lower than 0.02 M, with the hope of reducing the extent of reverse solute flux (J_s), as well as achieving a longer experimental duration and higher water recovery (R_e).

7.3 Recommendations

The following recommendations are made based on the challenges faced and results obtained from the study in question.

> ➤ To obtain a more accurate and reliable account of the power consumption of a dye-driven FO system, a pump such as a centrifugal pump should be employed. The changing of tubing due to wear of the peristaltic pump between experiments had a negative impact on the power consumption data. Furthermore, it is advised that the correct pump size is taken into consideration before commencing with experiments to ensure that the right pump is being utilised for the FO system being used.
>
> ➤ To better determine the extent of membrane fouling, it is advised that the membranes should be re-used (i.e. more than twice) and experiments should be run for a longer period to attain data that is substantial and conclusive enough to make correlations in relation to membrane fouling.
>
> ➤ There should be magnetic stirrers in both the FS and DS reservoirs. The magnetic stirrers should be utilised to achieve homogenous solutions, thus, ensuring a constant and accurate solution EC and OP readings.

REFERENCES

Achilli, A., Cath, T.Y. and Childress, A.E. 2009a. Power generation with pressure retarded osmosis: An experimental and theoretical investigation. *Journal of Membrane Science*, 343(1):42-52.

Achilli, A., Cath, T.Y. and Childress, A.E. 2010. Selection of inorganic-based draw solutions for forward osmosis applications. *Journal of Membrane Science*, 364(1):233-241.

Achilli, A., Cath, T.Y., Marchand, E.A. and Childress, A.E. 2009b. The forward osmosis membrane bioreactor: a low fouling alternative to MBR processes. *Desalination*, *239*(1-3):10-21.

Akther, N., Sodiq, A., Giwa, A., Daer, S., Arafat, H.A. and Hasan, S.W. 2015. Recent advancements in forward osmosis desalination: A review. *Chemical Engineering Journal*, 281:502-522.

Al Mazrooei, M. 2013. *Modeling Water Flux in Forward Osmosis: Implications for Improved Membrane Design* (Doctoral dissertation).

Aljeboree, A., Alkaim, A. and Alshirifi, A. 2014. Kinetics and equilibrium study for the adsorption
of textile dyes on coconut shell activated carbon. *Arabian Journal of Chemistry, 150*(10) 1016:1-14.

Alsvik, I.L. and Hägg, M.B. 2013. Pressure retarded osmosis and forward osmosis membranes: materials and methods. *Polymers*, 5(1):303-327.

Amy, G. 2008. Fundamental understanding of organic matter fouling of membranes. *Desalination*, *231*(1-3):44-51.

Augustine, R., 2017. *Forward osmosis membranes for direct fertigation within the South African wine industry*. Unpublished Doctoral dissertation, Cape Peninsula University of Technology.

Boo, C., Elimelech, M. and Hong, S. 2013. Fouling control in a forward osmosis process integrating seawater desalination and wastewater reclamation. *Journal of Membrane Science*, 444:148-156.

Boo, C., Elimelech, M. and Hong, S. 2013. Fouling control in a forward osmosis process integrating seawater desalination and wastewater reclamation. *Journal of Membrane Science*, 444:148-156.

Boo, C., Lee, S., Elimelech, M., Meng, Z. and Hong, S. 2012. Colloidal fouling in forward osmosis: Role of reverse salt diffusion. *Journal of Membrane Science*, *390*:277-284.

Burton, R. 2008. *Biomedical calculations: principles and practice*. John Wiley and Sons. University of Glasgow, United Kingdom.

Cai, Y., Shen, W., Loo, S.L., Krantz, W.B., Wang, R., Fane, A.G. and Hu, X. 2013. Towards temperature driven forward osmosis desalination using Semi-IPN hydrogels as reversible draw agents. *Water Research*, 47(11):3773-3781.

Cartinella, J.L., Cath, T.Y., Flynn, M.T., Miller, G.C., Hunter, K.W. and Childress, A.E. 2006. Removal of natural steroid hormones from wastewater using membrane contactor processes. *Environmental Science and Technology*, 40(23):7381-7386.

Cath, T.Y., Childress, A.E. and Elimelech, M. 2006. Forward osmosis: principles, applications, and recent developments. *Journal of Membrane Science*, *281*(1):70-87.

Cath, T.Y., Gormly, S., Beaudry, E.G., Flynn, M.T., Adams, V.D. and Childress, A.E. 2005. Membrane contactor processes for wastewater reclamation in space: Part I. Direct osmotic concentration as pretreatment for reverse osmosis. *Journal of Membrane Science*, 257(1):85-98.

Chanukya, B.S., Patil, S. and Rastogi, N.K. 2013. Influence of concentration polarization on flux behavior in forward osmosis during desalination using ammonium bicarbonate. *Desalination*, 312:39-44.

Chaoui, I., Abderafi, S., Vaudreuil, S. and Bounahmidi, T. 2019. Water desalination by forward osmosis: draw solutes and recovery methods–review. *Environmental Technology Reviews*, 8(1):25-46.

Chen, X., Xu, J., Lu, J., Shan, B. and Gao, C. 2017. Enhanced performance of cellulose triacetate membranes using binary mixed additives for forward osmosis desalination. *Desalination*, 405:68-75.

Chou, S., Wang, R., Shi, L., She, Q., Tang, C. and Fane, A.G. 2012. Thin-film composite hollow fiber membranes for pressure retarded osmosis (PRO) process with high power density. *Journal of Membrane Science*, 389: 25-33.

Cui, Y., Ge, Q., Liu, X.Y. and Chung, T.S. 2014. Novel forward osmosis process to effectively remove heavy metal ions. *Journal of Membrane Science*, 467:188-194.

Darwish, M.A., Abdulrahim, H.K., Hassan, A.S., Mabrouk, A.A. and Sharif, A.O. 2016. The forward osmosis and desalination. *Desalination and Water Treatment*, 57(10):4269-4295.

De Jager, D., Sheldon, M.S. and Edwards, W. 2014. Colour removal from textile wastewater using a pilot-scale dual stage MBR and subsequent RO system. *Separation and Purification Technology,* 135(2014):135-144*.*

Elimelech, M. and Phillip, W.A. 2011. The future of seawater desalination: energy, technology, and the environment. *Journal of Membrane Science*, 333(6043):712-717.

Fioramonti, L. 2015. Water shortages about to put load-shedding in the dark. Business Day http://www.waterrhapsody.co.za/2015/06/30/water-shortages-about-to-put. [8 December 2016].

Ghaly A.E., Ananthashankar. R., Alhattab. M. and Ramakrishnan, VV. 2014. Production, characterization and treatment of textile effluents: A Critical Review. *Journal of Chemical Engineering Process Technology*, 5(1):1-19.

Goh, P.S., Ismail, A.F., Ng, B.C. and Abdullah, M.S. 2019. Recent progresses of forward osmosis membranes formulation and design for wastewater treatment. *Water*, 11(10):2043.

Gonotec. 2014. User Guide: Osmomat 3000. Version 1.05. Available online at http://www.gonotec.com/ [8 September 2016].

Gray, G.T., McCutcheon, J.R. and Elimelech, M. 2006. Internal concentration polarization in forward osmosis: Role of membrane orientation. *Desalination*, 197(1-3):1-8.

GreenCape. Water: market intelligence report. 2017. *Intellectual property policy*. http:// www. greencape.co.za [29 June 2017].

Han, G., Liang, C.,Zeng, C., Tai Shung, W., Staudt,M.C. and Maletzko, C. 2016. Combination of forward osmosis (FO) process with coagulation/flocculation (CF) for potential treatment of textile wastewater. *Water Research*, 91:361–370.

Hancock, N.T. and Cath, T.Y. 2009. Solute coupled diffusion in osmotically driven membrane processes. *Environmental Science and Technology*, *43*(17):6769-6775.

Hsiang, T.C. 2011. Modeling and Optimization of the Forward Osmosis Process-Parameters Selection, Flux Prediction and Process Applications. Unpublished Doctoral dissertation. National University of Singapore, Singapore.

Jingxi, E.Z. 2017. Forward osmosis: a desalination technology for the textile industry. Unpublished Masters dissertation, Cape Peninsula University of Technology, South Africa.

Jung, D.H., Lee, J., Lee, Y.G., Park, M., Lee, S., Yang, D.R. and Kim, J.H. 2011. Simulation of forward osmosis membrane process: Effect of membrane orientation and flow direction of feed and draw solutions. *Desalination*, 277(1):83-91.

Keane, J. and te Velde, D.W. 2008. The role of textile and clothing industries in growth and development strategies. *Overseas Development Institute*, 7:7-9.

Kim, D.I., Kim, J., Shon, H.K. and Hong, S. 2015. Pressure retarded osmosis (PRO) for integrating seawater desalination and wastewater reclamation: Energy consumption and fouling. *Journal of Membrane Science*, 483:34-41.

Klaysom, C., Cath, T.Y., Depuydt, T. and Vankelecom, I.F. 2013. Forward and pressure retarded osmosis: potential solutions for global challenges in energy and water supply. *Chemical Society Reviews*, 42(16):6959-6989.

Koyuncu, I. and Cakmakci, M. 2010. Nanofiltration for Water and Wastewater treatment. *Nanotechnology in water treatment applications*, 18(13):103-113.

Kutchai, H. 2003. *Self-instructional packages on diffusion, osmosis, ionic equiilibria and resting membrane potential: General physiology course*. Sackler School of Medicine, Tel Aviv University.

Lambrechts, R. 2018. A performance and energy evaluation of a fertiliser-drawn forward osmosis (FDFO) system. Unpublished Doctoral dissertation, Cape Peninsula University of Technology, South Africa.

Lay, W.C., Chong, T.H., Tang, C.Y., Fane, A.G., Zhang, J. and Liu, Y. 2010. Fouling propensity of forward osmosis: investigation of the slower flux decline phenomenon. *Water Science and Technology*, *61*(4):927-936.

Lay, W.C., Zhang, J., Tang, C., Wang, R., Liu, Y. and Fane, A.G. 2012. Factors affecting flux performance of forward osmosis systems. *Journal of Membrane Science*, *394*:151-168.

Le,N.L. and Nunes, S.P. 2016. Materials and membrane technologies for water and energy sustainability. *Sustainable Materials and Technologies,* 7:1-28.

Lee, S., Boo, C., Elimelech, M. and Hong, S. 2010a. Comparison of fouling behaviour in forward osmosis (FO) and reverse osmosis (RO). *Journal of Membrane Science*, *365*(1-2), 34-39.

Lee, W., Ahn, C.H., Hong, S., Kim, S., Lee, S., Baek, Y. and Yoon, J. 2010b. Evaluation of surface properties of reverse osmosis membranes on the initial biofouling stages under no filtration condition. *Journal of Membrane Science*, 351(1):112-122.

Li, D., Zhang, X., Simon, G.P. and Wang, H. 2013. Forward osmosis desalination using polymer hydrogels as a draw agent: Influence of draw agent, feed solution and membrane on process performance. *Water Research*, 47(1):209-215.

Ling, M. M., Wang, K. Y. and Chung, T. S. 2010. Highly water-soluble magnetic nanoparticles as novel draw solutes in forward osmosis for water reuse. *Industrial and Engineering Chemistry Research*, 49(12):5869–5876.

Ling, M.M. and Chung, T.S. 2011. Desalination process using super hydrophilic nanoparticles via forward osmosis integrated with ultrafiltration regeneration. *Desalination*, 278(1-3):194-202.

Liu, Y. 2013. Fouling in forward osmosis membrane processes: Characterization, mechanisms and mitigation. Unpublished PhD thesis, University of Maryland, United States of America.

Lorimer, J.P., Mason, T.J., Plattes, M., Phull, S.S. and Walton, D.J. 2001. Degradation of dye effluent. *Pure and Applied Chemistry*, 73(12):1957-1968.

Lutchmiah, K., 2014. Reclaiming Water from Wastewater using Forward Osmosis.

Martinetti, C.R., Childress, A.E. and Cath, T.Y. 2009. High recovery of concentrated RO brines using forward osmosis and membrane distillation. *Journal of Membrane Science*, *331*(1):31-39.

McCutcheon, J.R. and Elimelech, M. 2006. Influence of concentrative and dilutive internal concentration polarization on flux behaviour in forward osmosis. *Journal of Membrane Science*, 284(1):237-247.

McCutcheon, J.R., McGinnis, R.L. and Elimelech, M. 2005. A novel ammonia—carbon dioxide forward (direct) osmosis desalination process. *Desalination*, 174(1):1-11.

McCutcheon, J.R., McGinnis, R.L. and Elimelech, M. 2006. Desalination by ammonia–carbon dioxide forward osmosis: Influence of draw and feed solution concentrations on process performance. *Journal of Membrane Science*, *278*(1):114-123.

McGinnis, R.L. and Elimelech, M. 2007. Energy requirements of ammonia–carbon dioxide forward osmosis desalination. *Desalination*, 207:370-382.

McGovern, R.K. and Lienhard, V.J.H. 2014. On the potential of forward osmosis to energetically outperform reverse osmosis desalination. *Journal of Membrane Science*, 469:245–250.

Mehta, D., Gupta, L. and Dhingra, R. 2014. Forward Osmosis in India: Status and comparison with other desalination technologies. *International Scholarly Research Notices,* 2014:9.

Mekonnen, M.M. and Hoekstra, A.Y. 2016. Four billion people facing severe water scarcity. *Science Advances*, *2*(2):4-10.

Mi, B. and Elimelech, M. 2008. Chemical and physical aspects of organic fouling of forward osmosis membranes. *Journal of Membrane Science*, 320(1–2):292–302.

Motsa, M.M., Mamba, B.B., Hoek, E.M.V. and Verliefde, A.R.D. 2014. Organic fouling in forward osmosis membranes: The role of feed solution chemistry and membrane structural properties. *Journal of Membrane Science*, 460:99-109.

Naidu, L.D., Saravanan, S., Chidambaram, M., Goel, M., Das, A. and Sarat, J. 2015. Nanofiltration in transforming surface water into healthy water: Comparison with reverse osmosis. *Journal of Chemistry*, 15:1-6.

Nicoll, P.G. 2013. Forward osmosis—A brief introduction. In *Proceedings of the international desalination association world congress on desalination and water reuse, Tianjin, China*, 1:20- 25.

Ntuli, F., Omoregbe, D.I., Kuipa, P.K., Muzenda, E. and Belaid, M. 2009. Characterization of effluent from textile wet finishing operations. World Congress on Engineering and Computer Science, San Francisco, USA, 1:2-6.

Peñate, B. and García-Rodríguez, L. 2011. Energy optimisation of existing SWRO (seawater reverse osmosis) plants with ERT (energy recovery turbines): Technical and thermoeconomic assessment. *Energy*, 36(1):613-626.

PerkinElmer precisely. 2005. *FT-IR Spectroscopy Attenuated Total Reflectance (ATR).* USA: PerkinElmer Life and Analytical Sciences.

Phuntsho, S., Sahebi, S., Majeed, T., Lotfi, F., Kim, J. E.and Shon, H. K. 2013. Assessing the major factors affecting the performances of forward osmosis and its implications on the desalination process. *Chemical Engineering Journal*, 231:484–496.

Phuntsho, S., Shon, H.K., Hong, S., Lee, S. and Vigneswaran, S. 2011. A novel low energy fertilizer driven forward osmosis desalination for direct fertigation: evaluating the performance of fertilizer draw solutions. *Journal of Membrane Science*, 375(1):172-181.

Phuntsho, S., Shon, H.K., Hong, S., Lee, S., Vigneswaran, S. and Kandasamy, J. 2012. Fertiliser drawn forward osmosis desalination: The concept, performance and limitations for fertigation. *Reviews in Environmental Science and Bio/Technology*, 11(2):147-168.

Rana, D. and Matsuura, T. 2010. Surface modifications for antifouling membranes. *Chemical Reviews*, *110*(4):2448-2471.

Sagiv, A., Zhu, A., Chistofides, P.D., Cohen, Y. and Semiat, R. 2014. Analysis of forward osmosis desalination via two-dimensional FEM model. *Journal of Membrane Science*, *464*:161-172.

Saren, Q., Qiu, C.Q. and Tang, C.Y. 2011. Synthesis and characterization of novel forward osmosis membranes based on layer-by-layer assembly. *Environmental Science and Technology*, 45(12):5201-5208.

Schader, G.A. 2006. *Direct nanofiltration of wastewater treatment plant effluent*. Unpublished Doctoral dissertation, University of Twente, Netherlands:

Schwab, K. 2010. The global competitiveness report 2015-2016. Geneva: World Economic Forum (15th September).

Seidel, A. and Elimelech, M. 2002. Coupling between chemical and physical interactions in natural organic matter (NOM) fouling of nanofiltration membranes: Implications for fouling control. *Journal of Membrane Science*, *203*(1):245-255.

Shaffer, D.L., Werber, J.R., Jaramillo, H., Lin, S. and Elimelech, M. 2015. Forward osmosis: Where are we now? *Desalination*, 356:271-284.

She, Q., Jin, X., Li, Q and Tang, C.Y. 2012. Relating reverse and forward solute diffusion to membrane fouling in osmotically driven membrane processes. *Water Research*, *46*(7): 2478- 2486.

Sheldon, M., Jingxi, E.Z., De Jager, D., Augustine, R., Korenak, J., Helix-Nielsen, C. and Petrinic, I. 2018. Potential of dyes as draw solutions in forward osmosis for the South African textile industry. *Water SA*, *44*(2):258-268.

Shon, H. K., Phuntsho, S., Chaudhary, D. S., Vigneswaran, S. and Cho, J. 2013. Nanofiltration for water and wastewater treatment – a mini review. *Drinking Water Engineering and Science,* 6:47- 53.

Strathmann H, Giorno L, Drioli E. 2006. An introduction to membrane science and technology, chapter 2. CNR Publisher, Roma. ISBN 88-8080-063-9.

Suh, C. and Lee, S. 2013. Modelling reverse draw solute flux in forward osmosis with external concentration polarization in both sides of the draw and feed solution. *Journal of Membrane Science*, 427:365-374.

Sunohara, T. and Masuda, T. 2011. Cellulose triacetate as a high-performance membrane. *Contributions to Nephology*, 173:156-163.

Tang, C.Y., She, Q., Lay, W.C., Wang, R. and Fane, A.G. 2010. Coupled effects of internal concentration polarization and fouling on flux behaviour of forward osmosis membranes during humic acid filtration. *Journal of Membrane Science*, *354*(1-2):123-133.

Tang, W. and Ng, H.Y. 2008. Concentration of brine by forward osmosis: performance and influence of membrane structure. *Desalination*, *224*(1-3):143-153.

Thompson, N.A. and Nicoll, P.G. 2011. Forward osmosis desalination: a commercial reality. In IDA World Congress–Perth Convention and Exhibition Centre (PCEC), Perth, Western Australia, 4-9 September, 2011.

Tow, E.W. and McGovern, R.K. 2015. Raising forward osmosis brine concentration efficiency though flowrate optimization. *Desalination*, 366:71-79.

Truett, L. J., and Truett, D. 2010. New challenges for the South African textile and apparel industries in the global economy. *Journal of Economic Development,* 35(4):73-91.

Van der Bruggen, B., Vandecasteele, C., Van Gestel, T., Doyen, W.and Leysen, R. 2003. A review of pressure-driven membrane processes in wastewater treatment and drinking water production. *Environmental Progress*, *22*(1):46-56.

Von Bormann, T and Gulati, M. 2014. The food energy water nexus: Understanding South Africa's most urgent sustainability challenge. WWF-SA, South Africa: 1-35.

Wang, K.Y., Chung, T.S. and Amy, G. 2012a. Developing thin-film-composite forward osmosis membranes on the PES/SPSf substrate though interfacial polymerization. *AIChE Journal*. *58*(3):770-781.

Wang, R., Setiawan, L. and Fane, A.G. 2012b. Forward osmosis: Current status and perspectives. *Journal of Membrane Science*, 281:70-87.

Wei, J., Liu, X., Qiu, C., Wang, R. and Tang, C.Y. 2011. Influence of monomer concentrations on the performance of polyamide-based thin film composite forward osmosis membranes. *Journal of Membrane Science*, *381*(1):110-117.

Wilson, A.D. and Stewart, F.F. 2013. Deriving osmotic pressures of draw solutes used in osmotically driven membrane processes. *Journal of Membrane Science*, 431:205-211.

Wong, M.C., Martinez, K., Ramon, G.Z. and Hoek, E.M. 2012. Impacts of operating conditions and solution chemistry on osmotic membrane structure and performance. *Desalination*, 287:340-349.

World Resources Institute: annual report. 2015. *Intellectual property policy*. http:// www.wri.org. [June 2015].

WWAP 2017. *United Nations World Water Assessment Programme. The United Nations World Water Development Report 2017. Wastewater: The Untapped Resource*. Paris, UNESCO.

Xiang, X., Zou, S. and He, Z. 2017. Energy consumption of water recovery from wastewater in a submerged forward osmosis system using commercial liquid fertilizer as a draw solute. *Separation and Purification Technology*, 174:432-438.

Yen, S.K., Haja N, F.M., Su, M., Wang, K.Y. and Chung, T. 2010. Study of draw solutes using 2-methylimidazole-based compounds in forward osmosis. *Journal of Membrane Science,* 364:242-252.

Yip, N.Y., Tiraferri, A., Phillip, W.A., Schiffman, J.D. and Elimelech, M. 2010. High performance thin-film composite forward osmosis membrane. *Environmental Science and Technology*, 44(10):3812-3818.

Zhang, H., Cheng, S. and Yang, F. 2014. Use of a spacer to mitigate concentration polarization during forward osmosis process. *Desalination*, 347:12-119.

Zhang, S., Wang, K.Y., Chung, T.S., Chen, H., Jean, Y.C. and Amy, G. 2010. Well-constructed cellulose acetate membranes for forward osmosis: Minimized internal concentration polarization with an ultra-thin selective layer. *Journal of Membrane Science*, *360*(1):522-535.

Zhao, P., Gao, B., Yue, Q., Liu, S. and Shon, H.K. 2016. Effect of high salinity on the performance of forward osmosis: Water flux, membrane scaling and removal efficiency. *Desalination*, 378:67-73.

Zhao, S., Huang, K and Lin, H. 2015. Impregnated Membranes for Water Purification Using Forward Osmosis. *Industrial and Engineering Chemistry Research.* 54(49):1235–1236.

Zhao, S., Zou, L., Tang, C.Y. and Mulcahy, D. 2012. Recent developments in forward osmosis: opportunities and challenges. *Journal of Membrane Science*, 396:1-21.

Zhou, Z., Lee, J.Y. and Chung, T.S. 2014. Thin film composite forward-osmosis membranes with enhanced internal osmotic pressure for internal concentration polarization reduction. *Chemical Engineering Journal*, 249:236-245.

Zou, S. and He, Z. 2016. Enhancing wastewater reuse by forward osmosis with self-diluted commercial fertilizers as draw solutes. *Water Research*, 99:235-243.

Zou, S., Gu, Y., Xiao, D. and Tang, C.Y. 2011. The role of physical and chemical parameters on forward osmosis membrane fouling during algae separation. *Journal of Membrane Science*, *366*(1-2), 356-362.

Zou, S., Yuan, H., Childress, A. and He, Z. 2016. Energy consumption by recirculation: a missing parameter when evaluating forward osmosis. *Environmental Science and Technology*, 6827-6829.

APPENDICES

APPENDIX A: Feed solution (FS) and draw solution (DS) preparation

All equipment used was calibrated and prepared in accordance with manufacturer instructions, respectively. Two 2 L beakers were cleaned meticulously with foamy water after which it was rinsed thoroughly with tap water to remove all presence of the foamy substance. Furthermore, the beakers were then rinsed vigorously with deionised (DI) water as a preventative measure to eliminate the presence of any form of contaminants. The beakers were then dried with a paper towel and were then ready for solution preparation.

A1. FS preparation procedure for baseline 1 and baseline 2 experiments

The FS utilised for baseline 1 and baseline 2 experiments comprised of a 1 M NaCl solution. The solution was stored in a 2 L beaker. A 0.5 L FS was prepared through the addition of 29.22 g NaCl in 0.5 L DI water and was stirred thoroughly until a homogenous solution was achieved.

A2. DS preparation procedure for baseline 1 and baseline 2 experiments

The DS utilised for baseline 1 and baseline 2 experiments were characterised by Dyeing solutions of Reactive Black 5 and Maxilon Blue GRL dye, respectively. The 0.2 L DS comprised of Reactive Black 5 dye was prepared through the addition of 3.96 g of dye and 39.6 g of NaCl to 0.2 L DI water. The 0.2 L DS comprised of Maxilon GRL dye was prepared through the addition of 1.93 g of dye and 19.3 g of NaCl to 0.2 L DI water. Both solutions were stirred thoroughly until a homogenous solution was achieved.

A3. FS preparation procedure for the main experiment (dye-driven FO system)

The FS utilised for the main experiment was characterised by an SBW5 solution with a salt content of 5 g NaCl per litre of water. The solution was stored in a 2 L beaker and was prepared through the addition of 10 g of NaCl to 2 L DI water and was stirred thoroughly until a homogenous solution was achieved.

A4. DS preparation procedure for the main experiment (dye-driven FO system)

The DS utilised for the main experiments were characterised by Dyeing solutions of Reactive Black 5 and Maxilon Blue GRL dye, respectively. The 0.2 L DS comprised of Reactive Black 5 dye was prepared through the addition of 3.96 g of dye and 39.6 g of NaCl to 0.2 L DI water. The 0.2 L DS comprised of Maxilon GRL dye was prepared through the addition of 1.93 g of dye and 19.3 g of NaCl to 0.2 L DI water. Both solutions were stirred thoroughly until a homogenous solution was achieved.

APPENDIX B: Membrane integrity test procedure

All equipment used was calibrated and prepared in accordance with manufacturer instructions, respectively. Two 2 L beakers were cleaned meticulously with foamy water after which it was rinsed thoroughly with tap water to remove all presence of the foamy substance. Furthermore, the beakers were then rinsed vigorously with DI water as a preventative measure to eliminate the presence of any form of contaminants. The beakers were then dried with a paper towel and were then ready for solution preparation.

B1. FS preparation procedure for the membrane integrity test

The FS utilised for the integrity test was characterised by a methyl violet dye solution. The 0.5 L FS was stored and prepared in a 2 L beaker. The solution was prepared by adding 30 drops of a 0.01% methyl violet dye solution to 0.5 L DI water and stirred thoroughly until a homogenous solution was achieved.

B2. DS preparation procedure for the membrane integrity test

The FS utilised for the integrity test was characterised by a 2 M NaCl solution which was stored and prepared in a 2 L beaker. The solution was prepared by adding 58.44 g NaCl in 0.5 L DI water and stirred thoroughly until a homogenous solution was achieved.

APPENDIX C: Cellulose triacetate (CTA) membrane preparation

An adjustment with regards to the size of the CTA membranes which were supplied with a parameter of 40 cm × 40 cm was made in order to fit perfectly into the FO membrane cell which was characterised by a membrane area of 42 cm^2. A membrane sheet was placed onto a sterilised working surface after which a plastic membrane stencil (SterlitechTM Co., Washington, USA) was placed above the membrane sheet in order to trace the shape of the plastic membrane stencil onto the membrane sheet. With the aid of a scissor and latex laboratory gloves, the membrane was cut into the respective size after which it was immediately stored in a ziplock plastic bag filled with 50 ml of DI water and kept in a laboratory refrigerator at 5℃. The cut membrane was stored in DI water as a preventative measure to ensure that the membrane maintains its physical properties.

APPENDIX D: Colour Hazen

Colour determination using colour Hazen

Samples were preserved at room temperature ($\pm 25\,°C$). A 0.45 µm Luer Lock syringe was used to filter 5 ml of the sample of which 2 ml of the filtered sample was transferred into a 50 mm glass cuvette through the use of a P5000 Gilson pipette. The 50 mm glass cuvette was then placed into a cell compartment of the Nova 60 Spectroquant, after which the code 179 was pressed in order to select the method.

For the measuring range: 0 – 1000 Pt/Co (Hz):

➢ Ensure samples being utilised are at room temperature before conducting the analysis. Filter 5 ml of the liquid sample through a membrane filter with a 0.45 µm pore size, using a Luer Lock syringe.

➢ Transfer $\pm$ 2 ml of the filtered sample into a 50 mm glass cuvette, using a P5000 Gilson pipette.

➢ Place the 50 mm glass cuvette into the cell compartment of the NOVA 60 Spectroquant and select the method (code no. 179) on the menu.

For the measuring range: 0 – 500 Pt/Co (Hz)/0 – 250 Pt/Co (Hz)/0 – 100 Pt/Co (Hz):

➢ Ensure samples being utilised are at room temperature before conducting the analysis. Filter 5 ml of the liquid sample through a membrane filter with a 0.45 µm pore size, using a Luer Lock syringe.

➢ Transfer $\pm$ 2 ml of the filtered sample into a 10 mm glass cuvette for the 0 – 500 Pt/Co (Hz) measuring range, a 20 mm glass cuvette for the 0 – 250 Pt/Co (Hz) measuring range and a 50 mm glass cuvette for the 0 – 100 Pt/Co (Hz) measuring range through the use of a P5000 Gilson pipette.

➢ Place the respective glass cuvette into the cell compartment of the NOVA 60 Spectroquant and select the method (code no. 032) on the menu.

Notes:

- Unfiltered sample = Apparent colour
- Filtered sample = True colour
- Ensure the exterior of the glass cuvette is free of scratches and marks (wipe the cuvette surface with soft tissue before inserting into the NOVA 60 Spectroquant)
- All samples are read in triplicate.
- For the measuring range: 0 – 1000 Pt/Co (Hz), code number 179 must be selected on the NOVA 60 Spectroquant menu.
- For the measuring ranges: 0 – 500 Pt/Co (Hz)/0 – 250 Pt/Co (Hz)/0 – 100 Pt/Co (Hz) the code number 032 must be selected on the NOVA 60 Spectroquant menu.

APPENDIX E: Sample calculations

E1. Dye DS sample calculation

Table E1: Known properties of the dye

Dye	M_r (dye) (g/mol)	V (L)	C (mol/L)
Reactive Black 5	991	0.2	0.02
Maxilon Blue GRL	482	0.2	0.02

Calculating moles of dye:

$$C = \frac{n}{V}$$

$$\therefore n_{dye} = C \times V$$

$$\therefore n_{dye} = 0.02 \frac{mol}{L} \times 0.2L = 4 \times 10^3 \, mol$$

Calculating the mass of dye to produce a 0.02 mol/L of Reactive Black 5 dye solution:

$$n = \frac{m}{M_r}$$

$$\therefore m_{dye} = n \times M_r$$

$$\therefore m_{dye} = 4 \times 10^3 \, mol \times 991 \frac{g}{mol} = 3.96 \, g$$

Calculating the mass of salt:

- Apply salt/dye mass ratio of 1:10

$$m_{NaCl} = m_{dye} \times 10$$

$$\therefore m_{NaCl} = 3.96 \, g \times 10 = 39.6 \, g$$

- Salt/dye mass ratio validation

$$Ratio = \frac{39.6 \, g}{3.96 \, g} = 10$$

E2. Osmotic pressure sample calculation

$$1\frac{mOsmol}{kg} \, water = 19.32 \, mmHg$$

$$1 \, mmHg = 0.13 \, kPa$$

$$\therefore \ 19.32 \, mmHg = 2.51 \, kPa$$

$$\therefore \ 6000 \, \frac{mOsmol}{kg} = 15060 \, kPa$$

E3. Water flux sample calculation

$$J_w = \frac{\Delta V}{A_m \times \Delta t} = \frac{V_f - V_i}{A_m \times (t_2 - t_1)}$$

Where:

V_f = Final volume of DS (L)

V_i = Initial volume of DS (L)

A_m = Effective membrane area (m²)

t_1 = Time interval 1 (hr)

t_2 = Time interval 2 (hr)

Calculating water flux

$$\therefore J_w = \frac{V_f - V_i}{(A_m)(t_2 - t_1)} = \frac{(0.32) - (0.29)}{(0.0042) \times (2 - 1)} = 6.74 \, L/m^2 . h$$

E4. Reverse solute flux sample calculation

$$J_s = \frac{\Delta(C_t V_t)}{A_m . \Delta t} = \frac{\left[(C_{FS_{t2}})(V_{FS_{t2}}) - (C_{FS_{t1}})(V_{FS_{t1}}) \right]}{(A_m)(t_2 - t_1)}$$

Where:

$C_{FS_{t1}}$ = Mass concentration of the FS at time interval 1 (g/L)

$C_{FS_{t2}}$ = Mass concentration of the FS at time interval 2 (g/L)

$V_{FS_{t1}}$ = Volume of the FS at time interval 1 (L)

$V_{FS_{t2}}$ = Volume of the FS at time interval 1 (L)

A_m = Effective membrane area (m²)

t_1 = Time interval 1 (hr)

t_2 = Time interval 2 (hr)

Calculating reverse solute flux

$$J_s = \frac{\left[(C_{FS_{t2}})(V_{FS_{t2}}) - (C_{FS_{t1}})(V_{FS_{t1}}) \right]}{(A_m)(t_2 - t_1)}$$

$$\therefore J_s = \frac{\left[(0.59)(1.96 \times 10^{-3}) - (0.55)(1.98 \times 10^{-3}) \right]}{(0.0042)(2 - 1)} = 0.02 \ g/m^2 . h$$

E5. Water recovery sample calculation

Water recovery = $\frac{\Delta V}{V_{f_i}} \times 100 = \frac{V_{FS_{t2}} - V_{FS_{t1}}}{V_{f_i}} \times 100$

Where:

$V_{FS_{t1}}$ = Volume of the FS at time interval 1 (L)

$V_{FS_{t2}}$ = Volume of the FS at time interval 1 (L)

V_{F_i} = Initial volume of FS (L)

Calculating water recovery

Water recovery = $\frac{0.28 - 0.26}{2} \times 100 = 0.9 \approx 1\%$

E6. System specific energy consumption (SEC) sample calculation

$$SEC = \frac{P_{power}}{Water\ flux\ volumetric\ flowrate}$$

- $P_{power} = P_{amp} \times P_{volt}$
- $Water\ flux\ volumetric\ flow\ rate = \frac{V_{f_{DS}} - V_{i_{DS}}}{\rho_{water} \times (t_2 - t_1)}$

NB: It was considered that the solution crossing the membrane from the FS to the DS mimics the properties of water, therefore it was assumed that the ρ_{water} was 1000 g/L.

Where:

$V_{f_{DS}}$ = Final volume of DS (L)

$V_{i_{DS}}$ = Initial volume of DS (L)

t_1 = Time interval 1 (hr)

t_2 = Time interval 2 (hr)

ρ_{water}= Density of water (g/L)

P_{amp}= Pump current (A)

P_{volt}= Pump voltage (V)

Calculating system specific energy consumption

$$SEC = \frac{P_{amp} \times P_{volt}}{\dfrac{V_{f_{DS}} - V_{i_{DS}}}{\rho_{water} \times (t_2 - t_1)}}$$

$$\therefore SEC = \frac{\dfrac{(0.046)(225.3)}{1000}}{\dfrac{(0.32) - (0.29)}{(1000)(2 - 1)}} = 345.46 \, kW.h/m^3$$